Optimising Continuous Flow Chemoenzymatic Processes Towards Fine Chemical Manufacturing

Harrison James Johnson-Evans

Submitted in accordance with the

requirements for the degree of

Doctor of Philosophy

University of Leeds

School of Chemistry

December 2023

The candidate confirms that the work submitted is his own and that appropriate credit has been given where reference has been made to the work of others.

Acknowledgements

This research has been carried out as part of a team which has included both academic (Prof. Steve Marsden, Prof. Nikil Kapur and Prof. John Blacker) and industrial (Dr Mark Muldowney, Greg Holgate and Dr Mark Dow) supervisors. I would like to thank my academic supervisors for providing stimulating discussions and encouragement around my academic interests, and my industrial supervisors for reiterating the industrial relevance of the work, all contributing to the formulation and success of this project. Thank you also to the technical staff at the University of Leeds for all their help (Mark, Alex, Jeanine and Matt).

I would also like to gratefully acknowledge the Engineering and Physical Sciences Research Council (EPSRC), Sterling Pharma Solutions and AstraZeneca for the funding of this research.

My thanks and appreciation to all members of the Centre for Doctoral Training in Molecules to Product for their willingness to use their abilities to develop my own insight as a researcher.

I would like to thank the members of G56, past and present, who I've worked with throughout my time in Leeds who have made the experience so enjoyable. With a special mention to Emily, Dan, Sam, Scott, Alex, and Drew for your help in the early days and throughout, and for ensuring there was never a dull day in the lab! Special thanks goes to Dan for the begrudging assistance with all of the microbiology, biochemistry and photochemistry, to Sam for the never ending enthusiasm, morning motivations and perseverance with all my mumbling and to Alex for the regular humbling. Good luck to the remaining PhDs; Julian, Callum, Muneeba, Karan and Emma, its been lovely to work alongside you and I will miss you all (don't play too much BGA!).

Finally, I would like to thank all my family and friends for their continuous support and belief in me.

Abstract

The advancement in enzyme engineering has led to the integration of biocatalytic transformations into the synthesis of commercial fine chemical and pharmaceutical products becoming increasingly widespread. Whilst the combination of bio- and chemo-catalysis within a continuous flow system opens new synthetic avenues, the limited number of literature reported [1, 2], highlights the challenges within the field.

The core technological challenges associated with synergistic bio- and chemo-catalysis, namely the divergent reaction conditions and cofactor recycling, may be overcome with a combination of enzyme immobilisation, reaction compartmentalization and continuous separations. Consequently, new synthetic routes to complex chiral molecules through chemoenzymatic cascades will become more readily available.

The focus of this work is the enhancement of chemoenzymatic cascades in continuous flow, fusing enzyme immobilisation, reaction compartmentalisation and chemocatalytic methodologies, for the synthesis of pharmaceutically relevant chiral amines (Figure 1).

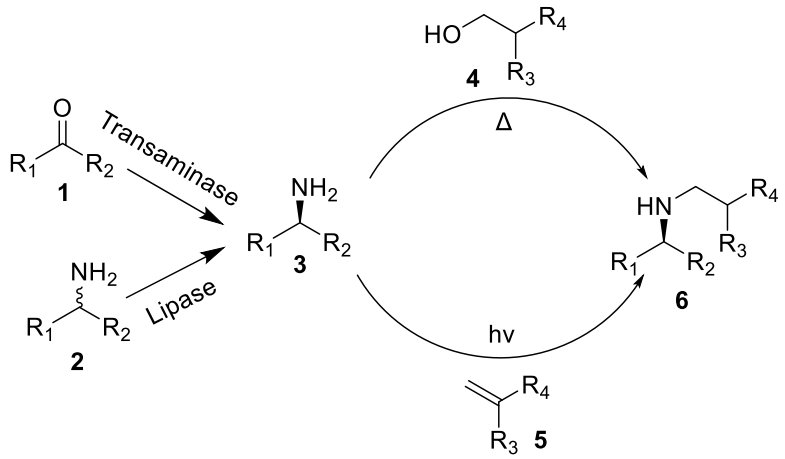

Figure 1: Four alternative routes to enantiomerically enriched secondary amines via chemoenzymatic continuous flow cascades. Two alternative enzymes, transaminase and lipase, can be used to access the same primary amine intermediate, whilst two

chemocatalytic processes can be used to access pharmaceutically-relevant secondary amines.

Two complementary enzymatic routes will be described for the synthesis of two pharmaceutically-relevant chiral primary amines, methylbenzylamine (MBA) and 1-(1-naphthyl)ethylamine (NEA). Reactions were initially screened and optimised under batch conditions and then translated to continuous flow platforms to afford space-time yields of 244 – 471 $gL^{-1}day^{-1}$ at steady state.

The amines generated in the biocatalytic processes then serve as starting materials within two complementary 'clean' *N*-alkylation methods to yield secondary alkylamines in high enantiomeric excess. The two target molecules, cinacalcet and evocalcet, can each be accessed from an enzymatically generated primary amine through application of borrowing hydrogen chemistry with an alcohol or photoredox anti-Markovnikov hydroamination with an alkene (or enecarbamate).

The two biocatalytic steps were then combined with the two *N*-alkylation methods into single continuous flow processes to yield 18 unique secondary amines in isolated yields of 5-73% equating to space-time yields of 34-250 $gL^{-1}day^{-1}$ at steady state.

List of abbreviations

δ	chemical shift
δ_{obs}	observed chemical shift
δ_H	fully protonated chemical shift
δ_L	fully deprotonated chemical shift
λ	wavelength
ν	frequency
Ac	acetyl
ADH	Alcohol dehydrogenase
AmDH	Amine dehydrogenase
Ar	aryl
Bn	benzyl
Boc	*tert*-butyloxycarbonyl
br	broad
Bu	butyl
Bz	benzoyl
b.p.	boiling point
CaLB	*Candida antarctica* lipase B
Cbz	carboxybenzyl
CFL	Compact fluorescent lamp
CLEA	Cross-linked enzyme aggregate
CLEC	Cross-linked enzyme crystals
*c*logP	logarithm of the partition coefficient (fragment-based prediction)
CSI	chemical shift index
CSTR	continuous stirred tank reactor
COSY	correlation spectroscopy
d	doublet
DBU	1,8-diazabicyclo[5.4.0]undec-7-ene

DCM	dichloromethane
DEPT	distortionless enhancement through polarisation transfer
DES	deep eutectic solvent
DIPEA	*N,N*-diisopropylethylamine
DKR	dynamic kinetic resolution
DMAP	4-(dimethylamino)pyridine
DMSO	dimethylsulfoxide
dr	diastereomeric ratio
ee	enantiomeric excess
e.g.	*exempli gratia*
EI	electron impact
ESI	electrospray ionisation
eq	equivalents
er	enantiomeric ratio
Et	ethyl
HAT	Hydrogen atom transfer
HEH	Ethyl Hantzsch ester
HMBC	heteronuclear multiple bond connectivity
HMQC	heteronuclear multiple quantum coherence
HNL	Hydroxy nitrile lyase
HPLC	high performance liquid chromatography
HRMS	high resolution mass spectroscopy
HTS	high-throughput screening
IL	ionic liquid
IR	infrared
IRED	Imine reductase
J	coupling constant
KCN	potassium cyanide

KR	Kinetic resolution
KRED	Ketone reductase
LCMS	liquid chromatography-mass spectrometry
LDA	lithium diisopropylamide
LED	light-emitting diode
logD	logarithm of the distribution coefficient
logP	logarithm of the partition coefficient
logS	logarithm of the solubility
m	meta
Me	methyl
MsAcT	*Mycobacterium smegmatis*
MTBE	methyl *tert*-butyl ether
mw	molecular weight
m.p.	melting point
n	primary
NADH	Nicotinamide adenine dinucleotide (reduced form)
NADPH	Nicotinamide adenine dinucleotide phosphate (reduced form)
n.d.	not determined
NMR	nuclear magnetic resonance
No.	number
nOe	nuclear Overhauser effect
NOESY	nuclear Overhauser effect spectroscopy
o	*ortho*
OD	optical density
p	*para*
p	pentet
PAD	Phenolic acid decarboxylase
PBR	packed-bed reactor

Ph	phenyl
PG	protecting group
pK_a	logarithm of the acid dissociation constant
ppm	parts per million
Pr	propyl
q	quartet
RedAm	Reductive aminase
R_f	retention factor
rt	room temperature
s	singlet
SCRAM	$[Cp^*IrI_2]_2$
SDS-PAGE	sodium dodecyl sulfate–polyacrylamide gel electrophoresis
SET	single electron transfer
SFC	Supercritical fluid chromatography
SLB	sample loading buffer
S_N	nucleophilic substitution
STY	Space-time yield
t	triplet
t	*tert* (tertiary-)
TFA	trifluoroacetyl
TFAA	trifluoroacetic anhydride
THF	tetrahydrofuran
TLC	thin layer chromatography
TRIP	triisopropylbenzene
Ts	*p*-toluenesulfonyl
TSA	*p*-toluenesulfonic acid
UV	ultraviolet
VT	variable temperature

Table of Contents

1 Introduction 1

1.1 Prevalence of chiral amines within pharmaceuticals 1

1.2 Asymmetric reductive amination 2

1.3 Enzymatic asymmetric reductive aminations 5

1.4 Chemoenzymatic synthesis in one-pot batch reactions 7

1.4.1 One-pot, multiple-step bio/chemocatalytic processes 9

1.4.1.1 Integration of biocatalysis with photoredox catalysis 11

1.5 Continuous Flow Chemoenzymatic synthesis 14

1.5.1 Heterogeneous-Heterogeneous Cascades 15

1.5.2 Heterogeneous-Homogeneous Cascades 21

1.5.3 Homogeneous-Homogeneous Cascades 23

1.6 Chapter summary 26

1.7 Project aims and objectives 27

2 Enzymatic access to pharmaceutically relevant chiral amines 30

2.1 Investigation of transaminase-mediated synthesis of chiral amines 31

2.1.1 Overview of transaminase mechanism 32

2.1.2 Transaminase at the industrial scale 34

2.1.3 Examination and optimisation of transaminase catalysed generation of chiral amines from pro-chiral ketones 35

2.1.3.1 Effect of amino donors on the transaminase catalysed generation of chiral amines from pro-chiral ketones 38

2.1.4 Strategies for Enzyme Immobilisation 41

2.1.4.1 Cross-linking 42

2.1.4.2 Encapsulation 44
2.1.4.3 Binding to Supports 46
2.1.4.3.1 Reactive Supports for Covalent Attachment 48
2.1.4.3.2 Reactive Supports for Non-Covalent Attachment 50
2.1.5 Comparison of alternative supports for enzyme immobilisation 52
2.1.5.1.1 Assessing catalyst loading after enzyme immobilization 54
2.1.5.2 Activity retention of enzyme-support complexes 58
2.1.6 Optimisation of *(R)*-selective ATA-436 64
2.1.6.1 Effect of substrate concentration on the transaminase catalysed generation of chiral amines from pro-chiral ketones 65
2.1.6.2 Effect of pH within ATA-436 catalysed reactions 67
2.1.7 pH-based liquid-liquid extraction of amines in continuous flow 68
2.1.8 Homogeneous transaminase reactions in continuous flow 71
2.1.8.1 Homogeneous Transaminase Reactions with in-line separation in continuous flow 73
2.1.9 Immobilised Transaminase Reactions in Continuous Flow 74
2.1.9.1 Reactor set up 75
2.1.9.2 Stability of immobilized transaminase within a PBR in continuous flow 76
2.1.9.3 Reaction Metrics 80
2.2 Examination of lipase-mediated kinetic resolution of racemic amines 81
2.2.1 Screening of potential non-enzymatic acylation of amines 82
2.2.2 Screening of immobilised lipases in batch 83
2.2.3 Lipase-mediated kinetic resolution in continuous flow 85
2.2.3.1 Reactor set up 86
2.2.3.2 Stability of Novozym 435 within a PBR in continuous flow 87
2.2.3.3 Reaction Metrics 90
2.3 Chapter summary 91
3 *N*-alkylation of enzymatically-generated primary amines 93
3.1 Borrowing Hydrogen *N*-Alkylation of MBA and NEA 94

3.1.1 Mechanistic insights of Borrowing Hydrogen *N*-Alkylation 94

3.1.2 Optimising the conditions for borrowing hydrogen reactions in batch 97

3.1.2.1 Effect of base on borrowing hydrogen *N*-alkylation 97

3.1.2.2 Effect of solvent on borrowing hydrogen *N*-alkylation 99

3.1.3 Exemplar targets accessed through borrowing hydrogen reactions .102

3.1.3.1 Use of borrowing hydrogen to access cinacalcet 102

3.1.3.2 Utilisation of borrowing hydrogen to access a key intermediate in the synthesis of evocalcet 105

3.1.4 Compatibility of borrowing hydrogen reactions with the enzymatic product stream(s).....107

3.1.4.1 Ketone compatibility within borrowing hydrogen chemistry 108

3.1.4.2 Amide compatibility within borrowing hydrogen chemistry 109

3.1.5 Reaction profile of batch borrowing hydrogen reactions.....110

3.1.6 Borrowing hydrogen at elevated temperatures with a back pressure regulator (BPR).....111

3.1.7 Borrowing Hydrogen Reactions in Continuous flow 114

3.1.7.1 Reactor set up..... 114

3.1.7.2 Optimised conditions for continuous flow borrowing hydrogen 116

3.2 Anti-Markovnikov Hydroamination *N*-alkylation 118

3.2.1 Mechanistic insights of photoredox hydroaminations 119

3.2.2 Hydroamination Substrate Screening 121

3.2.2.1 Utilisation of photoredox hydroamination to access cinacalcet and analogues 122

3.2.2.2 Utilisation of photoredox hydroamination to access a key intermediate in the synthesis of evocalcet 124

3.2.3 Enhancement of hydroamination reaction rates using photo fReactor units 128

3.2.3.1 Optimisation of anti-Markovnikov hydroamination reactions within fReactor CSTRs 128

3.2.3.2 Optimisation of enecarbamate hydroamination within fReactor CSTRs 130

3.2.4 Compatibility of photoredox hydroamination reactions with the enzymatic product stream 132

3.2.4.1 Ketone compatibility within photoredox hydroamination chemistry . 132

3.2.4.2 Amide compatibility within photoredox hydroamination chemistry .. 133

3.2.4.3 Retention of stereochemical purity within anti-Markovnikov hydroamination reactions 134

3.2.5 Stern-Volmer fluorescence quenching experiments 135

3.3 Chapter summary 139

4 Access to chiral secondary amines through chemoenzymatic cascades within continuous flow 140

4.1 Continuous flow chemoenzymatic cascades with an upstream lipase-mediated kinetic resolution 140

4.1.1 Lipase-mediated kinetic resolution in cascade with a photoredox hydroamination 141

4.1.1.1 Effect of photocatalyst loading in the downstream photoredox hydroamination chemistry 144

4.1.2 Lipase-mediated kinetic resolution cascaded with elevated temperature borrowing hydrogen 146

4.1.2.1 Inhibition of the borrowing hydrogen reaction in the chemoenzymatic continuous flow cascade 148

4.1.2.2 Strategies to overcome catalyst inhibition caused by Novozym leachate 148

4.1.2.2.1 Lipase-mediated kinetic resolution of a secondary amine 149

4.1.2.2.2 Utilisation of a carbon capture column in between reactor zones . 150

4.2 Continuous flow chemoenzymatic cascades with an upstream transaminase reaction 152

4.2.1 Extraction-hydroamination 153

4.2.2 Transaminase-hydroamination cascade 156

4.2.2.1 Ketone substrate scope within transaminase-hydroamination cascade 159

4.3 Chapter summary 161

5 Thesis Conclusion 162

5.1 Future Direction 164

6 Experimental 166

6.1 Chiral HPLC general method 167

6.2 Sequences of ω-transaminases 167

6.3 Expression and purification of recombinant protein 169

6.4 Immobilisation Procedures 170

6.4.1 EziG 170

6.4.2 Purolite 171

6.4.2.1 Epoxy Resins 171

6.4.2.2 Amino Resins 171

6.4.2.3 Adsorption Resins 172

6.4.3 Immobeads 172

6.4.4 Bradford Assay 173

6.5 General Procedures 173

6.5.1 General Procedure A (Batch, Transaminase) 173

6.5.2 General Procedure B (Continuous flow, Transaminase) 173

6.5.3 General Procedure C (Immobilised Transaminase Activity Retention) 174

6.5.4 General Procedure D (High Throughput Transaminase Screen) 174

6.5.5 General Procedure E (Batch, Lipase) 174

6.5.6 General Procedure F (Continuous flow, Lipase) 175

6.5.7 General Procedure G (Batch, Borrowing Hydrogen) 175

6.5.8 General Procedure H (Continuous flow, Borrowing Hydrogen) 175

6.5.9 General Procedure I (Batch, Hydroamination, in Vials) 175

6.5.10 General Procedure J (Batch, Hydroamination (enecarbamates) in Vials) 176

6.5.1 Photo fReactor set up 176

6.5.2 General Procedure K (Batch, Hydroamination, in fReactor) 178

6.5.3 General Procedure L (Continuous flow, Hydroamination) 178

6.5.4 Hydroamination General Workup Procedure 178

6.5.5 General procedure M for the continuous kinetic resolution/photocatalysed hydroamination 179

6.5.6 General procedure N for the continuous transaminase/photocatalysed hydroamination 180

6.5.7 Stern-Volmer Fluorescent Quenching 181

6.6 Characterisation data 181

6.6.1 Biocatalysis 181

6.6.2 Borrowing Hydrogen 193

6.6.3 Photoredox Hydroamination 206

6.6.4 Continuous kinetic resolution/hydroaminations 235

6.6.5 Continuous transaminase/hydroaminations 243

7 Appendix 267

7.1 HPLC Chromatograms 267

Table of FiguresFigure 1: A select example of pharmaceuticals containing α-chiral secondary amines. 1
Figure 2: Transition metal/Bronsted acid cooperative catalysis for asymmetric reductive amination.[25] 3
Figure 3: Organocatalytic reductive aminations employing a hydrogen bonding catalyst and Hantzsch ester.[31].....4
Figure 4: Biocatalytic access to α-chiral secondary amines using imine reductase (IRED) and reductive aminase (RedAm). 5
Figure 5: Specific activity of IRED for different amine coupling partners.[52] 5
Figure 6: Synthesis of chiral secondary amines by AmDH-catalysed asymmetric reductive amines of ketones with organic amines. 6
Figure 7: Dual-enzyme cascade for the borrowing hydrogen amination of alcohols with selected examples highlighted.....7
Figure 8: One-pot, two-step chemoenzymatic synthesis of (A) cinacalcet[79] and (B) the key intermediate of Pralsetinib.[80].....8
Figure 9: Integrated synthesis of α-aryl cycloketones via Pd-catalysed Suzuki cross-coupling and an enzymatic asymmetric hydrogenation.[96].....9
Figure 10: Integration of Buchwald-Hartwig couplings with amine dehydrogenase or imine reductase in one-pot.[86] 10
Figure 11: Chemoenzymatic synthesis of 2-substituted piperidines.[98].....10
Figure 12: Dynamic kinetic resolution (DKR) through the combination of Novozym 435 and photoredox catalysis.[101] 12
Figure 13: Asymmetric 2,2-disubstituted indol-3-one synthesis via one-pot photocatalytic oxidation and lipase-catalysed Mannich-type enolate addition. CFL = compact fluorescent lamp.[102] 12
Figure 14: Photoenzymatic one-pot synthesis of benzothiazoles. [104].....13
Figure 15: One-pot C-H bond oxidation/reduction cascade.[107].....14
Figure 16: Continuous flow dynamic kinetic resolution.....16
Figure 17: Dynamic kinetic resolution of chiral amines by lipase-palladium tandem catalysis.[126].....17
Figure 18: DKR of rac-1-phenylethanol utilising a single PBR containing CaLB and $VOSO_4$ separated by cotton layers.[127].....18
Figure 19: Continuous flow chemoenzymatic synthesis 19
Figure 20: A 2-step chemoenzymatic synthesis of selected cinnamoyl tryptamines in continuous flow.[130] 20
Figure 21: Attempted integration of bio-catalysed resolution and chemo-catalysed N-alkylation.[132].21
Figure 22: Two-step continuous flow synthesis of protected cyanohydrins. [135] 23
Figure 23: Sequential aldol-ADH chemoenzymatic cascade.[140] 25
Figure 24: Tandem aldol-ADH continuous flow cascade.[140] 26
Figure 25: Enzymatic access to α-aryl primary amines, applying transaminase or lipase. 28
Figure 26: Access to N-alkyl α-aryl amines, applying borrowing hydrogen or photoredox hydroamination methodologies.....28
Figure 27: Four alternative routes to enantiomerically enriched secondary amines via chemoenzymatic continuous flow cascades. 29
Figure 28: Enzymatic access to pharmaceutically relevant chiral amines, Ar = phenyl or naphthyl. ...30
Figure 29: Schematic of transaminase catalysed reactions (kinetic resolution and asymmetric synthesis) where at least one of the R groups on each of the amine donor and acceptor must be small (methyl or ethyl). 31
Figure 30: Mechanism of Transaminase Action.....33
Figure 31: Synthesis of Sitagliptin utilising an engineered transaminase, resulting in a reduction in process steps and replacement of a transition metal catalyst from the original chemocatalytic route. 34

Figure 32: Transaminase catalysed conversion of 1-acetonaphthone to 1-(1'-naphthyl)ethylamine. Reactions were performed with purified transaminase at 50 mM ketone with 5 equivalents of isopropylamine, 0.02 mM PLP in 100 mM phosphate buffer. 36
Figure 33: pH optimisation of transaminase catalysed conversion of 1-acetonaphthone to 1-(1'-naphthyl)ethylamine. Reactions were performed with purified transaminase at 30 °C in an aqueous buffer (100 mM K_2PO_4, 0.02 mM PLP) containing 50 mM 1-acetonaphthone and 250 mM $^{i}PrNH_2$ for 24 h. n = 1. Conversions were calculated using standard curves for both 1'-acetonaphthone and NEA. 36
Figure 34: Temperature effects on the conversion of the transaminase reaction. Reactions were performed in an aqueous buffer (100 mM K_2PO_4, 0.02 mM PLP, pH 8) containing 50 mM 1-acetonaphthone and 250 mM $^{i}PrNH_2$ for 24 h. Enantiomeric excess is shown in parentheses; Bm-TA produces the (S)-amine and Hyp-TA produces the (R)-amine. n = 1. Conversions were calculated using standard curves for both 1'-acetonaphthone and NEA. 37
Figure 35: 1,2-diaminopropane as a "smart" amine donor.....39
Figure 36: Effects of different amino donors on the conversion of the transaminase reaction (enantiomeric excess / %). Reactions were performed at 40 °C in an aqueous buffer (100 mM K_2PO_4, 0.02 mM PLP, pH 8) containing 50 mM 1-acetonaphthone and 250 mM amino donor for 24 h. Enantiomeric excess is shown in parentheses; Bm-TA produces the (S)-amine and Hyp-TA produces the (R)-amine. MBA denotes methylbenzylamine. Conversions were calculated using standard curves for both 1'-acetonaphthone and NEA.....40
Figure 37: Formation of cross-linked enzyme aggregates (CLEAs). 43
Figure 38: Formation of encapsulated enzymes in a hydrogel matrix 45
Figure 39: Covalent attachment of enzymes to a support.....47
Figure 40: Immobilisation of enzymes using a Purolite®.....49
Figure 41: His-tagged immobilisation of enzymes. 51
Figure 42: Percentage binding of two enantiocomplementary transaminase on a range of different immobilisation supports. Binding is calculated using the Bradford assay on the supernatant after immobilisation, assuming protein not present in supernatant is bound. 100 % binding equates to 10 wt%. 55
Figure 43: Average binding represented in terms of surface functionality. Hydrophilic, n = 11; hydrophobic, n = 9. EziG3 excluded due to semi-hydrophilic surface.....56
Figure 44: Average binding represented in terms of binding mode. His Tag, n = 3; covalent, n = 6; adsorption, n = 7; ionic, n = 5. 57
Figure 45: Standard conditions used for activity retention assays. Reactions were performed at 40 °C in an aqueous buffer (100 mM K_2PO_4, 0.02 mM PLP, pH 8) containing 50 mM 1-acetonaphthone and 250 mM $^{i}PrNH_2$ for 24 h in a thermomixer at 800 rpm. 58
Figure 46: Activity retention assay for immobilised transaminase from Bacillus megaterium on a range of immobilisation supports, runs 1-3, n = 1. Reactions were performed at 40 °C in an aqueous buffer (100 mM K_2PO_4, 0.02 mM PLP, pH 8) containing 50 mM 1-acetonaphthone and 250 mM $^{i}PrNH_2$ for 24 h in a thermomixer at 800 rpm. 'Protein' refers to a fresh non-immobilised, purified enzyme in solution-phase. Conversions were calculated using standard curves for both 1'-acetonaphthone and NEA. 59
Figure 47: Activity retention assay for immobilised transaminase from Bacillus megaterium on selected immobilisation supports, n = 1. Reactions were performed at 40 °C in an aqueous buffer (100 mM K_2PO_4, 0.02 mM PLP, pH 8) containing 50 mM 1-acetonaphthone and 250 mM $^{i}PrNH_2$ for 24 h in a thermomixer at 800 rpm. 'Protein' refers to a fresh non-immobilised, purified enzyme in solution-phase. Conversions were calculated using standard curves for both 1'-acetonaphthone and NEA.....61
Figure 48: Activity retention assay for immobilised transaminase from Hyphomonas neptunium on a range of immobilisation supports, run 1-3. Reactions were performed at 40 °C in an aqueous buffer (100 mM K_2PO_4, 0.02 mM PLP, pH 8) containing 50 mM 1-acetonaphthone and 250 mM $^{i}PrNH_2$ for 24

h in a thermomixer at 800 rpm. 'Protein' refers to a fresh non-immobilised, purified enzyme in solution-phase. Conversions were calculated using standard curves for both 1'-acetonaphthone and NEA. 62
Figure 49: Activity retention assay for immobilised transaminase from Hyphomonas neptunium on selected immobilisation supports. Reactions were performed at 40 °C in an aqueous buffer (100 mM K_2PO_4, 0.02 mM PLP, pH 8) containing 50 mM 1-acetonaphthone and 250 mM $^{i}PrNH_2$ for 24 h in a thermomixer at 800 rpm. 'Protein' refers to a fresh non-immobilised, purified enzyme in solution-phase. Conversions were calculated using standard curves for both 1'-acetonaphthone and NEA..... 63
Figure 50: Use of ATA-436 within the synthesis of Savolitinib. 64
Figure 51: Effect of substrate concentration on yield of transaminase reaction. Reactions were performed in buffer (100 mM KH_2PO_4, pH 9) containing 500 mM isopropylamine, 1 mM PLP, 10 mg enzyme, ketone with 10% DMSO, n =3. Yields were calculated using standard curves for both 1'-acetonaphthone and NEA. 66
Figure 52: Effect of pH on yield of transaminase reaction. Reactions were performed in buffer (100 mM KH_2PO_4, pH 8-11) containing 500 mM isopropylamine, 1 mM PLP, 10 mg enzyme and 10 mM ketone with 10% DMSO. Yields were calculated using standard curves for both 1'-acetonaphthone and NEA. 67
Figure 53: Theoretical speciation and extraction efficiency curves for selective extraction of MBA vs isopropylamine. Volume ratio organic : aqueous = 50:50. 69
Figure 54: Theoretical speciation and extraction efficiency curves for selective extraction of NEA vs isopropylamine. Volume ratio organic : aqueous = 50:50. 69
Figure 55: Continuous flow transaminase catalysed reaction of 1'-acetonaphthone. Reactions were performed in a buffered solution (10% DMSO, 100 mM KH2PO4, pH 9) containing 1'-acetonaphthone (200 mM), isopropylamine (500 mM), PLP (1 mM) and ATA-436 (2.5 mg mL^{-1}) within fReactor CSTR units with a T_{res} of 60 min. Yields were calculated using standard curves for both 1'-acetonaphthone and NEA. 72
Figure 56: Schematic of homogeneous transaminase reaction with in-line separation in continuous flow. Reactions were performed within a series of fReactor CSTR units, with a 60 min residence time with a buffered solution (10% DMSO, 100 mM KH_2PO_4, pH 9) containing 1'-acetonaphthone (200 mM), isopropylamine (500 mM), PLP (1 mM) and ATA-436 (2.5 gL^{-1}). 73
Figure 57: Photo of membrane of disassembled membrane separator after 2.5h of operation. 74
Figure 58: Continuous PBR set up where (A) is a Harvard Apparatus Model 22 syringe pump (B) a syringe containing 100 mM ketone, 500 mM $^{i}PrNH_2$ and 0.02 mM PLP in a buffered solution (100 mM KH_2PO_4, pH 8) and (C) a PBR containing EziG1-BmTA. 75
Figure 59: Conversion of 1'-acetonaphthone to 1-(1-naphthyl)ethylamine in continuous flow, catalysed by EziG1-BmTA. Reactions were performed at 40 °C in an aqueous buffer (100 mM K_2PO_4, 0.02 mM PLP, pH 8) containing 100 mM 1-acetonaphthone and 500 mM $^{i}PrNH_2$ with a residence time (T_{res}) of 30min. Conversions were calculated using standard curves for both 1'-acetonaphthone and NEA. 77
Figure 60: Conversion of 1'-acetonphenone to 1-phenylethylamine in continuous flow catalysed by EziG1-BmTA. Reactions were performed at 40 °C in an aqueous buffer (100 mM K_2PO_4, 0.02 mM PLP, pH 8) containing 100 mM 1-acetonaphthone and 500 mM $^{i}PrNH_2$ with a residence time (T_{res}) of 30min. Conversions were calculated using standard curves for both 1'-acetophenone and 1-phenylethylamine. 78
Figure 61: Protein concentration in the product stream for the conversion of 1'-acetonphenone to 1-phenylethylamine in continuous flow by EziG1-BmTA. Reactions were performed at 40 °C in an aqueous buffer (100 mM K_2PO_4, 0.02 mM PLP, pH 8) containing 100 mM 1-acetonaphthone and 500 mM $^{i}PrNH_2$ with a residence time (T_{res}) of 30min, n =1. 79
Figure 62: Previously demonstrated kinetic resolution of MBA (0.08 M) in continuous flow, using various acyl donors (0.32 M) at a range of temperatures within toluene. 82

Figure 63: Non-enzymatic acylation screen using NEA within isopropyl acetate. Reaction was performed in isopropyl acetate with 100 mM NEA at reflux (90 °C). *83*
Figure 64: Batch screen results of 6 different immobilised lipase. Reactions were performed at 40 °C in isopropyl acetate containing 100 mM NEA for 24 h in a thermomixer at 800 rpm. Enzymes immobilised on beads are represented with an asterisk, with the remaining immobilised enzymes being powder-based. Conversions were calculated using standard curves for both 130 and 148. ..... *84*
Figure 65: Synthesis of racemic amide products from the corresponding amine. *85*
Figure 66: Continuous PBR set up where (A) is a Harvard Apparatus Model 22 syringe pump (B) a syringe containing 200 mM amine in ^{i}PrOAc and (C) a PBR containing Novozym 435. ..... *86*
Figure 67: Conversion of rac-1-(1-naphthyl)ethylamine to (R)-N-acetyl-1-(1-naphthyl)ethylamine in continuous flow catalysed by Novozym 435. Reactions were performed at 40 °C in isopropyl acetate containing 200 mM rac-amine with a residence time (T_{res}) of 30 min and a PBR volume of 2.61 mL. Conversion was monitored by ^{1}H NMR against an internal standard and ee determined by HPLC. *88*
Figure 68: Conversion of rac-1-phenyl-ethylamine to (R)-N-acetyl-1-phenylethylamine in continuous flow catalysed by Novozym 435. Reactions were performed at 40 °C in isopropyl acetate containing 200 mM rac-amine with a residence time (T_{res}) of 30 min and a PBR volume of 2.61 mL. Conversion was monitored by ^{1}H NMR against an internal standard and ee determined by HPLC. *89*
Figure 69: Summary of enzymatic access of two chiral primary amines. Steady-state conversions within continuous flow reactions are shown. *92*
Figure 70: Target molecules for the two complementary chemocatalytic stages *93*
Figure 71: Equilibria of the dimeric and monomeric species of $[Cp^*IrCl_2]_2$. *95*
Figure 72: Two hydrogen borrowing catalysts synthesised by previous group members.[150, 257] *95*
Figure 73: Noyori-type catalyst, used in the asymmetric transfer hydrogenation of aromatic ketones.[258] *96*
Figure 74: Previously proposed mechanism for the iridium-catalysed N-alkylation of amines with primary and secondary alcohols, using $[Cp^*IrCl_2]_2$, adapted from Fistrup et al.[256] *96*
Figure 75: Effect of base for 4 catalysts for the N-alkylation screening reaction of MBA and 4-bromo benzylalcohol. Reactions were performed in toluene (1.0 M) with MBA, 4-bromo benzylalcohol, 2 mol% Ir and 5 mol% base at reflux. Reactions with catalyst 2 were performed at 80 °C due to constraints of the support resin. Yield was determined by ^{1}H NMR against and internal standard and ee retention was determined by chiral HPLC. *98*
Figure 76: Effect of solvent for 4 catalysts for the N-alkylation screening reaction of MBA and 4-bromo benzylalcohol. Reactions were performed at 1.0 M concentration with MBA, 4-bromo benzylalcohol and 2 mol% Ir at reflux. Reactions with catalyst 2 were performed at 80 °C, due to constraints of the resin. Yield was determined by ^{1}H NMR against and internal standard and ee retention was determined by chiral HPLC. *100*
Figure 77: Borrowing hydrogen reaction of MBA and 4-bromobenzylalcohol in isopropyl acetate (1.0 M). The reaction was performed in the absence of catalyst at reflux for 24 h. *101*
Figure 78: Access to cinacalcet utilising a borrowing hydrogen reaction of NEA and 3-(3-(trifluoromethyl)phenyl)propan-1-ol, with the C-N bond to be formed highlighted in red *102*
Figure 79: Synthesis of 3-(3-(trifluoromethyl)phenyl)propan-1-ol, starting from 3-bromobenzotrifluoride and propargyl alcohol. *103*
Figure 80: Substrate scope for hydrogen borrowing reactions of primary alcohols and α-aryl amines. Reactions were performed at reflux in isopropyl acetate (1.0 M) with 1 mol% $[Cp^*IrCl_2]_2$ for 20h. .. *104*
Figure 81: Mitsubishi Tanabe Pharma synthesis of evocalcet from (R)-NEA and N-Boc pyrroldininol.[274] *105*
Figure 82: Steric bulk positioned adjacent to the basic nitrogen in the second-generation study. *106*
Figure 83: Substrate scope for hydrogen reactions of cyclic, secondary alcohols and α-aryl amines. Reactions were performed at reflux in isopropyl acetate (1.0 M) with 1 mol% $[Cp^*IrCl_2]_2$ for 20h. .. *107*

Figure 84: N-alkylation of NEA with 4-methoxybenzyl alcohol, doped with 1'acetonaphthone. The reaction was performed in isopropyl acetate (1.0 M), with 0.5 equivalents of 1'-acetonaphthone and 1 mol% $[Cp^*IrCl_2]_2$ at reflux for 16 h. 108
Figure 85: N-alkylation of NEA with 4-methoxy benzylalcohol, doped with N-acetyl-1-(1-naphthyl)ethylamine. The reaction was performed in isopropyl acetate (1.0 M), with 1.0 equivalents of N-acetyl-1-(1-naphthyl)ethylamine and 1 mol% $[Cp^*IrCl_2]_2$ at reflux for 16 h. 109
Figure 86: Kinetic study for the borrowing hydrogen reaction of MBA and 4-bromobenzylalcohol. The reaction was performed in isopropyl acetate (1.0 M) with 1 mol% $[Cp^*IrCl_2]_2$ at reflux. Yield was determined from the crude ^1H NMR against an internal standard. 110
Figure 87: Vapour pressure plot for isopropyl acetate, using the Clausius-Clapeyron equation, Equation 6. 112
Figure 88: Effects of elevated temperature of the rate of the borrowing hydrogen reaction of NEA and 4-methoxybenzyl alcohol. Reactions were performed in isopropyl acetate (0.1 M) with 1 mol% $[Cp^*IrCl_2]_2$ within fReactor CSTRs fitted with a BPR. Yield was calculated by ^1H NMR against an internal standard. 113
Figure 89: Continuous borrowing hydrogen set up where (A) is a JASCO PU-980 HPLC pump (B) hydroamination feedstock containing 100 mM alcohol, 100 mM amine and 1 mM $[Cp^*IrCl_2]_2$ in ^{i}PrOAc (C) is a series of fReactor CSTRs, heated by a stirrer hot plate and (D) is a back pressure regulator (BPR). 115
Figure 90: Continuous flow borrowing hydrogen reaction between NEA and 4-bromo benzylalcohol. Reactions were performed in isopropyl acetate (0.1 M), with 1 mol% $[Cp^*IrCl_2]_2$ for a residence time of 1 h and fluid temperature of 140 °C. 116
Figure 91: Borrowing hydrogen reaction between NEA and 4-bromobenzylalcohol in a three-solvent system in batch. The reaction was performed in 50:45:5 isopropyl acetate/toluene/acetonitrile (0.1 M) at reflux for 16 h. 117
Figure 92: Borrowing hydrogen reaction between NEA and 4-bromobenzylalcohol in a three-solvent system in continuous flow. The reaction was performed with a residence time of 1 h and a fluid temperature of 140 °C maintained by a 100 psi BPR. Yield was determined by ^1H NMR against and internal standard. 118
Figure 93: Iridium photocatalysts used in the photoredox hydroaminations. 119
Figure 94: Complete reaction cycle for photoredox hydroamination proposed by Knowles. ET = electron transfer; BET = back-electron transfer; PT = proton transfer; HAT = hydrogen atom transfer, adapted from Qin et al.[294] 120
Figure 95: Alternative mechanistic pathway based on photocatalyst quenching by an enecarbamate.[149, 292] 121
Figure 96: Synthesis of 3-[(3-trifluoromethyl)phenyl]-1-propene from 3-bromobenzotrifluoride and 1.8 equivalents of allylboronic acid pinacol ester. The reaction was performed in THF (0.13 M) with 2 equivalents of CsF, 5 mol% $PdPh_3$ and 10 mol% PPh_3 at reflux for 22 h. 122
Figure 97: Isolated yields of 3 amines reacting with 6 alkenes in anti-Markovnikov hydroamination photoredox reactions. Reactions were performed in dry 1,4-dioxane (0.05 M), with 3 equivalents of alkene, 2 mol% $[Ir(dF(CF_3)ppy)_2(4,4'\text{-}CF_3\text{-}bpy)PF_6$, 50 mol% TRIP thiol and irradiated with a blue LED for 64 h. 123
Figure 98: General reaction conditions for hydroamination photochemical reactions between enecarbamates and primary amines. 124
Figure 99: Synthesis of tert-Butyl 3,4-dihydropyridine-1(2H)-carboxylate in three steps from piperidine (239). 125
Figure 100: Synthesis of N-Boc 2-azetine in two steps from N-Boc 3-hydroxyazetidine. 125
Figure 101: Effect of ring size on conversion within hydroamination photochemical reactions between enecarbamates and primary amines. Reactions were performed in toluene (0.05 M), with 2 mol%

photocatalyst B, 50 mol% TRIP thiol and 5 equivalents of amine, irradiated with a blue LED for 16 h. 126
Figure 102: Side product formation between N-Boc 2-azetine and TRIP thiol. 126
Figure 103: Investigating the cause of side product formation between enecarbamates and TRIP thiol. Reactions were performed in isopropyl acetate (0.05 M), with 1 mol% photocatalyst B, 50 mol% TRIP thiol and irradiated with a blue LED for 16 h. 127
Figure 104: Hydroamination reaction of 4-methoxystyrene with MBA or NEA in the photo fReactor units compared to the same reactions performed in a vial with a 40W Kessil A160WE tuna blue LED. Reactions were performed in dry or degassed solvent (0.05 M), with 3 equivalents of alkene, 2 mol% [Ir(dF(CF$_3$)ppy)$_2$(4,4'-CF$_3$-bpy)PF$_6$ and 50 mol% TRIP thiol. Conversions were determined by ^{1}H NMR against an internal standard.....129
Figure 105: Absorbance spectrum of [Ir(dF(CF$_3$)ppy)$_2$(4,4'-CF$_3$-bpy)PF$_6$.....130
Figure 106: Optimisation of ene-carbamate hydroamination within fReactor CSTRs for the reaction of NEA and N-Boc-2,3-dihydropyrrole. Reactions were performed using 2 mol% (Ir[dF(CF$_3$)ppy]$_2$(dtbpy))PF$_6$ and 50 mol% TRIP thiol. Yields were determined from the crude ^{1}H NMR against an internal standard.....132
Figure 107: Photoredox hydroamination of NEA with 4-methoxystyrene, doped with 1'-acetonaphthone. The reaction was performed in isopropyl acetate (0.05 M), with 0.5 equivalents of 1'-acetonaphthone, 3 equiv. alkene, 2 mol% iridium photocatalyst A, 50 mol% TRIP thiol and irradiated with blue LEDs for 16 h. 133
Figure 108: Photoredox hydroamination of NEA with 4-methoxystyrene, doped with N-acetyl-1-(1-naphthyl)ethylamine. The reaction was performed in isopropyl acetate (0.05 M), with 1.0 equivalents of N-acetyl-1-(1-naphthyl)ethylamine, 3 equiv. alkene, 2 mol% iridium photocatalyst A, 50 mol% TRIP thiol and irradiated with blue LEDs for 16 h. Yields were determined from the crude ^{1}H NMR against an internal standard. 133
Figure 109: Enantiomeric retention within photoredox hydroamination reactions. Reactions were performed in isopropyl acetate (0.1 M), with 3 equivalents of alkene, 2 mol% [Ir(dF(CF$_3$)ppy)$_2$(4,4'-CF$_3$-bpy)PF$_6$ and 50 mol% TRIP thiol and irradiated at 365 nm for 1h. 135
Figure 110: Stern-Volmer fluorescence quenching of catalyst 202 ("F" catalyst). Measurements were performed at 0.42 mM photocatalyst in isopropyl acetate with sequential additions of 20 µL of quencher (360 mM). Photocatalyst was irradiated at 380 nm with the luminescence recorded at 582 nm. 136
Figure 111: Stern-Volmer fluorescence quenching of catalyst 203 ("CF$_3$" catalyst). Measurements were performed at 0.42 mM photocatalyst in isopropyl acetate with sequential additions of 20 µL of quencher (360 mM). Photocatalyst was irradiated at 380 nm with the luminescence at 478 nm. ...137
Figure 112: Comparison of the two iridium photocatalyst for the hydroamination reaction of NEA and N-(tert-butoxycarbonyl)-2,3-dihydropyrrole. Reactions were performed using 2 mol% photocatalyst and 50 mol% TRIP thiol. Yields were determined against an internal standard.....138
Figure 113: Photo of the lipase-hydroamination continuous flow cascade with a) the biocatalytic feedstock b) a PBR containing Novozym 435 inside an aluminium heating block c) a syringe pump containing the hydroamination feedstock d) a series of photo fReactor units with the organic outlet of the PBR and the hydroamination feedstock as inlets and e) an external cooling fan.....142
Figure 114: Chemoenzymatic continuously flow synthesis of chiral secondary amines through a lipase-mediated kinetic resolution, hydroamination cascade. Reactions were performed with 200 mM of rac-amine in isopropyl acetate with a separate feed containing photocatalyst (1 mM) and TRIP thiol (50 mM) with either an alkene (300 mM) or enecarbamate (150 mM) in isopropyl acetate for a total residence time of 90 min. Conversions are determined by ^{1}H NMR against an internal standard from the racemic primary amine (maximum theoretical = 50% following kinetic resolution). 143
*Figure 115: Affect of iridium loading and multipoint injection on the conversion of the lipase-photo chemoenzymatic cascade for the exemplar product (S)-231. *Extra iridium infusion into fReactor 2,*

***Average flow rate used to calculate. Conversions are determined by ^{1}H NMR against an internal standard.* 145
Figure 116: Lipase-mediated kinetic resolution cascade with elevated temperature borrowing hydrogen. Reactions were performed with two stock solutions, the first a 200 mM stock of rac-amine in isopropyl acetate and the second a solution containing 100 mM of alcohol and 2 mM $[Cp^*IrCl_2]_2$ in a 90:10 mixture of toluene/acetonitrile. Resolution was performed at 40 °C with a residence time of 30 min and the borrowing hydrogen performed at a fluid temperature of 140 °C for a residence time of 60 min. A back pressure of 100 psi was applied to the system. Steady state conversion was determined from the crude ^{1}H NMR against an internal standard. 147
Figure 117: Borrowing hydrogen reaction of MBA and 4-bromobenzylalcohol at 0.1 M using isopropyl acetate containing leachate from Novozym 435 as a component in the solvent system. 148
Figure 118: Synthesis of 4-bromobenzyl-(1-phenyl-ethyl)-amine via reductive amination. 149
Figure 119: Attempted lipase-mediated kinetic resolution of 4-bromobenzyl-(1-phenyl-ethyl)-amine. Reactions were performed in isopropyl acetate (0.1 M), with 10 wt% lipase at 40 °C for 16h. 149
Figure 120: Affect of different capture column additives on the borrowing hydrogen reaction of NEA and 4-bromobenzyl alcohol. Reactions were performed at 0.1M with 100 mg of additive stirred with the solvent system for 30 min before addition of reagents and catalysts. The reactions were then refluxed for 16h, filtered through celite and analysed by ^{1}H NMR. 151
Figure 121: Continuous flow extraction coupled with downstream hydroamination. Reactions were performed with, NEA (84 mM), 1'-acetonaphthone (16 mM), PLP (0.02 mM) and isopropylamine (416 mM) in a buffered solution (100 mM KH_2PO_4, pH 10) and a hydroamination feed containing catalyst A (1 mM), TRIP thiol (50 mM) and 4-vinyl anisole (300 mM) in isopropyl acetate. Steady state yield was determined by ^{1}H NMR, in reference to an internal standard. 152
Figure 122: Continuous flow extraction of NEA from a buffered solution (100 mM KH_2PO_4, pH 8) containing isopropylamine (400 mM), NEA (100 mM), 1'-acetonaphthone (50 mM) and PLP (0.02 mM). pH was adjusted using NaOH (0.05 M) at various flow rates. Concentrations were determined against an internal standard for each compound. 154
Figure 123: Continuous flow extraction coupled with downstream hydroamination. Reactions were performed with, NEA (84 mM), 1'-acetonaphthone (16 mM), PLP (0.02 mM) and isopropylamine (416 mM) in a buffered solution (100 mM KH_2PO_4, pH 8). NEA was extracted with 0.05 M NaOH and isopropyl acetate, with a hydroamination feed containing catalyst A (1 mM), TRIP thiol (50 mM) and 4-vinyl anisole (300 mM) in isopropyl acetate. Steady state yield was determined by ^{1}H NMR against an internal standard. 155
Figure 124: Photos of the transaminase-hydroamination continuous flow cascade. A shows the whole set-up with a) the biocatalytic feedstock b) a JASCO PU-980 HPLC pump c) a PBR containing EmTA@EziG^1 inside an aluminium heating block d) a syringe pump containing 0.05 M NaOH e) a Zaiput SEP-10 membrane-based separator, fitted with an OB-900 membane and f) a syringe pump fitted with two syringes; one containing isopropyl acetate and the other containing the hydroamination feedstock. B shows a photo of the hotplate containing g) a fReactor unit with the PBR outlet and NaOH as inlets h) a fReactor unit with the basified solution from g) and isopropyl acetate as inlets and h) a series of three photo fReactor units with the organic outlet of the zaiput and the hydroamination feedstock as inlets. 156
Figure 125: Chemoenzymatic continuous flow synthesis of chiral secondary amines through a transaminase-hydroamination cascade. Reactions were performed with BmTA@EziG^1 and a buffered solution (100 mM KH_2PO_4, pH 8) containing 100 mM ketone, 500 mM isopropylamine and 0.02 mM PLP. Extraction was implemented through basification using NaOH (0.05 M) and isopropyl acetate. A Zaiput membrane separator was used to separate the biphasic mixture and the organic phase fed into a series of CSTR units and irradiated at 365 nm with a separate feed containing photocatalyst (1 mM) and TRIP thiol (50 mM) with either an alkene (300 mM) or enecarbamate (150 mM) in isopropyl

acetate for a total residence time of 90 min. Conversions were determined by ^{1}H NMR against an internal standard. *157*
Figure 126: Batch screen of alternative ketones, with view to expand the scope of the transaminase-hydroamination cascade. Reactions were performed at 40 °C in an aqueous buffer (100 mM K_2PO_4, 0.02 mM PLP) containing 50 mM ketone and 250 mM $^iPrNH_2$ for 24 h. *159*
Figure 127: Expansion of the ketone substrate scope within the transaminase-hydroamination continuous flow cascade. Reactions were performed with BmTA@EziG[1] and a buffered solution (100 mM KH_2PO_4, pH 8) containing 100 mM ketone, 500 mM isopropylamine and 0.02 mM PLP. Extraction was implemented through basification using NaOH (0.05 M) and isopropyl acetate. A Zaiput membrane separator was used to separate the biphasic mixture and the organic phase fed into a series of CSTR units and irradiated at 365 nm with a separate feed containing photocatalyst (1 mM) and TRIP thiol (50 mM) with methylenecyclohexane (300 mM) in isopropyl acetate for a total residence time of 90 min. Conversions were determined by ^{1}H NMR against an internal standard. .. *160*
Figure 128: A summary of products accessed in each chapter. *164*
Figure 129: Arrangement of the photo-flow modules on the individual CSTRs. Here, a complete set of five modules in series are shown. *177*
Figure 130: Schematic of enantioselective chemoenzymatic flow synthesis of secondary amines, employing immobilised lipase and hydroamination photochemistry. *180*
Figure 131: Schematic of enantioselective chemoenzymatic flow synthesis of secondary amines, employing immobilised transaminase and hydroamination photochemistry. *181*

1 Introduction

1.1 Prevalence of chiral amines within pharmaceuticals

Many chiral pharmaceuticals and natural products contain secondary or tertiary amines, often masked as amides.[3] A consequence of this is that α-chiral amines have become one of the most valuable building blocks adopted by synthetic chemists for the syntheses of pharmaceuticals and natural products.[4, 5]

Despite the prevalence of α-chiral secondary amines in active pharmaceutical ingredients (Figure 1) there are relatively few methods for direct chemocatalytic synthesis of *N*-alkylamines either by direct reductive amination[6-10] or through reduction of *N*-alkylketimines[11-14], especially when compared to *N*-aryl or *N*-carbamoyl/acyl derivatives.

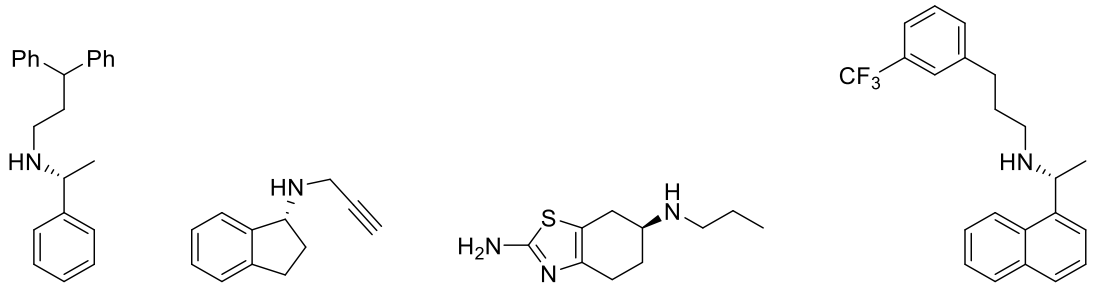

7 fendiline **8** rasagiline **9** pramiprexole **10** cinacalcet

Figure 1: A select example of pharmaceuticals containing α-chiral secondary amines.

The use of biocatalysis has been exploited by synthetic chemists to build molecular complexity as a direct result of the unparalleled specificity that biocatalysts boast.[15] Despite the potential of enzymatic reactions, their applications are often limited by economics.[16] In particular, the use of biocatalysis has traditionally been hindered by the high cost associated with recombinant proteins.[17]

Ensuring the stability and sufficient activity of enzymes under required reaction conditions is an area that still requires significant development.[18] Owing to the discovery and development of new and highly efficient enzymes through directed

evolution, the cost of using recombinant proteins is beginning to decrease.[16] A combination of this reduced cost and new synthetic approaches, including immobilised enzymes in continuous flow, has placed an impetus on improving the overall outlook for biocatalysis.[19] In order to be successfully implemented into an industrial setting, substrate concentration (>50 gL^{-1}) and activity (50-100 $gL^{-1}h^{-1}$) as well as the range of transformations need improving.[20] Each of these can be improved through the use of new to Nature enzymes, exploiting *de novo* design[21] and/or directed evolution.[22]

In this thesis, we describe our work on continuous bio/chemocatalytic sequences for the generation of enantioenriched amines. In order to put this in context, in this section, we will review some methods for chiral amine synthesis using chemo or biocatalysis individually, identifying some of the key limitations. We will then examine recent research into combined bio/chemocatalytic sequences in batch and in continuous flow.

1.2 Asymmetric reductive amination

In 1999, Blaser reported the first example of asymmetric reductive amination for the synthesis of a key intermediate of metolachlor.[23] The one-pot process was carried out with an iridium-based catalyst with a Xyliphos chiral ligand in the presence of hydrogen. Since this initial work, various groups have attempted to expand the field to both increase the scope as well as considering the practical implications of the methodology.[24]

The use of a cooperative catalyst system using an iridium complex and chiral phosphoric acid was employed by Xiao and co-workers to access a range of chiral anilines.[25]

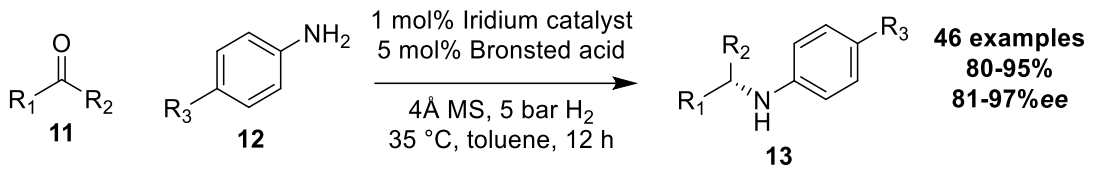

Figure 2: Transition metal/Bronsted acid cooperative catalysis for asymmetric reductive amination.[25]

Through this methodology, 46 chiral anilines were accessed with excellent yields and enantiomeric excess, with the substrate scope including both aliphatic and aromatic ketones as well as a range of substituted anilines. Since this report, the group investigated the use new chiral cyclometalated iridium complexes without a chiral phosphoric acid, however, despite excellent yields, only moderate stereocontrol was possible.[26]

There have been multiple reports building on the work of Xiao, with various metal-based catalysts including iron[27], iridium[28], palladium[29] and nickel[30], all requiring a chiral phosphine ligand and/or chiral Bronsted acid co-catalyst. Due to the difficulty in controlling enantioselectivity with alkyl-alkyl ketones, examples in the literature are extremely rare, with the majority of reports consist of akyl-aryl substrates.

In 2006, MacMillan reported the first organocatalytic asymmetric reductive amination.[31] Taking inspiration from transferase enzymes to selectively activate pyruvate-derived ketimines toward hydride delivery through hydrogen bonding, the replacement of enzymes and cofactors with small organic catalysts and NADH analogues enabled access to a range of α-chiral secondary amines.

After a catalyst screen, an *ortho*-triphenylsilyl variant of the Akiyama-Terada catalyst (16) was found to perform the desired reductive amination at moderate temperatures with diethyl Hantzsch ester (HEH) serving as an NADH analogue.[31]

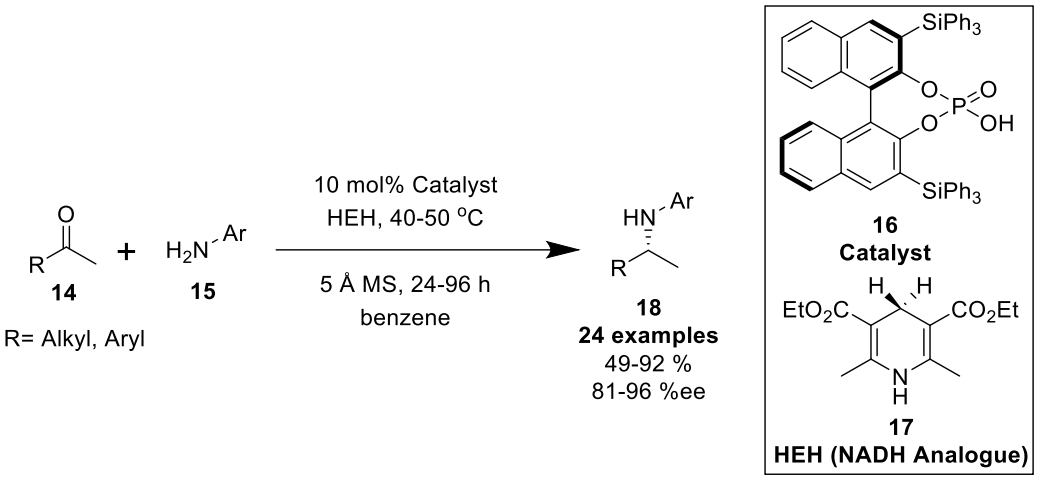

Figure 3: Organocatalytic reductive aminations employing a hydrogen bonding catalyst and Hantzsch ester.[31]

The scope of these reaction conditions was demonstrated through application to complex fragment couplings. A variety of electronically diverse aryl and heteroaromatic amines were coupled with both aryl ketones and bialkyl ketones with good to excellent enantioselectivities and moderate to excellent yields. The scope of the reaction was not reported with aliphatic amines, either because they were unsuccessful in the reaction or were not examined.

Since the initial report of asymmetric organocatalytic reductive aminations, the toolbox of available reducing agents has expanded from Hantzsch esters[31, 32] to include benzothiazoles[33-35], hydrosilanes[36-38] and boranes[39-42].

Whilst organocatalysts have several advantages compared to transition metals, including mild reaction conditions and operational simplicity, there are several challenges that remain within the field.[43] Often, the reactions suffer from low catalytic efficiency, which is compounded by the poor atom economy associated with the processes.[43]

1.3 Enzymatic asymmetric reductive aminations

Biocatalytic access to α-chiral secondary amines can be realised using imine reductase (IRED)[44-47] or reductive aminases (RedAm)[48, 49] often with very high levels of enantioselectivity, Figure 4.

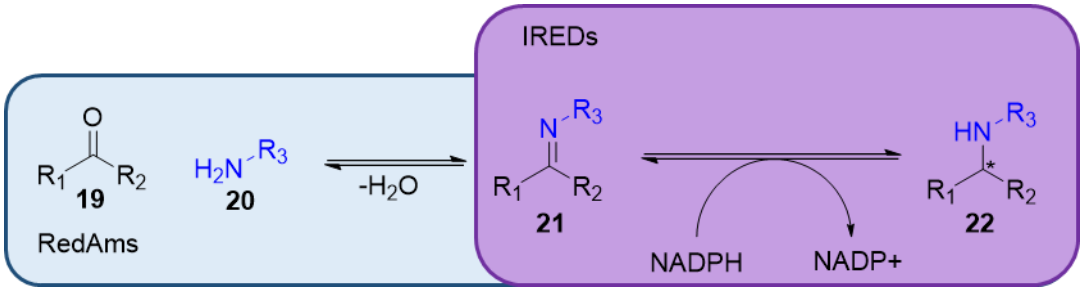

Figure 4: Biocatalytic access to α-chiral secondary amines using imine reductase (IRED) and reductive aminase (RedAm).

Whilst IRED and RedAm transformations allow access to *N*-alkyl chiral secondary amines, often the scope can be limited by the size of the coupling partner.[50-52]

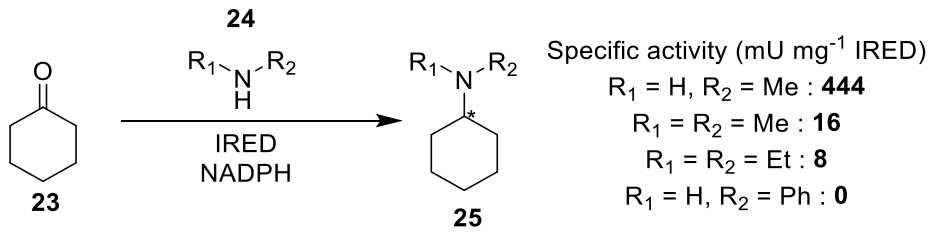

Figure 5: Specific activity of IRED for different amine coupling partners.[52]

Both IREDs and RedAms also suffer from poor activity towards aryl amine substrates, which is a consequence of the nucleophilicity of the substrates and would be difficult to circumvent through enzyme engineering.[44, 45, 53]Moreover, both class of enzyme suffer from instability under process conditions required for industrial application.[53, 54]

Biocatalytic asymmetric reductive amination of ketones can also be performed using amine dehydrogenases (AmDHs).[55, 56 47, 57] Despite the subtle differences in reactivity

between IREDs, RedAms and AmDHs, the catalytic mechanisms are closely related. As NADH-dependent enzymes, the key step within the mechanism involves a hydride transfer from NADH to the *in situ* formed imine intermediate.[57] It was, therefore, theorized that the use of amino donors, other than ammonia, could be applied within AmDH reactions, allowing access to secondary and tertiary amines, Figure 6.[57]

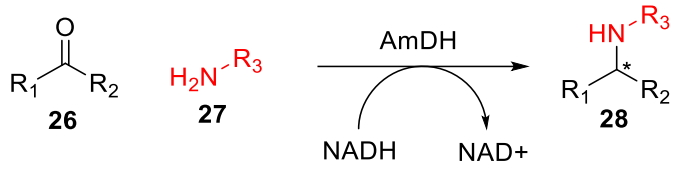

Figure 6: Synthesis of chiral secondary amines by AmDH-catalysed asymmetric reductive amines of ketones with organic amines.

As nicotinamide-dependent enzymes, a cofactor recycling system is essential to implement sub-stoichiometric quantities of the reductant as well as shifting the equilibrium of IRED, RedAm and AmDH catalysed reactions.[58] There are many different routes in which cofactors can be regenerated, including chemical, electrochemical and enzymatic reactions.[59-61] Enzymatic cofactor regeneration is generally the most preferred cofactor regeneration route as a broad range of substrates can be applied within the second enzymatic system to achieve a large thermodynamic driving force.[59, 60] The most commonly employed system to implement recycling of the nicotinamide cofactor is the use of glucose dehydrogenase (GDH)[15] where the two enzymes work in an antagonistic manner to drive the equilibrium and recycle the NAD(P)H cofactor.[60]

Whilst the scope of AmDHs has previously been demonstrated on a range of diverse substrates,[62] it was shown the scope could be further expanded through a dual-enzyme borrowing hydrogen cascade with alcohol dehydrogenases (ADHs).[63, 64] Furthermore, the principles of this type of cascade was exploited by Turner, applying a RedAm in place of AmDH to access secondary amines in high enantiomeric excess.[65]

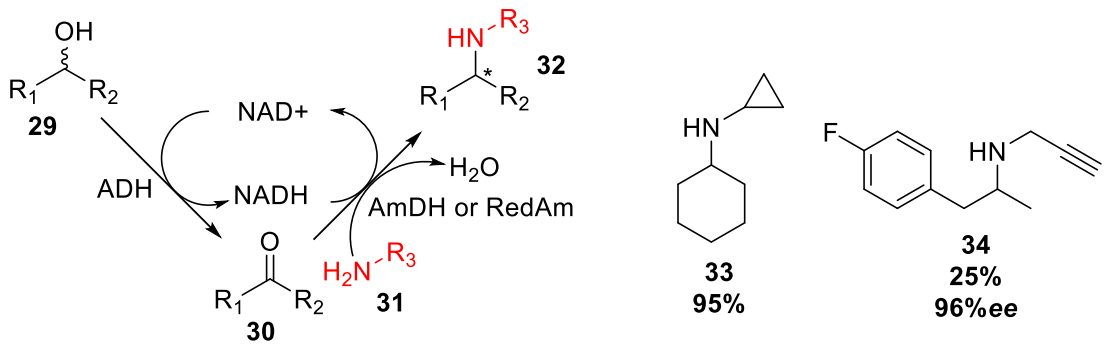

Figure 7: Dual-enzyme cascade for the borrowing hydrogen amination of alcohols with selected examples highlighted.

Despite the application of dual-enzyme cascades, the scope of the transformation(s) can still be limited by the size of the amine coupling partner,[50, 51] and expanding the substrate range available with these enzymes is a key challenge within the field. Moreover, enhancing enzyme stability within organic solvents would allow for higher substrate concentrations and increased productivity of enzymatic systems.[43]

1.4 Chemoenzymatic synthesis in one-pot batch reactions

The integration of continuous flow biocatalysis with chemo-catalysed step(s) has the potential to enable access to complex molecules, including pharmaceutical intermediates due to the synergistic synthetic abilities that cannot be achieved by each catalyst individually.[1, 2, 66, 67] Through the incorporation of the two catalytic systems, synthetic pathways can be dramatically shortened, improving the cost-efficiency and green profile of the route.[68-70]

As a consequence of the rapid advancement of protein engineering, the number of reported chemoenzymatic syntheses of natural products[71-73] and pharmaceuticals[74-78] is becoming increasingly widespread, with notable examples including cinacalcet[79] and the key intermediate in the synthesis of Pralsetinib, Figure 8.[80] Currently, these processes are performed in a step-wise, iterative manner, with few examples being performed in one-pot reactions.

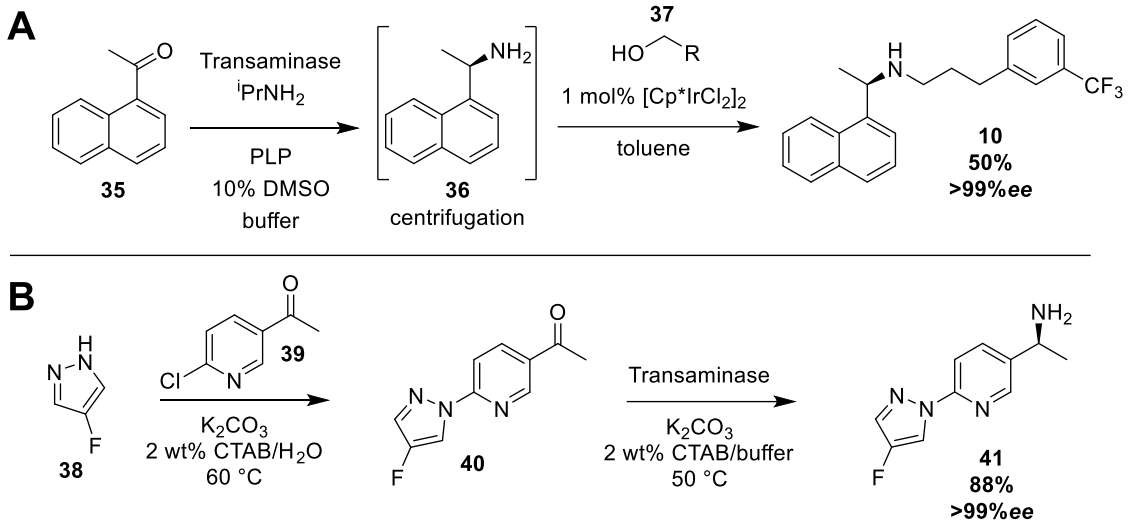

Figure 8: One-pot, two-step chemoenzymatic synthesis of (A) cinacalcet[79] and (B) the key intermediate of Pralsetinib.[80]

As a consequence of the divergent reaction conditions that biocatalysts and chemocatalysts require, performing one-pot chemoenzymatic reactions has proved difficult.[1, 66, 67] Recently, application of deep eutectic solvents (DES)[81, 82], ionic liquids[83-85] or designer surfactants [80, 86-88] have been used to overcome some of these limitations.

Each of these approaches have their limitations. Ionic liquids and DESs can be costly, with the counter ions often having a drastic effect upon reaction rates[89] as well as often having deleterious effects upon biological systems.[90, 91] Moreover, both solvent systems often suffer from chemical instability, with the possibility of reacting with various reaction components,[92, 93] especially under electro- and photochemical conditions.[94]

Use of surfactants allows for compartmentalisation of heterogeneous catalysis and for partitioning of homogeneous catalysts into the micellar phase.[88] It also limits the solvent of the reaction to aqueous solutions, with the water/surfactant ratio having a dramatic effect upon the rate of reaction in the organic phase.[95]

1.4.1 One-pot, multiple-step bio/chemocatalytic processes

Despite the above limitations, there have been some notable recent examples of chemo/biocatalytic sequences, and some examples are discussed here.

Access to chiral α-aryl cycloketones from 2-iodocycloenones, combining a Pd-catalysed cross coupling and an enzymatic asymmetric hydrogenation was recently demonstrated by Jiang and co-workers, Figure 9.[96]

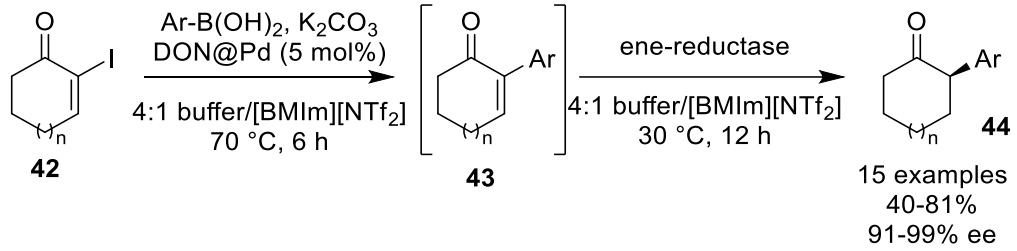

Figure 9: Integrated synthesis of α-aryl cycloketones via Pd-catalysed Suzuki cross-coupling and an enzymatic asymmetric hydrogenation.[96]

Through utilisation of immobilised Pd nanoparticles (DON@Pd), it was possible to implement a two-step, one-pot chemoenzymatic cascade. Despite immobilisation eliminating Pd/ligand inhibition of the ene-reductase, the reaction still needed to be carried out in two steps as residual boronic acid was found to inhibit the enzyme, resulting in a maximum yield of 41%.[96]

Substrates containing electron-donating and electron-withdrawing substituents were equally tolerated, however, the increased steric bulk associated with substrates with ortho-substitution resulted in lower yields. Both 5- and 6-membered cycloeneones were successfully converted to their corresponding products, however, α-phenyl cycloheptenone could not be converted which demonstrates the limited substrate scope of the ene-reductase.[97]

To circumvent the poor activity of AmDHs and IREDs towards aryl amine substrates, in 2020, Turner reported the combination of engineered AmDH or IRED with a palladium-catalysed amination to access a range of anilines, Figure 10.[86]

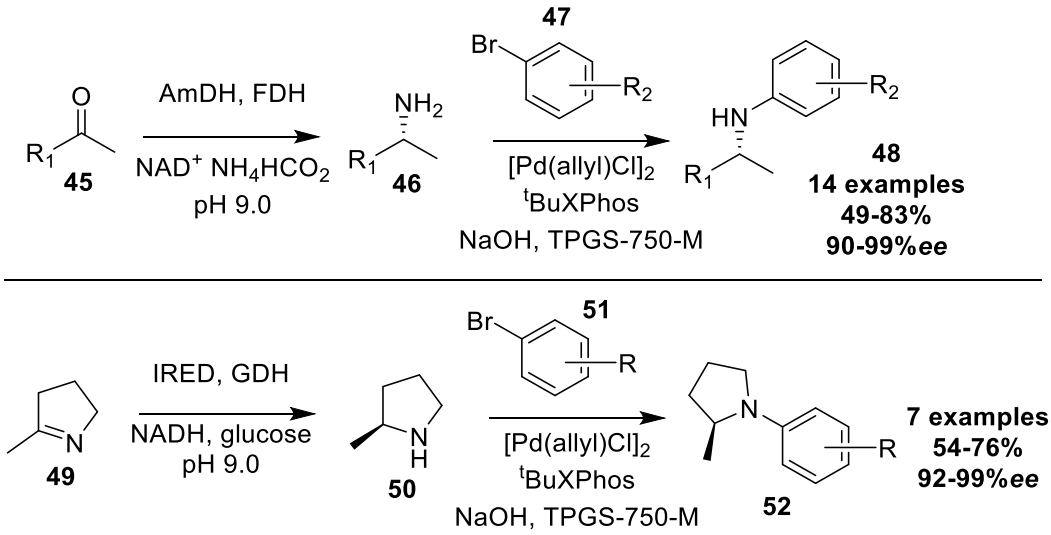

Figure 10: Integration of Buchwald-Hartwig couplings with amine dehydrogenase or imine reductase in one-pot.[86]

The reactions were performed sequentially, with addition of the reagents required for the amination after 48h of reaction. Use of TPGS-750-M, a designer surfactant, enabled the palladium-catalysed coupling to be performed in the crude biocatalytic reaction mixture as it allowed for the low solubility of aryl bromides in water through the surfactant's lipophilic core.

In 2022, O'Reilly reported a hybrid bio-organocatalytic approach for the synthesis of 2-substituted piperidines.[98] Within the cascade, a piperideine intermediate is formed *in situ*, through the transaminase reaction of a diamine, before a proline-catalysed Mannich reaction yields the desired 2- substituted piperidines.[98]

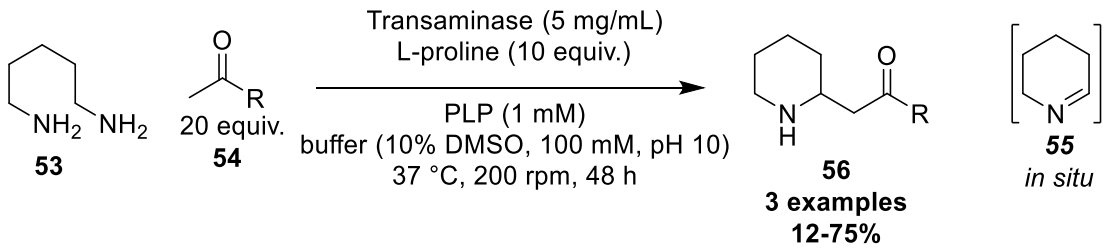

Figure 11: Chemoenzymatic synthesis of 2-substituted piperidines.[98]

The best conversions were obtained with acetone as the ketone partner, with the conversion decreasing as the ketone chain length increased. The lower conversions observed with longer chain length ketone nucleophiles was thought to be caused by competing enamine formation, however, this was not investigated further.

At least two equivalents of the ketone partner are required within the reaction as one is required as the amine acceptor within the transaminase reaction and a second equivalent is required in the subsequent Mannich reaction. On an analytical scale, 20 equivalents of the ketone partner were required within the reaction. This high excess of ketone substate was lowered when performed on a preparative scale, with just four equivalents of acetone required to obtain a 60% isolated yield of the pelletierine product.

1.4.1.1 Integration of biocatalysis with photoredox catalysis

In recent years, photoredox catalysis has emerged as a powerful strategy for the activation of small molecules. With improved energy efficiency through milder reaction conditions, as well as lower waste production, there is a desire to implement photoredox methodologies within industrial applications.[99, 100]

As part of this work will focus on photoredox methodologies and its combination with biocatalysis in continuous flow, this section will review the current literature regarding the integration of biocatalysis with photoredox catalysis.

There have been several reported processes that combine biocatalysis and photoredox methodologies in either a sequential or concurrent manner in batch.[66] The success of combining these two catalytic systems is a consequence of the mild reaction conditions under which photocatalysts can operate, including in aqueous environments.

Through a combination of iridium-catalysed photochemical racemisation with the stereoselectivity of Novozym 435, Yang and coworkers achieved dynamic kinetic resolutions (DKR) of a range of primary amines, Figure 12.[101]

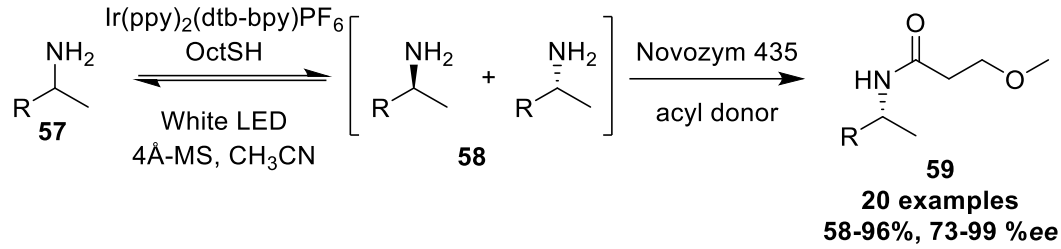

Figure 12: Dynamic kinetic resolution (DKR) through the combination of Novozym 435 and photoredox catalysis.[101]

Within the DKR, it was possible to access 20 amides in good to excellent yields and excellent enantiomeric excess, with the substrate scope including arene-substituted amines, long chain aliphatic amines and a 1,4-diamine.

A lipase enzyme has also been employed in a concurrent photochemical-biocatalytic one-pot cascade for the synthesis of 2,2-disubstituted indol-3-ones, Figure 13.[102] Utilising a ruthenium photocatalyst under aerobic conditions, the first step of the reaction involves a photooxidation of 2-arylindoles to give 2-arylindolones. The indolone intermediates then underwent lipase-catalysed asymmetric Mannich reactions with ketones to yield 2,2-disubstituted indol-3-ones.[102] This exploited the catalytic promiscuity of wheat germ lipase, that had previously been found capable of performing asymmetric Mannich reactions of ketimines.[103]

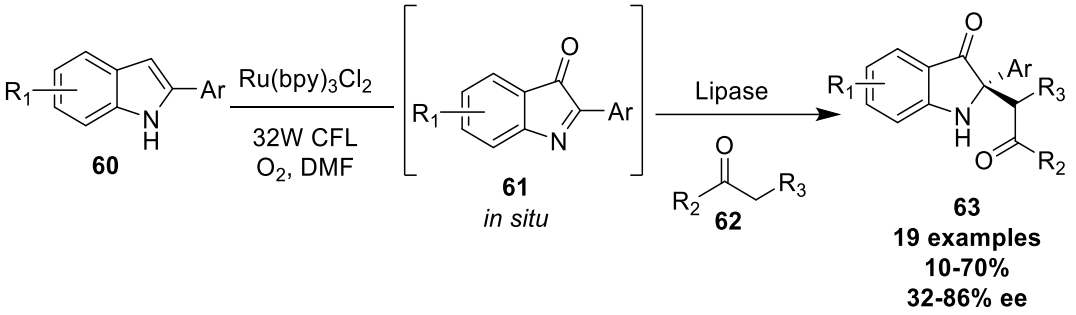

Figure 13: Asymmetric 2,2-disubstituted indol-3-one synthesis via one-pot photocatalytic oxidation and lipase-catalysed Mannich-type enolate addition. CFL = compact fluorescent lamp.[102]

Several control experiments were performed, proving that the reaction could only proceed in the presence of both catalysts, light, and oxygen. Further control experiments concluded that the Asp-His-Ser catalytic triad of the lipase was vital for

this concurrent photoenzymatic reaction. Moreover, it was concluded that the oxidation reaction proceeded by a radical mechanism as only trace amounts of product were identified when the reaction was conducted in the presence of free-radical scavengers. Substrates with *N*-substitution were unsuccessful in the reaction, likely due to the imine intermediate limiting the scope to free indoles.

In a similar manner, a trypsin-catalysed condensation was coupled with a photocatalytic oxidation to access benzothiazoles in a one-pot photoenzymatic manner, Figure 14.[104] The non-native reactivity of the enzyme is consistent with previous reports where trypsin had been applied to a Biginelli reaction[105] as well as an asymmetric aldol reaction.[106]

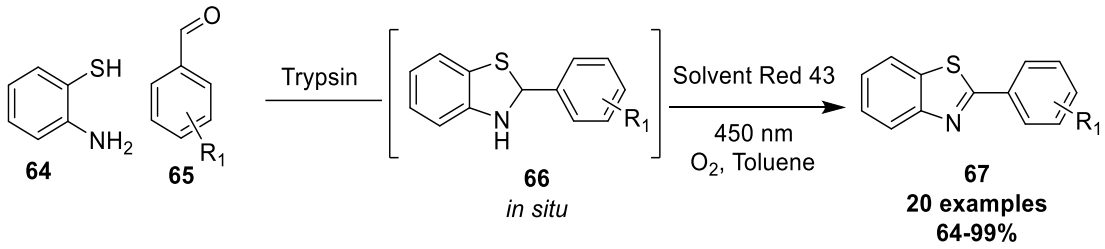

Figure 14: Photoenzymatic one-pot synthesis of benzothiazoles. [104]

Control experiments demonstrated that no 2,3-dihydrobenzothiazole was formed in the absence of enzyme, with trypsin identified as the best enzyme; but no conversion to the oxidised product was observed in the presence of enzyme, which required the photocatalytic step.

After screening photocatalysts (both in presence and absence of trypsin), as well as wavelength and solvent, a range of benzaldehydes (and 2-thiophenecarboxaldehyde) were then applied to the one-pot photoenzymatic reaction.

Within another example of photo-enzymatic one-pot synthesis, photocatalytic oxidation of benzylic C–H bonds was coupled to an asymmetric ketone reductase (KRED) catalysed reduction, Figure 15.[107] The reactions were performed in a one-pot, two-step cascade due to the incompatibility of isopropanol with the photocatalytic oxidation. Despite this incompatibility, all other components of the reaction could be

added from the beginning of the reaction without interfering with the formation of the keto-intermediates.

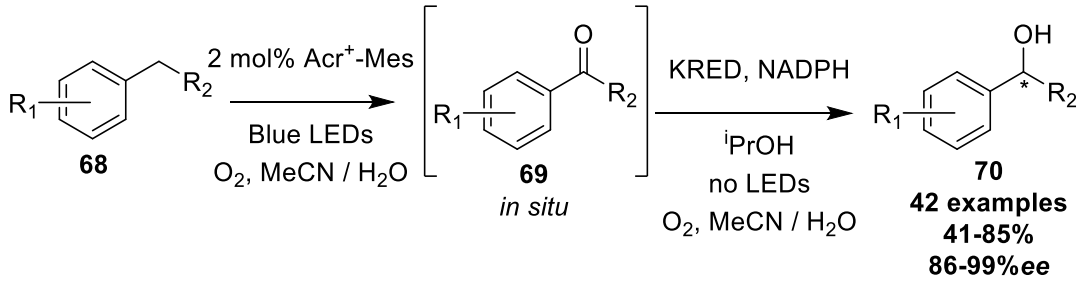

Figure 15: One-pot C-H bond oxidation/reduction cascade.[107]

The reaction was performed on a range of benzylic substrates, accessing aryl-alkyl alcohols, diarylmethanols, γ and δ-lactones, α-hydroxy esters and 1,2-amino alcohols, with moderate to excellent yields and good to excellent enantioselectivities.[107] Moreover, the one-pot photo-enzymatic process was successfully performed on a 5g scale for two substrates with excellent yields (77-83%) and enantioselectivity (99%).

1.5 Continuous Flow Chemoenzymatic synthesis

Traditionally, multi-step reaction sequences are performed in a batch-wise, iterative manner.[108] Not only is this time-consuming, it is also extremely wasteful as it often requires the isolation and purification of each intermediate.[109-112] Consequently, there are considerable environmental, economic and efficiency-based driving forces for implementing cascade reactions in continuous flow.[113-115] Furthermore, cascading a reaction can be used to drive unfavourable equilibria, whilst also obviating the need for the isolation and purification of intermediates.[108, 116, 117]

Through continuous flow cascade reactions, it is possible to use substrate channelling to drive a reaction.[117] The substrate channelling effect, where the direct transfer of a product as a substrate in a subsequent reaction, can overcome diffusion limitations that are often observed in heterogeneously catalysed reactions resulting in increased reaction rates and shorter cycle times. These advantages are further enhanced by

the potential of continuous flow cascade reactions to offer synthetic routes with fewer unit operations, lower reactor volumes and less waste generation.[118]

Significant challenges associated with chemo-enzymatic cascade reactions are the mismatching of the reaction conditions or catalyst inhibition caused by reagents or products from a previous step.[119, 120] These issues can be alleviated through telescoping, where each stage of the reaction takes place in a different reaction zone.[121] This allows for sequential optimisation of each reaction zone as biocatalysis is typically performed in aqueous, mild conditions compared to elevated conditions in organic solvents that chemocatalysis is usually performed. In addition, utilisation of immobilised enzymes can vastly enhance the synergy of bio- and chemo-catalysis in a cascade, especially when compartmentalisation is required.[118, 122]

Telescoping alone is not sufficient to prevent cross-inhibition between sequential reactions[119], placing emphasis on efficient separation strategies. The integration of sequential reactions and separations results in processes becoming more streamlined, efficient and, therefore, inherently "green".[123]

The literature surrounding chemoenzymatic synthesis in continuous flow is extremely limited, highlighting the complexity of the field.[2] The current literature can be grouped by the reactor configurations and/or catalyst homogeneity and will be discussed in the next section.

1.5.1 Heterogeneous-Heterogeneous Cascades

In 2019, Falus and coworkers reported the first continuous flow dynamic kinetic resolution through the combination of an enzyme with a catalytic racemisation.[124] The enantioselective amidation of a racemic mixture of *N*-Boc-phenylalanine ethyl thioester was catalysed using subtilisin A, to selectively generate *(S)*-*N*-Boc-phenylalanine benzylamide from benzylamine.

Entrapment, cross-linked enzyme crystals (CLECs) and cross-linked enzyme aggregates (CLEAs) were all methods of immobilisation that had previously been

used to immobilise subtilisin A. Each of these immobilisation methods were considered sub-optimal for continuous flow operation due to low specific activities as well as the propensity to clog. Instead, the group used surface modified silica gels to adsorb the enzyme, which has greater compatibility with continuous flow, but can often result in leaching.[125] The optimal support, an ethyl grafted macroporous silica gel, was identified after the screening of 24 differently modified silica gels.

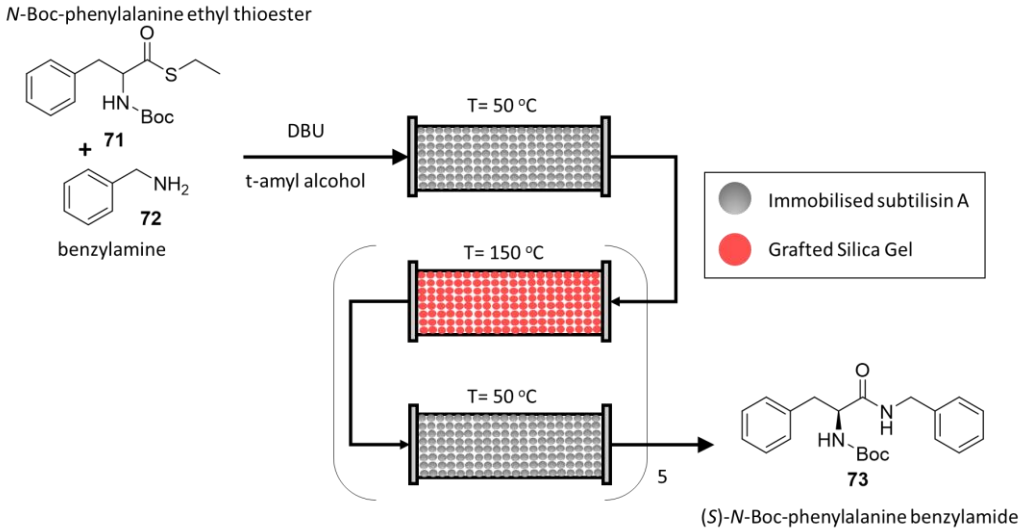

Figure 16: Continuous flow dynamic kinetic resolution of (S)-N-Boc-phenylalanine benzylamide using immobilised subtilisin A.[124]

In order to achieve their dynamic kinetic resolution (DKR) alternating packed-bed columns containing either immobilised subtilisin A (to perform the kinetic resolution) or ethyl grafted macroporous silica gel for racemisation were required. A total of eleven columns were required (six containing immobilised subtilisin A and five containing ethyl grafted macroporous silica gel), with compartmentalisation allowing different and optimum temperatures to be used for each zone, Figure 16. Under optimum conditions, *(S)-N*-Boc-phenylalanine benzylamide was produced in excellent yield (79%) and enantiomeric excess (98%), approaching the limit of kinetic control.

Farkas and co-workers recently described a heterogeneous-heterogeneous continuous flow system for the DKR of racemic amines applying palladium catalysed

hydrogen transfer catalysis as the mode of racemisation.[126] As the two heterogeneous catalysts were found to operate efficiently within similar conditions, the integration of the two catalysts into one PBR drastically reduced the number of PBR units required to implement a DKR.[2]

In contrast to the report of Falus and coworkers that utilised eleven PBRs, Figure 16,[124] only two PBRs were required to implement the DKR. The first PBR in series contained a sol-gel immobilised *Candida antarctica* lipase B (CaLB) that then feeds a resolved mixture into the second PBR containing a mix of palladium immobilised on 3-aminopropyl-functionalized silica and the immobilised lipase.

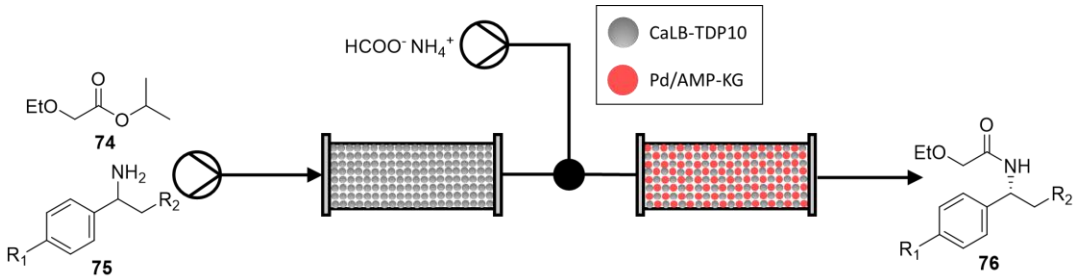

Figure 17: Dynamic kinetic resolution of chiral amines by lipase-palladium tandem catalysis.[126]

A range of benzylic amines were transformed with good to excellent conversions (62-99%) and excellent enantioselectivity (>99%). For some of the bulkier substrates, two PBRs containing lipase were required ahead of the mixed PBR to achieve satisfactory conversions. Moreover, the process was found to be incompatible with substrates that contain functional groups that are reducible under transfer hydrogenation conditions.

A 48 h run showed no major decrease in productivity, demonstrating the operational stability of the system, with a space-time yield (STY) of 103 $kgm^{-3}day^{-1}$ and an *ee* >99.8%.

In an attempt to circumnavigate the unit number dependency of PBR cascades, de Souza and co-workers applied a single PBR containing CaLB and $VOSO_4$ for the DKR of 1-phenylethanol.[127] The incompatibility of the two catalysts, that prevents their

use together in batch,[128] was overcome using thin cotton layers between the layers of lipase and $VOSO_4$, Figure 18.

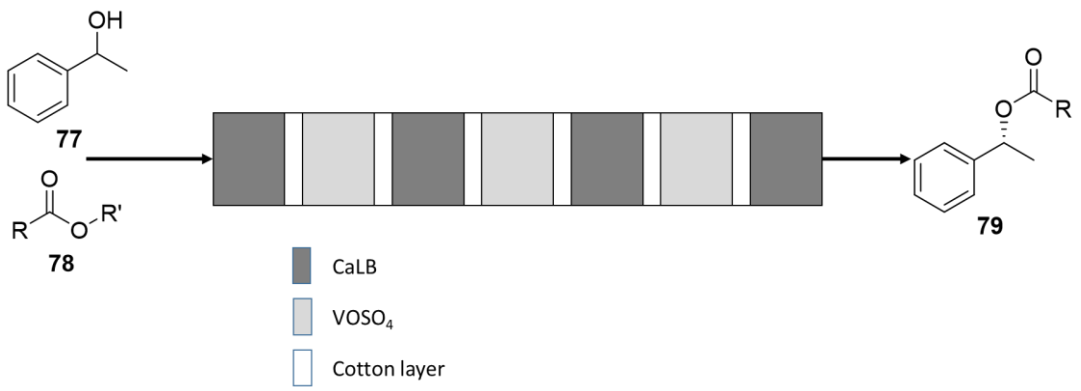

Figure 18: DKR of rac-1-phenylethanol utilising a single PBR containing CaLB and $VOSO_4$ separated by cotton layers.[127]

Through the translation to continuous flow, it was possible to increase the concentration of the reaction to 0.1M, almost ten times that of the previously performed batch reaction (0.0127 M).[128] Moreover, the design of the PBR in this manner allowed for 4 kinetic resolution and 3 racemisation alternating sections within the PBR, resulting in conversions of up to 93.8% and >99%*ee*.

A chemoenzymatic continuous flow synthesis recently reported by Grabner and coworkers utilised DES's for the synthesis of *(E)*-4-hydroxystilbene, Figure 19.[129] The use of DES's minimised compatibility issues as they increased the substrate solubility, whilst also maintaining high enzyme stability and activity. The first step of their synthesis utilised phenolic acid decarboxylase (PAD) for an enzymatic decarboxylation of *para*-coumaric acid.

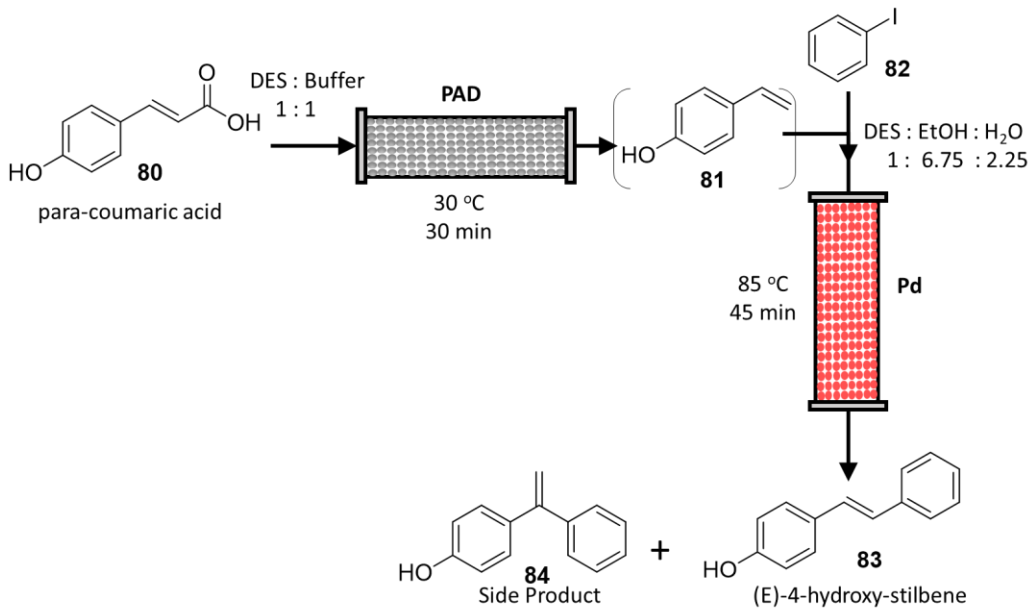

Figure 19: Continuous flow chemoenzymatic synthesisof (E)-4-hydroxy-stilbene using DES's.

The second step, a Heck cross-coupling with iodobenzene, was catalysed by a Pd-substituted Ce-Sn-oxide. The two catalysts (PAD and Pd) were compartmentalised into different PBRs, allowing them to operate at optimal reaction temperatures, 30 °C and 85 °C respectively, as well as allowing for different solvent compositions in each step. Compartmentalisation of the reaction also supressed side product formation caused by polymerisation of the 4-ethenylphenol intermediate as isolation was not required.

Despite compartmentalisation, leaching from the PAD remained an issue as deposited protein clogged the pre-heating tube before the Pd-packed reactor, increasing the formation of the homo-coupled product.

The majority of reports to date involve an upstream biocatalytic stage feeding into a downstream chemocatalytic reaction. In 2021, Padrosa and Contente reported a 2-step chemoenzymatic synthesis of selected cinnamoyl tryptamines in continuous flow, through the utilisation of immobilised $Pd(OAc)_2$ and an immobilised acyl transferase.[130] Cinnamoyl tryptamines were accessed from cinnamic acids through a palladium catalysed transvinylation and an enzymatic *N*-acylation in a sustainable

and cost-effective manner in continuous flow, Figure 20. Performing the reaction in flow, using immobilised palladium not only negated a filtration that is required to remove the transition metal in batch, but it also increased the yields of the reaction from 40-45% after 24h to 70-75% with a residence time of 30 min.[130]

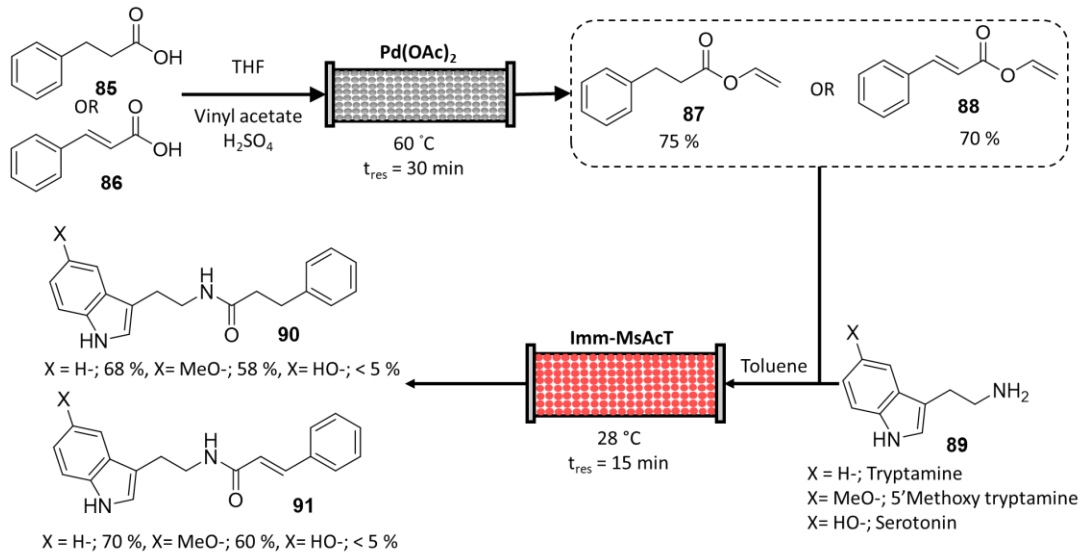

Figure 20: A 2-step chemoenzymatic synthesis of selected cinnamoyl tryptamines in continuous flow.[130]

The stability of the acyl transferase from *Mycobacterium smegmatis* (MsAcT) was enhanced through immobilisation onto glyoxyl-agarose beads, with high recovery of enzyme activity (73%) at a low loading (1 mg/g_{resin}). This enabled the enzymatic reaction to be carried out in organic solvents,[131] which was of great benefit, as the poor water solubility of the vinyl cinnamates, even after the addition of DMSO cosolvent, prohibited the enzymatic reaction from being performed within aqueous buffers, resulting in the immobilised MsAcT reaction carried out in toluene.

The yields of the enzymatic reaction were enhanced and reaction time drastically reduced by moving from batch (25-35%, 24 h) to flow (58-70%, t_{res} = 15 min) with the aid of enzyme immobilisation. The bioreactor stability was tested through a continuous 24 h run, yielding 2.33 g of pure product at a catalyst productivity of 5.33 mmol/mg.[130]

Whilst both stages of synthesis were performed in flow, isolation of the vinyl cinnamates through an ion exchange resin and column chromatography was required in between the two steps. The requirement for purification in between the two flow reactions highlights the difficulty of combining transition metal catalysts and biocatalysts in continuous flow.

1.5.2 Heterogeneous-Homogeneous Cascades

The complexity of integrating chemocatalysts and biocatalysts in one continuous system was further highlighted within a PhD thesis from the Blacker group at the University of Leeds.[132] The group combined Novozym 435 with a homogenous amine alkylation catalyst, $[IrCp^*I_2]_2$ (SCRAM),[133] within a single continuous flow system with the aim of preparing enantiomerically enriched *N*-alkylated MBAs, Figure 21.

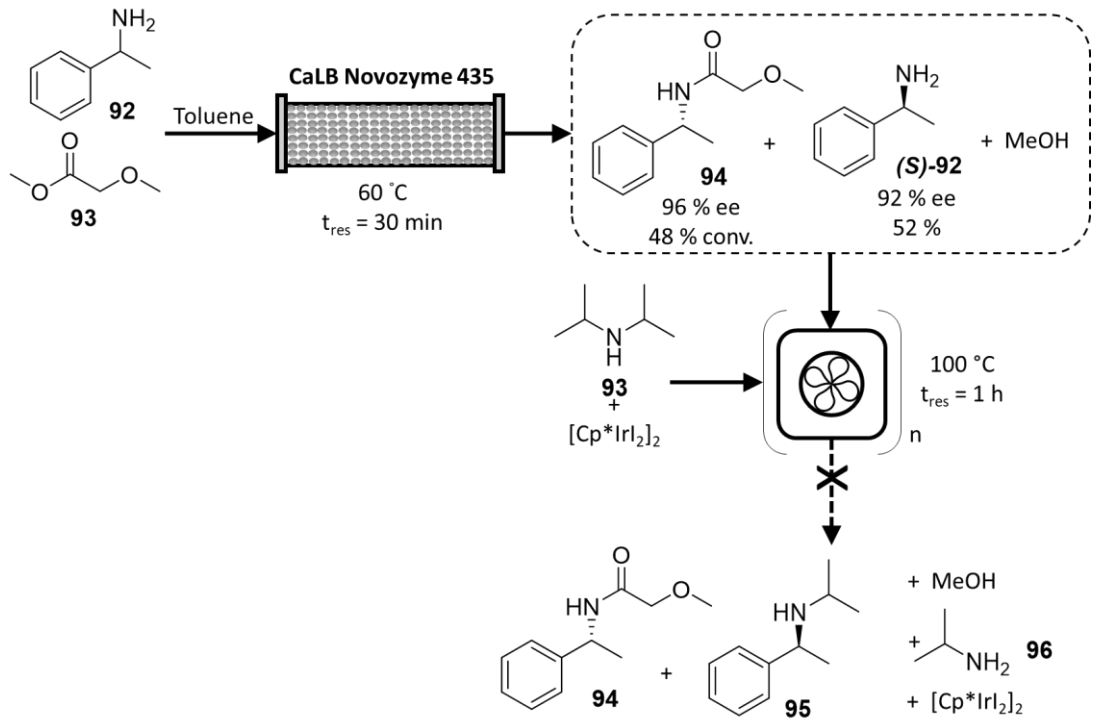

Figure 21: Attempted integration of bio-catalysed resolution and chemo-catalysed N-alkylation.[132]

Novozym 435 was used within a PBR to resolve *rac*-MBA through the selective acylation of the *(S)*-enantiomer using methyl methoxyacetate as the acyl donor in toluene at 60 °C. A 48% conversion to the *(S)*-amide was observed at steady state

with a 30 min residence time, resulting in an enantiomeric excess of 96 %. The unreacted *(R)*-MBA had separately been shown to react with the diisopropylamine in batch with the SCRAM catalyst, with a 97% conversion observed after 1 h at 150 °C, with minimal racemisation. When this reaction was carried out in a CSTR with a t_{res} of 1 h, only 33% conversion was observed (95% *ee*). This low conversion was put down to a lower catalyst loading within the reaction as some solid was observed within the reaction stock solution and was enhanced by increasing the catalyst loading in the stock solution.[132]

To check the compatibility of the two steps, the components of the *N*-alkylation reaction were added to the stream of the enzymatic reaction to ensure that no inhibition would occur if the *N*-alkylation reaction components were recirculated through the PBR. No inhibition was observed as the same level of conversion was reached. In addition, it demonstrated that the *N*-alkylation would not work at the lower temperature of 60 °C, emphasising the need for two separately heated reactors.

To check the compatibility of the enzymatic product steam within the downstream borrowing hydrogen reaction, methyl methoxyacetate and the *(S)*-amide were added to the alkylation reaction, which resulted in an enhancement of the conversion from 33% to 73%. This increase in reactivity was attributed to a favourable coordination of the ester to the SCRAM catalyst. Importantly, it was assumed that as the enzyme was immobilised it would not interfere with the downstream *N*-alkylation and was consequently omitted from the inhibition studies.

Once the two systems were brought together, it was found that the enzymatically catalysed resolution gave a 42% conversion, but the second step only produced a 4% yield of the *N*-alkylated product. With the only difference between the inhibition studies and the combined system was the presence of Novozym 435, a leachate from the immobilised enzyme was proposed to be poisoning the SCRAM catalyst,

however, it is not currently fully understood what part of the immobilised enzyme is causing the inhibition.[132]

1.5.3 Homogeneous-Homogeneous Cascades

One of the main hindrances to chemoenzymatic synthesis in flow can be the divergent reaction conditions of each catalyst, highlighted by the combined efforts of Romano and Tamborini (see 1.5.2).[134] The use of phase-switching separations can potentially address this problem and has been investigated by several groups.

In 2015, Delville *et al.* utilised a liquid-liquid separator, to allow the first reported two step chemoenzymatic cascade with incompatible reaction conditions, Figure 22.[135]

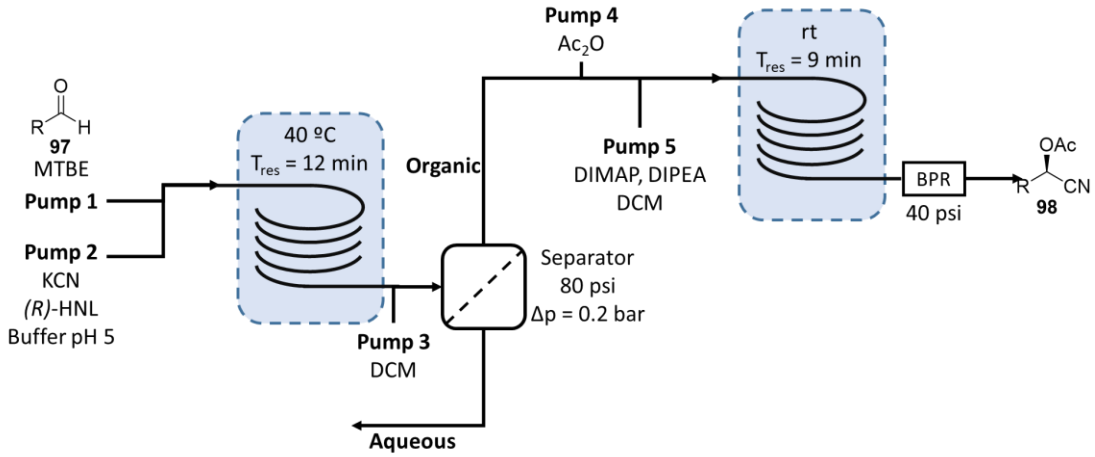

Figure 22: Two-step continuous flow synthesis of protected cyanohydrins. [135]

Each reaction step was optimised separately, utilising previously defined flow conditions.[136, 137] The first step involved the chemoenzymatic formation of cyanohydrins, involving an *(R)*-selective hydroxynitrile lyase (HNL) and potassium cyanide (KCN) in a biphasic reaction mixture, in a 5:1 ratio of pH 5 buffer to methyl *tert*-butyl ether (MTBE).[135] Upon increasing the residence time from 5 to 12 min and heating the reactor (40 °C), the conversion was increased from 57 to 83 %.

A commercially available liquid-liquid separator[138] allowed for the integration of the downstream protection step. Dichloromethane (DCM) was required in the downstream protection step due to solubility complications and efficient separation

was achieved with a phase ratio of 4:1 DCM:biphasic mixture, with a pressure differential of 0.2 bar required to prevent clogging caused by crude enzyme lysate.

Despite the removal of the aqueous buffer by the membrane separator, titration experiments found that the MTBE in the organic phase showed a water concentration of 460 mM, the presence of which reduced the yield of the protection step to 79% from a 90% yield obtained when dry MTBE was used.[135] It was also essential for Ac_2O to be added to the product stream from the first stage before the addition of base, to prevent racemisation. Despite this, some racemisation was observed when the reaction was performed at 50 °C with DIPEA as a base. Upon cooling the reaction temperature to 21 °C and the addition of 10% DMAP the enantioselectivity of the reaction was increased to 98%, with an isolated yield of 64%.[135]

The two-step process, whilst not using a transition metal, demonstrates that it is possible to perform sequential reactions with incompatible conditions within a flow system, with the aid of *in-line* separation. It also highlights one of the safety benefits of flow chemistry, the safe handling of *in situ* generated and toxic HCN formed in the enzyme-catalysed addition to aldehydes.

After successfully demonstrating a one-pot generation of 1,3-diols with *d.r.* up to >25:1 and 99%*ee* utilising an asymmetric aldol catalyst and alcohol dehydrogenase (ADH),[139] Groger and coworkers transferred the chemoenzymatic cascade into flow to access all four stereoisomers of the 1,3-diol product.[140] Having previously performed the same reaction in both sequential and tandem batch modes, direct comparison of the sequential (Figure 23) and tandem continuous flow set ups was possible (Figure 24).

Within a sequential, two-step flow process, the aldol reaction could be performed under optimal conditions, with conditions adjusted through a third inlet after the first reaction zone, Figure 23. Dilution (1:20) was required in between reaction zones from an initial concentration of 500 mM due to the biocatalyst being unstable in high

substrate concentrations. This dilution also ensured that the aldol reaction didn't proceed outside of the first reactor.

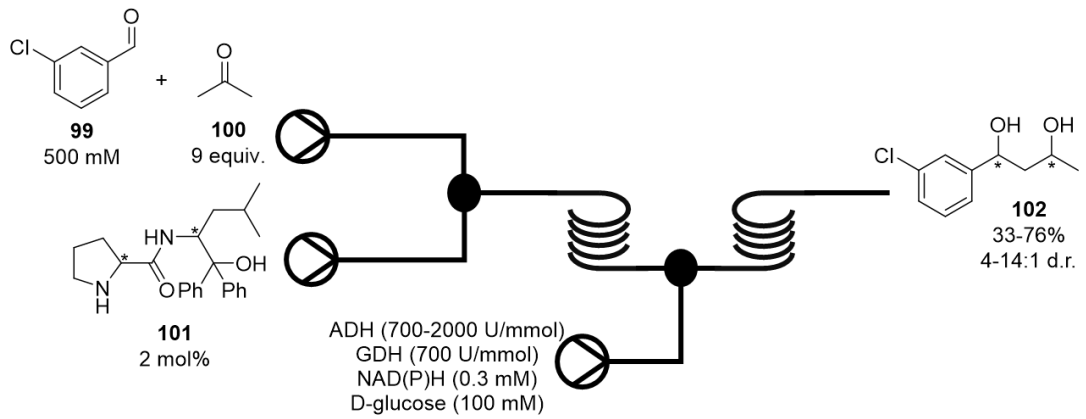

Figure 23: Sequential aldol-ADH chemoenzymatic cascade.[140]

The desired 1,3-diol product was accessed in 33-76% yield with a diastereomeric ratio ranging from 4:1 to 14:1. From the mass balance of the reaction, the differences in productivity of the four stereoisomers is a consequence of the enzymatic reaction. Productivity of the biocatalytic reaction was further limited by the concentration of biocatalyst within the reaction as precipitation was observed, leading to clogging within the continuous reactor configuration.

The "tandem cascade" approach combined both reactions into a single reaction zone, Figure 24. Reagents were required to be separated into three feed solutions, to prevent any reactions occurring before entering the reactor.

Combination of the two steps into a single reaction zone required compromise on substrate and isopropanol concentration. This limited the tandem set-up to just the *(R)*-selective ADH as the *(S)*-selective ADH was not stable in the high concentration of acetone required in the reaction.

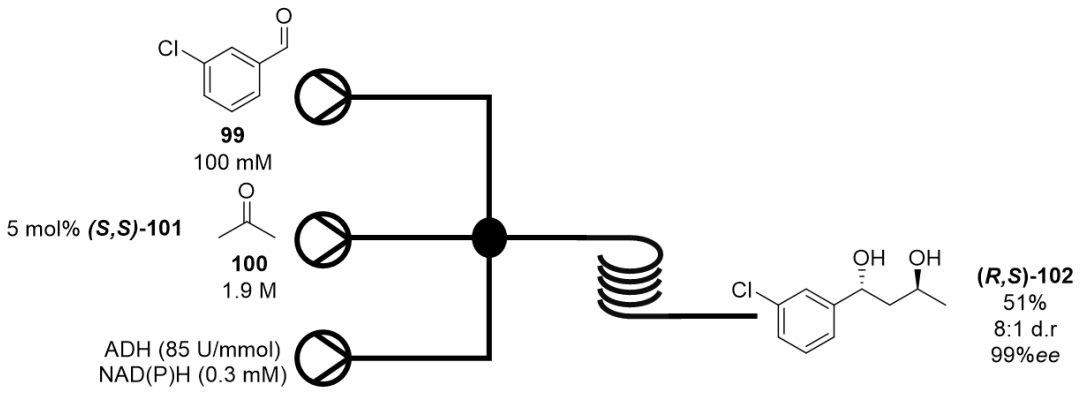

Figure 24: Tandem aldol-ADH continuous flow cascade.[140]

Reactions were performed at 100 mM substrate concentration in a buffered solution containing 14 v% isopropanol and 14 v% acetone, with a 2h residence time. Through this process, the *(1R,3S)*-1,3-diol product was accessed in 51% yield with >99%*ee*. Within the tandem set up, significant formation of 3-chlorobenzyl alcohol as a side product was observed due to competition of ADH reduction of the starting material with the organocatalytic aldol reaction.

Overall, both continuous flow cascades resulted in an increase in productivity with respect to the corresponding batch reaction. The sequential flow reaction provided the greatest productivity of 182 µmol h^{-1} compared to 153 µmol h^{-1} for the tandem flow reaction, in part due to the shorter residence time of 2h compared to 2.5h.

1.6 Chapter summary

Whilst telescoping offers the possibility of solvent switching, it often leads to dilute reaction solutions, with prohibitively slow reaction rates. Moreover, the solubility of both the reactants and products for each reaction in the sequence needs to be considered, in order to optimise the process.[119] Ultimately, the low substrate loadings limits the scalability of cascade systems.[120]

In order to expand the utility of telescoped reactions within flow systems, there is a need for the integration of solution-based work-ups and their subsequent phase separations.[108] Currently, there are only a limited number of reported examples of

tandem work up and separations in continuous flow.[123, 141-144] This is mainly a consequence of the use of heterogenous catalysts that negate the need for work up and/or purification.[108] Heterogeneous catalysts can often suffer from fouling,[145] leaching[146, 147] and/or loss of activity through poisoning[145], all of which require downtime of the continuous flow set up to resolve.

The complexity of combining chemo- and bio-catalysis in a single continuous flow system is highlighted by the limited literature in this field.[1, 2] In part, this is due to the divergent reaction conditions that each step requires. Compartmentalisation has the potential to enable access to these combined systems, with DES also minimising the solvent compatibility issues between the different catalysts. Combining several reactors in tandem, however, often results in a substantial build-up of pressure as well as dilute reaction solutions, both of which can hinder the application of multiple reactors sequentially in flow.[108]

1.7 Project aims and objectives

The focus of this work is the enhancement of chemoenzymatic cascades in continuous flow, fusing enzyme immobilisation, continuous separation and chemocatalytic methodologies.

There are three areas of focus within this project:

Objective one: Enzymatic generation of α-aryl primary amines

The first objective concerns the generation of enantioenriched α-aryl primary amines through two alternative enzymatic pathways, illustrated in Figure 25. Through the optimisation of the performance of supported biocatalysts in different reactor configurations, translation of the biocatalytic reactions from batch to continuous flow could lead to accelerated reaction rates, as a consequence of better heat and mass transfer. Moreover, translation to continuous flow could help drive the equilibrium of the transaminase reaction through continuous product removal.

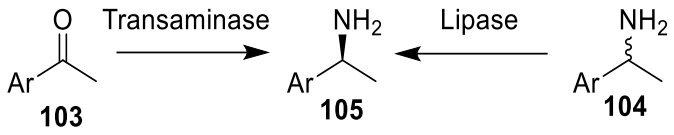

Figure 25: Enzymatic access to α-aryl primary amines, applying transaminase or lipase.

Objective two: Translation of 'clean' *N*-alkylation methodologies into continuous flow

With access to chiral α-aryl primary amines provided through enzymatic routes, *N*-alkylated secondary amines will be accessed through two complementary 'clean' *N*-alkylation methods, iridium-catalysed borrowing hydrogen and photoredox hydroamination, previously demonstrated within the group, Figure 26.[133, 148-151] Once these methodologies are demonstrated in batch, translation to continuous flow within the fReactor platform will enable accelerated reaction rates.

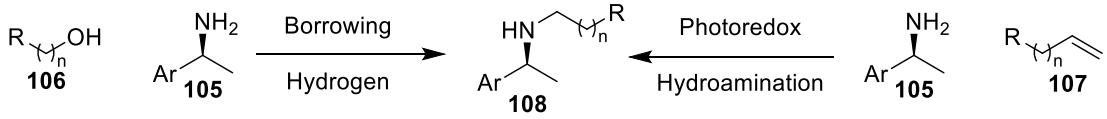

Figure 26: Access to N-alkyl α-aryl amines, applying borrowing hydrogen or photoredox hydroamination methodologies

Objective three: Continuous flow chemoenzymatic synthesis of α-aryl secondary amines

The last objective is to demonstrate the union of continuous bio- and chemo-catalytic processes for the synthesis of exemplar products, combining the outcomes of the previous two objectives.

In addition, efficient extraction of reaction components, with the intention of facilitating downstream cascade reactions and/or co-factor recycling will be implemented.

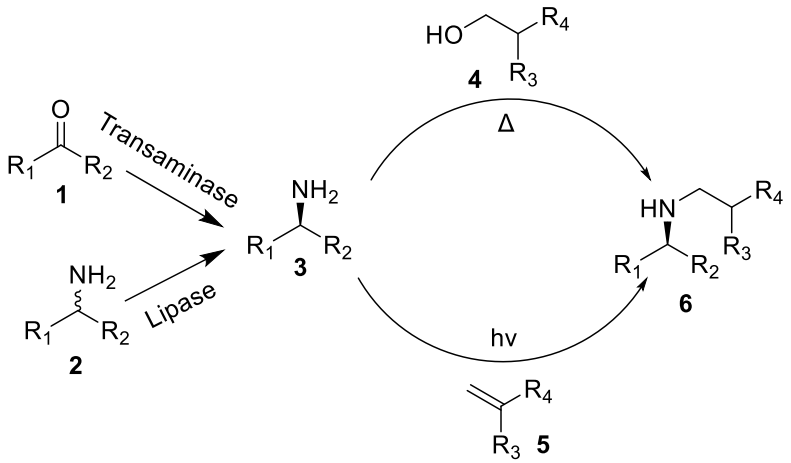

Figure 27: Four alternative routes to enantiomerically enriched secondary amines via chemoenzymatic continuous flow cascades.

Through the combination of bio- and chemo-catalysis, as well as selective extractions, access to α-aryl secondary amines will be possible with excellent enantiomeric excess.

2 Enzymatic access to pharmaceutically relevant chiral amines

Chiral amines are prevalent in many fine chemicals, especially pharmaceuticals, and consequently play an important role in organic synthesis. As a result of the specificity of enzymes and their increasing use in organic synthesis, there is an ever-growing interest in accessing pharmaceutically relevant chiral amines through enzymatic routes.

The use of biocatalysts in flow is an attractive prospect. There are several benefits that can stem from using biocatalysis in flow, such as; reduced enzyme inhibition through a continuous removal of products, improved turnover numbers, enhanced mass transfer, substantially decreased reaction times as well as modulated mixing which aids downstream separations.[16, 19, 118, 152, 153]

Limitations of using enzymes homogeneously in continuous flow synthesis revolve around contamination of product with protein. Recently, immobilisation strategies have emerged as a method to circumvent these reservations, however, there is a need for these strategies to be more efficient and generic.[16] Moreover, leaching of protein from a solid support can often remain an issue despite immobilisation.[154-156]

Within this chapter, two complementary enzymatic routes to the same chiral amine intermediates will be described for the synthesis of two pharmaceutically-relevant chiral primary amines, methylbenzylamine (MBA) and 1-(1-naphthyl)ethylamine (NEA). Reactions were initially screened and optimised under batch conditions and then transferred to continuous flow systems.

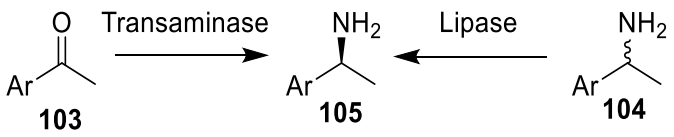

Figure 28: Enzymatic access to pharmaceutically relevant chiral amines, Ar = phenyl or naphthyl.

2.1 Investigation of transaminase-mediated synthesis of chiral amines

Traditional routes to chiral amines often require the use of transition metals, which are often toxic and unfavourable from an environmental perspective. Furthermore, extensive and often costly downstream processes to remove the metal are sometimes required.[157] Over the past decade, the development and application of enzymes as biocatalysts for the asymmetric synthesis of chiral amines has started to receive considerable attention.[158] Biocatalysts, in particular transaminases, offer a promising, sustainable alternative route to chiral amines, with high chemo-, regio- and stereoselectivity as well as the ability to function in mild reaction conditions.

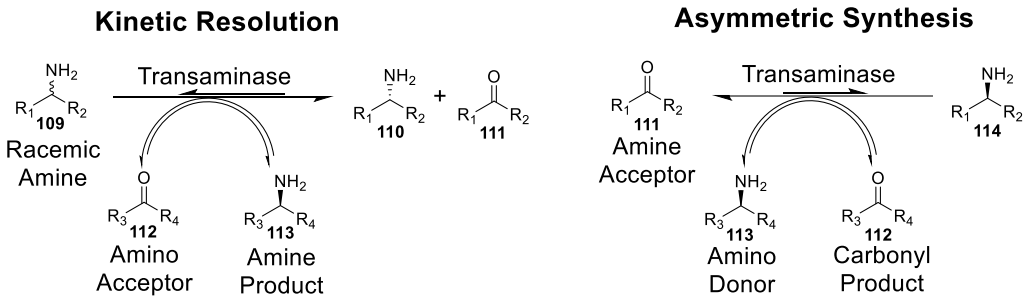

Figure 29: Schematic of transaminase catalysed reactions (kinetic resolution and asymmetric synthesis) where at least one of the R groups on each of the amine donor and acceptor must be small (methyl or ethyl).

Transaminases belong to a group of pyridoxal-5'-phosphate (PLP) dependent enzymes and are required for the synthesis of amino acids within the body. Within organic synthesis, transaminases are most commonly applied to the formal asymmetric reductive amination of pro-chiral ketones to yield chiral amines.[159]

For successful transaminase reactions, substrates have to fit within two binding pockets, commonly known as the large and small binding pockets.[160] There has been considerable attention in increasing the substrate scope of transaminases by increasing the capacity of the small binding pocket.[161] With successful protein engineering, the scope of transaminases can be increased, facilitating cascade reactions and the synthesis of complex molecules with multiple stereocentres.[161]

There are various types of transaminases, classified by the position of the amine group that is being transferred, relative to the carboxyl group of the substrate.[160] Both α- and ω-transaminases have been identified for use in organic synthesis. Due to the location of the binding pockets, α-transaminases can only convert α-amino and α-keto acids. In comparison, ω-transaminases offer larger substrate versatility and are subsequently of highest interest to the pharmaceutical industry.[161]

Transaminases can be used to access enantiopure amines through two approaches: kinetic resolution and asymmetric synthesis. Within a kinetic resolution, one enantiomer of a racemic mixture is converted to a keto-product with use of an amino acceptor, resulting in an enantioenriched amine product, Figure 29. Conversely, within a transaminase-mediated asymmetric synthesis reaction, a prochiral ketone is converted to an amino product, with use of an amino donor, often in high enantiomeric excess, Figure 29. Prochiral ketones are extremely attractive starting materials, owing to their structural simplicity as well as their relatively low cost and broad availability.[158]

Asymmetric synthesis is commonly the most desirable route as it offers a theoretical yield of 100% compared to the 50% maximum yield that kinetic resolution can provide. Additionally, product separation is considerably more challenging in kinetic resolution reactions due to the high concentration of co-products produced. Kinetic resolution is still a valuable tool, however, especially when the substrate scope does not allow for asymmetric synthesis.

2.1.1 Overview of transaminase mechanism

The mechanism by which transaminases function has been studied in extensive detail.[162-164] Transaminase catalysed reactions proceed by a bi-uni-uni-bi ping-pong mechanism that can be divided into two half reactions. A bi-uni-uni-bi mechanism denotes that the reaction is catalysed by one enzyme and converts two substrates into two products, whilst ping-pong means that it is not until the first substrate is converted to its subsequent product that the next substrate binds to the protein.

The first step of the mechanism involves the formation of an internal aldimine between the aldehyde group of a PLP that is bound to the enzyme *via* a lysine residue of the active site, Figure 30. This is subsequently replaced by an external aldimine, which is formed by the amino donor and the PLP, releasing the lysine residue.[165]

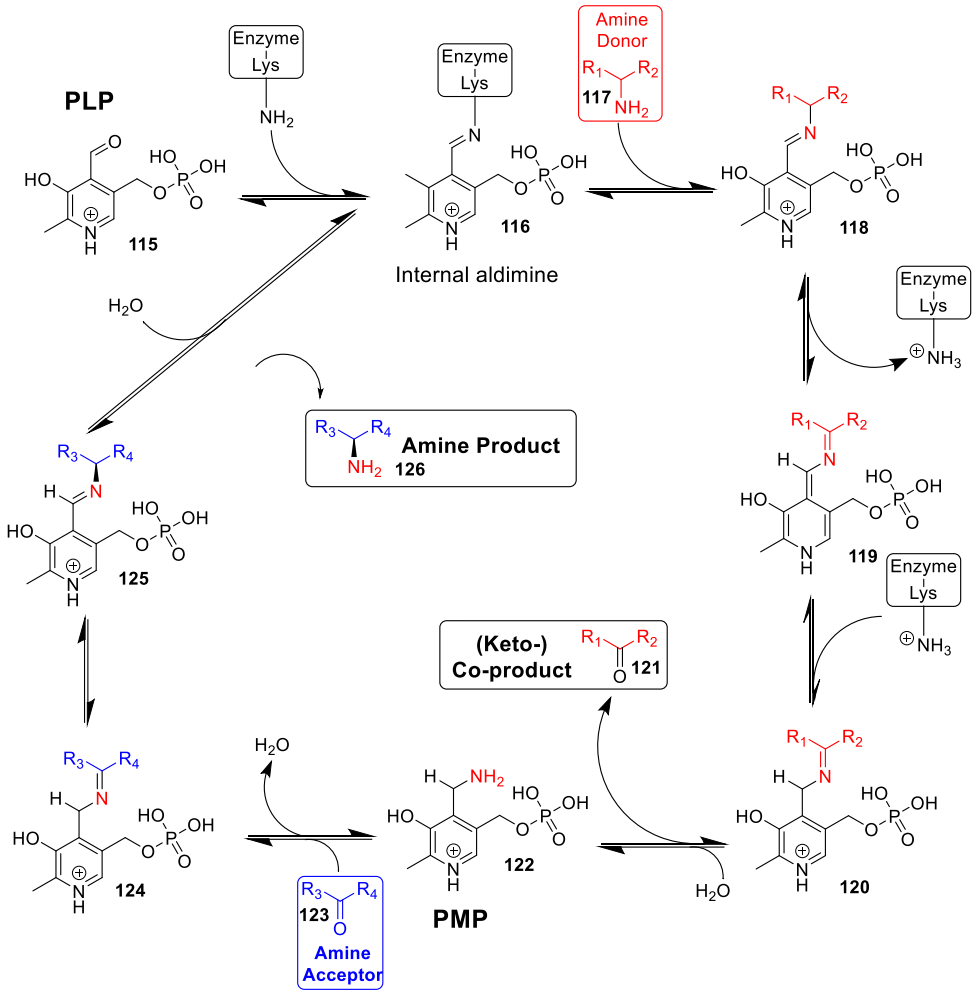

Figure 30: Mechanism of Transaminase Action, showing the regeneration of PLP and the use of both the amine donor and acceptor. Adapted from Szmedjda et al., 2017. [164]

The free lysine functions as a base in the next step of the mechanism, facilitating a 1,3-hydogen shift from the α-proton of the external aldimine to the imine of the co-enzyme, *via* a quinonoid intermediate, which stereoselectively yields a ketimine.[165] The quinonoid intermediate is stabilised by a hydrogen bond to a tyrosine residue that resides within the active site. Hydrolysis of the ketimine yields the ketone product along with pyridoxamine-5'-phosphate (PMP).

The second half-reaction is initiated through the formation of a Michaelis complex involving an amino acceptor and the PMP bound to the enzyme.[165] This second ketimine complex is then converted to an aldimine *via* a 1,3-hydrogen shift. The subsequent hydrolysis regenerates PLP and in the process, yields the amine product.

The two binding site model was proposed by Shin and Kim in 2002, where the large binding pocket functions as a carboxylate trap, relying on strong repulsion from the small pocket. In their model, it is this repulsion that determines the substrate specificity and stereoselectivity.[166] This model is also built on the principle that the structure of the enzyme is essential for orientating the substrate in a manner in which it yields high stereoselectivity due to the small binding pocket accommodating the side chain of the substrate in one specific orientation.[166]

2.1.2 Transaminase at the industrial scale

Perhaps the most famous industrial-scale use of transaminase is in the synthesis of the antidiabetic drug, sitagliptin. At the time, the substrate scope of transaminase enzymes was extremely limited.[76, 77, 165] Starting from a completely inactive wild-type transaminase, a combination of substrate walking, to engineer the large binding pocket, and directed evolution, to enhance activity, resulted in an evolved transaminase that could replace a rhodium-catalysed step in the synthesis sitagliptin.[77]

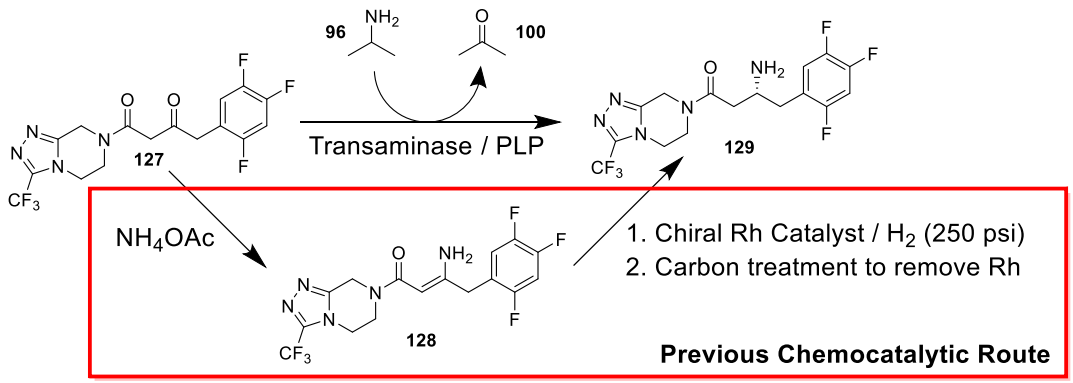

Figure 31: Synthesis of Sitagliptin utilising an engineered transaminase, resulting in a reduction in process steps and replacement of a transition metal catalyst from the original chemocatalytic route.

To overcome the equilibrium limitation, the group used a large excess of the amine donor, which could lead to issues with product separation in downstream processes.[167-169] Moreover, a large amount of dimethyl sulfoxide (DMSO) co-solvent as well as high reaction temperatures were required due to the solubility of the ketone substrate.[77] All these conditions increased the demand on the enzyme and placed further emphasis on the protein evolution.

The final evolved enzyme contained 27 mutations compared to the original wild-type, of which 12 involved the active site (5 small binding pocket, 5 large binding pocket, 2 outside the binding pockets).[77] Not only did the transaminase-catalysed reaction reduce the number of steps and environmental impact of the process, but compared to the rhodium-catalysed synthesis, the biocatalytic process delivered a 13 % higher yield and a 53 % increase in productivity.[77]

Due to the broad substrate scope of the newly evolved enzymes generated for this study, a wide variety of ketone substrates were successfully converted to their amine counterparts, including various phenylethylamines and trifluoromethyl substituted amines.[77] This compounded the sitagliptin synthesis in demonstrating the potential use of transaminases in industrial synthesis for desirable chiral amine products.

2.1.3 Examination and optimisation of transaminase catalysed generation of chiral amines from pro-chiral ketones

We decided to employ two stereo-complementary transaminases, an *(S)*-selective ω-transaminase originating from *Bacillus megaterium* (Bm)[170-172] and an *(R)*-selective ω-transaminase originating from *Hyphomonas neptunium* (Hyp)[173-175], donated by the Turner group (University of Manchester). Both enzymes have previously demonstrated good substrate tolerance for aliphatic and aromatic ketones with a variety of amino donors.[171, 172, 174, 175] The solution-phase behaviour of these two ω-transaminases was examined for the conversion of 1'-acetonaphthone to 1-(1-naphthyl)ethylamine (NEA), Figure 32. Optimisation of reaction conditions was

performed using a one variable at a time (OVAT) approach. First, pH optimisation was carried out for both enzymes at 30 °C with a pH range of 6-10, Figure 33.

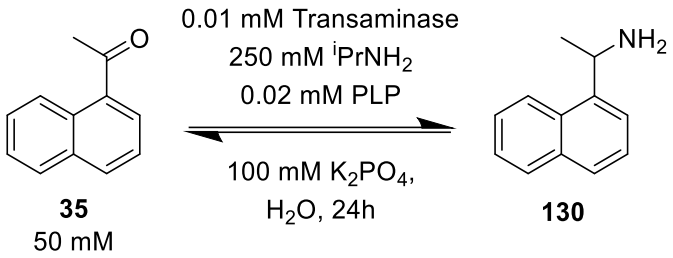

Figure 32: Transaminase catalysed conversion of 1-acetonaphthone to 1-(1'-naphthyl)ethylamine. Reactions were performed with purified transaminase at 50 mM ketone with 5 equivalents of isopropylamine, 0.02 mM PLP in 100 mM phosphate buffer.

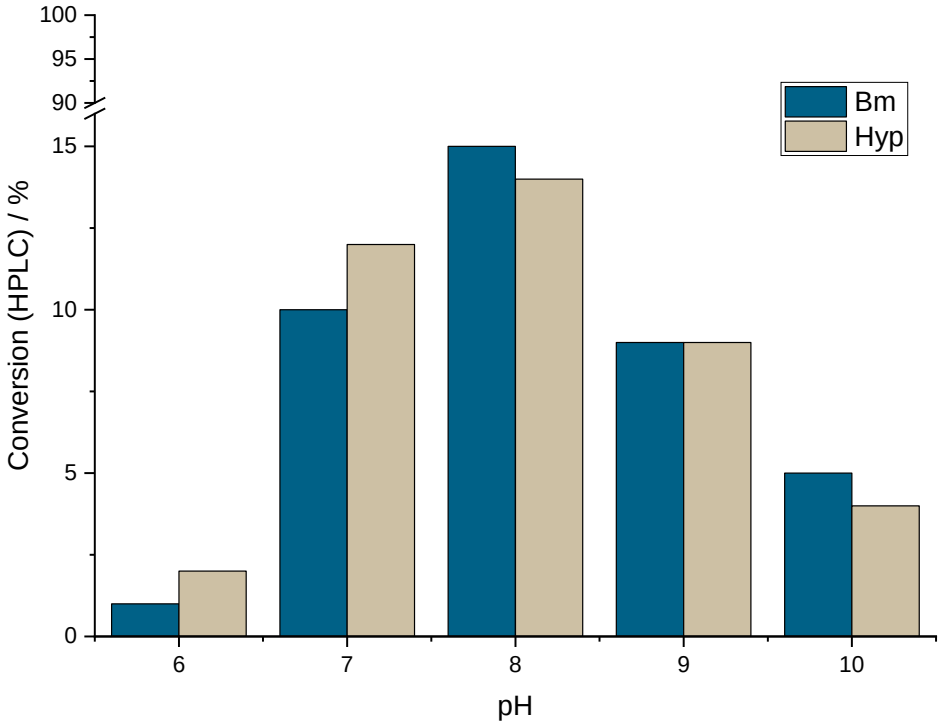

Figure 33: pH optimisation of transaminase catalysed conversion of 1-acetonaphthone to 1-(1'-naphthyl)ethylamine. Reactions were performed with purified transaminase at 30 °C in an aqueous buffer (100 mM K_2PO_4, 0.02 mM PLP) containing 50 mM 1-acetonaphthone and 250 mM $^{i}PrNH_2$ for 24 h. n = 1. Conversions were calculated using standard curves for both 1'-acetonaphthone and NEA.

On the basis of these results, all subsequent transaminase reactions were carried out at pH 8. With the low conversions observed at 30 °C, the temperature of the reaction was then varied with the view of increasing the conversion.

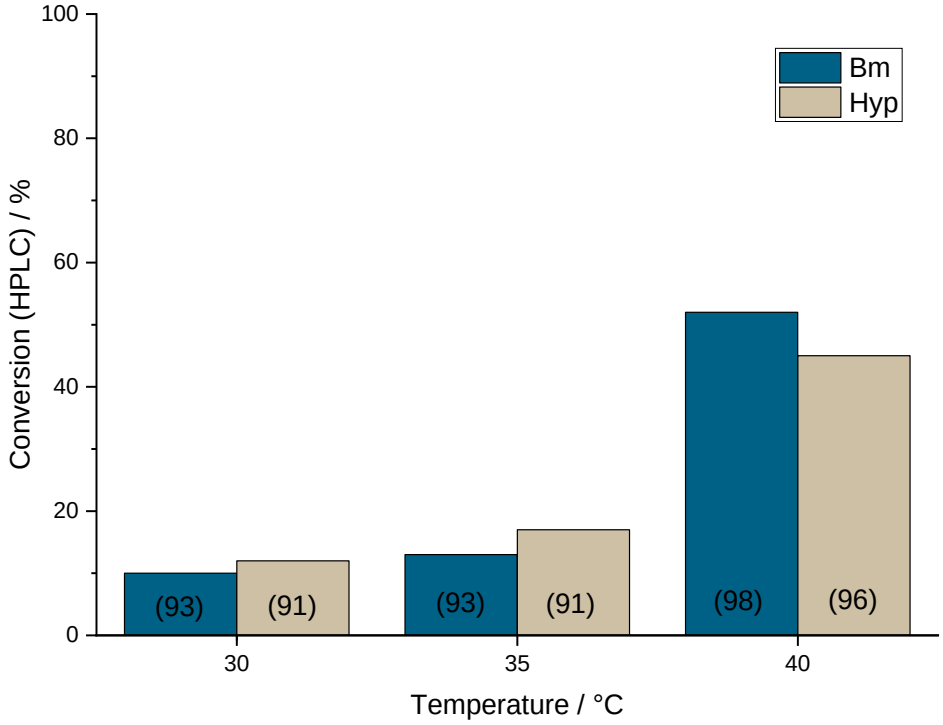

Figure 34: Temperature effects on the conversion of the transaminase reaction. Reactions were performed in an aqueous buffer (100 mM K_2PO_4, 0.02 mM PLP, pH 8) containing 50 mM 1-acetonaphthone and 250 mM $^{i}PrNH_2$ for 24 h. Enantiomeric excess is shown in parentheses; Bm-TA produces the (S)-amine and Hyp-TA produces the (R)-amine. n = 1. Conversions were calculated using standard curves for both 1'-acetonaphthone and NEA.

At a lower temperature of 30 °C, there was minimal effect upon conversion when compared to the 35 °C reaction, however, when the temperature was increased to 40 °C, conversion increased dramatically. The temperature wasn't increased above 40 °C due to the potential for protein denaturation. As the highest conversion was observed at 40 °C, which is consistent with previous optimised conditions described for Bm-TA,[176] all future reactions were carried out at 40 °C and pH8.

2.1.3.1 Effect of amino donors on the transaminase catalysed generation of chiral amines from pro-chiral ketones

The reversible nature of the transaminase reaction means conversion is dependent on the position of the equilibrium.[161, 177] Several strategies have been outlined to displace the reaction equilibrium in favour of the amine product. These strategies include using an excess of the amine donor, the removal of the volatile ketone co-products by evaporation or distillation,[167, 178] enzyme catalysed degradation or recycling of the co-product, [179-184] and a spontaneous follow up reaction of the co-product.[158, 185, 186]

Of all these strategies, the use of an excess of the amine donor is the simplest to deploy. Whilst this does shift the equilibrium in favour of product formation according to Le Chatelier's principle, the excess of co-substrate can lead to enzyme inhibition as well as incurring difficulties with separations and product purification.

It was found that 1'-acetonaphthone has a limited solubility within the aqueous buffer at room temperature. The addition of DMSO as a co-solvent has been applied to many biocatalytic reactions in which the solubility of a substrate within an aqueous buffer has been a limiting factor. Therefore, addition of 5% DMSO was proposed to aid the solubility of 1'-acetonaphthone, potentially increasing the conversion of the reaction.

Moreover, initial reactions were carried out using isopropylamine, as it is the most frequently used amino donor in transaminase reactions.[183] Two alternative amino donors, that are also frequently used in transaminase reactions, alanine and methylbenzyl amine (MBA) were also screened in the reaction.

Irreversible or "smart" amine donors can be used to drive the equilibrium of the transaminase step in favour of the chiral amine product in accordance with Le Chatelier's principles. The use of 1,2-diaminopropane as a cheap, irreversible amino donor has been previously proposed by O'Reilly and coworkers, Figure 35.[187]

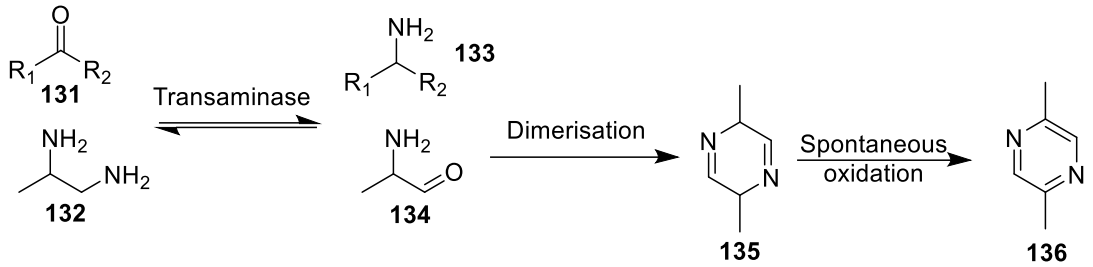

Figure 35: 1,2-diaminopropane as a "smart" amine donor.

With the potential rapid dimerization of the initially formed 2-aminopropanal and subsequent spontaneous oxidation of the resultant diimine species, the amino donor would be driven out of the equilibrium, displacing it favourably and increasing the conversion of the reaction.

A potential issue with this strategy is that the pyrazine co-product would partition into the organic stream within the separations step and would be present within the reaction mixture in the downstream chemistries unless multiple separation steps are incorporated. Additionally, any effects the pyrazine has upon subsequent transformations, such as serving as a ligand for an iridium catalyst, would need to be investigated as it could lead to reduced reaction rates or catalyst poisoning.

The results of screening various amine donors and reaction conditions are shown in Figure 36. Reactions were performed at 40 °C in an aqueous buffer (100 mM K_2PO_4, 0.02 mM PLP, pH 8) containing 50 mM 1-acetonaphthone and 250 mM amino donor for 24 h.

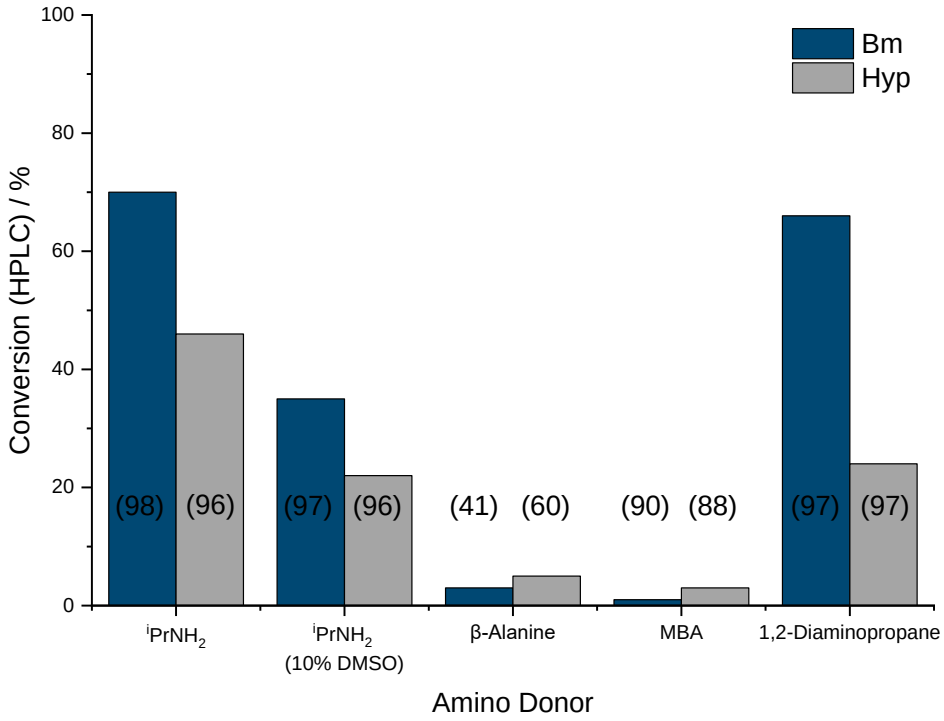

Figure 36: Effects of different amino donors on the conversion of the transaminase reaction (enantiomeric excess / %). Reactions were performed at 40 °C in an aqueous buffer (100 mM K_2PO_4, 0.02 mM PLP, pH 8) containing 50 mM 1-acetonaphthone and 250 mM amino donor for 24 h. Enantiomeric excess is shown in parentheses; Bm-TA produces the (S)-amine and Hyp-TA produces the (R)-amine. MBA denotes methylbenzylamine. Conversions were calculated using standard curves for both 1'-acetonaphthone and NEA.

Despite 1'-acetonaphthone having a limited solubility within the aqueous buffer, addition of 5% DMSO resulted in a decrease in conversion for both enzymes. This decrease in activity suggests the DMSO co-solvent is not tolerated by the wild-type enzymes and, therefore, DMSO was not used in any further reactions.

Moreover, when the reaction was performed with alternative 'simple' amino donors (β-alanine, MBA), a dramatic loss of conversion was also observed, as well as a drastic drop in enantiomeric excess with β-alanine serving as the amino donor. This is likely due to β-amino acids being poor amino donors with wild-type transaminase, with the development of transaminase which accept β-amino acids being a key area for development within the field.[174]

1,2-Diaminopropane gave similar conversions to isopropylamine for BmTA, however, there was a sizeable drop in conversion for HypTA. For simplicity of the downstream chemistry, not having to consider the effects of the pyrazine side product, coupled with isopropylamine performing greater than 1,2-diaminopropane for both wild-type transaminase, isopropylamine was used as the amino donor in all subsequent reactions.

2.1.4 Strategies for Enzyme Immobilisation

Biocatalysts are neither consumed nor destroyed during their activity and, therefore, isolation from the reaction mixture facilitates their reuse.[188] Isolation or retention of biocatalysts is paramount in order to reduce process costs through the subsequent reuse of the catalyst. Various techniques have been employed in order to retain the catalyst, including; phase separation where a hydrophobic polytetrafluoroethylene (PTFE) membrane is used to separate the stream containing the enzyme and the product stream[189] and attaching the biocatalyst to beads or the walls of a microchannel through immobilisation in order to fix the biocatalyst within the reaction zone.[119]

Immobilisation of biocatalysts has attracted considerable interest from both academia and industry, especially when biocatalysts are to be used in continuous flow.[118] The attachment of the soluble biocatalyst to a heterogeneous support not only simplifies the retention of the catalyst, it can also enhance the catalytic stability, often an issue with biological catalysts in organic chemistry, and increase the loading of the catalyst.[190] Moreover, immobilisation can also increase the stability of an enzyme towards organic solvents.[116, 129, 154, 191] The benefits of this are two-fold: simplification of work-up, reducing waste generation and processing time as well as increasing the solubility of hydrophobic substrates. Furthermore, for enzymes to be used industrially, it is essential that they are stable and fully functional under the process conditions.[190]

Whilst the primary function of immobilisation is to facilitate the reuse of the catalyst, it is also possible for the immobilisation process to trigger hyperactivity of the catalyst through conformational changes to the protein's quaternary structure[192] or through the generation of a favourable microenvironment.[190] Despite the successes of immobilisation, many strategies suffer from significant loss in activity compared to that of the free enzyme.[15]

As every enzyme is unique, there is currently no immobilisation technique that works for all enzymes.[122] The unique relationship between the enzyme and its support mean that the development of immobilisation has followed a trial and error approach.[193]

Routes to immobilisation can be grouped into three categories; cross-linking, encapsulation and binding to a support. The extensive screening and optimisation of immobilisation conditions presently employed to achieve immobilisation are a significant drawback to the trial and error style approach. For this reason, there is a drive to make immobilisation strategies as general and broadly applicable as possible.

2.1.4.1 Cross-linking

Cross-linking of enzymes has been used as a strategy of immobilisation since the 1960s.[194] Originally achieved through the reaction of primary amines on the surface of the enzymes with bifunctional cross-linkers, the philosophy of cross-linking is to produce an insoluble enzyme. This technique, however, had low retention of catalytic activity as well as having low mechanical stability, limiting the use of these enzymes.[154]

The first commercially available form of cross-linked enzymes were produced by Altus Biologics in the 1990s.[154] Their broadly applicable method of immobilisation involved allowing the enzyme to crystallise before adding a bifunctional reagent, commonly glutaraldehyde, subsequently this type of immobilisation is known as cross-linked enzyme crystals (CLECs). This resulted in robust, highly active enzymes

with an easily controllable particle size. Whilst this method is applicable for all classes of enzyme, the need to crystallise the enzyme can become a prohibitive factor due to the necessity of highly pure enzymes and the cost associated with them.[154]

Despite no longer being commercially available, CLECs paved way for an analogous technique for immobilisation. Cross-linked enzyme aggregates (CLEAs) are formed in a similar manner to CLECs, however, instead of crystallisation, the enzymes are precipitated. Precipitation of enzymes through the addition of salts, non-organic polymers or organic solvents generates aggregates of protein without denaturation.[154] The pre-organised aggregate can be held together in a permanent manner through the addition of a cross-linker, whilst retaining a high catalytic activity. Furthermore, the manner in which CLEAs are produced combines purification and immobilisation, meaning that crude enzyme preparations can be used to generate CLEAs.

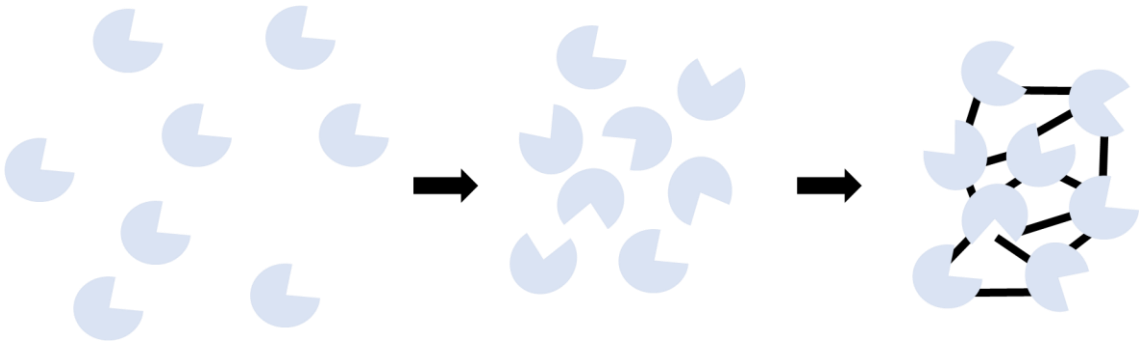

Figure 37: Formation of cross-linked enzyme aggregates (CLEAs). *Step 1, enzymes are precipitated, coming into close contact and forming and aggregate. Step 2, a cross-linking agent is introduced, resulting in the formation of a CLEA*

The particle size and shape of CLEAs can have a significant effect on its activity and is dependent on the number of enzyme molecules and the manner in which they pack within the aggregate.[195] It has also been found that conformational changes that occur as a result of the aggregated state can lead to hyperactivation.[195] As such, close control over the aggregation processes is highly desirable. There are various methods of controlling the size of an aggregate, such as choice of solvent, altering the time allowed for precipitation, and changing the precipitant concentration.[195]

One of the advantages of cross-linking is that the low weight percentage of carrier, compared to enzyme, meaning that there is minimal dilution of activity caused by non-catalytic material. In addition, the lack of non-catalytic bulk means that reactors can be loaded with a higher proportion of enzyme.

Recent expansion of CLEAs has occurred, with the development of CLEA composites that facilitate higher enzyme loads or in some instances an easier means to separation.[154] Moreover, there have also been reports of combi-CLEAs, where several enzymes are cross-linked within the same aggregate.[154] Not only does this facilitate one-pot cascade reactions, the close proximity of the different enzymes reduces mass transfer limitations.

The inherent disadvantage of CLEAs is the requirement for a different precipitation and cross-linking protocol for each enzyme. This requirement indicates the preparation conditions need to be optimised for each new enzyme as the technique is not ubiquitous.[19, 195]

Moreover, the relatively low mechanical stability of carrier-free immobilised enzymes means than CLEAs are not yet amenable for industrial scale processes.[195] One approach to overcome this is to cross-link the CLEA with magnetic nanoparticles, forming a “smart” CLEA.[154, 195] Aside from the higher operational stability, this enhances separation through the application of a magnetic field. Another route to alleviate the low mechanical stability is to use another route of immobilisation (encapsulation) of the whole aggregate.

2.1.4.2 Encapsulation

The desire to trap enzymes in their active state was the main driving force and the reason for the surge in popularity of encapsulation as an immobilisation technique.[19] Due to the enzyme being in its native state, gel encapsulation provides greater activity retention than the other immobilisation tecniques.[196] Additionally, compared to the conditions required for other immobilisation techniques, encapsulation is often a much milder process, commonly taking place in an aqueous environment at

room temperature.[122, 197] Consequently, the preparation of porous polymeric particles around the biocatalyst is applicable for almost all types of enzyme.

The most commonly used form of polymeric particles are hydrogels made up of polysaccharides, owing to allowance of cell growth inside of the polymeric structure.[197] These hydrogels do, however, suffer from low mechanical stability as well as high ratios of enzyme distorting the particle structure, limiting the enzyme load.

As a consequence of the limitations of natural polymers, attention has turned to the use of synthetic polymers, applied in a similar manner. Polyvinyl alcohol (PVA) has been used to overcome the disadvantages experienced with natural polymers as, unlike their natural counterparts, PVA hydrogels exhibit excellent mechanical stability, are very elastic and are not biodegradable.[198] Furthermore, PVA is an inexpensive material, meaning encapsulation using PVA hydrogels provides a cheap and accessible route to immobilisation.

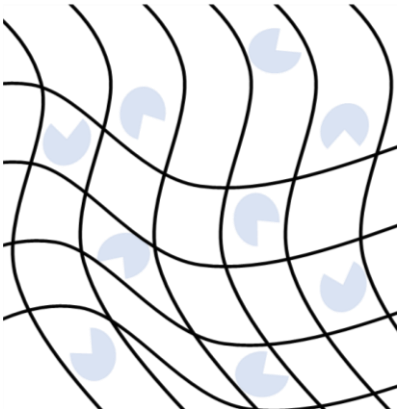

Figure 38: Formation of encapsulated enzymes in a hydrogel matrix

Incorporation of enzymes into a gel-network ensures they become mechanically robust, whilst also increasing their chemical tolerance. As such, encapsulation could prove to be a viable route to one-pot chemo-enzymatic cascades owing to a greater spatial and temporal separation of the enzymes in an aqueous environment and the organic solvent in which the metal-catalysed step occurs in.[129]

The structure surrounding the enzyme provides greater thermal, pH and storage stability as the structure of the protein is confined, delaying the denaturation process. Despite these advantages, the network that surrounds the enzyme introduces a diffusion barrier, which often leads to a reduction in activity.[19, 193] Furthermore, the lack of covalent linkages causes significant issues in regards to catalyst leaching, which is a considerable problem if a high purity product is required.[19]

2.1.4.3 Binding to Supports

The most ubiquitous immobilisation technique involves the binding of the enzyme to a support.[19] This method of immobilisation was first realised in 1916, when Nelson and Griffin adsorbed invertase to a solid charcoal support.[199] Through their immobilisation, they found that removing an enzyme from an aqueous solution had little effect on its activity.

The binding of biocatalysts to supports can be generally categorized into “covalent” and “noncovalent” groups. In “covalent” attachment, the biocatalyst is bound to the support through a covalent bond between reactive groups on the support and surface amine groups on the protein, whereas in “noncovalent” attachment, the protein is bound to the support by any number of physicochemical interactions, including; hydrophobic, charge-charge and affinity tags.[19]

There are multiple different functional groups found on proteins that can be used for covalent immobilisations, including; α- and ε-amino groups, α-carbonyl and β- and γ-carboxyl groups, phenols, thiols, hydroxyls, imidazole and indoles.[200] Considering the multitude of possible binding groups, it is critical that there is no covalent linkage to a functional group that is involved in the catalytic activity of the enzyme. Selectively targeting particular functional groups on the protein allows for directed orientation of immobilisation, resulting in good steric accessibility of the active site.[200]

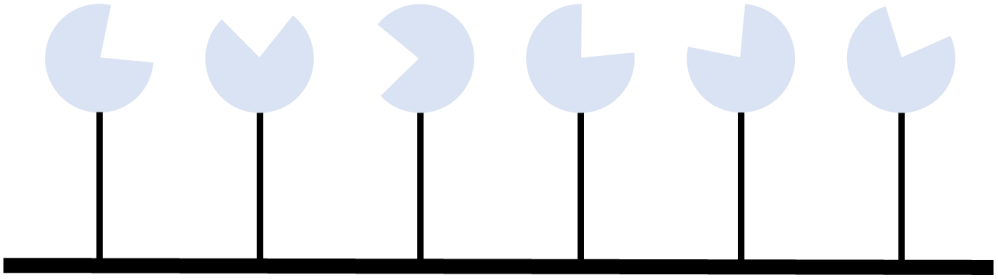

Figure 39: Covalent attachment of enzymes to a support

One of the major disadvantages associated with covalent immobilisation is that the link between the enzyme and the support is permanent. This is not as big of as issue after successful immobilisation, however, if the enzyme is denatured during the immobilisation process, it renders both the support and the enzyme obsolete.

Conversely, one of the advantages of noncovalent attachment is that any conformational changes that occur upon immobilisation are less significant than they would be if the enzyme was covalently bound.[200] There is, however, significantly less control over the orientation in which the enzyme adsorbs to the surface, compared to covalent immobilisation.[201]

Often regarded as the simplest way of preparing an immobilised enzyme, there are numerous means of non-covalent binding to a support.[200] The main limitation of non-covalent attachment is the stability of the adsorbed layer, which is typically much weaker than that of the covalent alternative. The utilisation of affinity tags is a novel route to immobilisation that has potential to alleviate the stability issues that non-covalent binding poses.

In order to facilitate multipoint attachment, immobilisation supports possess a plethora of available groups on their surface which can result in unwanted reactions between the reactant and the support. To avoid these unwanted reactions, it is paramount that after immobilisation any unreacted active groups on the surface of the support are blocked.[200]

The main issue with binding to a support is that a large amount of non-catalytic bulk is introduced to the system, resulting in a dilution in activity.[19] This dilution effect can be somewhat controlled through the targeting of specific groups for attachment which result in the least significant conformational change of the enzyme. Moreover, sufficient porosity of the support can limit the reduction in activity by increasing accessibility to the enzymes active site. Additionally, the immobilisation geometry can improve access to an enzymes active site, often this leads to hyper-activation of the bound enzyme.[125]

Whilst there may not be one immobilisation support that is optimal for all enzymes, there are several characteristics that define a suitable support. A large surface area with sufficient functional groups capable of attachment is a necessity in order to achieve a high catalyst load.[153] Consequently, it is important to consider the size and shape of the support as both these parameters dictate the surface area of the material. Further, other physical properties of the support that can affect the maximum catalyst load also need to be taken into account, including its chemical nature, density and porosity.[190]

In addition, one of the primary reasons for immobilisation is an increase in stability and as such the support needs to be chemically and thermally stable, with respect to the reaction conditions. Moreover, the support ought to have a level of rigidity, be non-toxic and carry a low cost.[153] Another reason for immobilisation is reusability of the attached enzyme. As many enzymatic reactions take place in aqueous conditions, the support needs so be insoluble in water to allow for efficient extraction.[153]

2.1.4.3.1 Reactive Supports for Covalent Attachment

In a similar manner to Merrifield's seminal work, Lifetech™ have developed a catalogue of resins for enzyme immobilisation, commonly referred to as Purolite® resins. Within this catalogue, there are two different types of resin which use covalent binding to immobilise the enzyme, epoxy-activated and amino-activated. Both resin backbones provide mechanical stability, maximising the lifetime of the

support. Further, each resin is available in different porosities, synthesised with a high degree of cross-linking and a porogenic agent, allowing precise control of the porosity. This allows a resin to be selected based on the size of the enzyme, maximising their scope whilst reducing any mass transfer limitations.

Additionally, the mechanical strength, hydrophilicity and porosity of the resin can be altered by varying the amount of cross-linking. This increases the ease of tailoring the resin to enzyme desired to be immobilised, for example highly hydrophobic resins have been found to be optimal for *Candida antarctica* Lipase B (CALB)[125, 202], whereas transaminases have been found to function best when attached to hydrophilic resins.[203, 204]

The reactivity of epoxy-activated resins makes them perfectly suitable for multipoint covalent attachment between the enzyme and the resin, as reactions can occur between the epoxy group and any number of amino, thiol or phenolic groups present on the enzyme. This multipoint attachment significantly reduces the extent of leaching from the support.

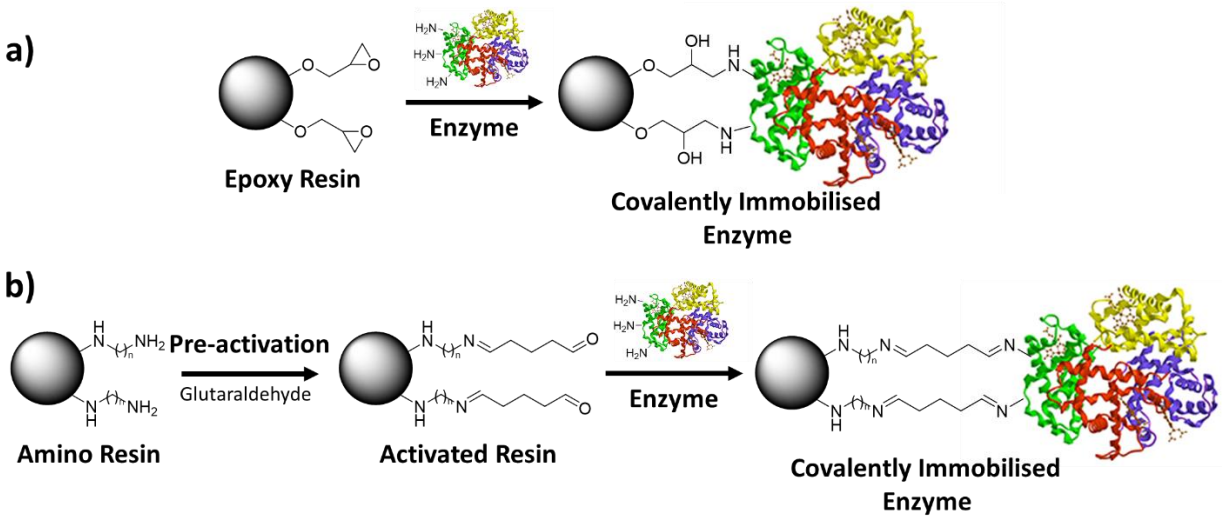

Figure 40: Immobilisation of enzymes using a Purolite® *a) epoxy b) amino resin. Not to scale. Adapted from www.purolite.com*[205]

Unlike their epoxy counterparts, the amino resins require an additional pre-activation step, involving glutaraldehyde. The resulting aldehyde can then undergo a

rapid reaction with amino groups of the enzyme, forming a Schiff base. Whilst this linkage is satisfactorily strong enough to bind the enzyme with minimal leaching, especially with multipoint attachment, access to a more stable attachment is possible through reduction of the imine with use of borohydrides.

Both epoxy- and amino-activated resins have similar routes to immobilisation, with the difference being the need for a glutaraldehyde pre-activation step when using amino-activated resins. For optimum immobilisation onto Purolite® resins, a high ionic strength buffer is required,[202] which could limit the solubility of the enzyme and, therefore, the loading capacity.

Due to the reactivity of the binding groups on the resin support, it is possible that covalent bonds to residues involved in the catalytic activity of the enzyme may be formed. In order for this to be avoided, it would be desirable to incorporate a targeting binding approach, through considering the reactivity of target residue(s) on the protein and functionalising the support appropriately thereafter.

2.1.4.3.2 Reactive Supports for Non-Covalent Attachment

Affinity tags are a convenient non-covalent means to facilitate immobilisation. The poly-histidine tag was invented by Roche[206] and have since been engineered into countless enzymes, typically consisting of at least 6 histidine (His_6) residues. The function of a His-tag is to dramatically increase the protein's affinity for a metal ion enabling selective purification from crude protein solutions.

Through harnessing His_6-tags, which are expressed on nearly all recombinant proteins, the EziG™ platform combines immobilisation and purification steps, reducing process time and enzyme preparation costs. The core of the EziG™ material consists of controlled pore glass (CPG) and chelated metal ions. The CPG is an extremely porous material, possessing many interconnecting pores, minimising any diffusion or accessibility limitations commonly experienced in similar type systems.[15] Additionally, the CPG core is both non-swelling and mechanically stable, enabling use in both batch and continuous flow reactors.

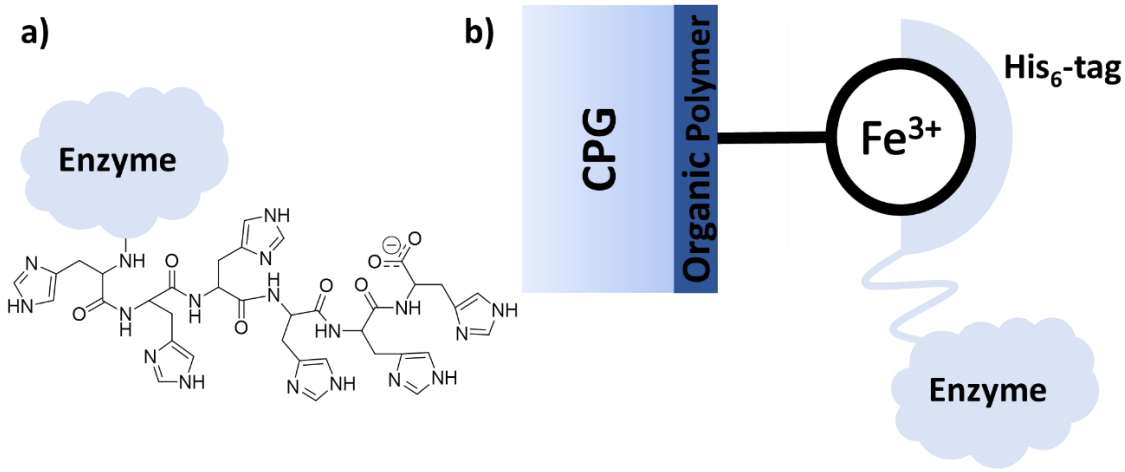

Figure 41: His-tagged immobilisation of enzymes. *a) the chemical structure of a His_6-tag attached to an enzyme b) EziG™ technology employing a His_6-tag to immobilise and enzyme to a controlled pore glass (CPG) support. Not to scale.*

As the binding of the His_6-tags to the metal ion is non-covalent, high enzyme loadings can be achieved using EziG™ immobilisation, whilst also experiencing the other advantages of non-covalent immobilisation. Moreover, the binding of the His_6-tag to the metal ion is so strong that, unlike other non-covalent immobilisation methods, enzyme leaching is minimal.[15] Despite the strong binding, however, it is possible to "swap out" the bound enzymes with use of a strip and reload step, allowing for regeneration of the biocatalytic system.

A further benefit of EziG™ technology is that there are currently three different commercially available variations of the CPG core, with different surface functionalisation (hydrophilic, hydrophobic, and semi-hydrophilic). Coupled with the fact many enzymes have been engineered to contain His_6-tags, this makes this method of immobilisation accessible to almost all classes of enzymes. It is important to consider the substrates of a reaction when using EziG™ immobilised enzymes as competitive binding can occur between the substrate and support, resulting in leaching of the enzyme.

In addition, utilisation of metal-ion affinity to immobilise enzymes can only be applied to non-metalloenzymes, else the protein will be stripped of its metal, resulting in denaturation. In the same manner, the use of metal buffers or metal

cofactors is also restricted, which limits the potential application of metal-ion affinity immobilisation.

Despite each immobilisation technique carrying a unique set of advantages and disadvantages, it is often difficult to make direct comparisons. Furthermore, each of the methods of immobilisation vary in terms of both activity retention and cost. It is well documented that each of the techniques result in a loss of activity[15, 122, 153, 154, 197], however, this is more than compensated by the increased stability and reusability.[116] In addition, the trade-off between activity, recyclability, preparation and overall cost constantly needs to be considered.[19]

2.1.5 Comparison of alternative supports for enzyme immobilisation

The binding of an enzyme to a support is dependent on the surface functionality of the support as well as the mode of binding. The catalyst loading of a support can be quantified using a Bradford assay, which uses the absorbance shift of the Coomassie brilliant blue G-250 dye to quantify the amount of protein in the supernatant.[207]

21 different immobilisation supports were screened against each transaminase. The 21 different supports originate from 3 different suppliers; Enginzyme (EziG), Immobeads (IB) and Purolite. Each support differs by either binding mode, surface functionality or both, with all the screened supports shown in Table 1.

Table 1: The 21 immobilisation supports examined for the immobilisation of two transaminases. Mode of immobilisation, matrix of the support, surface functionality and binding group are all displayed.

Supplier	Support	Mode of binding	Matrix	Surface functionality	Binding group
EziG	1 (Opal)	His-tag	CPG	hydrophilic	chelated Fe^{3+}
EziG	2 (Coral)	His-tag	CPG, poly vinyl benzyl chloride	hydrophobic	chelated Fe^{3+}

EziG	3 (Amber)	His-tag	CPG	semi hydrophlic	chelated Fe^{3+}
IB	ADS-1	adsorption	polyacrylic	hydrophobic	alkyl
IB	ADS-2	adsorption	styrene	hydrophobic	phenyl
IB	ADS-3	adsorption	methacrylate	hydrophobic	octadecyl
IB	ADS-4	adsorption	styrene	hydrophilic	styrene, methyl
IB	COV-1	covalent	polyacrylic	hydrophobic	epoxide, butyl
IB	COV-2	covalent	polyacrylic	hydrophobic	epoxide
IB	COV-3	covalent	polyacrylic	hydrophobic	epoxide
IB	ANI-1	anionic	polyacrylic	hydrophobic	amino C_6 spacer
IB	ANI-2	anionic, weak	polystyrene	hydrophilic	tertiary amine
IB	ANI-3	anionic, weak	polystyrene	hydrophilic	quaternary ammonium type
IB	ANI-4	anionic, strong	polystyrene	hydrophilic	quaternary ammonium type
IB	CAT-1	cationic, strong	styrene	hydrophilic	sulphonic
Purolite	8285	covalent	epoxy/butyl methacrylate	hydrophobic	epoxy
Purolite	8204F	covalent	epoxy methacrylate	hydrophilic	epoxy

Purolite	8309F	covalent or ionic/ adsorption	amino C2 methacrylate	hydrophilic	NH_2 (short spacer)
Purolite	8806M	adsorption	octadecyl methacrylate	hydrophobic	octadecyl
Supplier	**Support**	**Mode of binding**	**Matrix**	**Surface functionality**	**Binding group**
Purolite	1090M	adsorption	macroporous divinyl benzene	hydrophobic	none
Purolite	1030M	adsorption	divinyl benzene/ methacrylate	hydrophobic	none

The mechanism of attachment that the solid support exploits to bind an enzyme impacts the protocol required for immobilisation. These differences in protocol can include incubation time and temperature, ionic strength of the buffer and the washing procedure.

2.1.5.1.1 Assessing catalyst loading after enzyme immobilization

The amount of protein that each support was exposed to was calculated to give a maximal binding of 10 wt%. After the relevant immobilization steps, 20µL of the supernatant was sampled and mixed with 980µL of Bradford reagent and incubated for 5 min at room temperature. After the incubation period, the protein concentration in the supernatant was determined by absorbance at 595 nm plotted against protein concentration obtained from an external standard.

The amount of enzyme remaining in solution was used to calculate the percentage of enzyme bound to the support. This was based on two assumptions. First that any protein not present in the supernatant was bound to the support and second that the only protein in the supernatant was the transaminase. The results of the binding assays are shown in Figure 13.

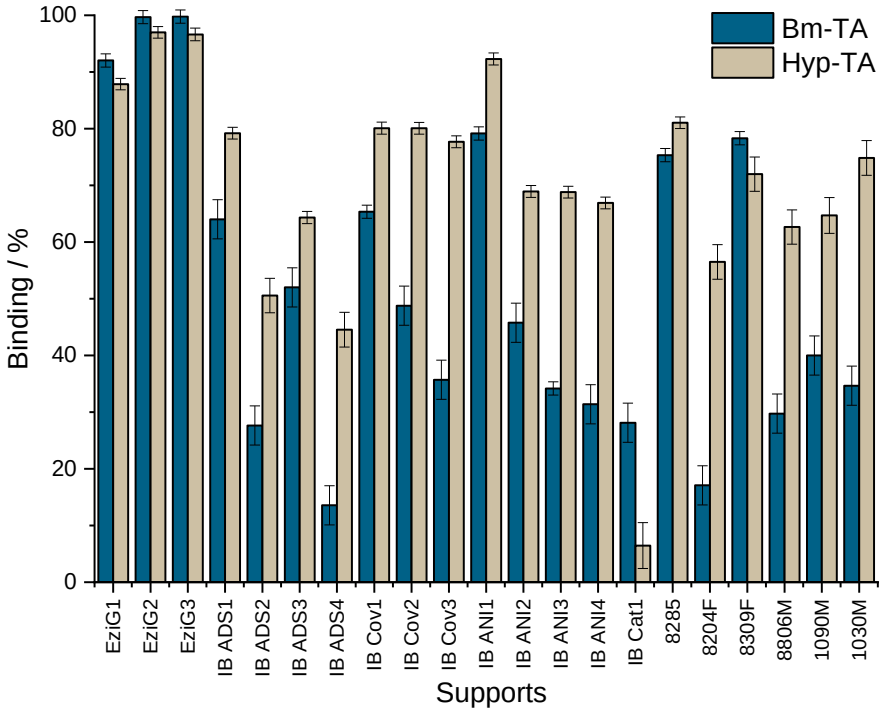

Figure 42: Percentage binding of two enantiocomplementary transaminase on a range of different immobilisation supports. Binding is calculated using the Bradford assay on the supernatant after immobilisation, assuming protein not present in supernatant is bound. 100 % binding equates to 10 wt%.

The group of supports which provide the greatest percentage binding are the EziG supports, which differ only by the surface functionality of their matrix, Table 1. The hydrophobic (EziG2) and semi-hydrophilic (EziG3) supports both give a similar level of binding (>95%), whilst the hydrophilic EziG1 gives a lower binding percentage. The smaller drop in binding percentage between the different surface functionalities of the EziG supports compared to the drop in binding percentage for the other supports suggests that the surface functionality of the support has a lesser effect on binding percentage than the mode of binding.

To determine which property of the support has a larger effect upon catalyst loading, the supports were then grouped according to their surface functionality and their mode of binding as displayed in Table 1.

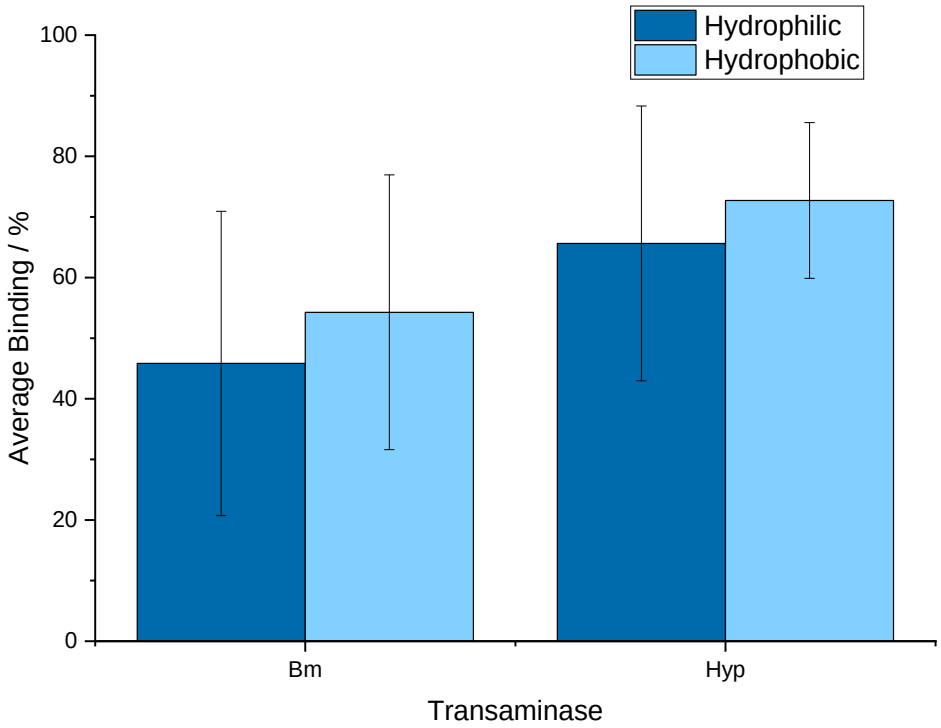

Figure 43: Average binding represented in terms of surface functionality. Hydrophilic, n = 11; hydrophobic, n = 9. EziG3 excluded due to semi-hydrophilic surface.

When grouped by surface functionality, there is a small preference for hydrophobic supports for both enzymes, as shown by the average binding, Figure 43. There is, however, no statistical significance between a hydrophilic or a hydrophobic surface for either transaminase, as shown by overlap of the error bars. This suggests that the surface functionality of the support does have an effect upon percentage binding of the two transaminases, but that surface functionality alone isn't the differentiating factor of binding percentage between the supports.

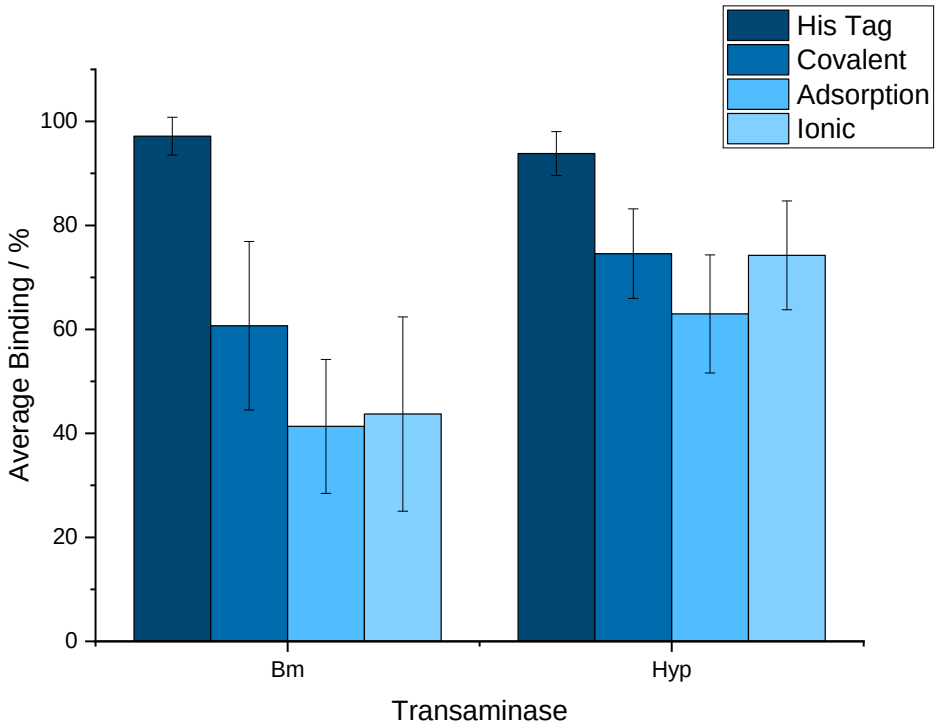

Figure 44: Average binding represented in terms of binding mode. His Tag, n = 3; covalent, n = 6; adsorption, n = 7; ionic, n = 5.

When the supports are grouped by binding mode, however, there is a statistical significance between the His-tag supports and the other three binding modes, Figure 44. It is evident that the His-tag supports bind the two transaminases better than any of the other binding modes, regardless of surface functionality.

For the other three binding modes, there is no statistical significance; however, covalent binding has the next highest average binding, followed by ionic and adsorption, respectively.

For some of the supports, there were large differences in binding percentage between the two enzymes, with higher loadings typically observed for HypTA. Here, the difference in binding can only be due to the enzymes themselves. The two enzymes differ in size by *ca*. 25 kDa, with BmTA (*ca.* 55 kDa) almost double the size of the HypTA (*ca*. 30 kDa). Therefore, it could be possible that the difference in binding could be due to size of the enzymes. Alternatively, differences in amino acid

residues present on the surface of each enzyme would dictate the protein's interactions with the support and would affect all modes of binding, except His-tags.

Whilst the Bradford assay can give an accurate account of protein bound to the support, it does not account for any denaturation of protein upon binding. Moreover, it is well documented that enzyme immobilisation frequently results in a loss of activity[15, 122, 153, 154, 197], however, this loss is often more than compensated by the increased stability and reusability of the enzyme.[116] In addition, the trade-off between activity, recyclability, preparation and overall cost constantly needs to be considered.[19]

2.1.5.2 Activity retention of enzyme-support complexes

The activity of the immobilized enzyme compared to the homogeneous enzyme needs to be assessed to identify the optimum enzyme-support complex. Furthermore, the reusability and activity retention of the support over several cycles are also important parameters to assess the success of immobilization.

The 21 different enzyme-support complexes were placed within 1.5 mL Eppendorf tubes and subjected to 0.5 mL of reaction mixture containing 50 mM acetonaphthone, 250 mM isopropylamine, 100 mM KH_2PO_4 and 0.02 mM PLP at pH 8. The Eppendorf tubes were then placed within a thermomixer and shaken (800 rpm) for 16 h at 40 °C. The reactions were performed within a thermomixer, to allow for even heating and non-destructive mixing.

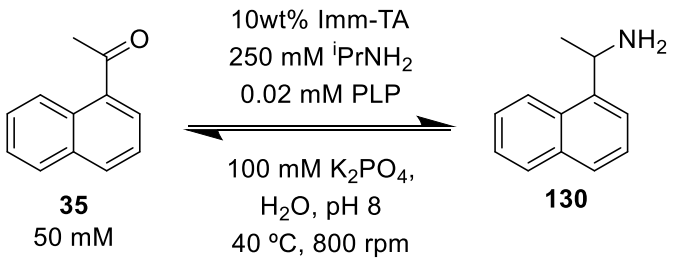

Figure 45: Standard conditions used for activity retention assays. Reactions were performed at 40 °C in an aqueous buffer (100 mM K_2PO_4, 0.02 mM PLP, pH 8) containing 50 mM 1-acetonaphthone and 250 mM $^{i}PrNH_2$ for 24 h in a thermomixer at 800 rpm.

After 16h the Eppendorfs were centrifuged before 100 µL of supernatant was sampled, diluted with 900 µL of acetonitrile and analysed by HPLC. The rest of the supernatant was then removed and replaced with 0.5 mL of fresh reaction mixture. A fresh homogeneous protein standard was also used for each run, to identify any loss of activity (see column 1 of Figures 14-17, labelled 'protein').

Each of the supports, with bound transaminase, were subject to three reaction cycles for the conversion of 1-acetonaphthone to NEA under the reaction conditions shown in Figure 45.

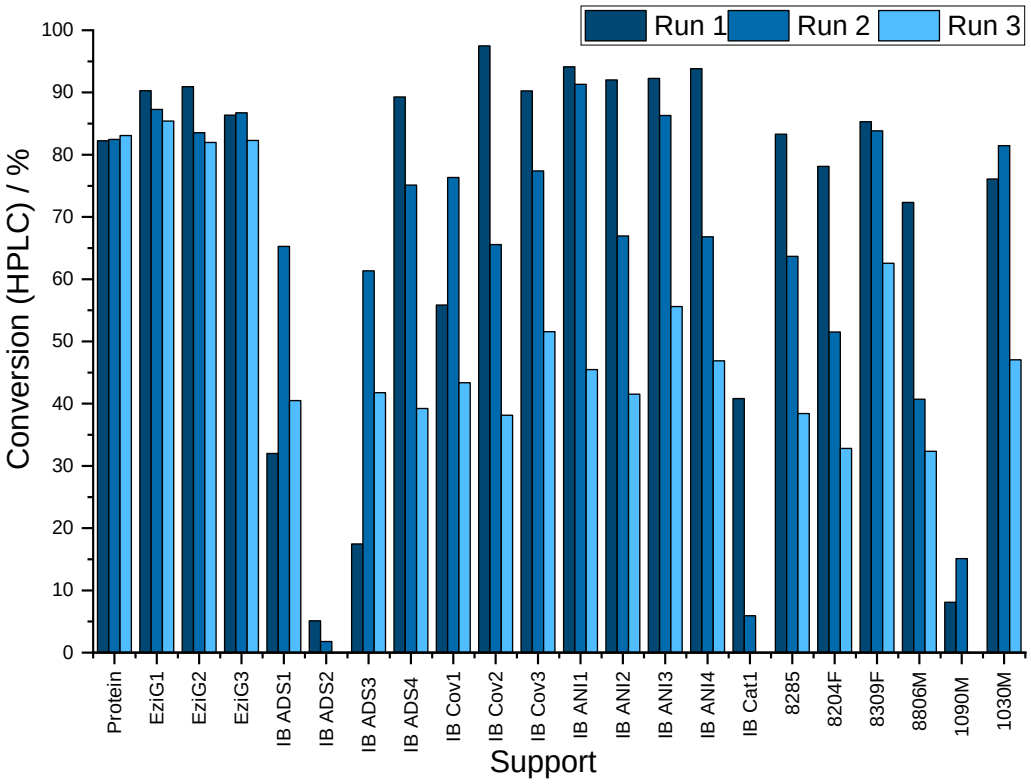

Figure 46: Activity retention assay for immobilised transaminase from Bacillus megaterium on a range of immobilisation supports, runs 1-3, n = 1. Reactions were performed at 40 °C in an aqueous buffer (100 mM K_2PO_4, 0.02 mM PLP, pH 8) containing 50 mM 1-acetonaphthone and 250 mM $^{i}PrNH_2$ for 24 h in a thermomixer at 800 rpm. 'Protein' refers to a fresh non-immobilised, purified enzyme in solution-phase. Conversions were calculated using standard curves for both 1'-acetonaphthone and NEA.

After three runs, it was clear that the supports that use the His-tag mode of binding retain activity much better than the other supports, with the enzymes attached to the three EziG supports all retaining over 80% conversion after the third run. This is likely due to the His-tag mode of binding occurring at the end of the protein and having minimal impact on the structure of the enzyme, therefore, less bound enzyme is denatured upon immobilisation.

Noticeably, only 6 supports maintained conversions over 50% after three runs. This suggests that many of the supports suffer from considerable enzyme leaching or deactivation, as >50% conversion is observed for many supports for the first 2 runs. Supports that resulted in <50% conversion in the first two runs correlate to a low binding affinity (IB ADS2, 1030M).

The 5 supports that maintained the highest conversion after three runs were selected for two further runs. For BmTA those supports were EziG1, EziG2, EziG3, ANI3 and 8309F.

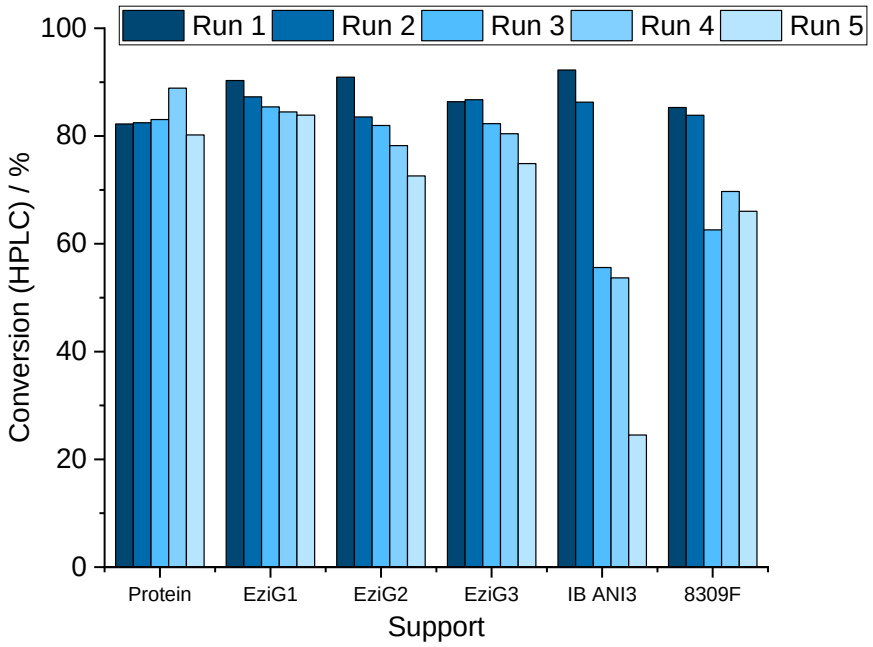

Figure 47: Activity retention assay for immobilised transaminase from Bacillus megaterium on selected immobilisation supports, n = 1. Reactions were performed at 40 °C in an aqueous buffer (100 mM K_2PO_4, 0.02 mM PLP, pH 8) containing 50 mM 1-acetonaphthone and 250 mM $^{i}PrNH_2$ for 24 h in a thermomixer at 800 rpm. 'Protein' refers to a fresh non-immobilised, purified enzyme in solution-phase. Conversions were calculated using standard curves for both 1'-acetonaphthone and NEA.

The poorest performing support, out of the 5 selected for additional runs, was IB ANI3, with the decreasing activity likely to be a result of catalyst leaching. This suggests that anionic immobilisation is not strong enough in this instance to allow for reusability of the catalyst.

The 8309F support, which uses a short chain amino linker to covalently bind to the protein, observed a dip in activity in the third run which is likely due to a sampling error as the activity then appears to plateau.

The highest retention of activity was observed with the EziG1 support, a hydrophilic support that uses the His-tag mode of binding. The next two best performing supports also used the His-tag mode of binding, however, both had an observable

decrease in activity by the fifth run. Based on these results, EziG1 was selected to be the support of choice for all future reactions with BmTA.

The activity retention assay was performed in the same way for HypTA as it was for BmTA. Despite a generally greater loading across all the supports (as seen in Figure 42), the activity retention compared to the native protein, as well as that observed for the various immobilised forms of BmTA activity retention, was poor, Figure 48.

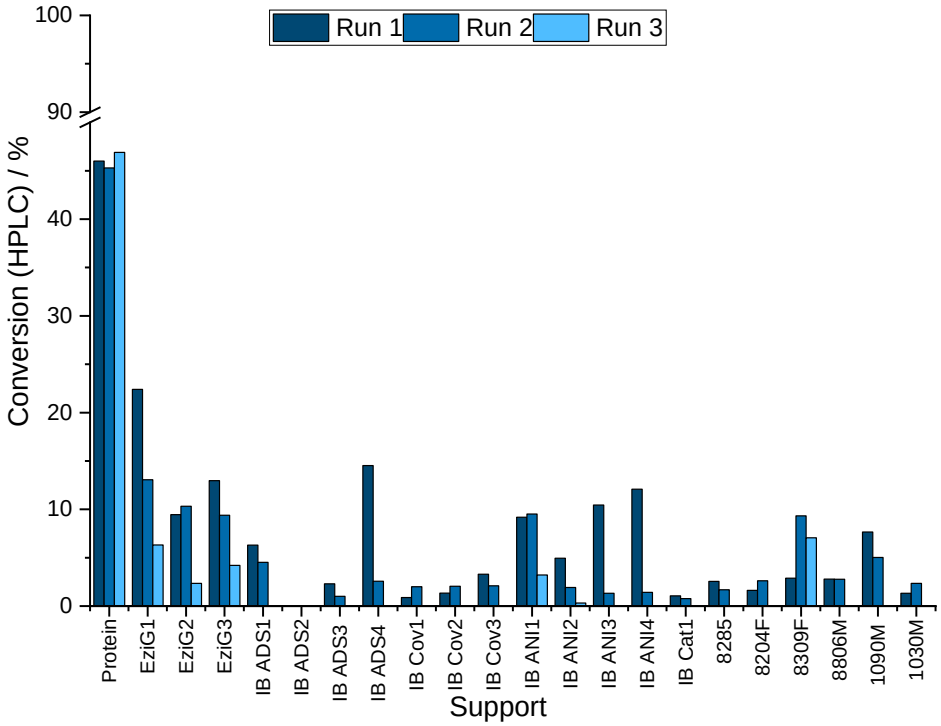

Figure 48: Activity retention assay for immobilised transaminase from Hyphomonas neptunium on a range of immobilisation supports, run 1-3. Reactions were performed at 40 °C in an aqueous buffer (100 mM K_2PO_4, 0.02 mM PLP, pH 8) containing 50 mM 1-acetonaphthone and 250 mM $^{i}PrNH_2$ for 24 h in a thermomixer at 800 rpm. 'Protein' refers to a fresh non-immobilised, purified enzyme in solution-phase. Conversions were calculated using standard curves for both 1'-acetonaphthone and NEA.

All the supports retained less than 50% activity of the native protein within the first run and activity appeared to be less well retained across the three runs when compared to BmTA. The supports utilising his-tag mode of binding (EziG) retain activity better than the other supports, but none with a high enough retention for application within an industrial process.

There was good agreement with BmTA as to the best performing supports, with EziG1, EziG2, EziG3 and 8309F, each retaining activity better than other supports for both enzymes. The fifth support that performed best for HypTA was ANI1 and, in an analogous manner to BmTA, the five best performing supports were subjected to a further 2 runs.

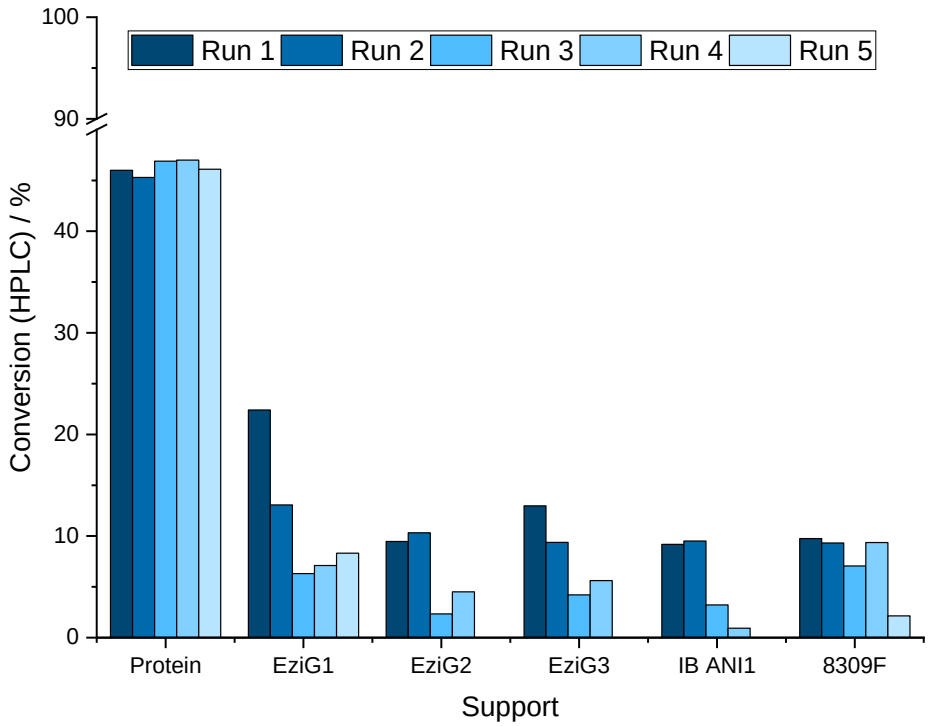

Figure 49: Activity retention assay for immobilised transaminase from Hyphomonas neptunium on selected immobilisation supports. Reactions were performed at 40 °C in an aqueous buffer (100 mM K_2PO_4, 0.02 mM PLP, pH 8) containing 50 mM 1-acetonaphthone and 250 mM $^{i}PrNH_2$ for 24 h in a thermomixer at 800 rpm. 'Protein' refers to a fresh non-immobilised, purified enzyme in solution-phase. Conversions were calculated using standard curves for both 1'-acetonaphthone and NEA.

The poorest performing support, out of the 5 selected for additional runs, was IB ANI1, with a rapid drop off in activity retained observed after the third run. This is in agreement with the observations from BmTA, that anionic immobilisation is not strong enough with these two enzymes to allow for reusability of the catalyst.

As with BmTA, the highest retention of activity was observed with the EziG1 support, a hydrophilic support that uses the his-tag mode of binding. The other two supports

using the his-tag mode of binding, EziG2 and EziG3, both demonstrated markedly different activity retentions to EziG1. After a slight increase in retained activity in the fourth run, likely due to a sampling error in run 3, neither support showed any activity in the fifth run.

The 8309F support, which performed reasonably well with BmTA, retained activity well for the first 4 runs before a considerable decrease in activity in the fifth run. It was, however, the only support aside from EziG1 to show any activity retention in the fifth run.

With EziG1 having the highest activity retention remaining after 5 runs, albeit < 10 %, it was selected to be the support of choice for all future reactions with HypTA. When placed in a PBR and operated within continuous flow, the high local concentration of catalyst may help to increase the conversion to a synthetically useful level.

2.1.6 Optimisation of *(R)*-selective ATA-436

An alternative commercially available transaminase, previously employed in the AstraZeneca route to Savolitinib**,** Figure 50,[208, 209] also made available to us by our industrial partners, was assessed for feasibility for the asymmetric generation of NEA.

Application of ATA-436 alleviated scalability issues with the previously proposed synthetic route, such as a classical resolution to access the desired enantiomer and chromatography requirements.[210]

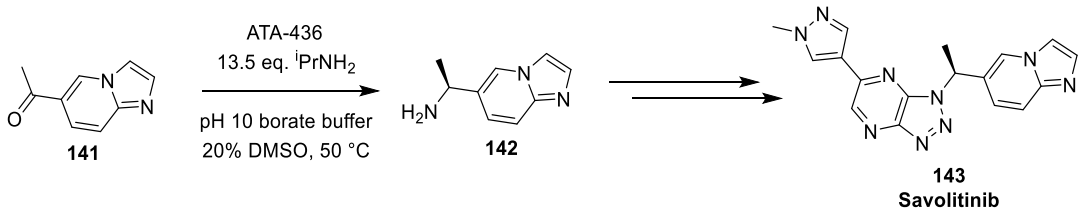

Figure 50: Use of ATA-436 within the synthesis of Savolitinib.

The first-generation mutant enzyme used within the Savolitinib process, ATA-436, is tolerable to high pH, high amino donor equivalency and high DMSO concentrations.

Moreover, due to substrate similarity of the imidazopyridine and naphthyl groups, it was hypothesized that ATA-436 would be a suitable enzyme for the transformation of 1'-acetonaphthone to NEA.

2.1.6.1 Effect of substrate concentration on the transaminase catalysed generation of chiral amines from pro-chiral ketones

Initial screening of the reaction was performed at 10 mM ketone concentration. Whilst this serves as a good comparison between different enzymes and/or different enzyme-support complexes, 10 mM concentration is not suitably high enough for a process.

Consequently, various substrate concentrations were screened. Reactions were performed in 2 mL Eppendorf tubes with 0.9 mL buffered solution (100 mM KH_2PO_4, pH 9) containing 500 mM isopropylamine, 1 mM PLP and 10 mg enzyme. Reactions were initiated upon addition of 100 µL of 1'-acetonaphthone in DMSO. The Eppendorf tubes were then heated (40 °C) and shaken (800 rpm) for 20 h. After this time, 500 µL of reaction mixture was added to 1 mL MeOH and analysed by SFC.

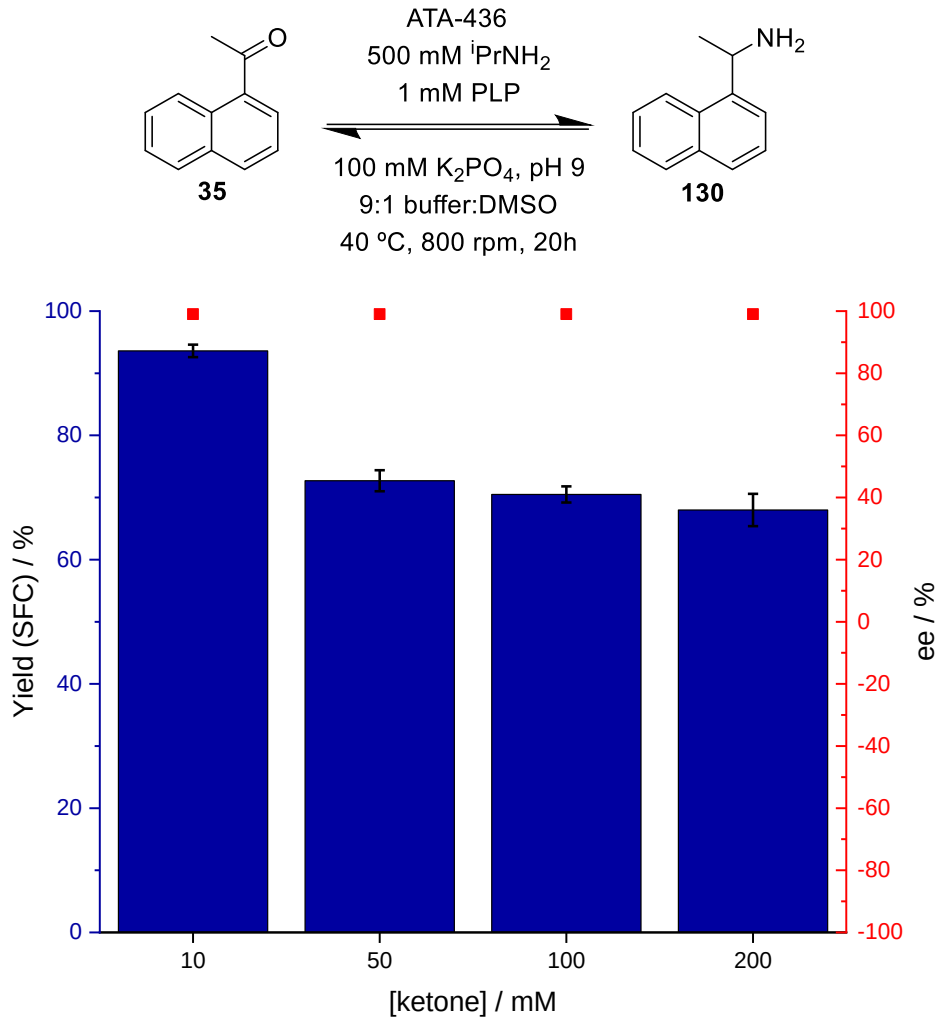

Figure 51: Effect of substrate concentration on yield of transaminase reaction. Reactions were performed in buffer (100 mM KH_2PO_4, pH 9) containing 500 mM isopropylamine, 1 mM PLP, 10 mg enzyme, ketone with 10% DMSO, n =3. Yields were calculated using standard curves for both 1'-acetonaphthone and NEA.

A large drop in conversion is observed when the ketone concentration is increased from 10 to 50 mM. The differences in yield between 50-200 mM, however, are within experimental error. Despite the addition of DMSO as a co-solvent, at 200 mM the reaction mixture remained biphasic due to the poor solubility of acetonaphthone. Subsequently, 100 mM was identified as the optimum concentration for the process.

2.1.6.2 Effect of pH within ATA-436 catalysed reactions

Reactions were performed in 2 mL Eppendorf tubes with 0.9 mL buffered solution (100 mM KH_2PO_4, pH 8-11) containing 500 mM isopropylamine, 1 mM PLP and 10 mg enzyme. Reactions were initiated upon addition of 100 µL of 1'-acetonaphthone (100 mM in DMSO) to give a final ketone concentration of 10 mM. The Eppendorf tubes were then heated (40 °C) and shaken (800 rpm) for 20 h. After this time, 500 µL of reaction mixture was added to 1 mL MeOH and analysed by SFC.

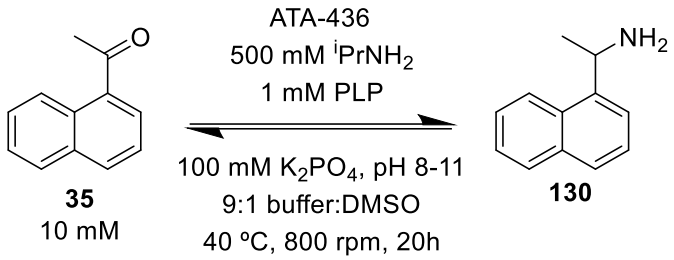

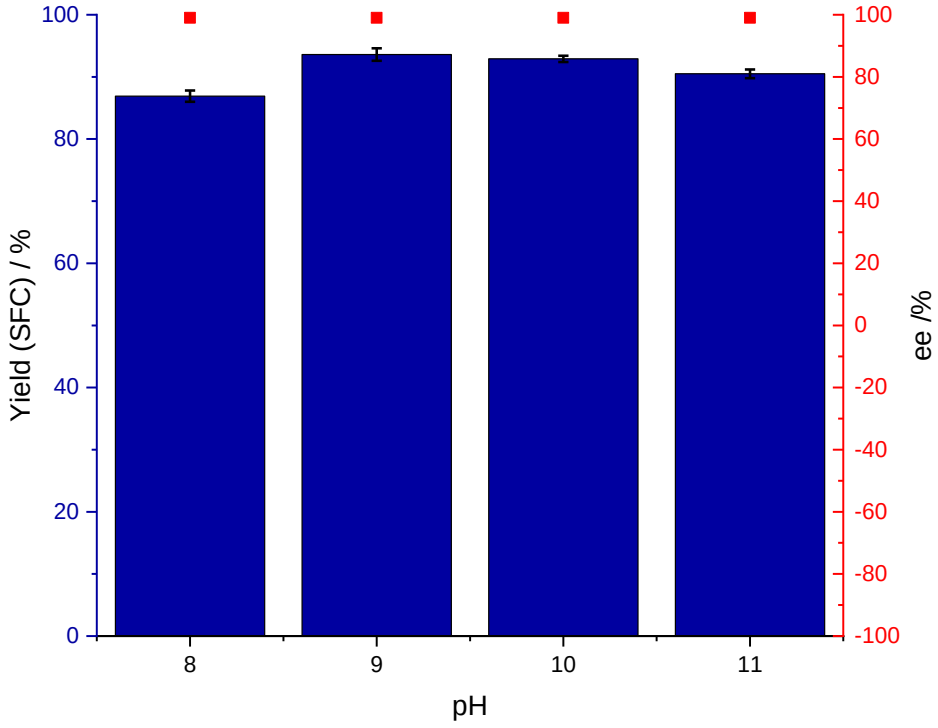

Figure 52: Effect of pH on yield of transaminase reaction. Reactions were performed in buffer (100 mM KH_2PO_4, pH 8-11) containing 500 mM isopropylamine, 1 mM PLP, 10 mg enzyme and 10 mM ketone with 10% DMSO. Yields were calculated using standard curves for both 1'-acetonaphthone and NEA.

As there is minimal difference in yield between the pH values, the optimal pH for the reaction was determined by the extraction properties of the reaction components, discussed in the next section.

2.1.7 pH-based liquid-liquid extraction of amines in continuous flow

With a view towards telescoping the transaminase reaction with a downstream chemocatalytic step in continuous flow, efficient extraction of the amine from the aqueous reaction mixture of the biocatalytic step into an organic solvent is required. The partitioning behaviour of the transaminase reaction components can be mapped using the logP and pKa values of each component, Table 2.

Table 2: Calculated pKa and logP values for the transaminase reaction components. Calculations were performed in percepta ACDlabs.

Compound	**pKa(s)**				**logP**
PLP	1.60 ± 0.1	3.60 ± 0.2	6.10 ± 0.3	8.20 ± 0.1	-0.53 ± 0.31
isopropylamine	10.70 ± 0.3				0.21 ± 0.19
1-acetophenone	-				1.66 ± 0.22
1'-acetonaphthone	-				2.90 ± 0.22
1-(1-phenyl)ethylamine	9.00 ± 0.1				1.44 ± 0.22
1-(1-naphthyl)ethylamine	9.30 ± 0.4				2.67 ± 0.22

Using the predicted values from ACD/Percepta, Table 2, speciation curves of each component can be plotted and the optimal pH for selective extraction can be extrapolated.

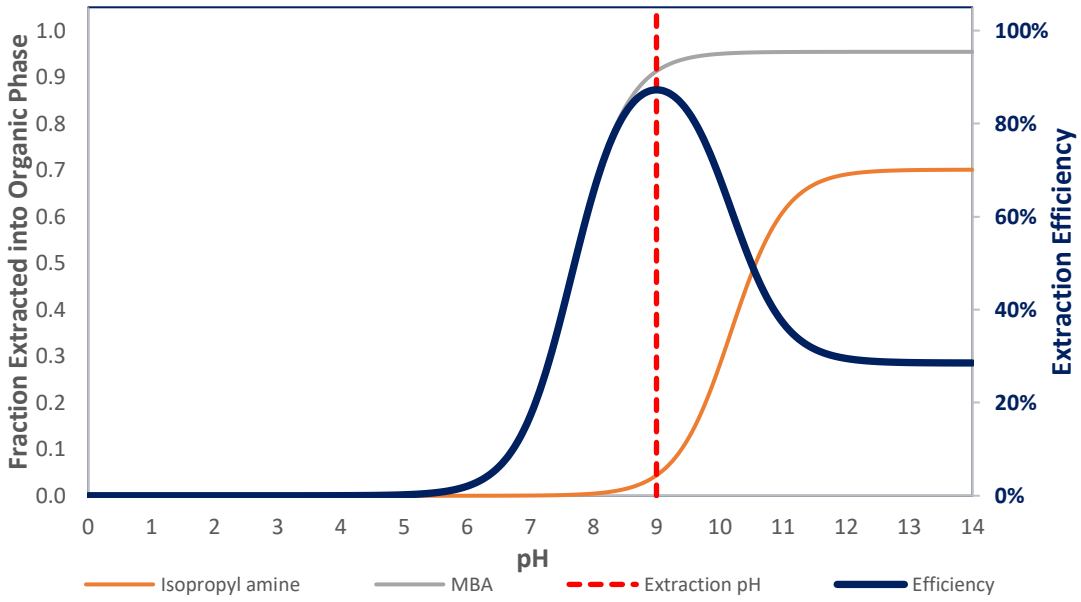

Figure 53: Theoretical speciation and extraction efficiency curves for selective extraction of MBA vs isopropylamine. Volume ratio organic : aqueous = 50:50.

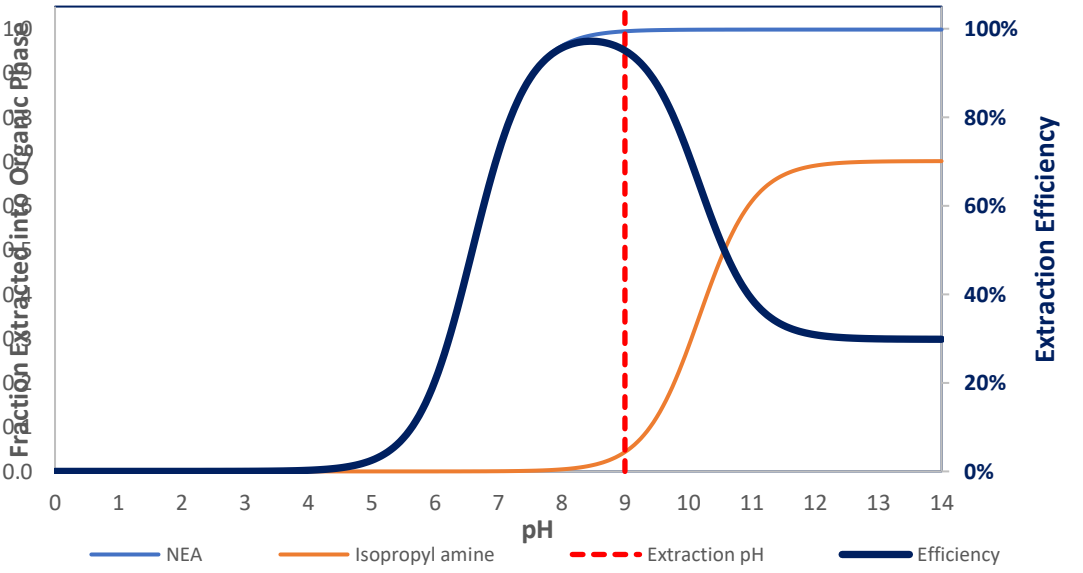

Figure 54: Theoretical speciation and extraction efficiency curves for selective extraction of NEA vs isopropylamine. Volume ratio organic : aqueous = 50:50.

Based on the extraction graphs for both MBA and NEA, the optimum pH for selective extraction of MBA/NEA over isopropylamine is predicted to be pH 8 for NEA and pH 9 for MBA. As the calculations for ACD/Percepta are based on three assumptions: the

solution is aqueous, the temperature is 25 °C and the ionic strength is zero, it is necessary to compare the predictive model to experimental results.

To assess the accuracy of the predictive model, extraction efficiency at three pH values was assessed. A buffered solution (100 mM KH_2PO_4) containing NEA (100 mM), isopropylamine (400 mM), 1'-acetonaphthone (50 mM) and PLP (1 mM) was prepared and adjusted to the relevant pH. An equal volume of buffered solution and isopropyl acetate were then mixed in an orbital shaker for 30 min. The organic layer was then sampled for analysis by GC.

Table 3: Partitioning of NEA, 1'acetonaphthone and isopropylamine at different pH values into isopropyl acetate. Volume ratio 1:1 buffer:isopropyl acetate, concentrations were determined by GC.

pH	[NEA] in organic / mM	[1'-acetonaphthone] in organic / mM	[$^{i}PrNH_2$] in organic / mM
8	56.7 ± 3.5	46.0 ± 1.1	0
9	69.9 ± 4.9	45.2 ± 1.7	0
10	85.3 ± 2.9	46.3 ± 2.3	93.5 ± 5.7

The extraction of 1'-acetonaphthone, as a non-ionisable compound, into isopropyl acetate is invariant to pH. As pH is increased, however, the extraction of NEA into the organic phase increases.

At pH 10, the selectivity of the extraction is decreased as isopropylamine also partitions into the organic phase. This gives an optimal extraction pH of 9, in agreement with the computational model. Subsequently, a pH adjustment after the enzymatic reaction is required when using BmTA or HypTA, to extract the desired amine for reaction in the downstream chemistries.

Whilst the extraction efficiency for NEA at pH 9 is only 70%, a second extraction with isopropyl acetate was able extract a further 21 mM to give a total extraction efficiency of 91%. This demonstrated that the use of a multi-stage or counter-current extraction unit within continuous flow could increase the extraction efficiency close to 100%.

2.1.8 Homogeneous transaminase reactions in continuous flow

Modification of ATA-436, including immobilisation, is prohibited by an intellectual property agreement with the enzyme's manufacturer (Codexis), and consequently a homogeneous-homogenous continuous flow cascade was hypothesized. Before the cascade could be realised, the activity of ATA-436 within a homogenous continuous flow system needed to be assessed.

Reactions were performed within a series of fReactor CSTR units, with a 60 min residence time. Into the first of the series of fReactors, a buffered solution (10% DMSO, 100 mM KH_2PO_4, pH 9) containing 1'-acetonaphthone (200 mM), isopropylamine (500 mM), PLP (1 mM) and ATA-436 (2.5 mg mL^{-1}) was fed.

The outlet of the final fReactor in series was collected in reactor volumes, sampled immediately, diluted with MeCN and analysed by HPLC. The collected reactor volumes were then left at room temperature overnight, to assess residual enzyme activity, sampled, diluted with MeCN and analysed by HPLC.

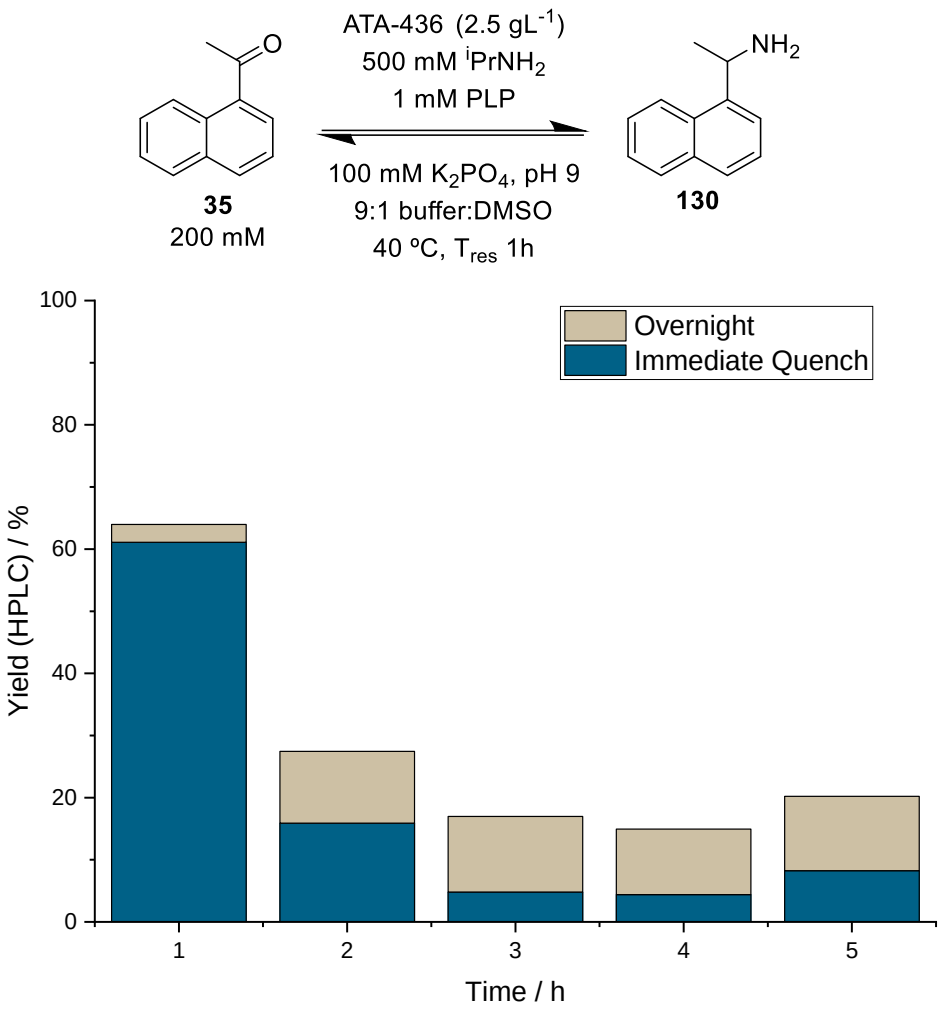

Figure 55: Continuous flow transaminase catalysed reaction of 1'-acetonaphthone. Reactions were performed in a buffered solution (10% DMSO, 100 mM KH2PO4, pH 9) containing 1'-acetonaphthone (200 mM), isopropylamine (500 mM), PLP (1 mM) and ATA-436 (2.5 mg mL^{-1}) within fReactor CSTR units with a T_{res} of 60 min. Yields were calculated using standard curves for both 1'-acetonaphthone and NEA.

After one reactor volume, the HPLC yield of NEA was pleasingly high (61%), however, this yield decreased in subsequent reactor volumes with steady state yield of ca. 10%. When the samples were re-analyzed after 18 h at room temperature, all the samples showed an increase in yield, indicating that the ATA-436 was still active, despite the active mixing within the fReactors.

Despite the low yield of the reaction at steady state, the retention of activity of the enzyme was promising. This suggested that if the enzyme could maintain activity after an in-line separation, it could be recirculated with the PLP cofactor.

2.1.8.1 Homogeneous Transaminase Reactions with in-line separation in continuous flow

To assess the feasibility of recycling the transaminase and cofactor, a continuous flow homogenous transaminase reaction was performed and coupled to a membrane-based extraction unit.

Reactions were performed within a series of fReactor CSTR units, with a 60 min residence time. Into the first of the series of fReactors, a buffered solution (10% DMSO, 100 mM KH_2PO_4, pH 9) containing 1'-acetonaphthone (200 mM), isopropylamine (500 mM), PLP (1 mM) and ATA-436 (2.5 gL^{-1}) was fed.

Into the final fReactor in series, a stream of isopropyl acetate was pumped to give a 1:1 buffer:isopropyl acetate ratio. The outlet of the CSTR containing a biphasic mixture was then allowed to flow through a SEP-10 liquid-liquid separator (Zaiput Flow Technologies) fitted with an OB-900 membrane. The aqueous and organic outlets of the liquid-liquid separator were collected separately in aliquots corresponding to the total reactor volume.

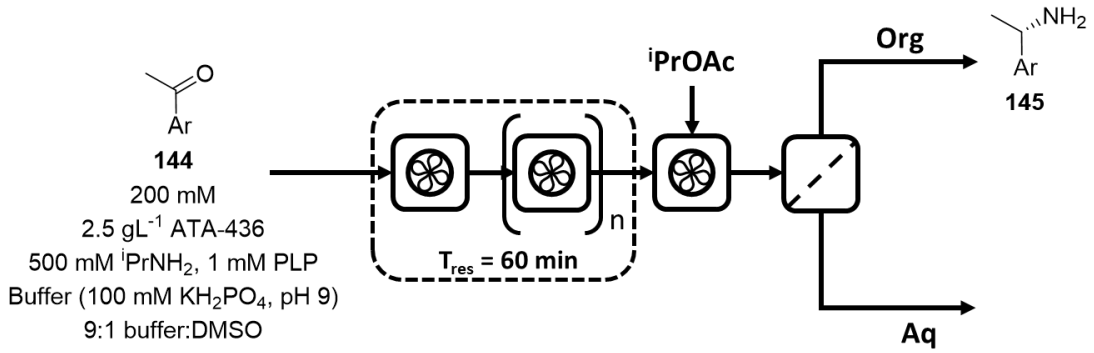

Figure 56: Schematic of homogeneous transaminase reaction with in-line separation in continuous flow. Reactions were performed within a series of fReactor CSTR units, with a 60 min residence time with a buffered solution (10% DMSO, 100 mM KH_2PO_4, pH 9) containing 1'-acetonaphthone (200 mM), isopropylamine (500 mM), PLP (1 mM) and ATA-436 (2.5 gL^{-1}).

After 2.5 h of operation, the organic phase began to be retained by the separator, suggesting that the membrane had become fouled. Upon disassembly of the separator, the extent of fouling was evident.

Figure 57: Photo of membrane of disassembled membrane separator after 2.5h of operation.

Whilst it was possible to recover the membrane through washing with weak HCl, the clogging of the membrane in under 3 h of operation drastically impacts the feasibility of using transaminase homogeneously in flow. Moreover, membrane recovery required the dismantling of the separator and could not be done in continuous flow.

With the low steady state conversions observed at 2.5 gL^{-1} enzyme and increasing enzyme loading likely to lead to elevated membrane fouling, using transaminase homogeneously in flow, for this process, was deemed inconceivable.

2.1.9 Immobilised Transaminase Reactions in Continuous Flow

With homogenous continuous flow transaminase reactions not feasible, attention was turned to performing reactions using immobilized forms of the wild-type BmTA.

2.1.9.1 Reactor set up

The continuous reactor set up consisted of immobilised enzyme loaded into an Omnifit® EZ glass chromatography column (10 mm ID, 2.75 mL reactor volume) contained within an aluminium heating block, heated by a stirrer hotplate, Figure 58. Reagent feeds were introduced into the system using a JASCO PU-980 HPLC pump or a Harvard Apparatus Model 22 syringe pump. PTFE tubing (1/8" ID) was used to connect the syringe pump to the reactor and from the outlet of the reactor to a collection vessel.

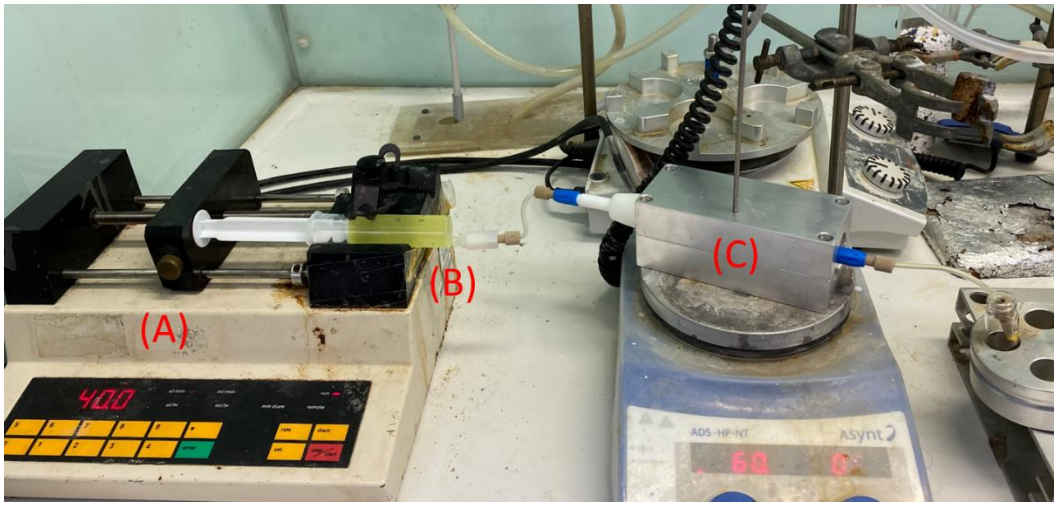

Figure 58: Continuous PBR set up where (A) is a Harvard Apparatus Model 22 syringe pump (B) a syringe containing 100 mM ketone, 500 mM $^{i}PrNH_2$ and 0.02 mM PLP in a buffered solution (100 mM KH_2PO_4, pH 8) and (C) a PBR containing EziG1-BmTA.

All future flow reactions followed the general procedure: 0.8 g of EziG1-BmTA was transferred into the Omnifit® column. The column was then installed within the heating block and a buffered solution (100 mM KH_2PO_4, 0.2 mM PLP, pH 8) pumped through the reactor at room temperature, to purge any air from the system, then the reactor was heated to 40 °C. A buffered solution (100 mM KH_2PO_4, 0.2 mM PLP, pH 8) of ketone (100 mM) and isopropylamine (500 mM) was then pumped through the reactor at the specified flow rate. The flow rate required was calculated using Equation 1, with a volume calculated using Equation 2 and the desired residence time.

$$Flow\ rate\ (mL\ min^{-1}) = \frac{Reactor\ volume\ (mL)}{Residence\ time\ (min)}$$

Equation 1: Flow rate calculation.

$$\boldsymbol{Reactor\ volume\ (mL) = \frac{mass\ of\ dry\ PBR\ (g) - mass\ of\ wet\ PBR\ (g)}{density\ of\ solvent\ (g\ mL^{-1})}}$$

Equation 2: Reactor volume calculation. Where mass of dry PBR denotes the mass of the enzyme-support complex within the PBR before addition of solvent and mass of wet PBR corresponds to the mass of the PBR after wetting with reaction solvent, until all air bubbles have been removed from the system.

The reactor volume was assigned as the volume of EziG[1]-BmTA within the Omnifit® column, as control reactions demonstrated that the reaction only proceeds in the presence of transaminase, therefore, no reaction was occurring in the PTFE tubing before entering the reactor or in the outlet PTFE tubing. The outlet stream was collected in aliquots corresponding to the total reactor volume and analysed by chiral HPLC before the solvent was removed under reduced pressure and the crude residue analysed by NMR.

2.1.9.2 Stability of immobilized transaminase within a PBR in continuous flow

For the continuous flow reactions, a packed bed reactor filled with immobilized enzyme was placed inside a heating jacket that was heated to 40 °C, Figure 59. The reactor was used in continuous flow mode for a duration of 8 h, with the conversion of the reaction monitored by chiral HPLC, Figure 59.

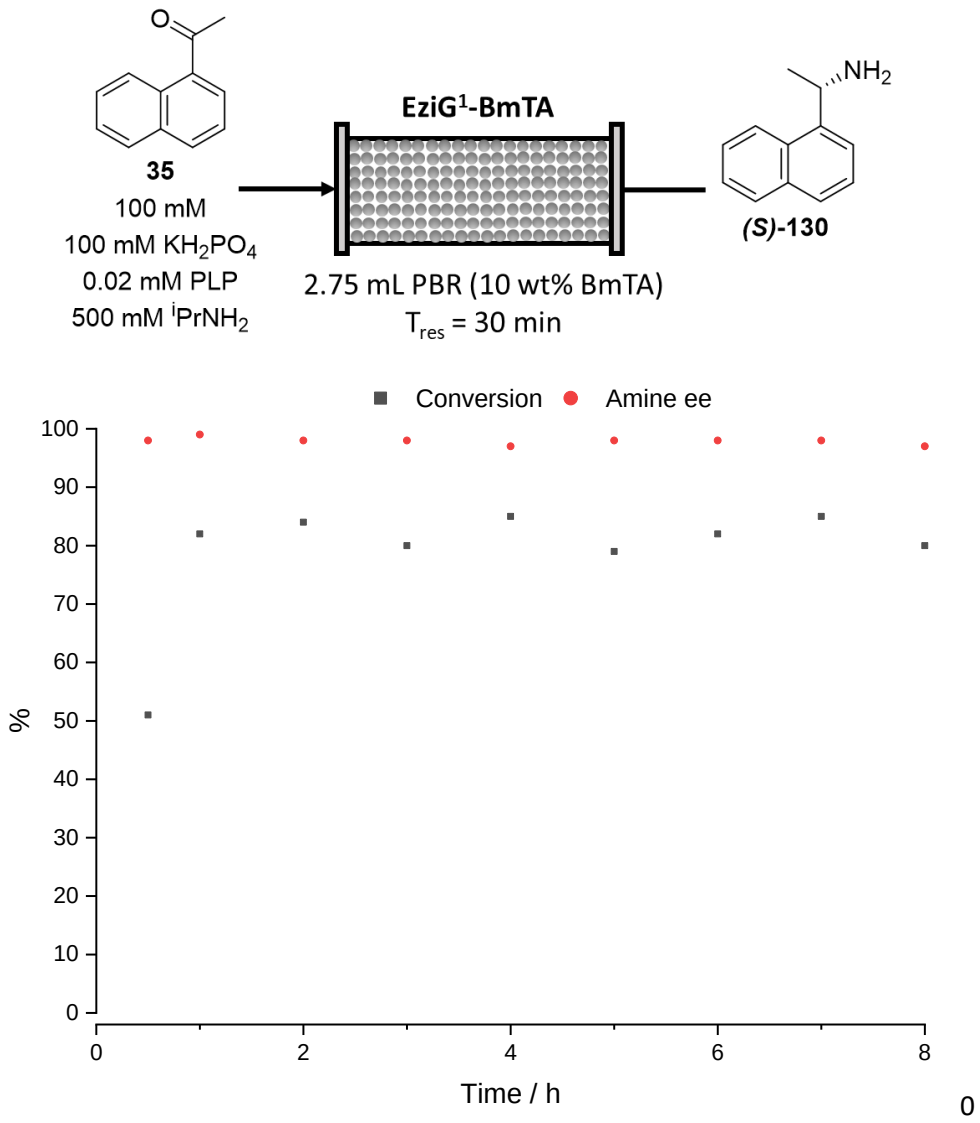

Figure 59: Conversion of 1'-acetonaphthone to 1-(1-naphthyl)ethylamine in continuous flow, catalysed by EziG1-BmTA. Reactions were performed at 40 °C in an aqueous buffer (100 mM K_2PO_4, 0.02 mM PLP, pH 8) containing 100 mM 1-acetonaphthone and 500 mM $^{i}PrNH_2$ with a residence time (T_{res}) of 30min. Conversions were calculated using standard curves for both 1'-acetonaphthone and NEA.

After 1h of operation, steady state equilibrium was reached, with an average conversion of 84% to NEA. This level of activity was maintained for 8h of operation. Pleasingly, the enantioselectivity of the BmTA was also maintained above 98% (determined by HPLC) for the duration of the process.

The stability of the catalyst after storage was also investigated. After use, the PBR filled with EziG1-BmTA was washed with 3x reactor volume of aqueous buffer (100

mM KH_2PO_4, 0.2 mM PLP, pH 8) and stored at 4 ºC for 12 h. There was no observable loss of activity when the catalyst was then re-used, with conversion maintained at 84% and *ee* >98%, Figure 59.

With promising results observed for NEA, attention was turned to the formation of MBA from acetophenone, Figure 60.

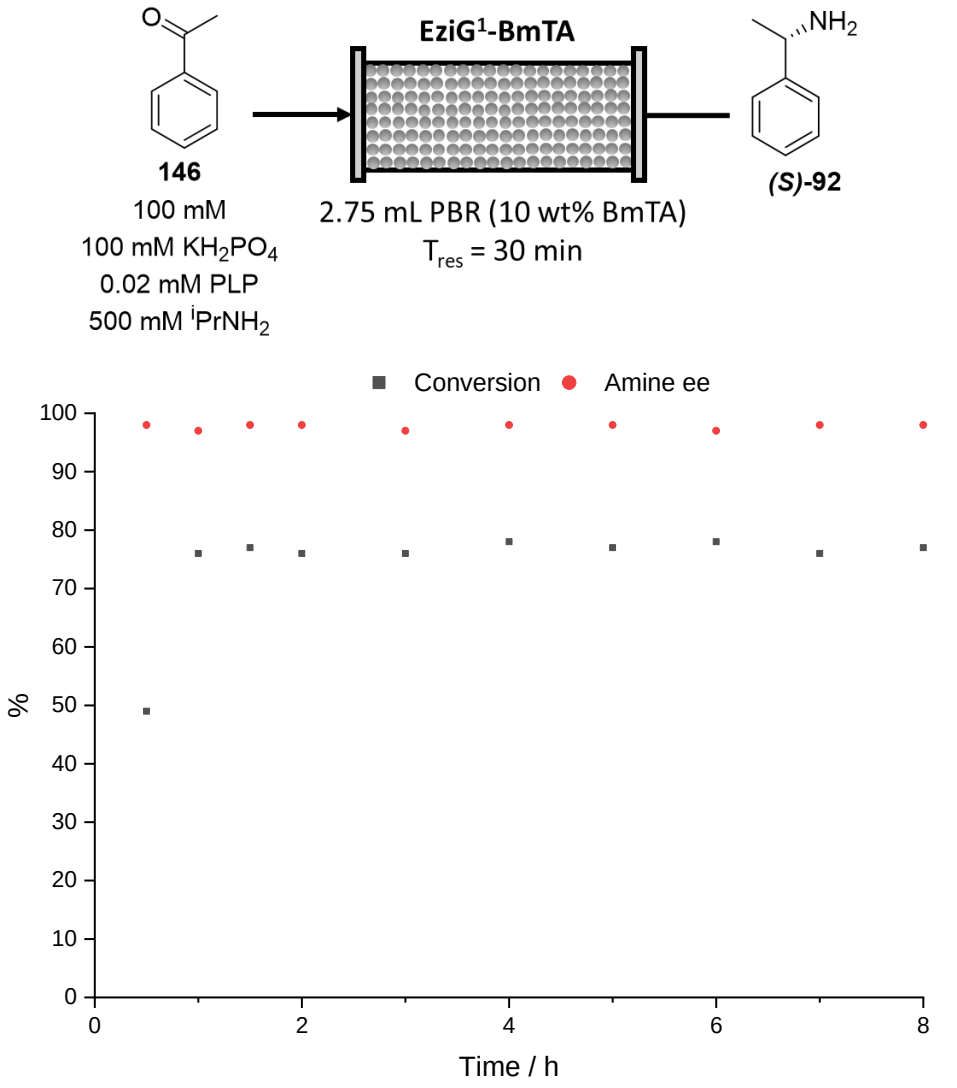

Figure 60: Conversion of 1'-acetonphenone to 1-phenylethylamine in continuous flow catalysed by EziG1-BmTA. Reactions were performed at 40 °C in an aqueous buffer (100 mM K_2PO_4, 0.02 mM PLP, pH 8) containing 100 mM 1-acetonaphthone and 500 mM $^iPrNH_2$ with a residence time (T_{res}) of 30min. Conversions were calculated using standard curves for both 1'-acetophenone and 1-phenylethylamine.

After 1h of operation, steady state equilibrium was reached, with an average conversion of 77% to MBA, slightly lower than that observed for NEA. This level of activity was maintained for 8h of operation. Pleasingly, the enantioselectivity of the BmTA was also maintained above 97% for the duration of the process.

Wary of the potential of enzyme leaching, the product stream from the 1'-acetophenone flow set up was also sampled for use in a Bradford assay. After each reactor volume, 40 µL was sampled from the product steam and mixed with 1960 µL stock solution of Bradford reagent. Absorption at 595 nm was measured, following a 5 min incubation at room temperature, and plotted against an external standard.

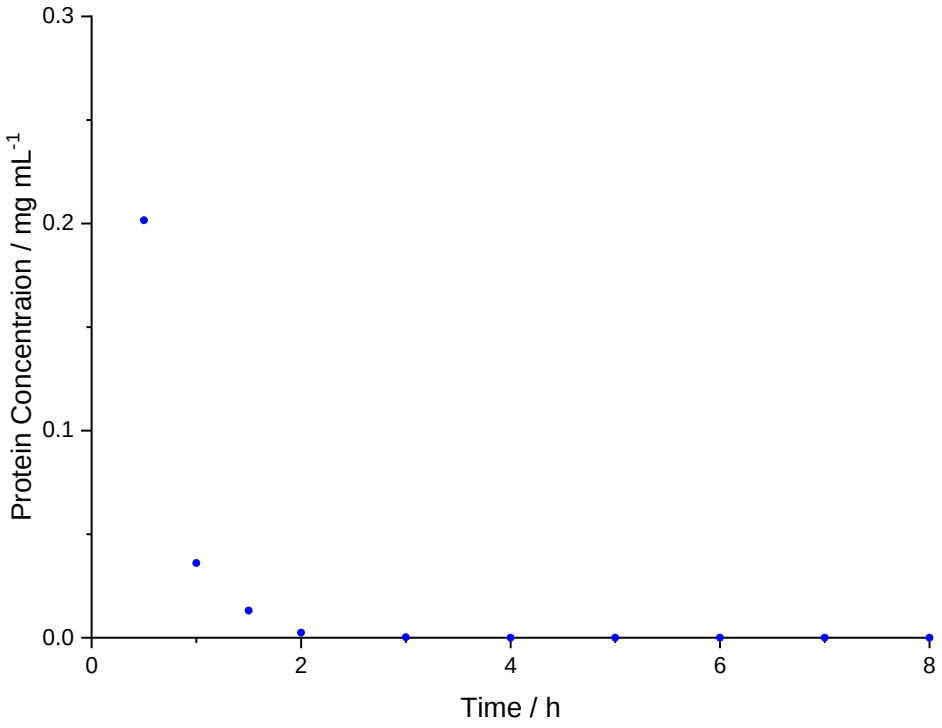

Figure 61: Protein concentration in the product stream for the conversion of 1'-acetonphenone to 1-phenylethylamine in continuous flow by EziG1-BmTA. Reactions were performed at 40 °C in an aqueous buffer (100 mM K_2PO_4, 0.02 mM PLP, pH 8) containing 100 mM 1-acetonaphthone and 500 mM $^{i}PrNH_2$ with a residence time (T_{res}) of 30min, n =1.

Within the first reactor volume, considerably more protein leached compared to other stages of the reaction. Over the next three reactor volumes, the concentration of protein in the product stream decreases dramatically. This suggests weakly bound protein is washed off the support in the early stages of the process whilst the reactor reaches steady state.

After four reactor volumes, the protein concentration appears to plateau, below the lower limit of quantification (LLOQ) of 12.5 µg mL^{-1} of protein for the Bradford assay, suggesting that there is minimal enzyme leaching throughout the rest of the process.

2.1.9.3 Reaction Metrics

With the optimum reaction conditions of 30 min T_{res}, 40 °C and 100 mM applied, a space time yield (STY) for the process was calculated according to Equation 3.[211]

$$STY\ (g\ L^{-1}h^{-1}) = \frac{Moles\ of\ Product\ (mol)\ x\ MW\ (g\ mol^{-1})}{t_{res}\ (h)\ x\ Reactor\ Volume\ (L)}$$

Equation 3: STY calculation, where MW is the molecular weight of the product and the reactor volume is the volume of the PBR calculated using Equation 2.

The optimum conditions determined in conversion to NEA (84 mM) provided a STY of 376 g L^{-1} day^{-1} and 244 g L^{-1} day^{-1} for the conversion to MBA (77 mM). Through increasing the reactor size, a larger amount of catalyst could be used, leading to a shorter reaction time and an increase in STY.

To compare the waste associated with the transaminase production of NEA and MBA, E factors were determined according to Equation 4.[212]

$$E\ factor = \frac{mass\ of\ amino\ donor + mass\ of\ ketone + mass\ of\ acetone - mass\ of\ amine}{mass\ of\ amine}$$

Equation 4: E factor calculation for transaminase catalysed reaction.

With 5 equivalents of isopropylamine as the amino donor, an E factor of 1.24 and 2.45 was calculated for NEA and MBA respectively. If fewer equivalents of amino

donor could be used, this would decrease the E factor, as less waste would be generated. The transaminase, support, co-catalyst and solvent were all excluded from the calculation as it was assumed that they could be recycled.

2.2 Examination of lipase-mediated kinetic resolution of racemic amines

Lipase-mediated kinetic resolution offers an alternative enzymatic system to access the same chiral amine intermediates produced by transaminase. Moreover, lipase-mediated kinetic resolution has previously been used as an alternative route to enantiopure aminoindanes in the place of a transaminase.[213]

Despite the well-documented high enantioselectivities possible using lipases,[214, 215] the maximum theoretical yield of a kinetic resolution is only 50%, in comparison to the transaminase reaction, where the maximum theoretical yield is 100%.

A potential advantage of lipase-mediated reactions over transaminases is compatibility with organic solvents.[216-218] Transaminases are generally limited to buffered aqueous solutions, with a relatively limited pH range, whilst also limited by compatibility with only small quantities of co-solvent.[160, 188, 219] In comparison, lipases have a broad solvent compatibility, with lipases frequently performing equally as well in organic solvents such as toluene and isopropyl acetate as they do in aqueous buffer.[216-218]

Moreover, lipases were one of the first classes of enzyme to be immobilized and mass produced in their immobilized form,[220] which is critical for operating within a PBR in continuous flow.

Novozym 435 was selected as one of the lipases that should be screened for the kinetic resolution, having previously been demonstrated for the kinetic resolution of MBA with a range of different acyl donors in continuous flow, Figure 62.[214]

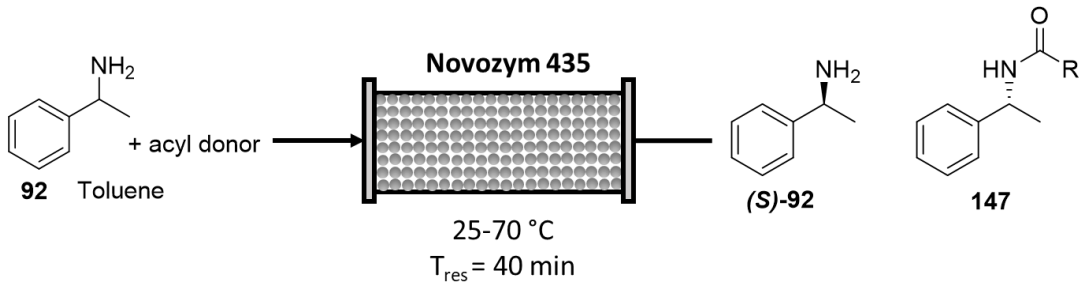

Figure 62: Previously demonstrated kinetic resolution of MBA (0.08 M) in continuous flow, using various acyl donors (0.32 M) at a range of temperatures within toluene.

The effect of the acyl donor was found to have a profound effect on the enantiomeric excess, with more reactive donors, such as isopropenyl acetate, resulting in non-enzymatic acylation. In contrast, use of simpler acyl donors such as ethyl acetate requires higher reaction temperatures and pre-loading of the enzyme with acyl donor to achieve better conversions.[132, 214]

The use of a solvent that also functions as an acyl donor would also be beneficial as it could facilitate the proposed downstream chemocatalytic methodologies without additional components being present in the reaction mixture. Isopropyl acetate, a green alternative to ethyl acetate,[221] would be able to serve as both the solvent and acyl donor, as previously demonstrated with ethyl acetate.[51]

2.2.1 Screening of potential non-enzymatic acylation of amines

As it has previously been demonstrated that more reactive acyl donors can lead to non-enzymatic acylation, it was important to investigate if any acylation occurred in absence of lipase. Subsequently, NEA (100 mM) was refluxed in isopropyl acetate, conditions that are considerably more extreme than the reaction conditions proposed for the enzymatic reaction, Figure 63.

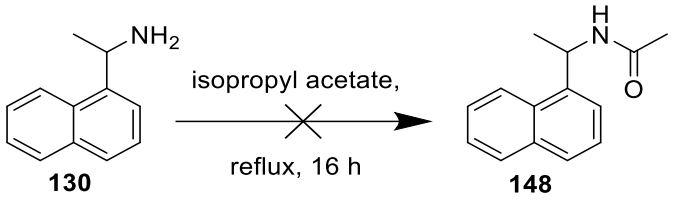

Figure 63: Non-enzymatic acylation screen using NEA within isopropyl acetate. Reaction was performed in isopropyl acetate with 100 mM NEA at reflux (90 °C).

After 16 h, no acetylated product was detected, therefore, it was concluded that acylation can only proceed in the presence of lipase.

2.2.2 Screening of immobilised lipases in batch

To investigate the feasibility of the lipase-mediated kinetic resolution, 6 different immobilized lipases were screened for the kinetic resolution of NEA, Figure 64. Within the pool of 6 commercially available lipases selected for screening, Novozym 435 (*Candida antarctica)*, Lipozme RM (*Rhizmucor miehei*) and Lipozyme TL 1M (*Thermomyces lanuginosus*) have all previously been reported for amine kinetic resolutions,[214] whilst ImmCalB-ADS4 (*Candida antarctica)*, Lipomod 34 MDP *(Candida Cylindracea (Rugosa))* and Lipase 004 have demonstrated high activity for resolution of esters[222] or for transesterification.[223]

Screening reactions for the kinetic resolution of NEA (100 mM) were performed in isopropyl acetate, with 0.1 wt% lipase at 40 °C for 16 h, Figure 64.

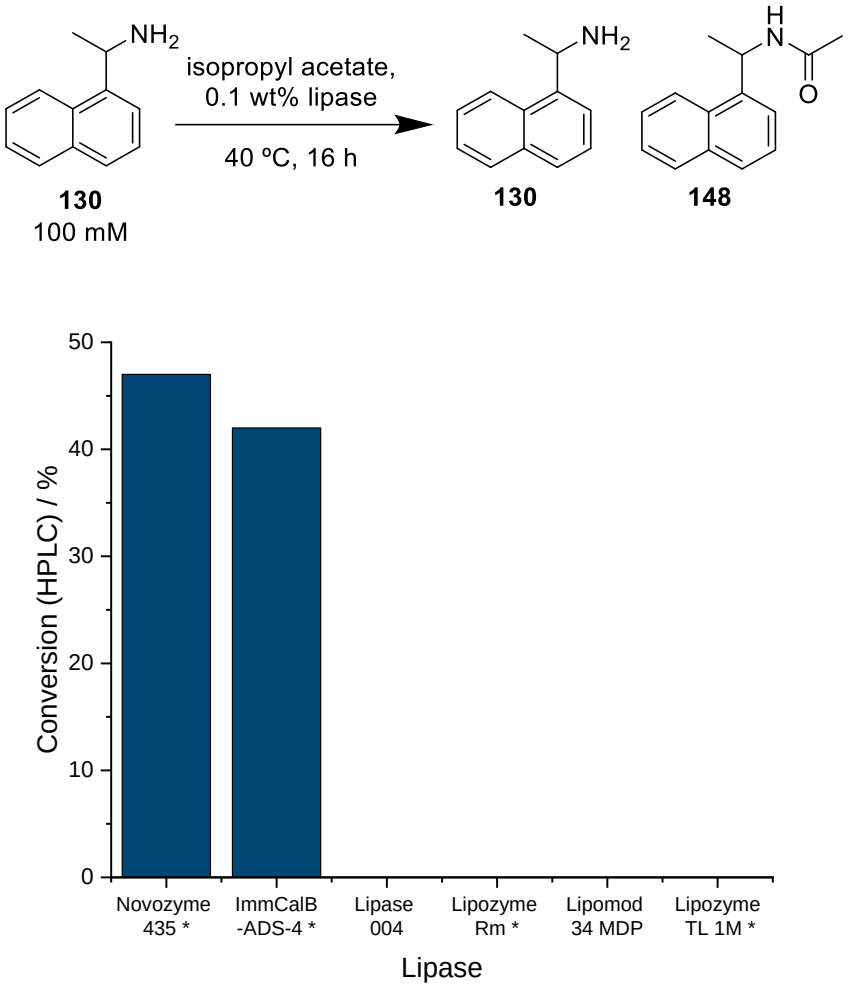

Figure 64: Batch screen results of 6 different immobilised lipase. Reactions were performed at 40 °C in isopropyl acetate containing 100 mM NEA for 24 h in a thermomixer at 800 rpm. Enzymes immobilised on beads are represented with an asterisk, with the remaining immobilised enzymes being powder-based. Conversions were calculated using standard curves for both 130 and 148.

Of the six enzymes screened, only two were found to be active in the reaction conditions. Both active catalysts were different immobilised forms of the same enzyme, *Candida antarctica* Lipase B (CaLB). Subsequently both forms of the enzyme had the same enantioselectivity within the reaction, producing the *(R)*-amide.

CaLB is one of the most stable commercially available lipases[224, 225] and is one of the most widely used lipases in synthetic chemistry.[215, 226, 227] Owing to its greater activity than ImmCalB-ADS-4, Novozym 435 was selected for the kinetic resolution of the racemic mixture of the corresponding chiral amine intermediate.

As Novozym 435 is a hydrophobic support, CaLB is adsorbed to the surface *via* interfacial activation, the mechanism of action for lipases. When CaLB is adsorbed to a hydrophobic surface, a polypeptide "lid" that covers the active site is fixed in an open state, fully exposing the active site. The "open" form of a lipase molecule can stabilise other lipases, often leading to the immobilisation of aggregates.[228-230]

One of the major limitations of interfacial activation as a mode of immobilisation is that enzyme leaching from the support is possible with use of detergents,[231] high temperatures or organic (co-)solvents.[232, 233] This has the potential to hinder the control of a reaction as it is possible for reactions to continue with leached enzyme outside of the reactor.[234]

Furthermore, the support itself being soluble in organic media is another cause of concern. It has previously been demonstrated that polymethacrylate and divinylbenzene, two components of the resin, can be found dissolved in short chain alcohols.[235-238] Currently, there are limited reports of this being a problem,[232] but it is possible that if this effect occurs with a broader range of organic solvents, it could be detrimental to the use of Novozym at an industrial level.

2.2.3 Lipase-mediated kinetic resolution in continuous flow

To allow for reaction monitoring, a racemic amide sample was prepared for both NEA and MBA, using standard conditions, Figure 65.[239]

Figure 65: Synthesis of racemic amide products from the corresponding amine.

For operation in continuous flow, the solubility limit of both the amine and amide in isopropyl acetate needed to be found. NEA, MBA and *N*-acetyl-1-phenylethylamine were all soluble up to 300 mM, however, *N*-acetyl-1-(1-naphthyl)ethylamine was

demonstrated to be insoluble above 100 mM. Therefore, all subsequent continuous flow lipase reactions were carried out with 200 mM of *rac*-amine in isopropyl acetate, to allow for the solubility of the amide product.

2.2.3.1 Reactor set up

The continuous reactor set up consisted of an Omnifit® EZ glass chromatography column (10 mm ID, 2.61 mL reactor volume) contained within an aluminium heating block, heated by a stirrer hotplate, Figure 66. Reagent feeds were introduced into the system using a JASCO PU-980 HPLC pump or a Harvard Apparatus Model 22 syringe pump. PTFE tubing (1/8" ID) was used to connect the syringe pump to the reactor and from the outlet of the reactor to a collection vessel.

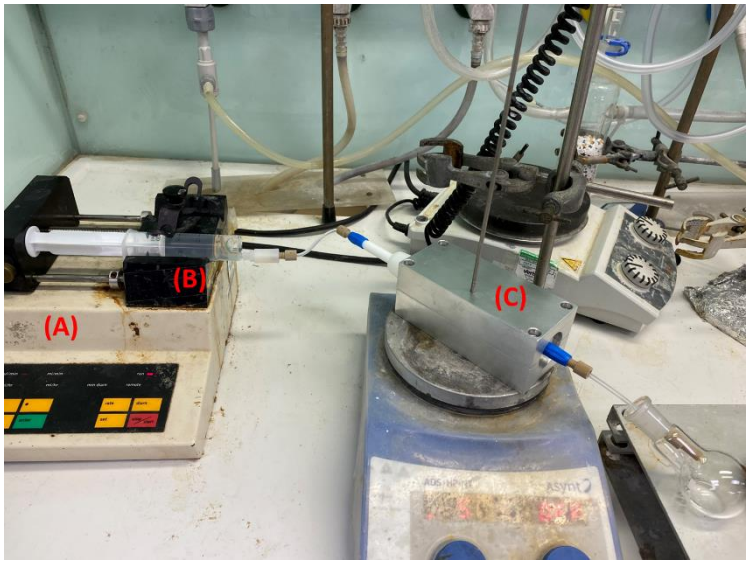

Figure 66: Continuous PBR set up where (A) is a Harvard Apparatus Model 22 syringe pump (B) a syringe containing 200 mM amine in ^{i}PrOAc and (C) a PBR containing Novozym 435.

All future flow reactions followed the general procedure: 1 g of Novozym 435 was transferred into an Omnifit® column. The column was then installed within a heating block and isopropyl acetate pumped through the reactor at room temperature, to purge any air from the system, before the reactor was heated to 40 °C. Once the reactor reached 40 °C, the reaction mixture was pumped through the reactor at the

specified flow rate. The flow rate required was calculated using Equation 1, with reactor volume calculated using Equation 2 and the desired residence time.

The reactor volume was assigned as the volume of Novozym 435 within the Omnifit® column, as control reactions demonstrated that the reaction only proceeds in the presence of Novozym 435, therefore, no reaction was occurring in the PTFE tubing before entering the reactor or in the outlet PTFE tubing. The outlet stream was collected in aliquots corresponding to the total reactor volume and the crude residue analysed by NMR and chiral HPLC.

2.2.3.2 Stability of Novozym 435 within a PBR in continuous flow

Novozym 435 has previously been demonstrated to function well within a PBR in a continuous flow step up for the kinetic resolution of MBA[132, 214], therefore, the PBR was subjected to a long operation time in order to observe any loss of activity.

Due to the lower solubility of the naphthylacetamide, as well as it being used in the previous screen, NEA was selected for the first lipase-mediated kinetic resolution in continuous flow, Figure 67. It had been previously demonstrated with MBA that 50 % conversion and 99% *ee* of both amide and amine can be achieved with a residence time of 30 min,[132] therefore, a 30 min residence time was selected to monitor any catalyst degradation for the kinetic resolution of NEA.

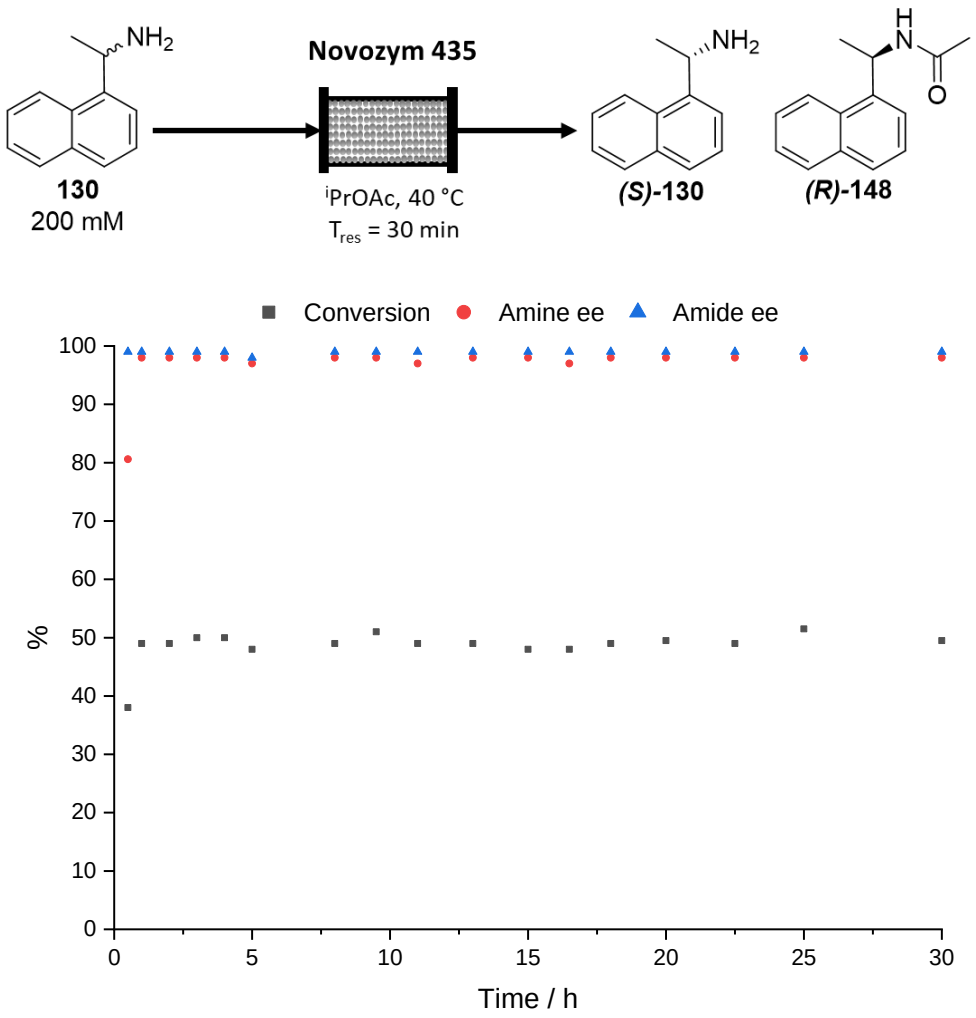

Figure 67: Conversion of rac-1-(1-naphthyl)ethylamine to (R)-N-acetyl-1-(1-naphthyl)ethylamine in continuous flow catalysed by Novozym 435. Reactions were performed at 40 °C in isopropyl acetate containing 200 mM rac-amine with a residence time (T_{res}) of 30 min and a PBR volume of 2.61 mL. Conversion was monitored by ^{1}H NMR against an internal standard and ee determined by HPLC.

There was no observable decrease in activity within this time scale, with excellent conversion (49.3% ± 0.5%) and enantiomeric excesses for amide (98.9% ± 0.1%) and residual amine (97.8% ± 0.2%). After 2 residence times (1 h) of operation, steady state was reached, with complete (50%) conversion to the acetamide being observed.

The stability of the catalyst after storage was also investigated. After use in a kinetic resolution of NEA, the PBR filled with Novozym 435 was washed with 3x reactor

volume of isopropyl acetate and stored at 4 °C for 24 h. There was no observable loss of activity when the catalyst was then re-used, with conversion maintaining > 49% for a further 8 h of operation.

With the longevity and reusability of the support already being demonstrated with NEA, a shorter length recyclability test was performed utilising MBA, utilising the same reaction conditions as above.

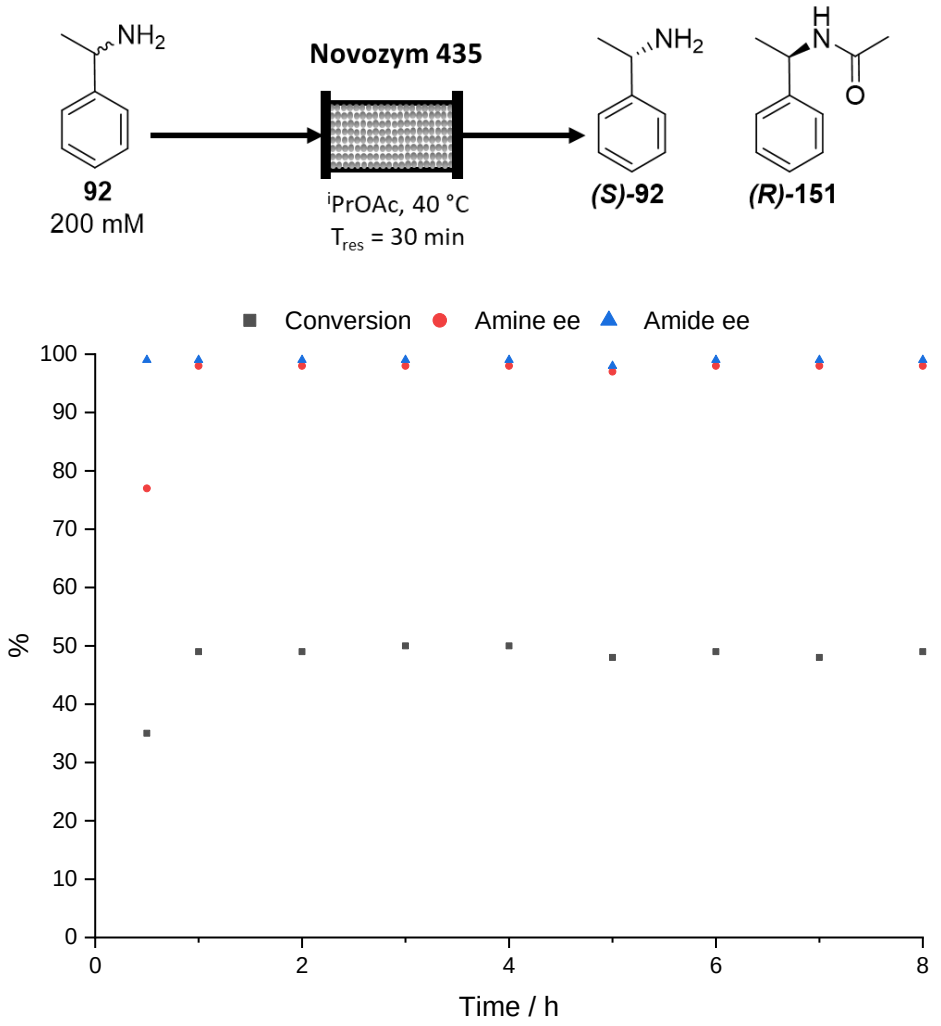

Figure 68: Conversion of rac-1-phenyl-ethylamine to (R)-N-acetyl-1-phenylethylamine in continuous flow catalysed by Novozym 435. Reactions were performed at 40 °C in isopropyl acetate containing 200 mM rac-amine with a residence time (T_{res}) of 30 min and a PBR volume of 2.61 mL. Conversion was monitored by ^{1}H NMR against an internal standard and ee determined by HPLC.

As observed for NEA, after 2 residence times of operation, steady state was reached and maintained for 8 h of operation with excellent conversion (49.5% $\pm$ 0.7%) and enantiomeric excesses for amide (98.8% $\pm$ 0.3%) and residual amine (97.9% $\pm$ 0.3%).

Wary of the potential for enzyme leaching, the product stream from the MBA flow set up was also sampled for use in a Bradford assay. After each reactor volume, 40 µL was sampled from the product steam and mixed with 1960 µL stock solution of Bradford reagent. Absorption at 595 nm was measured, following a 5 min incubation at room temperature, and plotted against an external standard.

At each time point, the absorbance value remained below the lower limit of quantification (LLOQ) of 12.5 µg mL^{-1} of protein for the Bradford assay. This suggests that there is no observable enzyme leaching of the enzyme from the support throughout its operation within a PBR.

2.2.3.3 Reaction Metrics

With the optimum reaction conditions of 30 min T_{res}, 40 °C and 200 mM *rac*-amine applied, a space time yield (STY) for the process was calculated according to, Equation 3.[211] The optimum conditions determined gave conversions of 471 g L^{-1} day^{-1} for *(S)*-NEA and 334 g L^{-1} day^{-1} for *(S)*-MBA. The productivity of the MBA resolution could hypothetically be increased at higher concentrations, as the solubility limit of the amide coproduct would allow for reactions up to 600 mM, which would result in a STY greater than 1 kg L^{-1} day^{-1} if the same level of conversion could be maintained. Moreover, through increasing the reactor size, a larger amount of catalyst could be used, leading to a shorter reaction time resulting in an increase in STY for both amine systems.

To compare the waste associated with the lipase production of *(S)*-NEA and *(S)*-MBA, E factors were determined according to Equation 5.[212]

$$E\ factor = \frac{mass\ of\ amide + mass\ of\ acyl\ donor - mass\ of\ amine}{mass\ of\ amine}$$

Equation 5: E factor calculation for lipase-mediated kinetic resolution.

With isopropyl acetate serving as both the solvent and the acyl donor, an E factor of 0.84 and 1.19 was calculated for NEA and MBA respectively. The E factor for MBA, is lower than the previously reported 1.34, where one equivalent of methyl methoxy acetate was used as the acyl donor with toluene as the solvent at 0.07 M.[132]

2.3 Chapter summary

A robust transaminase catalysed asymmetric synthesis was developed using an immobilised ω-transaminase within a PBR. A one variable at a time (OVAT) approach was used to obtain an optimised set of reaction conditions. The type of amino donor was investigated under batch conditions before the optimised conditions were applied within a continuous system. Through transfer of the reaction from batch to continuous flow, the reaction time was significantly reduced due to the high local concentration of catalyst facilitated by the PBR, resulting in an increase in productivity.

A second, complementary enzymatic route to the same chiral amine intermediates was developed utilising immobilised lipase within a PBR in continuous flow, following an initial batch screen of 6 commercially available lipases. Isopropyl acetate was demonstrated to serve as both the acyl donor and the solvent, allowing for a lower operating temperature than previously reported.[132, 214]

The stability of each immobilized flow system was investigated, with no observable decrease in activity observed at 8 h for the transaminase and up to 30 h for the lipase, indicating that the processes are amenable to the long operation window that is required for industrial application. Furthermore, the ability to store and reuse the same batch of catalyst makes the process more commercially desirable as the catalyst's contribution to the total process cost is drastically reduced.

Each system was subjected to enzyme leaching tests, monitored by a Bradford assay, with no protein detected in the product stream during steady state operation of both enzymatic system.

Both continuous flow systems have been demonstrated to produce a single enantiomer of two chiral aromatic amines in a highly productive manner, Figure 69. By coupling these systems to an *N*-alkylation step, access to enantiomerically rich secondary amines will be possible within one continuous flow system.

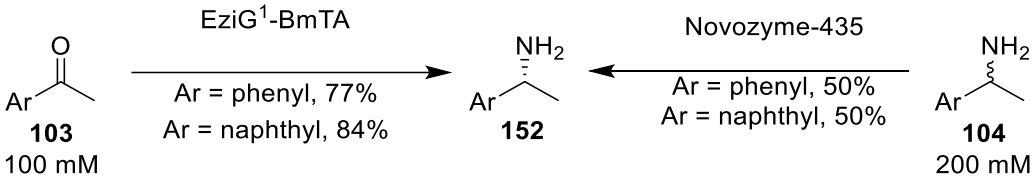

Figure 69: Summary of enzymatic access of two chiral primary amines. Steady-state conversions within continuous flow reactions are shown.

Within the next chapter, two alternative *N*-alkylation routes will be discussed to explore the range of secondary chiral amines that could be accessed by coupling to one of the two complementary enzymatic routes demonstrated within this chapter.

3 *N*-alkylation of enzymatically-generated primary amines

Despite the inherent inefficiency of many *N*-alkylation methodologies, it is still one of the most commonly used transformations within the pharmaceutical industry.[240-242] The most common *N*-alkylation routes consist of either an amine and an alkylating agent, typically an alkyl halide, or reductive amination. This leads to additional chemical steps, undesirable waste products and poor green credentials. [240, 243, 244]

Within this chapter, two complementary 'clean' *N*-alkylation methods will be applied to generate pharmaceutically relevant secondary amines, using the amines generated in the biocatalytic processes (Chapter 2) as starting materials.

Two target molecules, cinacalcet and evocalcet, can each be accessed through application of similar methodologies. Cinacalcet can be accessed through *N*-alkylation of an enzymatically generated chiral amine, applying either borrowing hydrogen, with a primary alcohol, or anti-Markovnikov hydroamination, with an alkene, Figure 70.

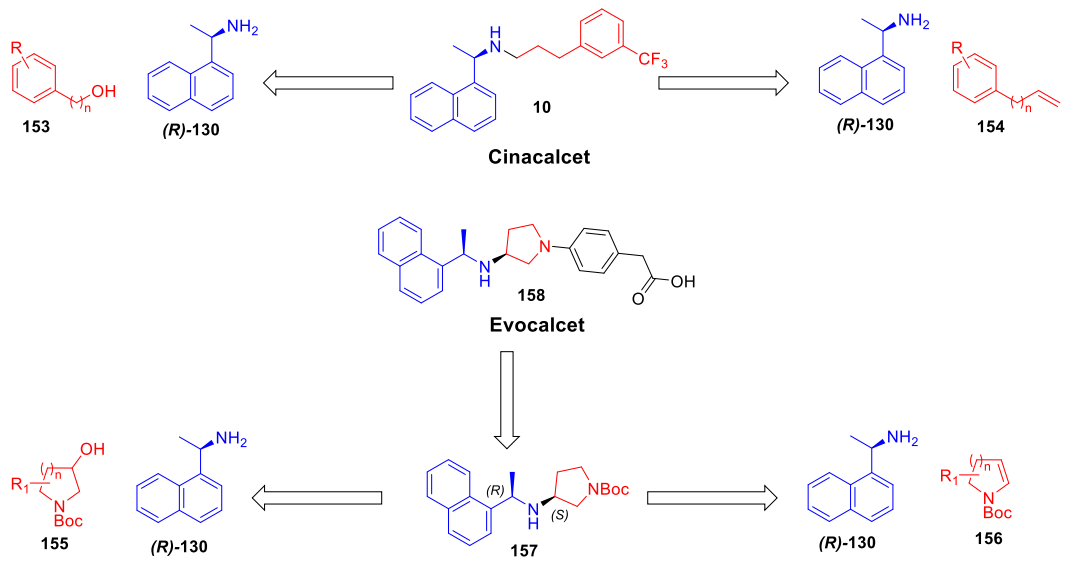

Figure 70: Target molecules for the two complementary chemocatalytic stages

Alternatively, with the same enzymatically generated amine, a cyclic alcohol can be applied within the borrowing hydrogen chemistry to access the key intermediate in

the synthesis of evocalcet. Moreover, building on previous work within the Marsden group,[149] an enecarbamate can be applied as a substrate in hydroamination photochemistry, Figure 70.

3.1 Borrowing Hydrogen *N*-Alkylation of MBA and NEA

Since its first report in 1981,[245-248] hydrogen borrowing chemistry has allowed a redox-neutral approach to the alkylation of amines. Extensively studied within academia, borrowing hydrogen *N*-alkylation methods are yet to be widely applied within an industrial setting.[240, 249] High loadings of expensive precious metal catalysts as well as undesirable reactions conditions (elevated temperatures, molar concentrations, nonpolar aromatic solvents) are some of the reasons behind the lack of applicability for transfer to large-scale applications.[240]

Despite several advancements in recent years (solvents, catalyst design)[150, 240, 249-252] the limitations of the borrowing hydrogen approach continue to inhibit its uptake at the industrial scale.[240] The heat and mass transfer that continuous flow provides would allow for accelerated reaction rates, negating some of these limitations.[253, 254] Moreover, the ability to operate above the atmospheric boiling point of a solvent could not only accelerate reaction rates but also enable lower catalyst loadings.[253, 254]

3.1.1 Mechanistic insights of Borrowing Hydrogen *N*-Alkylation

The most widely applied catalyst for borrowing hydrogen processes is the iridium dimer $[Cp^*IrCl_2]_2$, owing to its high functional group tolerance, great activity and generally high yields.[255] The active species of $[Cp^*IrCl_2]_2$ has previously been found to be a monomeric, 16-electron species that is in equilibrium with the dimeric complex, Figure 71.[150, 256] Previous investigation in to the rate of reaction showed there isn't a linear increase in reaction rate as catalyst loading increases, therefore, the formation of the monomeric, active species does not increase linearly as loading of the catalyst is increased.[150] The addition of a base could be used to shift the

equilibrium in favour of the active complex, with the hope of increasing the rate of reaction and enabling a decrease in reaction time.

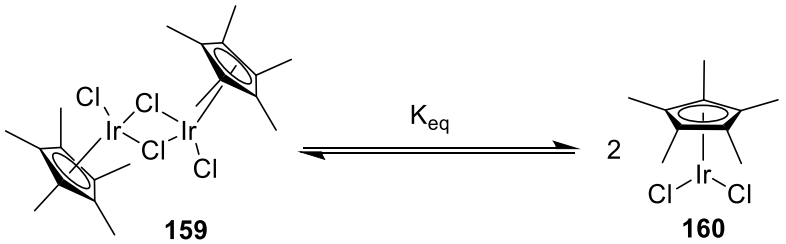

Figure 71: Equilibria of the dimeric and monomeric species of $[Cp^*IrCl_2]_2$.

Fujita and co-workers have previously demonstrated rate acceleration of $[Cp^*IrCl_2]_2$ catalysed *N*-alkylation upon addition of weak bases for a range of monoalkylated aniline products.[255] Catalyst 161 , Figure 72, has also been shown to have greater activity when 5 mol% of weak base (K_2CO_3) is present in the reaction mixture.[150] An immobilised iridium catalyst (catalyst 162), previously employed for the transfer hydrogenation of benzaldehyde,[257] could be applied to borrowing hydrogen methodologies, allowing for the potential recycling of the catalyst.

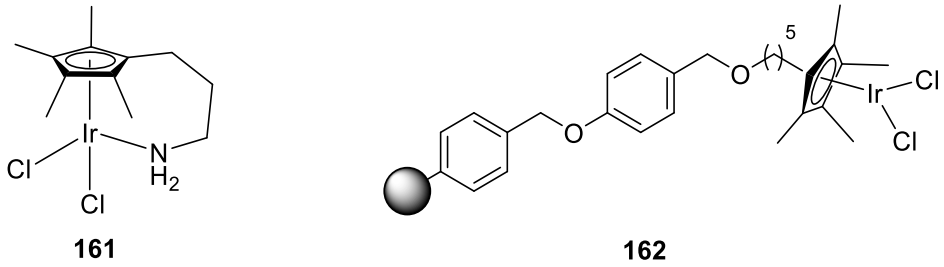

Figure 72: Two hydrogen borrowing catalysts synthesised by previous group members.[150, 257]

Moreover, Noyori and co-workers showed that strong bases, such as potassium hydroxide, were necessary to generate the active form of their catalyst, which has a similar structure to catalyst 161, Figure 73.[258]

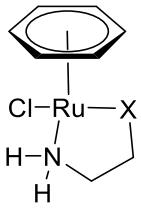

163

Figure 73: Noyori-type catalyst, used in the asymmetric transfer hydrogenation of aromatic ketones.[258]

More recent mechanistic studies of the catalytic cycle of $[Cp^*IrCl_2]_2$, however, uncovered that the active form of the catalyst could be generated in the absence of a base,[150] supporting an amine-coordination mechanism previously proposed by Madsen and co-workers, Figure 74.[256]

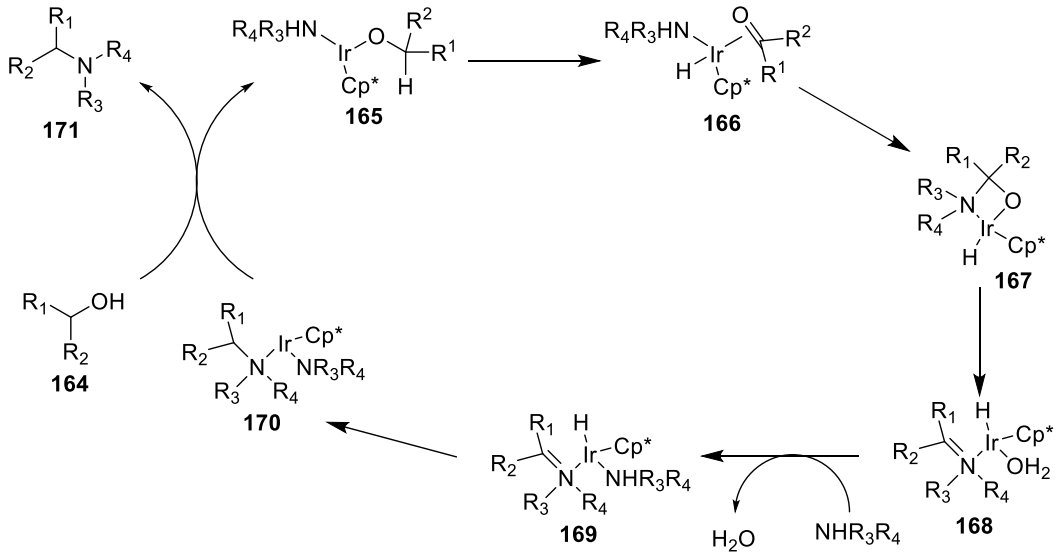

Figure 74: Previously proposed mechanism for the iridium-catalysed N-alkylation of amines with primary and secondary alcohols, using $[Cp^*IrCl_2]_2$, adapted from Fistrup et al.[256]

Within the amine-coordination mechanism, an alkoxy-metal species first forms an activated carbonyl that is then attacked by the amine to form a hemiaminal. After dehydration of the hemiaminal to form an imine, water is formed and released. This leaves a vacant site on the metal for a second molecule of amine. A second molecule of the alcohol provides the final hydrogen atom required to form and release the N-alkylated amine product, restarting the catalytic cycle.[256]

The rate determining step for the proposed mechanism has previously been determined to be either formation of the carbonyl, hemiaminal formation or the elimination of water.[256] Furthermore, an excess of alcohol has previously been found to give faster reaction rates than when the starting materials are equimolar. This is a consequence of the amine forming a more stable and inactive iridium complex, leading to catalytic inhibition.[150]

3.1.2 Optimising the conditions for borrowing hydrogen reactions in batch

To assess the feasibility of applying borrowing hydrogen to access the two target molecules, four iridium-based catalysts were screened for the *N*-alkylation reaction with MBA and 4-bromobenzylalcohol. In addition to $[Cp^*IrCl_2]_2$, a diiodo iridium dimer ($[Cp^*IrI_2]_2$, SCRAM) catalyst, a monomeric iridium complex (Catalyst 161)[150, 151, 259] and an immobilized iridium catalyst (Catalyst 162)[257] (Figure 72) were applied to the model reaction, Figure 75.

3.1.2.1 Effect of base on borrowing hydrogen *N*-alkylation

Owing to the contrasting previous reports in relation to the base requirement to generate the active species, all four catalysts were compared with weak (K_2CO_3) and strong (KOH) bases as well as in the absence of base.

Reactions were performed in toluene (1.0 M), with 2 mol% Ir and 5 mol% base. The reactions were heated at reflux for 24 h with yield determined from the crude ^{1}H NMR and *ee* retention determined by chiral HPLC.

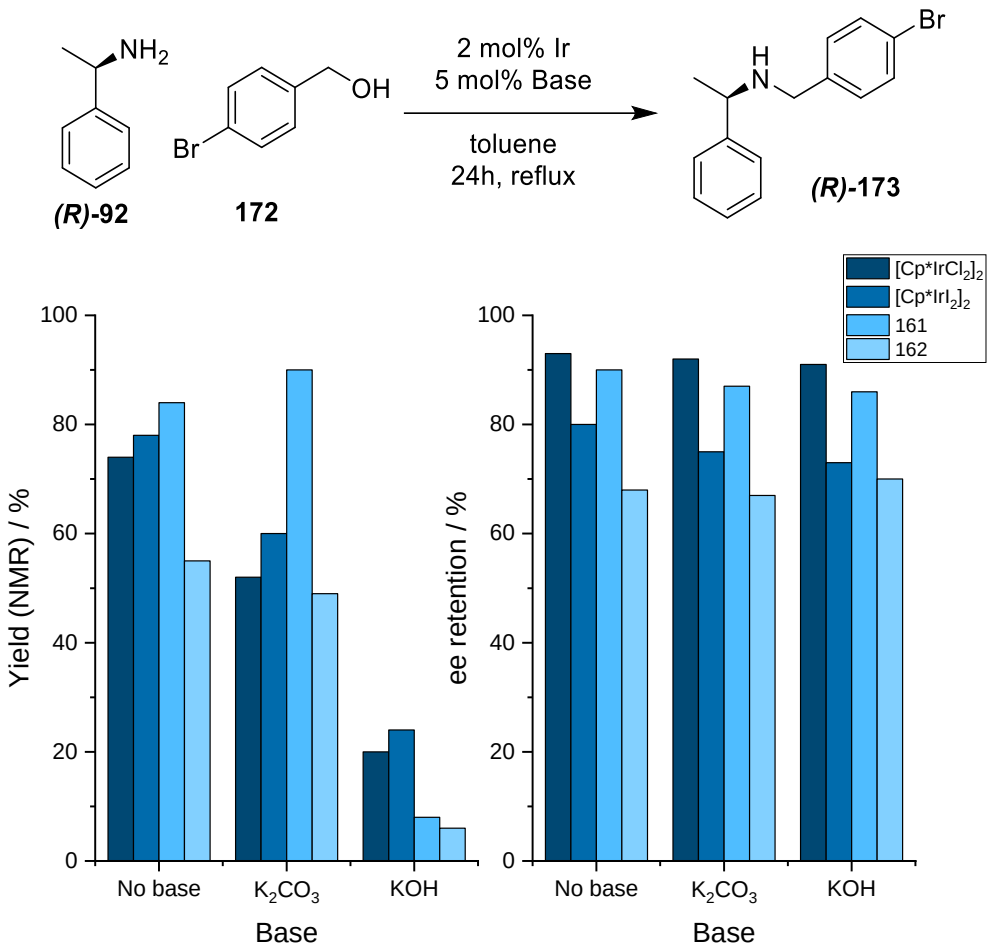

Figure 75: Effect of base for 4 catalysts for the N-alkylation screening reaction of MBA and 4-bromo benzylalcohol. Reactions were performed in toluene (1.0 M) with MBA, 4-bromo benzylalcohol, 2 mol% Ir and 5 mol% base at reflux. Reactions with catalyst 2 were performed at 80 °C due to constraints of the support resin. Yield was determined by ^{1}H NMR against and internal standard and ee retention was determined by chiral HPLC.

Comparable yields were observed for the three homogenous catalysts after 24 h without addition of a base, with catalyst 161 giving a higher NMR yield, Figure 75. As the high temperature of the reaction is required to dissociate the amine from the iridium center,[260] the lower yield observed with catalyst 162 could be due to the lower reaction temperature (80 °C) that was enforced by the presence of the Wang resin.[257]

As expected, a higher degree of racemisation was observed with the SCRAM catalyst and catalyst 162 as both catalysts have previously been reported for the racemisation

of chiral amines.[261, 262] In comparison, reactions utilising catalyst 161 and $[Cp^*IrCl_2]_2$ result in high retention of the stereocentre installed in the biocatalytic reaction (90 and 95% *ee* retention respectively).

Despite the previous findings of Noyori and coworkers[258], addition of potassium hydroxide had a detrimental effect upon the reaction with yields decreasing for all catalysts by 49-76% in comparison to the base-free reaction. This suggested that the presence of a strong base formed an inactive catalytic species instead of activating the complex for borrowing hydrogen.[150, 263]

Addition of potassium carbonate also resulted in lower conversions for the two dimeric complexes and catalyst 162, however, not as drastic a reduction (compared to the bass-free reactions) as observed with KOH. An increase in conversion from 84% to 90% was observed with catalyst 161 which is rationalized by the base deprotonating the coordinating amine, revealing a 16-electron complex capable of dehydrogenating the alcohol.[150, 151]

3.1.2.2 Effect of solvent on borrowing hydrogen *N*-alkylation

Traditionally, borrowing hydrogen is performed in toluene or xylene(s)[151, 240, 264] due to the high temperatures required within the reaction. With considerations of RRI and green chemistry, 2-MeTHF and isopropyl acetate were screened as solvents, to potentially provide a green alternative to toluene. Aside from its green credentials, isopropyl acetate was screened as a solvent owing to its compatibility with Novozym 435. If the reaction performed well in isopropyl acetate, it would alleviate the need for a solvent switch between the two reaction stages within a continuous flow system.

Water has previously been used as a green, alternative solvent for the iridium catalysed borrowing hydrogen reaction of various (di)amines and diols to form *N*-heterocycles.[133, 265] Whilst the use of water as a solvent would be ideal, with the incorporation of an upstream transaminase reaction, further studies demonstrated that the reaction didn't occur within the water and only on the surface, due to the

insolubility of the catalyst in water,[266-268] and therefore, would not be suitable for continuous flow. Subsequently, all four catalysts were compared within toluene, 2-MeTHF and isopropyl acetate.

Reactions were performed in batch (1.0 M), with catalyst loadings equating to 2 mol% total iridium. The reactions were heated at reflux for 24 h with conversion determined from the crude ^{1}H NMR and *ee* retention determined by chiral HPLC.

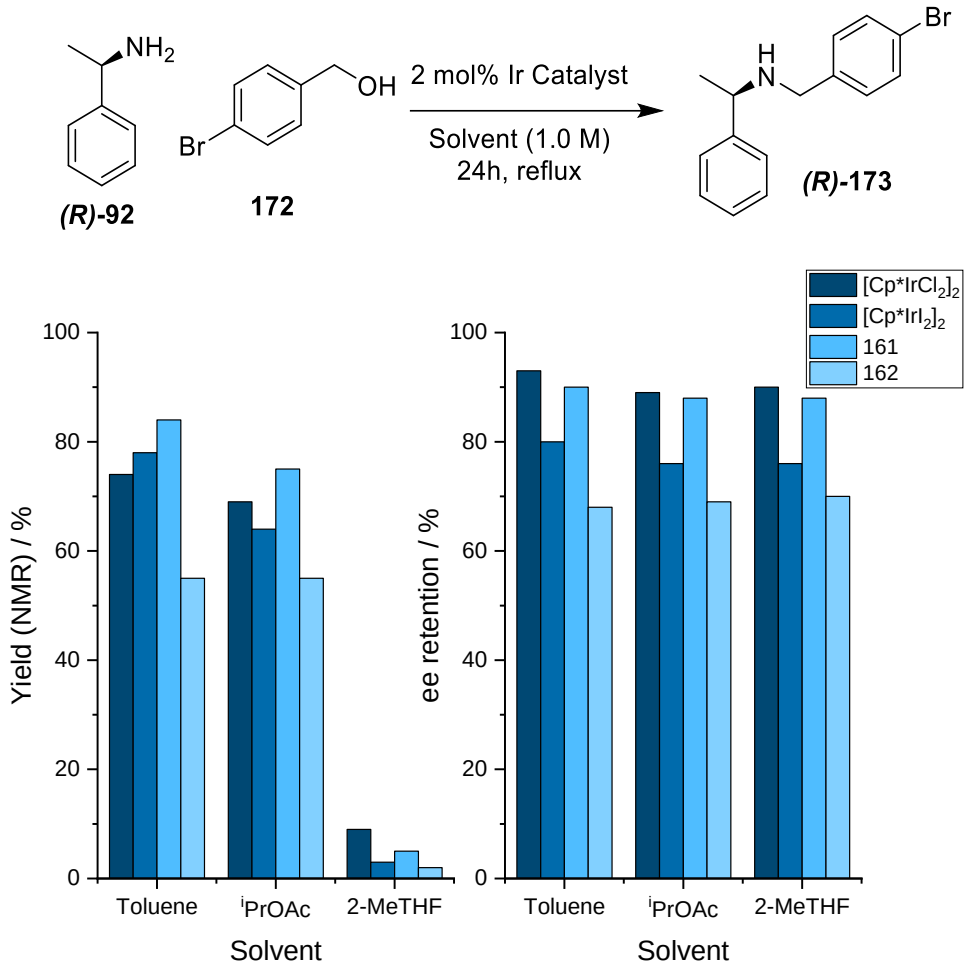

Figure 76: Effect of solvent for 4 catalysts for the N-alkylation screening reaction of MBA and 4-bromo benzylalcohol. Reactions were performed at 1.0 M concentration with MBA, 4-bromo benzylalcohol and 2 mol% Ir at reflux. Reactions with catalyst 2 were performed at 80 °C, due to constraints of the resin. Yield was determined by ^{1}H NMR against and internal standard and ee retention was determined by chiral HPLC.

The observed NMR yield when the reaction was performed in 2-MeTHF was significantly lower than the other two solvents. This was particularly surprising for catalyst **161**, as it had previously displayed great solvent tolerance and comparable activity within the two solvents.[150] Poor activity could be due to the lower boiling point (80 °C) of 2-MeTHF.

Isopropyl acetate proved a good solvent, with comparable yields to those obtained in toluene observed across all four catalysts. Owing to the high temperatures of the reaction, acylation of the amine could be possible when the reaction is performed in isopropyl acetate. To assess the rate of amide formation, a solution of MBA and 4-bromobenzylalcohol was refluxed in isopropyl acetate (1.0 M), in the absence of catalyst, Figure 77. This also served as an indication as to whether the desired reaction could proceed in the absence of the iridium catalyst.

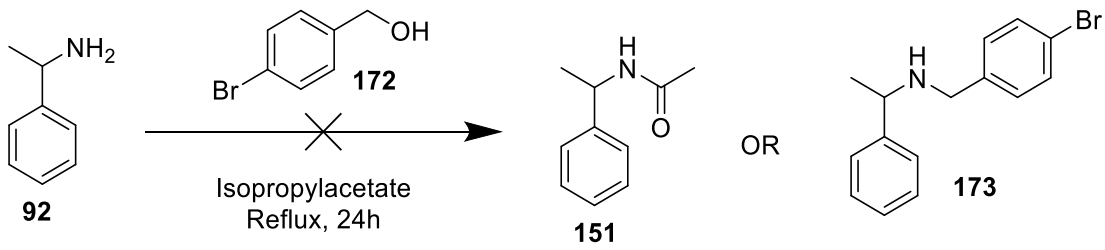

Figure 77: Borrowing hydrogen reaction of MBA and 4-bromobenzylalcohol in isopropyl acetate (1.0 M). The reaction was performed in the absence of catalyst at reflux for 24 h.

Pleasingly, after 24h neither the amide nor the borrowing hydrogen product were observed in the reaction mixture, with the starting materials recovered. This demonstrated that the reaction couldn't proceed in absence of the catalyst, whilst also emphasising the applicability of isopropyl acetate as a solvent.

Owing to its comparable activity to toluene as well as compatibility with Novozym 435, all future reactions were performed with 1 mol% $[Cp^*IrCl_2]_2$ in isopropyl acetate. With a view to telescoping the lipase-mediated kinetic resolution to the borrowing hydrogen reaction, being able to perform both reactions within the same solvent

negates the need for a solvent switch or in-line separation between the reaction zones.

3.1.3 Exemplar targets accessed through borrowing hydrogen reactions

Borrowing hydrogen chemistry has been demonstrated on a wide variety of substates.[150, 151, 240, 249] Exploring the scope of the methodology falls outside the remit of this work, instead a small number of drug and drug-like targets were selected to highlight the benefit of applying borrowing hydrogen chemistry in continuous flow.

3.1.3.1 Use of borrowing hydrogen to access cinacalcet

Cinacalcet, a calcimimetic drug used for the treatment of secondary hyperparathyroidism in patients with chronic kidney disease,[79] was highlighted as a potential target molecule as it is possible to access in two steps, Figure 78: first, the enzymatic generation of a 1-(1-naphthyl) ethylamine (NEA), followed by a borrowing hydrogen reaction with 3-(3-(trifluoromethyl)phenyl)propan-1-ol (alcohol 174).

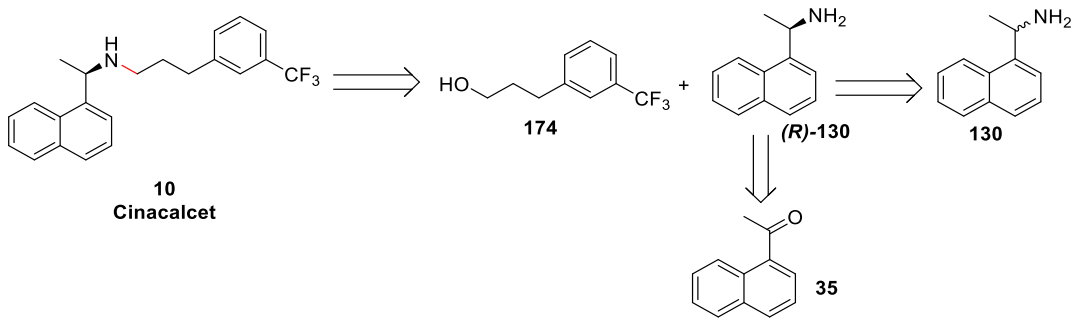

Figure 78: Access to cinacalcet utilising a borrowing hydrogen reaction of NEA and 3-(3-(trifluoromethyl)phenyl)propan-1-ol, with the C-N bond to be formed highlighted in red

It was possible to synthesize 3-(3-(trifluoromethyl)phenyl)propan-1-ol (174) in 2 steps in a 68% yield, according to a literature procedure, Figure 79.[269] The first step was performed in THF with 3 mol% CuI, 3 mol% $Pd(OAc)_2$ and 6 mol% PPh_3 at 55 °C for 22 h. The resultant alkyne was hydrogenated using 3.4 mol% Pd/C in EtOH under a H_2 atmosphere for 18 h.

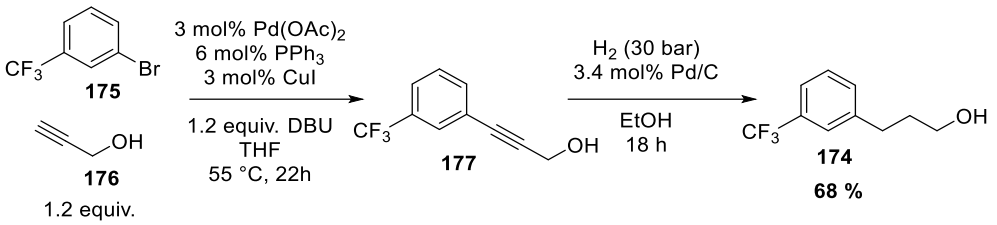

Figure 79: Synthesis of 3-(3-(trifluoromethyl)phenyl)propan-1-ol, starting from 3-bromobenzotrifluoride and propargyl alcohol.

In addition to 3-(3-(trifluoromethyl)phenyl)propan-1-ol, three benzylic alcohols were subjected to the borrowing hydrogen reaction to yield compounds found within the same patent(s) as cinacalcet.[270-272] Moreover, contacting the four alcohols with α-methylbenzylamine (MBA), the other amine enzymatically accessed in 0, would allow access to a panel of eight secondary amines. Reactions were performed in isopropyl acetate (1.0 M) with a catalyst loading of 1 mol% (2% iridium) for 20h, Figure 80.

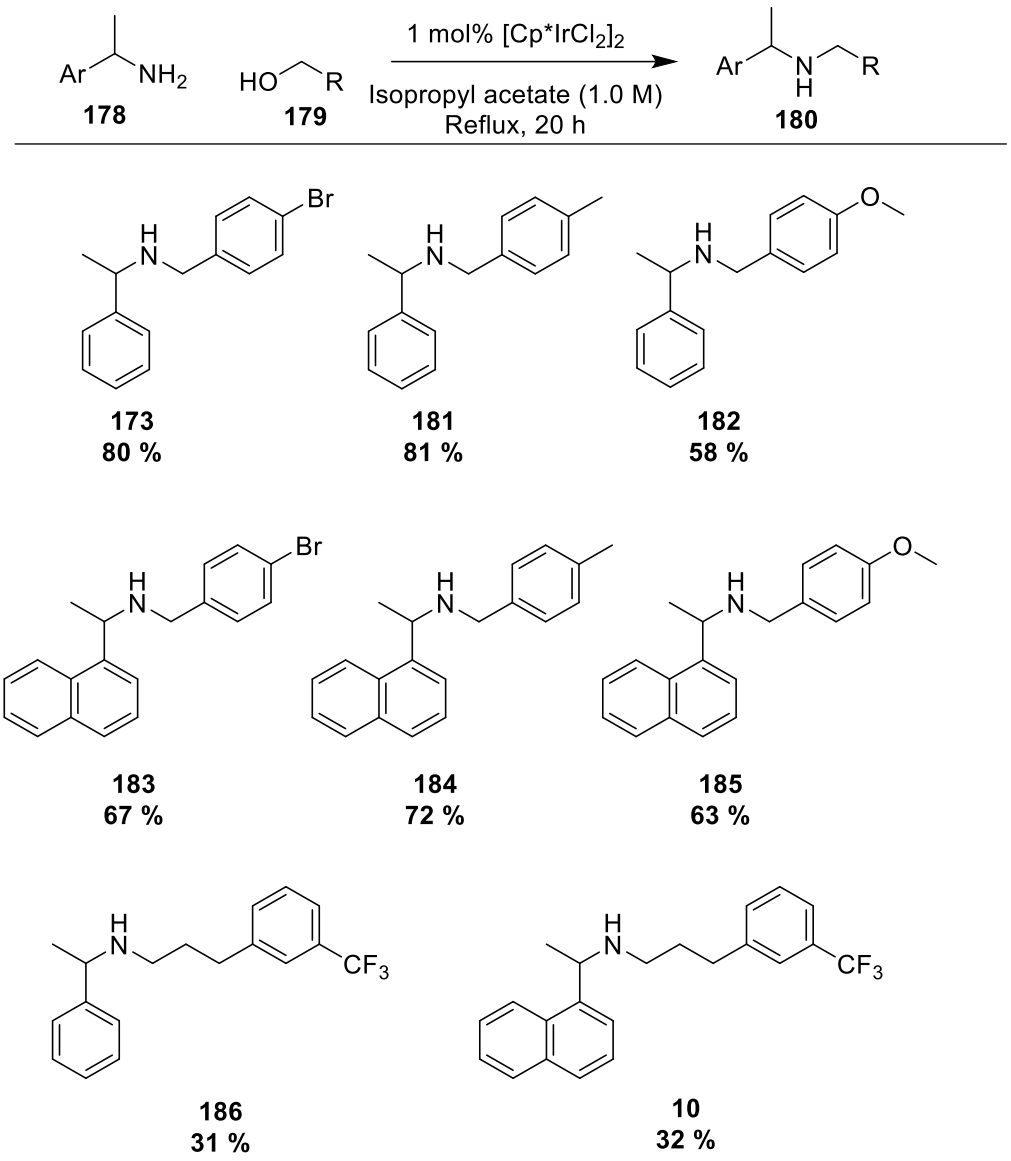

*Figure 80: Substrate scope for hydrogen borrowing reactions of primary alcohols and α-aryl amines. Reactions were performed at reflux in isopropyl acetate (1.0 M) with 1 mol% [Cp*IrCl₂]₂ for 20h.*

All 8 reactions were successful, with higher yields observed for the benzylic alcohols compared to 3-(3-(trifluoromethyl)phenyl)propan-1-ol. It was expected that the more activated benzylic alcohols would result in higher yields than 3-(3-(trifluoromethyl)phenyl)propan-1-ol (174) due to the stability of the carbonyl intermediate, which also explains the high prevalence of benzylic alcohols as model substrates within the literature.[240, 249, 252]

Despite the lower yields observed with 3-(3-(trifluoromethyl)phenyl)propan-1-ol (174), Figure 80, it was hoped that yield could be enhanced in continuous flow with utilisation of a back pressure regulator (BPR). Operating above the ambient boiling point of isopropyl acetate with use of a BPR would enable an enhancement of reaction rate and hence further optimisation was not investigated at this point.

3.1.3.2 Utilisation of borrowing hydrogen to access a key intermediate in the synthesis of evocalcet

Evocalcet is an oral allosteric calcium-sensing receptor (CaSR) agonist, with a similar mechanism of action as cinacalcet.[273] Within the synthesis of evocalcet, *syn*-aminopyrrolidine (157) is accessed as a mixture of diastereomers, from *(R)*-NEA and *N*-Boc pyrroldininol, Figure 81.[274]

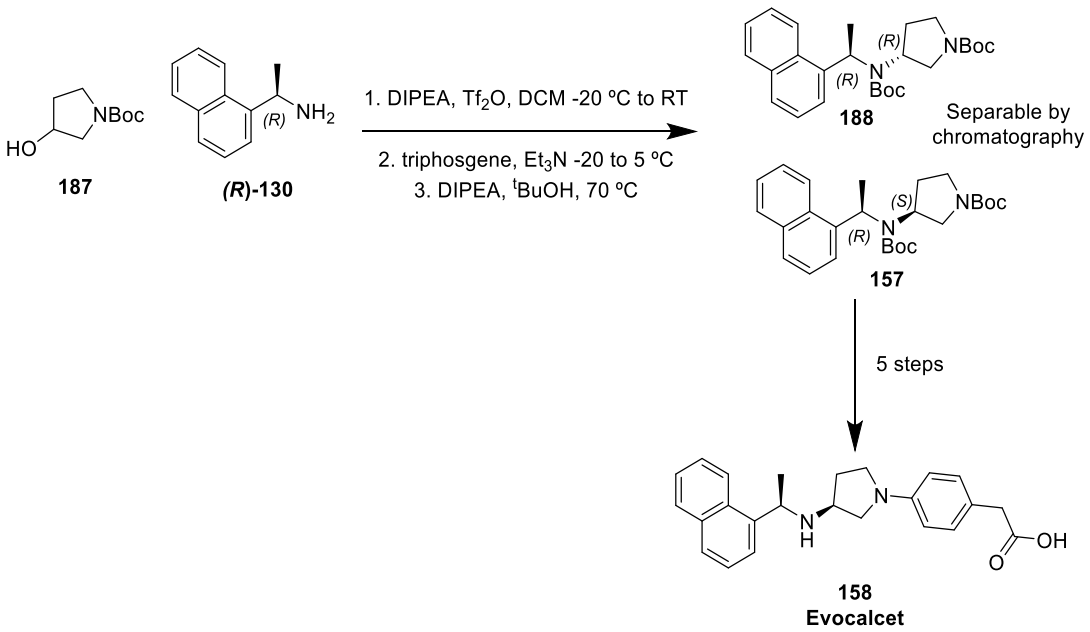

Figure 81: Mitsubishi Tanabe Pharma synthesis of evocalcet from (R)-NEA and N-Boc pyrroldininol.[274]

Owing to the shared chiral amine precursor with cinacalcet, evocalcet serves as a good alternative target molecule that can also be accessed with borrowing hydrogen chemistry using cyclic alcohols.

Typically, secondary alcohols react more slowly than primary alcohols within borrowing hydrogen reactions. Despite secondary alcohols being easier to oxidise

than primary alcohols, the decreased electrophilicity can result in imine formation becoming the rate determining step, slowing the rate of reaction.[240, 260] Within the mechanism, Figure 74, the alcohol is oxidized to the corresponding carbonyl, which then coordinates to an iridium hydride species. As ketones are poorer electrophiles than aldehydes, imine condensation within the coordination sphere of the iridium complex is considerably slower, resulting in slower reaction rates.[260]

Moreover, the difference in reactivity between primary and secondary alcohols is so extreme that it has previously been demonstrated that primary alcohols can react preferentially in the presence of a secondary alcohol with no undesired products being formed.[151]

The basic nitrogen of cinacalcet is essential for its agonistic activity,[275] however, it is also the cause of CYP2D6 inhibition[276] resulting in adverse effects on the gastrointestinal (GI) tract.[274] Through the addition of steric bulk, provided by the pyrrolidine ring adjacent to the basic nitrogen in evocalcet, Figure 82, the affinity for CYP2D6 was weakened and adverse effects considerably reduced.[274]

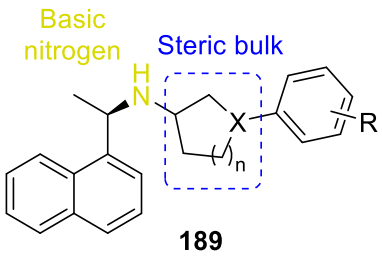

189

Figure 82: Steric bulk positioned adjacent to the basic nitrogen in the second-generation study.

As a piperidine moiety adjacent to the basic nitrogen was also screened in the search for a second-generation drug,[274] analogues of the aminopyrrolidine (157) with various ring sizes were also synthesised using borrowing hydrogen methodology. Reactions with cyclic, secondary alcohols were performed in isopropyl acetate (1.0 M) with 1 mol% $[Cp^*IrCl_2]_2$, Figure 83.

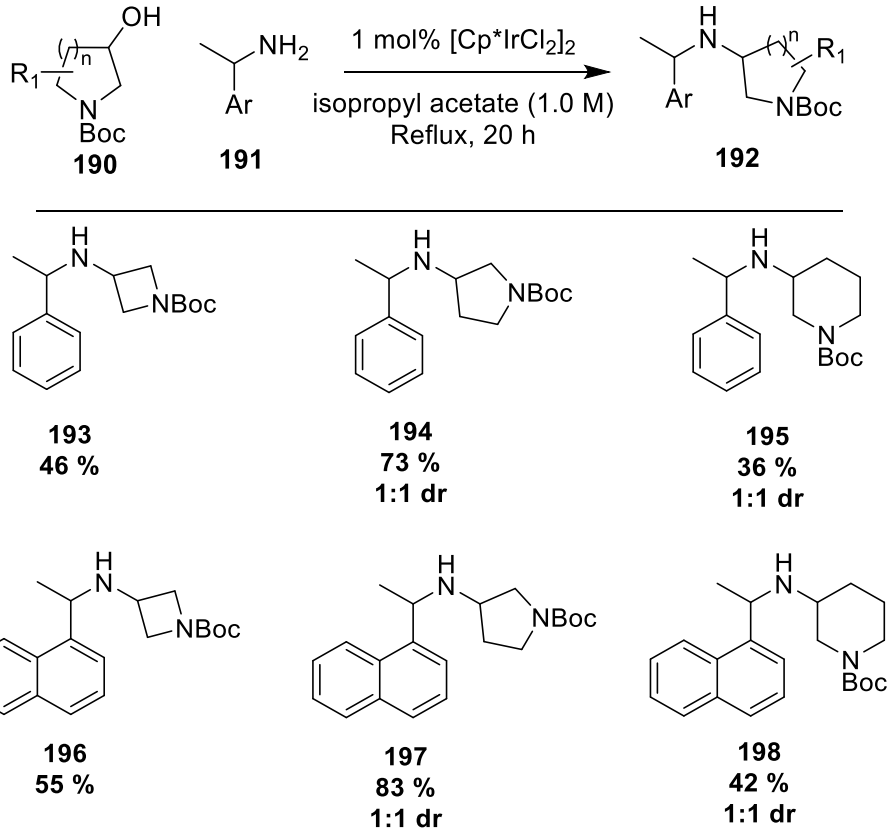

*Figure 83: Substrate scope for hydrogen reactions of cyclic, secondary alcohols and α-aryl amines. Reactions were performed at reflux in isopropyl acetate (1.0 M) with 1 mol% [Cp*IrCl$_2$]$_2$ for 20h.*

Each of the six reactions produced the desired product, in moderate to excellent yields, with reactions involving *N*-Boc-3-hydroxypyrrolidine providing yields comparable to those observed with benzylic alcohols (see 3.1.3.1). Both the azetidine and piperidine ring systems produce yields more typical of secondary alcohols.

In an analogous manner to cinacalcet and its analogues, through translation to continuous flow and with use of a BPR, it was hoped that the moderate yields of the azetidinol and piperidinol reactions could be enhanced through operation above the ambient boiling point of isopropyl acetate.

3.1.4 Compatibility of borrowing hydrogen reactions with the enzymatic product stream(s)

Unlike the reactions earlier within this chapter, in the continuous flow chemoenzymatic set up, components of the upstream biocatalytic reaction will be

present in the downstream chemistry. The compatibility of borrowing hydrogen chemistry in the presence of the extra reaction components, therefore, needs to be examined.

3.1.4.1 Ketone compatibility within borrowing hydrogen chemistry

Results from studies on separations demonstrated that unreacted ketone starting material from the transaminase reaction would partition into the organic layer (see 2.1.7) and would, therefore, be present in the downstream borrowing hydrogen reaction. Since *N*-alkylation of anilines with ketones has been previously demonstrated,[277, 278] any potential cross-reactivity needed investigating.

A reaction of NEA and 4-methoxybenzyl alcohol was performed in isopropyl acetate (1.0 M), with 0.5 equivalents of 1'-acetonaphthone doped into the reaction mixture, Figure 84.

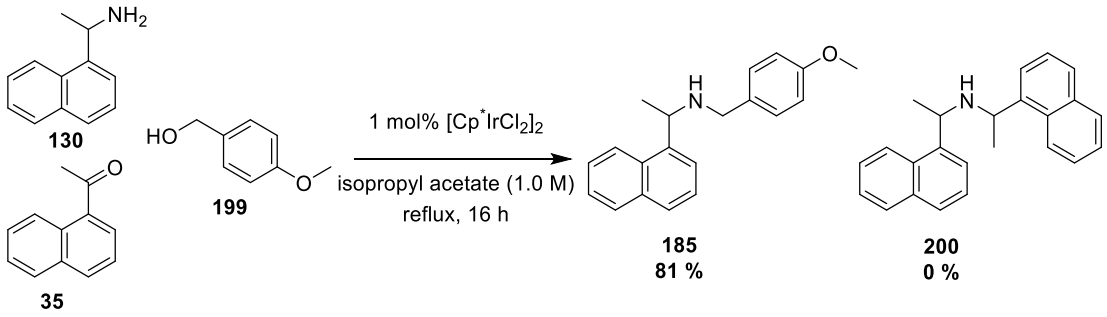

*Figure 84: N-alkylation of NEA with 4-methoxybenzyl alcohol, doped with 1'acetonaphthone. The reaction was performed in isopropyl acetate (1.0 M), with 0.5 equivalents of 1'-acetonaphthone and 1 mol% [Cp*IrCl$_2$]$_2$ at reflux for 16 h.*

No cross-reactivity product was observed, which can be rationalized by the considerably lower reactivity of ketones towards imine formation, when compared to aldehydes.

Additionally, from the mechanism in Figure 74, there would be no proton transfer to the amine or iridium-hydride to reduce the iminium species after dehydration of the hemiaminal if the ketone coordinates to the iridium center before the alcohol. For cross-reactivity to occur, the ketone must displace the alkoxide after elimination of

its β-hydrogen, however, the reactants within the proposed mechanism remain coordinated to the iridium centre for the entirety of the reaction.

3.1.4.2 Amide compatibility within borrowing hydrogen chemistry

An *N*-acetyl amide is produced as a by-product in the lipase-mediated kinetic resolution. As there is no solvent switch between the two stages when lipase is utilised as the upstream biocatalyst, the amide would be present in the borrowing hydrogen reaction and potential cross-reactivity needed investigating. A reaction of NEA and 4-methoxybenzyl alcohol was performed in isopropyl acetate with 1 equivalent of *N*-acetyl-1-(1-naphthyl)ethylamine doped into the reaction mixture, Figure 85.

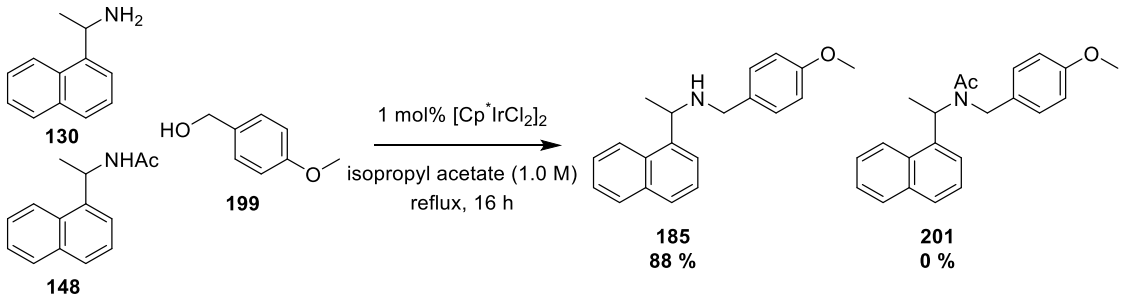

*Figure 85: N-alkylation of NEA with 4-methoxy benzylalcohol, doped with N-acetyl-1-(1-naphthyl)ethylamine. The reaction was performed in isopropyl acetate (1.0 M), with 1.0 equivalents of N-acetyl-1-(1-naphthyl)ethylamine and 1 mol% [Cp*IrCl$_2$]$_2$ at reflux for 16 h.*

Whilst there is no direct precedent of borrowing hydrogen reactions performed with *N*-alkylated amides, there has been reports of sulfonamides being used in place of alcohols.[148, 249] After 16 h at reflux, no cross-reactivity product was observed, with the yield observed comparable to when there is no doped amide in the reaction mixture. This therefore demonstrates the compatibility of the lipase reaction product stream within borrowing hydrogen reactions.

Moreover, as the yield observed within the reaction is comparable to the yield observed in the absence of amide, it can be suggested that the amide does not poison the iridium catalyst.

3.1.5 Reaction profile of batch borrowing hydrogen reactions

To facilitate a seamless transition from batch to continuous flow, a reaction employing MBA and 4-bromobenzyl alcohol was sampled at regular intervals and the yield of the reaction determined from the crude ^{1}H NMR against an internal standard, Figure 86.

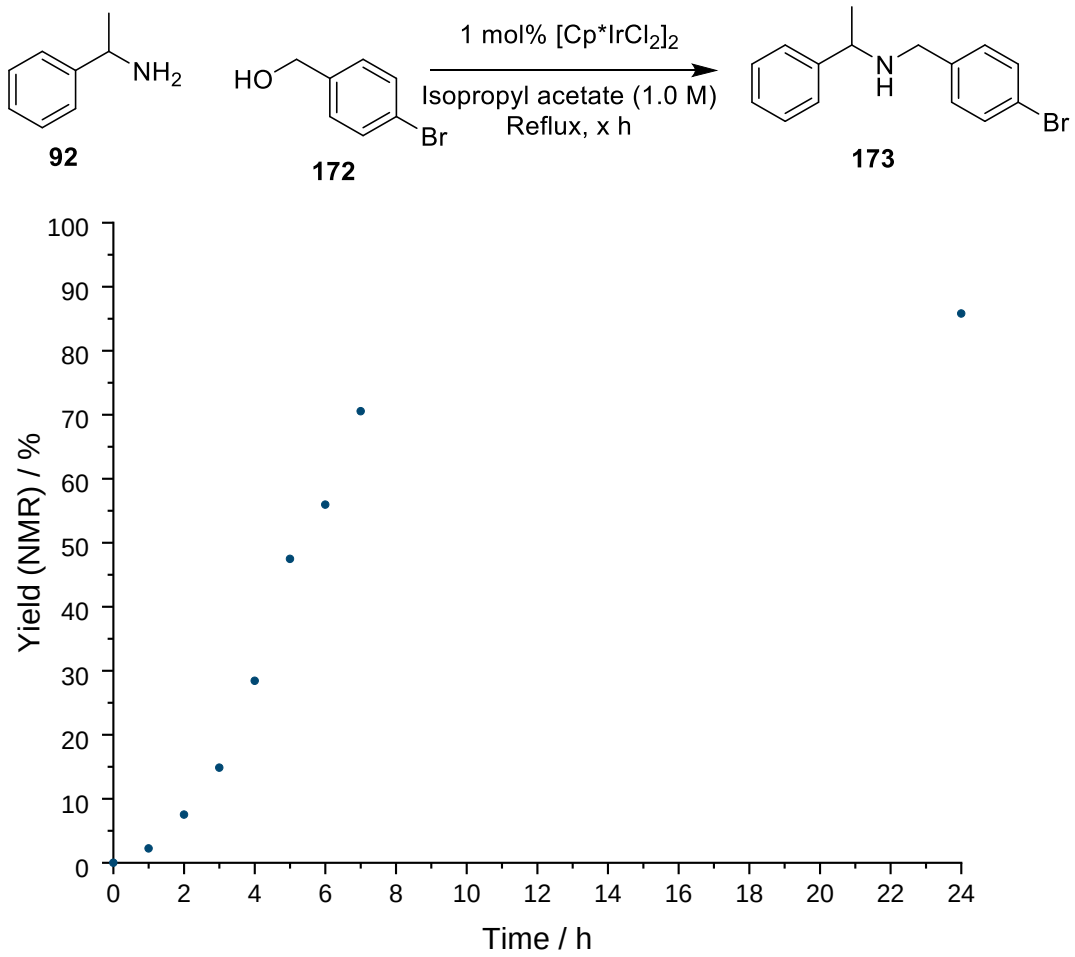

*Figure 86: Kinetic study for the borrowing hydrogen reaction of MBA and 4-bromobenzylalcohol. The reaction was performed in isopropyl acetate (1.0 M) with 1 mol% [Cp*IrCl$_2$]$_2$ at reflux. Yield was determined from the crude ^{1}H NMR against an internal standard.*

An initial lag period (0-2 h, Figure 86) suggests that the rate is limited initially by the formation of the active 16 electron species, Figure 71. After this initial period, yield increases linearly, up to 71% after 7h, with the reaction eventually reaching a final NMR yield of 86% after 24h.

These results suggest that after 7 h, the reaction is nearly complete. To be compatible with our proposed upstream PBR set-up, with a maximum volume of 4 mL, the residence time within the downstream CSTR set-up would be limited to a maximum of 2 h due to constraints of the reactor configuration.

As previously alluded to when discussing the substrate scope, utilisation of a BPR within a continuous flow reactor would enable solvent temperatures above the boiling point of isopropyl acetate at ambient pressure and subsequently lead to accelerated reaction rates. This could potentially reduce the reaction time of the borrowing hydrogen reaction to be within the 2 h residence time required for compatibility with the upstream reaction.

3.1.6 Borrowing hydrogen at elevated temperatures with a back pressure regulator (BPR)

When operating in continuous flow, it is possible to heat above a solvent's atmospheric boiling point if an appropriate BPR is applied to the system. Using the Clausius-Clapeyron equation, Equation 6, the pressure required to ensure the solvent does not vaporise and that the desired flow rate is maintained, can be calculated.

$$\ln\left(\frac{P_1}{P_2}\right) = \frac{\Delta H_{Vap}}{R}\left(\frac{1}{T_2} - \frac{1}{T_1}\right)$$

Equation 6: The Clausius-Clapeyron equation where P_1 and P_2 are vapour pressures at two temperatures T_1 and T_2, ΔH_{Vap} is the enthalpy of vaporisation and R is the gas constant.

Using the Clausius-Clapeyron equation, it is possible to calculate that a BPR of 10 Pa would allow isopropyl acetate to be heated to 172.4 °C without the solvent vaporising, Figure 87. Therefore, with a BPR of 10 Pa and a temperature lower than 172.4 °C, it is possible to operate under flow conditions and accurately record flow rates and residence times.

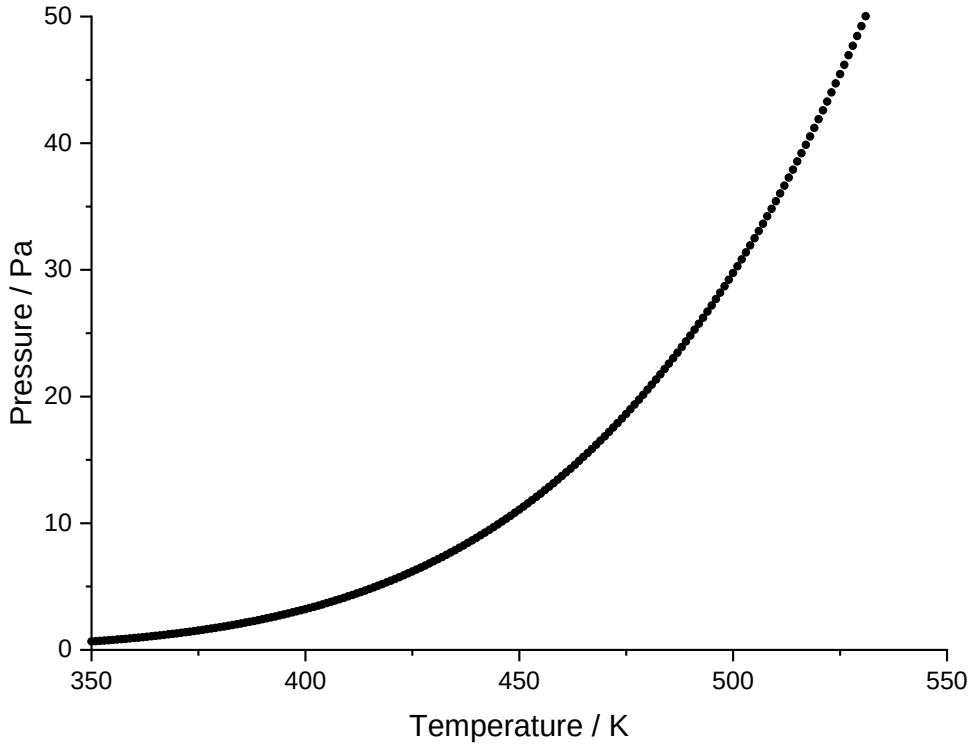

Figure 87: Vapour pressure plot for isopropyl acetate, using the Clausius-Clapeyron equation, Equation 6.

Furthermore, fluid temperature within the fReactors is lower than the temperature recorded on the aluminium base plate, due to the thermal resistance of PEEK. Subsequently, Equation 7 was used to calculate the temperature the hotplate should be set to, to reach the desired fluid temperature.

$$Hotplate\ temperature\ ℃ = (1.25\ \times desired\ fluid\ temperature\ ℃) - 5.5$$

Equation 7: Required hotplate temperature for the desired fluid temperature inside a fReactor CSTR.

To observe the influence of elevated temperature, three borrowing hydrogen reactions employing NEA and 4-methoxybenzyl alcohol were set up in batch within fReactor CSTRs. The reactions were performed in isopropyl acetate (0.1 M) with 1 mol% $[Cp^*IrCl_2]_2$, to replicate the concentration that would be utilised in continuous flow.

The first of these three reactions was performed for 16 h with a 90 °C fluid temperature, to mirror the previously performed reactions at reflux. The other two

were carried out with a fluid temperature of 120 °C for 1 and 2 h, respectively, with all three reactions using a BPR, Figure 88.

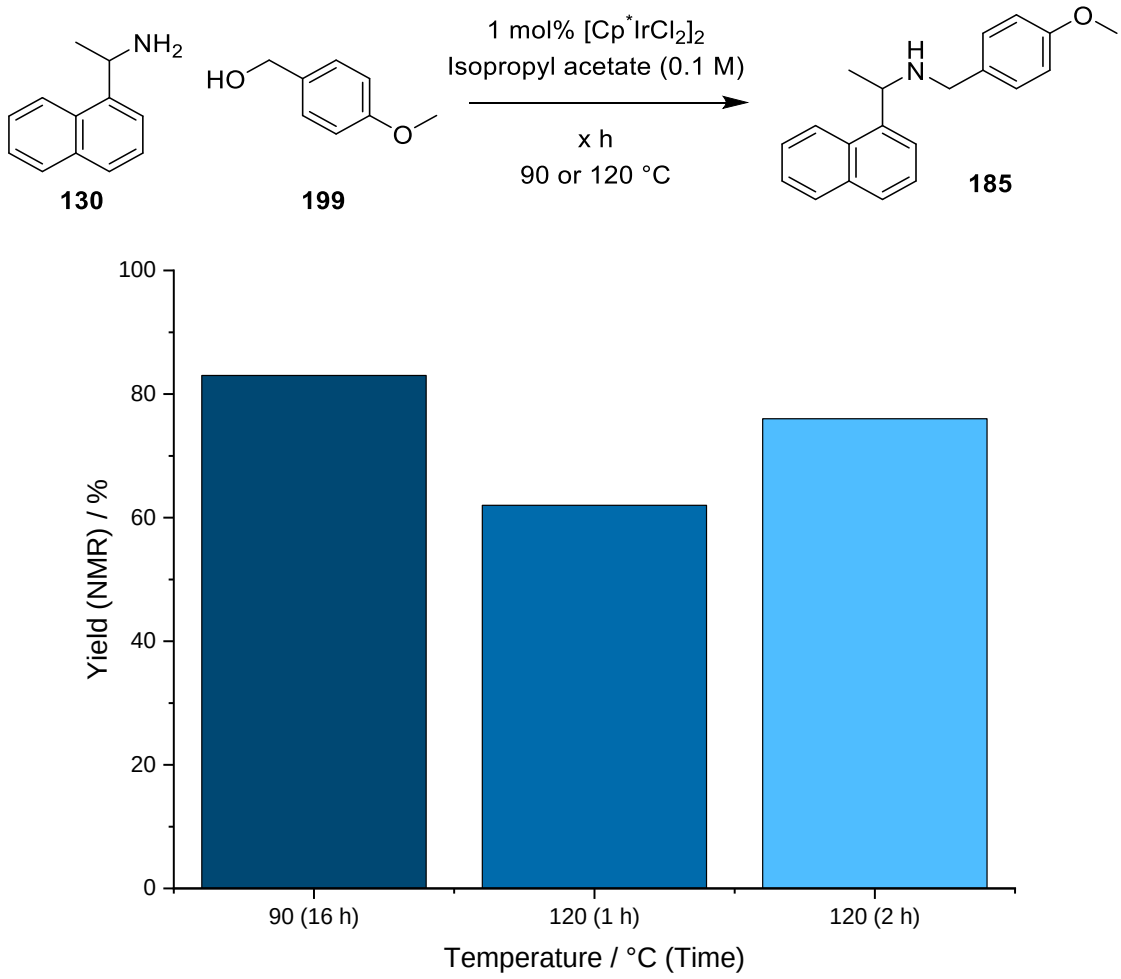

*Figure 88: Effects of elevated temperature of the rate of the borrowing hydrogen reaction of NEA and 4-methoxybenzyl alcohol. Reactions were performed in isopropyl acetate (0.1 M) with 1 mol% [Cp*IrCl$_2$]$_2$ within fReactor CSTRs fitted with a BPR. Yield was calculated by ^{1}H NMR against an internal standard.*

After 16 h at 90 °C, an NMR yield of 83% was observed which is higher than the yield obtained when the reaction was performed in batch, Figure 80. This could be due to greater heat and mass transfer within the fReactor CSTRs, resulting in enhanced reaction rate.

At the elevated fluid temperature of 120 °C, after 1 h an NMR yield of 62% was observed, which increased to 76% after 2 h. Both results demonstrated an increase in reaction rate at higher temperatures, especially with only 7% difference in yield between the 16 h 90 °C reaction and the 2 h 120 °C reaction.

The reduction of the residence time from 16 h to 2 h would allow for more compatible residence times with the upstream biocatalytic reactions. Moreover, increasing the fluid temperature inside the fReactor CSTRs or utilisation of an alternative flow reactor that would allow for extreme temperatures could enable faster reaction rates and shorter residence times.

3.1.7 Borrowing Hydrogen Reactions in Continuous flow

After demonstrating the use of BPR with fReactor CSTR devices in batch to accelerate the reaction rates of borrowing hydrogen reactions, the reactions next needed to be translated into continuous flow.

3.1.7.1 Reactor set up

The continuous reactor set up consisted of a series of fReactor CSTRs which in turn sit on a standard laboratory stirrer hotplate, Figure 89. Each reaction vessel (PEEK material, volume 1.7ml) contains a single cross stirrer bar and is equipped with 4 standard ports accepting standard low pressure HPLC fittings, allowing for flexibility in connecting reactors to each other.

Reagent feeds were introduced into the system using a JASCO PU-980 HPLC pump or a Harvard Apparatus Model 22 syringe pump. PTFE tubing (1/16” ID) was used to connect the pump to the reactor, in between each reaction vessel (1/8” ID) and from the outlet of the reactor to the PBR and into a collection vessel.

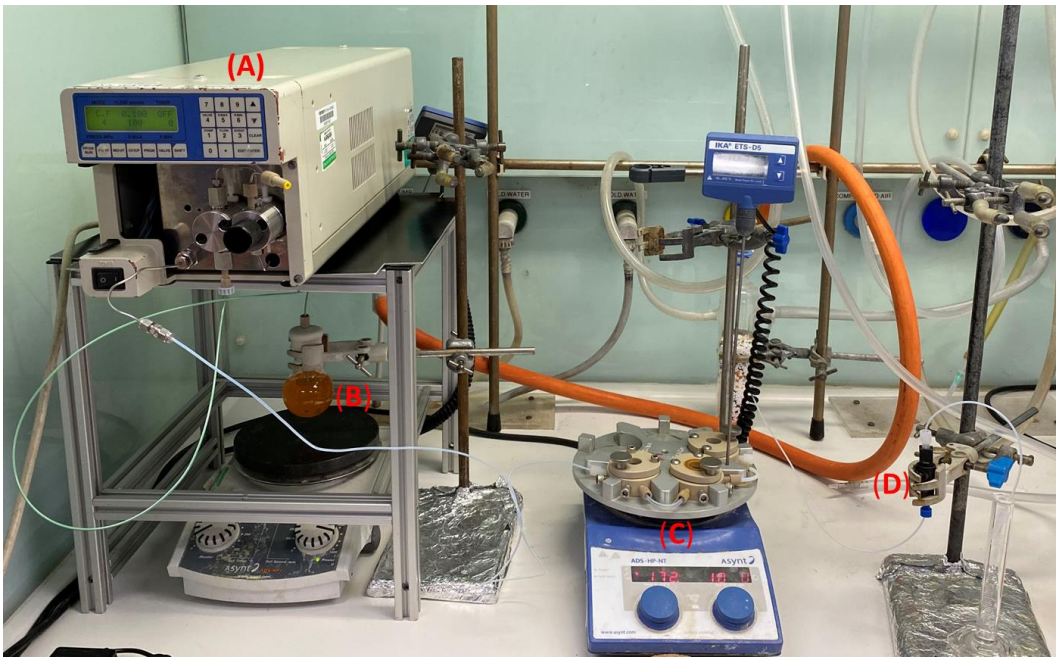

Figure 89: Continuous borrowing hydrogen set up where (A) is a JASCO PU-980 HPLC pump (B) hydroamination feedstock containing 100 mM alcohol, 100 mM amine and 1 mM $[Cp^*IrCl_2]_2$ in ^{i}PrOAc (C) is a series of fReactor CSTRs, heated by a stirrer hot plate and (D) is a back pressure regulator (BPR).

All future continuous flow reactions followed the general procedure: a solution containing 100 mM alcohol, 100 mM amine and 1 mM $[Cp^*IrCl_2]_2$ in isopropyl acetate was pumped through a series of fReactor CSTRs, purging any air from the system. A BPR was connected after the final device and the reactors then heated to give a fluid temperature of 140 °C.

Once the fluid temperature reached 140 °C, the reaction mixture was pumped through the reactor at the specified flow rate. The flow rate required was calculated using Equation 8, with a 1.7 mL volume per fReactor unit.

$$Flow\ rate\ (mL\ min^{-1}) = \frac{Reactor\ volume\ (mL)}{Residence\ time\ (min)}$$

Equation 8: Flow rate calculation within fReactor CSTRs.

The outlet stream was collected in aliquots corresponding to the total reactor volume and the crude residue analysed by ^{1}H NMR against an internal standard.

3.1.7.2 Optimised conditions for continuous flow borrowing hydrogen

With the benefits of elevated temperatures already being demonstrated, the reaction was then translated from batch to continuous flow. Initial screening reactions in flow were performed with 1 mol% $[Cp^*IrCl_2]_2$ in isopropyl acetate (0.1 M). A fluid temperature of 140 °C was achieved upon application of a 100 psi BPR and was contained within a series of three fReactor modules for a residence time of 1 h.

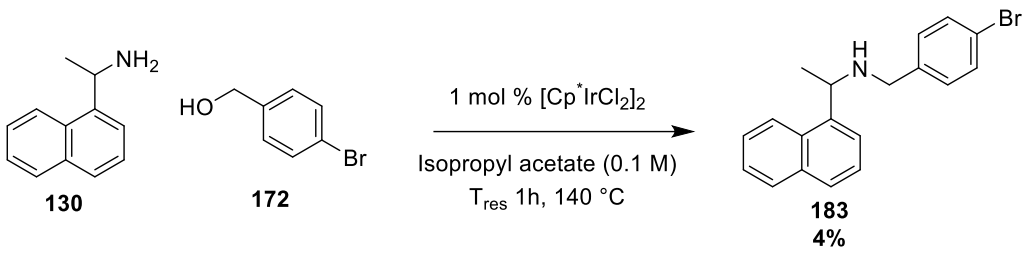

Figure 90: Continuous flow borrowing hydrogen reaction between NEA and 4-bromo benzylalcohol. Reactions were performed in isopropyl acetate (0.1 M), with 1 mol% $[Cp^*IrCl_2]_2$ for a residence time of 1 h and fluid temperature of 140 °C.

The poor (4%) conversion observed was proposed to be a consequence of low catalyst solubility in isopropyl acetate, with large deposits of catalyst remaining within the feed solution. Subsequently, a new solvent system was designed based on the solubility of the catalyst.

A 5 mM solution of $[Cp^*IrCl_2]_2$ was prepared in a range of solvents and solvent combinations and left unstirred for 72h. After this time, only one solvent combination contained no precipitate, a solution of 10% acetonitrile in toluene. With the prospect of an upstream lipase-mediated kinetic resolution performed within isopropyl acetate, the full solvent system that would be present in the downstream chemistry would be 50:45:5 isopropyl acetate/toluene/acetonitrile.

The newly derived solvent system was first applied in batch to assure its applicability within the reaction. A reaction between NEA and 4-bromobenzyl alcohol was

performed in 50:45:5 isopropyl acetate/toluene/acetonitrile (0.1 M) at reflux for 16 h, Figure 91.

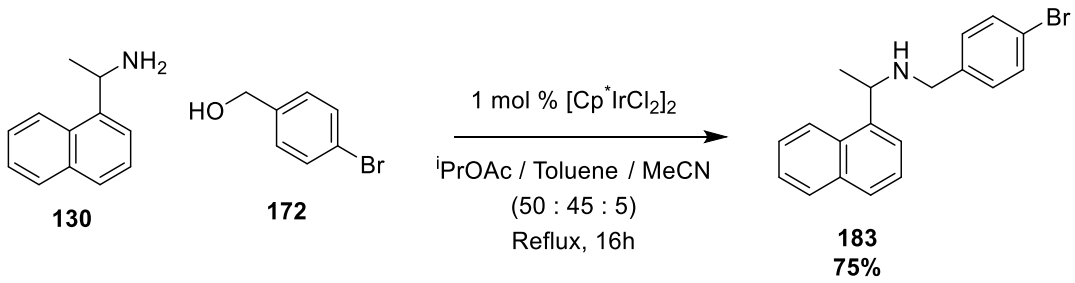

Figure 91: Borrowing hydrogen reaction between NEA and 4-bromobenzylalcohol in a three-solvent system in batch. The reaction was performed in 50:45:5 isopropyl acetate/toluene/acetonitrile (0.1 M) at reflux for 16 h.

With the new solvent system proving successful in batch, it was then applied to a continuous flow reaction. The catalyst loading was increased to 2 mol% and the reaction was performed with a fluid temperature of 140 °C and a residence time of 1 h.

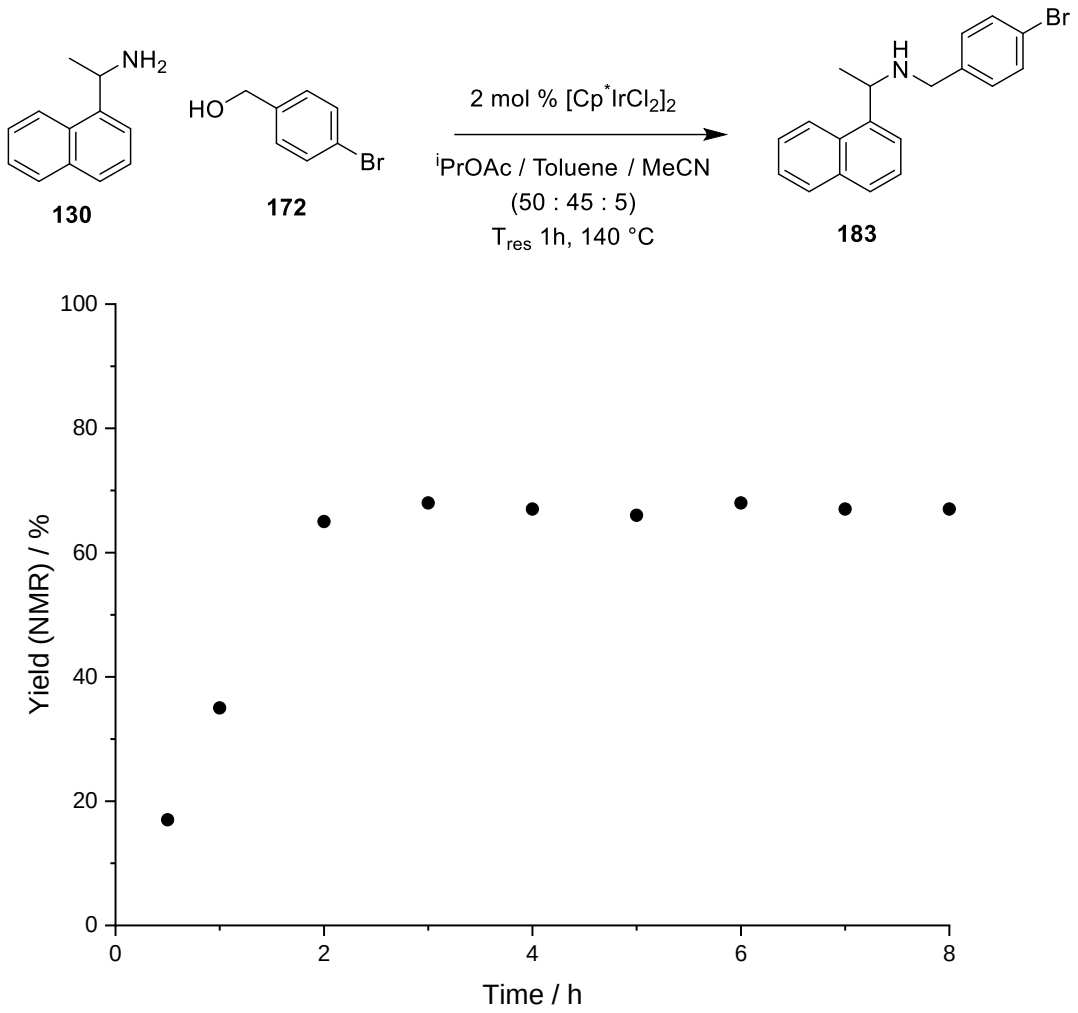

Figure 92: Borrowing hydrogen reaction between NEA and 4-bromobenzylalcohol in a three-solvent system in continuous flow. The reaction was performed with a residence time of 1 h and a fluid temperature of 140 °C maintained by a 100 psi BPR. Yield was determined by ^{1}H NMR against and internal standard.

A very good steady state conversion (66.8% ± 0.9%) was achieved after 2h reaction time (two residence times). This demonstrated the applicability of the chemistry within continuous flow, with a residence time compatible with the upstream biocatalytic reaction.

3.2 Anti-Markovnikov Hydroamination *N*-alkylation

As a result of considerable developments in photoredox catalysis, the application of photochemistry within organic synthesis has seen huge growth.[279, 280] Furthermore,

where transition metal catalysed hydroamination reactions of styrenes have previously been reported to give Markovnikov products,[281-284] recent advances in photoredox hydroamination catalysis have enabled control of regio-selectivity within hydroamination chemistry in an anti-Markovnikov manner.[285-288] Moreover, photoredox hydroamination reactions between primary amines and alkenes, with minimal over alkylation and excellent regioselectivity is now possible.[289]

In an analogous manner to borrowing hydrogen chemistry, photochemistry has potential downfalls that hinders its use at the industrial scale, with dilute reaction conditions and issues with light penetration both negatively influencing its scalability.[290, 291] Recent developments towards continuous flow photochemical reactors has negated the some of the scalability issues surrounding photochemical reactions.[291-293]

Within this section, two complementary photoredox hydroamination methodologies will be applied to a range of substrates to access the target compounds and analogues outlined at the start of this chapter.

3.2.1 Mechanistic insights of photoredox hydroaminations

To implement the two hydroamination pathways, two different photocatalysts with different redox potentials are required, Figure 93.

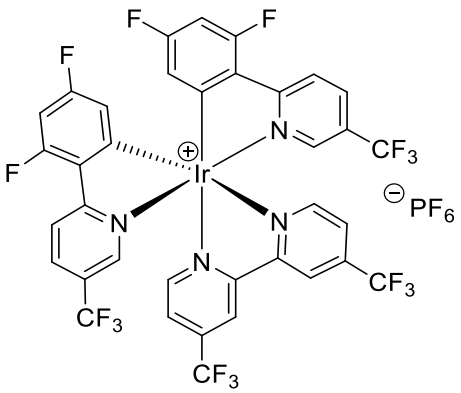

202

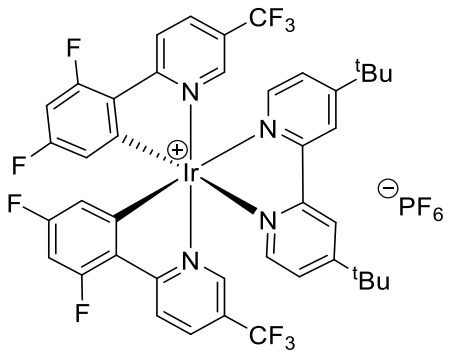

203

Figure 93: Iridium photocatalysts used in the photoredox hydroaminations.

Photocatalyst 202 ([Ir(dF(CF$_3$)ppy)$_2$(4,4'-CF$_3$-bpy)]PF$_6$) has previously been employed by Knowles to achieve anti-Markovnikov additions of primary amines with a range of alkene substrates.[285, 287, 289] Within the mechanism proposed by Knowles, for both primary and secondary amines, the reaction proceeds through the formation of aminium radicals with reductive quenching of the photocatalyst, Figure 94.[294]

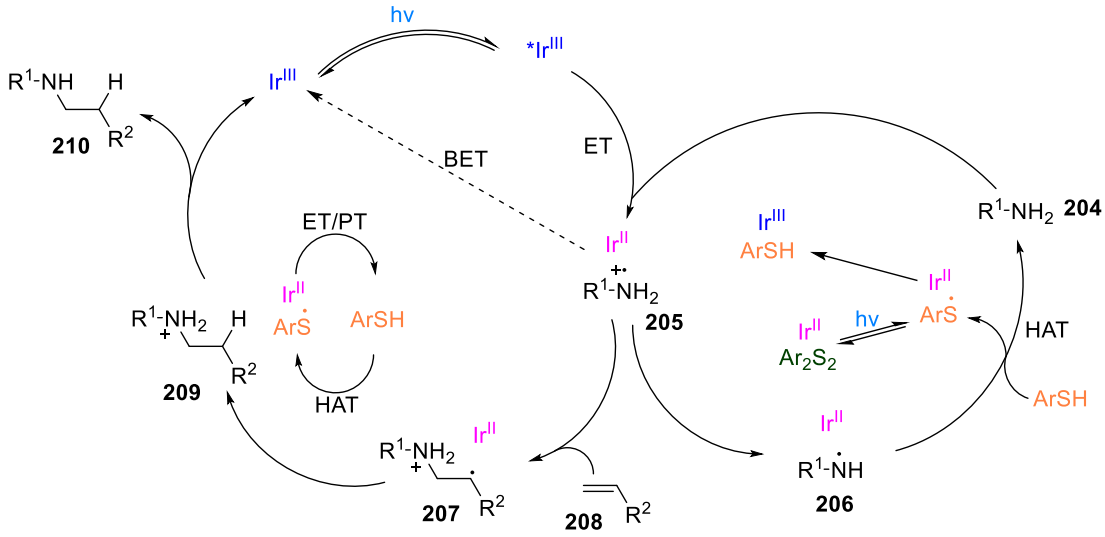

Figure 94: Complete reaction cycle for photoredox hydroamination proposed by Knowles. ET = electron transfer; BET = back-electron transfer; PT = proton transfer; HAT = hydrogen atom transfer, adapted from Qin et al.[294]

The aminium radical cation can then react with an alkene to generate the corresponding α-carbon-centred radical species, with subsequent hydrogen atom abstraction from the thiol co-catalyst.[285]

Knowles further demonstrated that secondary amine products are selectively obtained with little over-reaction to produce tertiary amines (*ca.* 2%). This chemoselectivity arises from faster addition of the primary aminium radical cations compared to secondary aminium radical cations to the alkene and was found not to be photocatalyst-specific.[294]

Photocatalyst 203 ([Ir(dF(CF$_3$)ppy)$_2$(dtbpy)]PF$_6$) has previously been employed within our group to achieve anti-Markovnikov additions of amines to enecarbamates and

eneamides.[149, 292] Whilst photocatalyst B is capable of performing hydroaminations with more easily oxidised secondary amines through the formation of aminium radical cations through a similar mechanism to that in Figure 94, we have previously found that with enecarbamates photocatalyst 203 could lead to hydroamination products with primary amines that are not oxidised by this catalyst.[149, 289] Subsequently, a mechanism distinct from that operating in Knowles' reactions was proposed for the coupling of enecarbamates and primary alkyl amines, Figure 95.[149, 292]

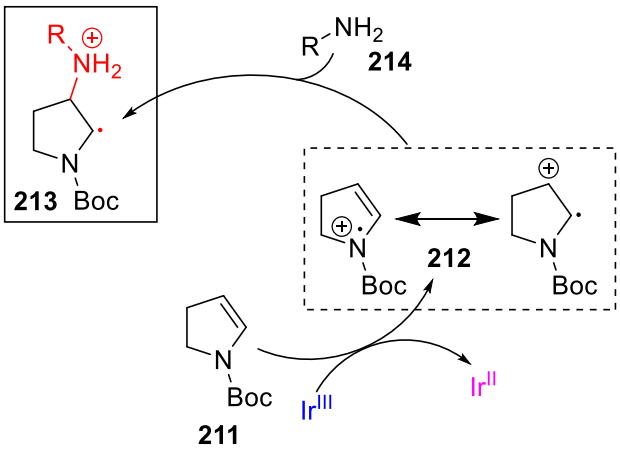

Figure 95: Alternative mechanistic pathway based on photocatalyst quenching by an enecarbamate.[149, 292]

Stern-Volmer fluorescence quenching analysis identified enecarbamates as better quenching agents for excited photocatalyst B than primary alkyl amines, giving further support to the proposed alternative mechanism.[149]

3.2.2 Hydroamination Substrate Screening

To access the model compounds outlined in section 3.1.3, both the Knowles-type and Marsden-type photoredox hydroaminations need to be applied to the amines generated in the biocatalytic stage. Within each of these reports, only two examples of α-aryl amines have previously been demonstrated (2-phenyl-2-propylamine and benzylamine).[149, 289]

We therefore selected three amines to examine the hydroamination photoredox reaction in our systems: cyclohexylamine, MBA and NEA. Cyclohexylamine was selected as it allowed direct comparisons to batch reactions that have been reported previously.[289]

3.2.2.1 Utilisation of photoredox hydroamination to access cinacalcet and analogues

For cinacalcet to be synthesised photochemically through anti-Markovnikov hydroamination it was necessary to produce 3-[(3-trifluoromethyl)phenyl]-1-propene, which could be accessed using a literature procedure,[295] with a 74 % yield achieved after 22 h, Figure 96.

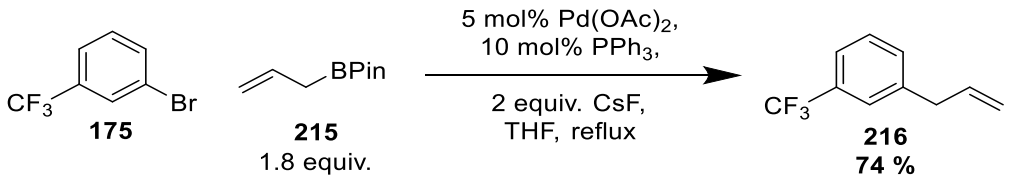

Figure 96: Synthesis of 3-[(3-trifluoromethyl)phenyl]-1-propene from 3-bromobenzotrifluoride and 1.8 equivalents of allylboronic acid pinacol ester. The reaction was performed in THF (0.13 M) with 2 equivalents of CsF, 5 mol% $PdPh_3$ and 10 mol% PPh_3 at reflux for 22 h.

In an analogous manner to cyclohexylamine being employed to allow direct comparisons to the literature, methylenecyclopentane, methylenecyclohexane and cyclohexene were employed to demonstrate the feasibility of MBA and NEA as substrates within the hydroamination photoredox process. Subsequently, the three amines were then reacted with six alkenes under standard conditions, yielding 16 isolated products shown in Figure 97.

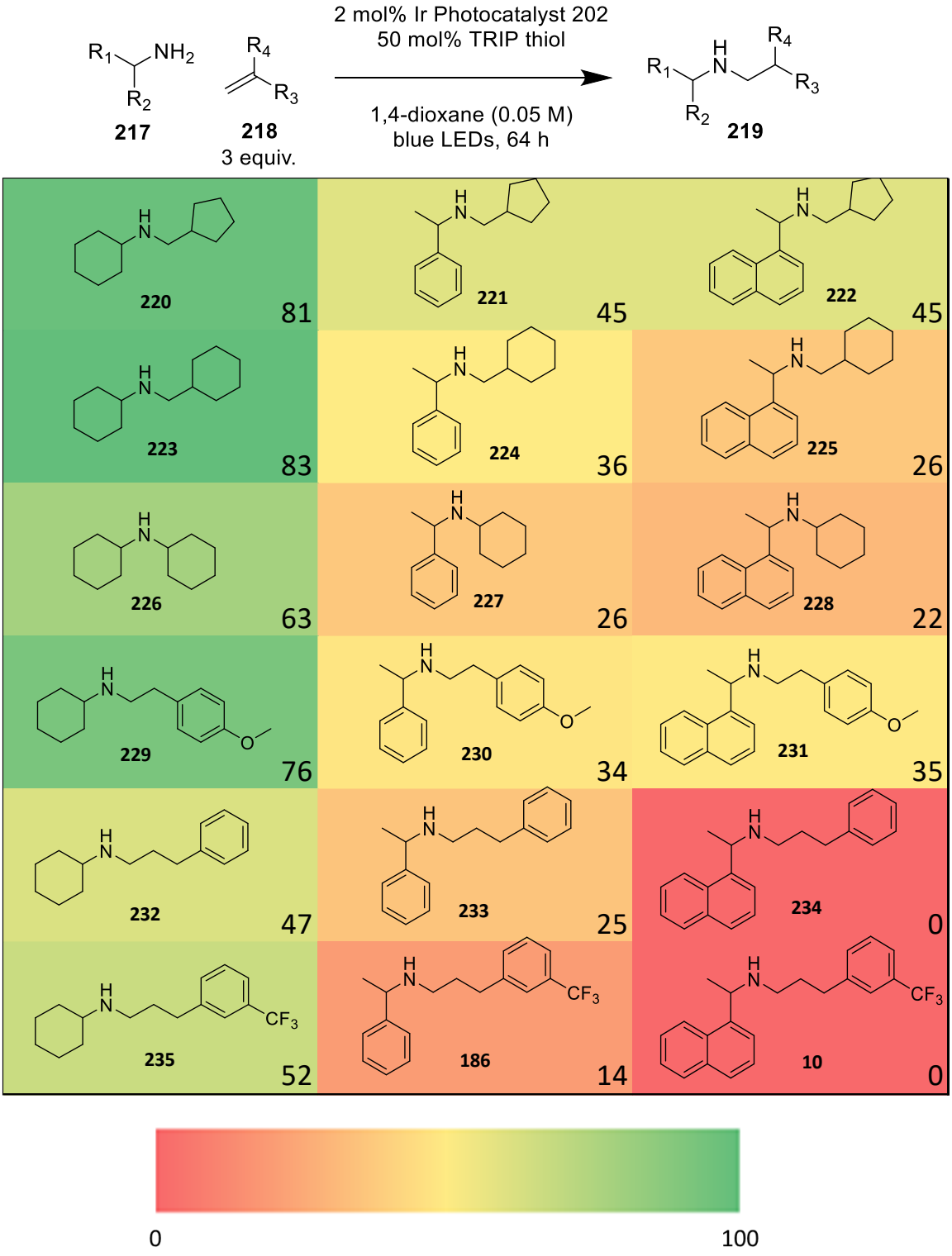

Figure 97: Isolated yields of 3 amines reacting with 6 alkenes in anti-Markovnikov hydroamination photoredox reactions. Reactions were performed in dry 1,4-dioxane (0.05 M), with 3 equivalents of alkene, 2 mol% [Ir(dF(CF₃)ppy)₂(4,4'-CF₃-bpy)PF₆, 50 mol% TRIP thiol and irradiated with a blue LED for 64 h.

The aliphatic cyclohexylamine performed better than the two α-aryl amines for all alkenes. Pleasingly, the more challenging, allyl benzene and 3-[(3-trifluoromethyl)phenyl]-1-propene substrates returned moderate yields, demonstrating their applicability within the reaction.

Both MBA and NEA returned poor to moderate yields across the six alkene substrates, with yields considerably lower than observed with cyclohexylamine, consistent with previous findings with α-aryl amines compared to primary alkyl amines.[149, 289] It is not currently clear what causes the differences in reactivity between the α-aryl amines and cyclohexylamine. One possible explanation is the larger α-substituent of the aryl amines results in more degrees of freedom compared to the more conformationally constrained cyclohexylamine.

Despite no product being observed for the target molecule 10, it was hoped that by translating the reactions into continuous flow, with a different reactor configuration and more powerful LEDs, not only could these yields be increased but the reaction time of 64 h be shortened drastically.

3.2.2.2 Utilisation of photoredox hydroamination to access a key intermediate in the synthesis of evocalcet

To access the key evocalcet intermediate and analogues, an alternative catalyst system was required. Using enecarbamates and primary amines with an alternative iridium photocatalyst 203 (Figure 93) it was possible to access the evocalcet intermediate as well as analogues with different ring size enecarbamates under conditions previously described by our group, Figure 98.[149]

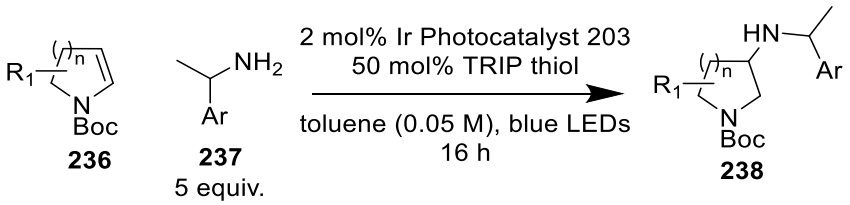

Figure 98: General reaction conditions for hydroamination photochemical reactions between enecarbamates and primary amines.

To access different ring sizes through this methodology, *N*-Boc-3,4-dihydro-2*H*-pyridine 240 and *N*-Boc 2-azetine 242 were synthesised from readily available starting materials.

N-Boc-3,4-dihydro-2*H*-pyridine 240 was accessed in three steps from piperidine (239), Figure 99. Boc-protected piperidine was subjected to an anodic oxidation, first described by Shono[296, 297], that has since been used to generate a range of enecarbamates[298, 299] as a consequence of the method being expanded to the functionalisation of simple cyclic protected amines.[300] MeOH was then eliminated from the intermediate α-methoxycarbamate,[301] to give 240 in 57% yield across the three steps.

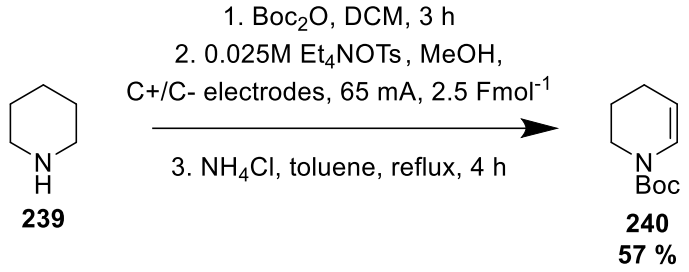

Figure 99: Synthesis of tert-Butyl 3,4-dihydropyridine-1(2H)-carboxylate in three steps from piperidine (239).

N-Boc azetidine was accessed in two steps from *N*-Boc-3-hydroxyazetidine (241), according to a literature procedure.[302]

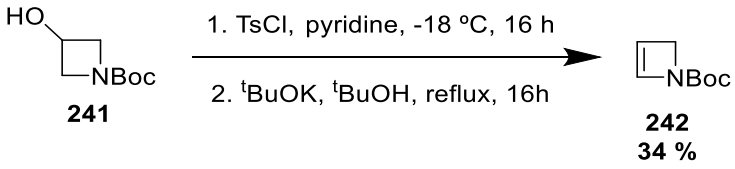

Figure 100: Synthesis of N-Boc 2-azetine in two steps from N-Boc 3-hydroxyazetidine.

Hydroamination reactions were performed on the two synthesised enecarbamates as well as the commercially available *N*-Boc-2,3-dihydropyrrole (211) with both MBA and NEA, applying the standard conditions in Figure 98. The desired product was obtained in all six reactions in poor to moderate yields, Figure 101.

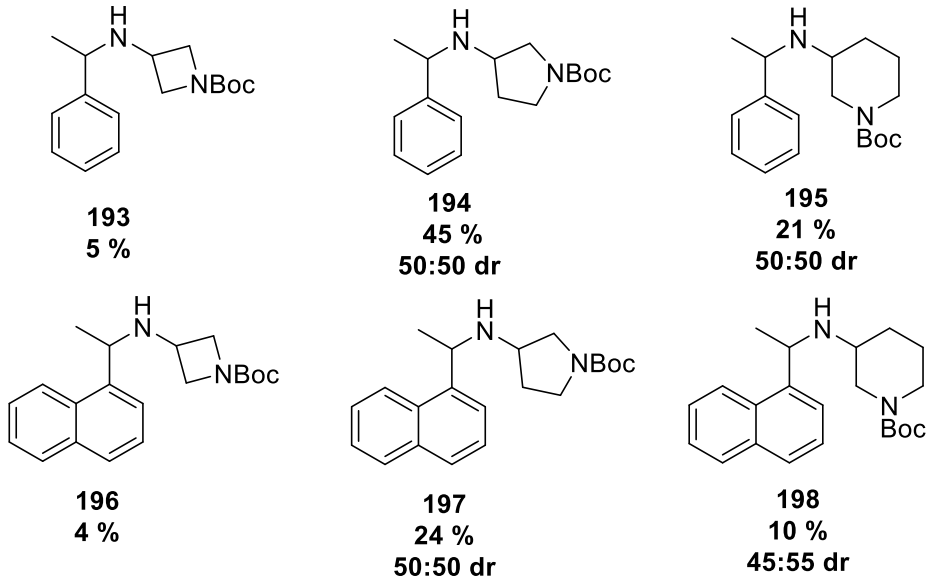

Figure 101: Effect of ring size on conversion within hydroamination photochemical reactions between enecarbamates and primary amines. Reactions were performed in toluene (0.05 M), with 2 mol% photocatalyst B, 50 mol% TRIP thiol and 5 equivalents of amine, irradiated with a blue LED for 16 h.

All the reactions were performed for a standard period of time (16 h) and in each of the crude ^{1}H NMRs, with the exception of the azetine reactions, there was evidence of unreacted enecarbamate. This suggests that if the reactions were left for longer, the yields would increase. As the ring size of the enecarbamate increases from a 5- to a 6-membered ring, the rate of the hydroamination reaction decreases, a trend previously observed within our group.[149, 299]

The reactions involving *N*-Boc 2-azetine were poor yielding owing to a competing side reaction which resulted in a near-quantitative yield of side product 244, Figure 102.

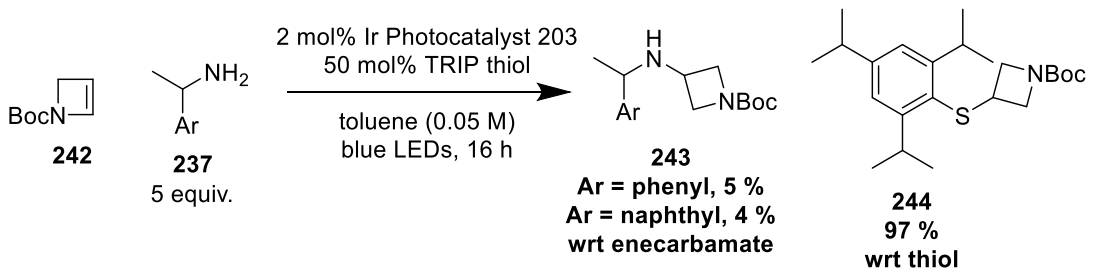

Figure 102: Side product formation between N-Boc 2-azetine and TRIP thiol.

This ‘thiol adduct’ side product 244 was not observed when any of the other enecarbamates were subjected to the reaction conditions. It is likely that the formation of 244 is only possible as the enecarbamate is small enough that the isopropyl groups of the thiol no longer prevent it from acting as a nucleophile.

To observe whether the formation of the thiol adduct product was due to the size of the enecarbamate, parallel reactions containing enecarbamate, iridium photocatalyst and thiol were performed, Figure 103.

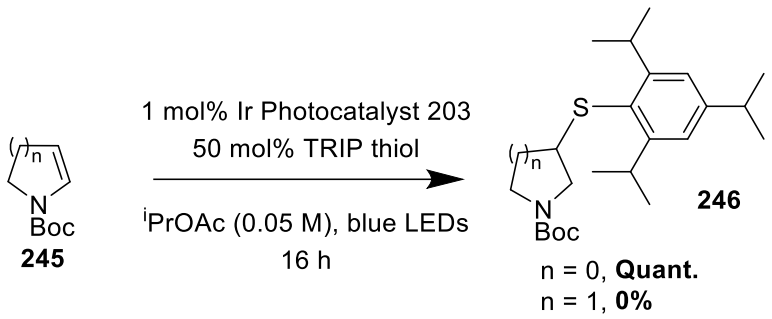

Figure 103: Investigating the cause of side product formation between enecarbamates and TRIP thiol. Reactions were performed in isopropyl acetate (0.05 M), with 1 mol% photocatalyst B, 50 mol% TRIP thiol and irradiated with a blue LED for 16 h.

After 16 h of irradiation, quantitative yield of the thiol adduct product was observed in the reaction involving the azetine (n = 0). In contrast, *N*-Boc-2,3-dihydropyrrole (n = 1) showed no signs of thiol addition, with the reaction returning only the starting materials. This demonstrated that the addition of the thiol to the azetine was likely due to the reduced steric bulk of this substrate; it also showed that thiol addition proceeds in absence of the amine co-substrate.

The reaction conditions applied in the screening reactions above were taken directly from literature,[149] where 5 equivalents of amine were required. With an upstream biocatalytic reaction generating a chiral amine, it would be wasteful to use the amine in excess. Therefore, for the reaction to be efficiently telescoped to an upstream biocatalytic reaction in continuous flow, the equivalency of the reaction would need to be lowered or have the enecarbamate in excess.

Despite the low yields observed in the reactions, it was hoped that these could be increased through the utilisation of an alternative reactor configuration, the photo fReactor, which can be operated in either batch or continuous flow modes.

3.2.3 Enhancement of hydroamination reaction rates using photo fReactor units

Photochemical reactions performed in batch are often limited by poor light penetration, particularly with larger vessels, leading to scaling issues. With greater control of thermal effects as well as shorter reaction times, continuous flow photochemical reactors are emerging as promising alternative to batch reactors.[291, 293]

Our group have recently developed a photochemical CSTR by interfacing LED units with the previously described fReactor platform.[292] Expanding on the original 'fReactor' platform, the LED photo-units sit atop the CSTR, allowing for a flexible, easy and safe-to-use platform for both batch and continuous flow photochemistry.[292] With the photo-fReactor, it was hoped that the reaction time could be drastically reduced from the extended reactions times that were necessary using a Kessil lamp.

3.2.3.1 Optimisation of anti-Markovnikov hydroamination reactions within fReactor CSTRs

The photo-units associated with the fReactor CSTRs were available in two fixed wavelength LEDs, 365 and 455 nm. Isopropyl acetate has previously been employed as a solvent in a literature mechanistic study of photoredox hydroamination, with a better yield observed than for reactions performed in 1,4-dioxane.[294] Moreover, toluene is the literature solvent for enecarbamate photoredox hydroaminations.[149] In addition to 1,4-dioxane, therefore, both isopropyl acetate and toluene were also screened as solvents within the fReactor photo-units at the two available wavelengths.

4-Methoxystyrene was selected as the alkene for the optimisation studies, owing to the comparable, but moderate, yields for both α-aryl amines after 64 h in batch (Figure 97).

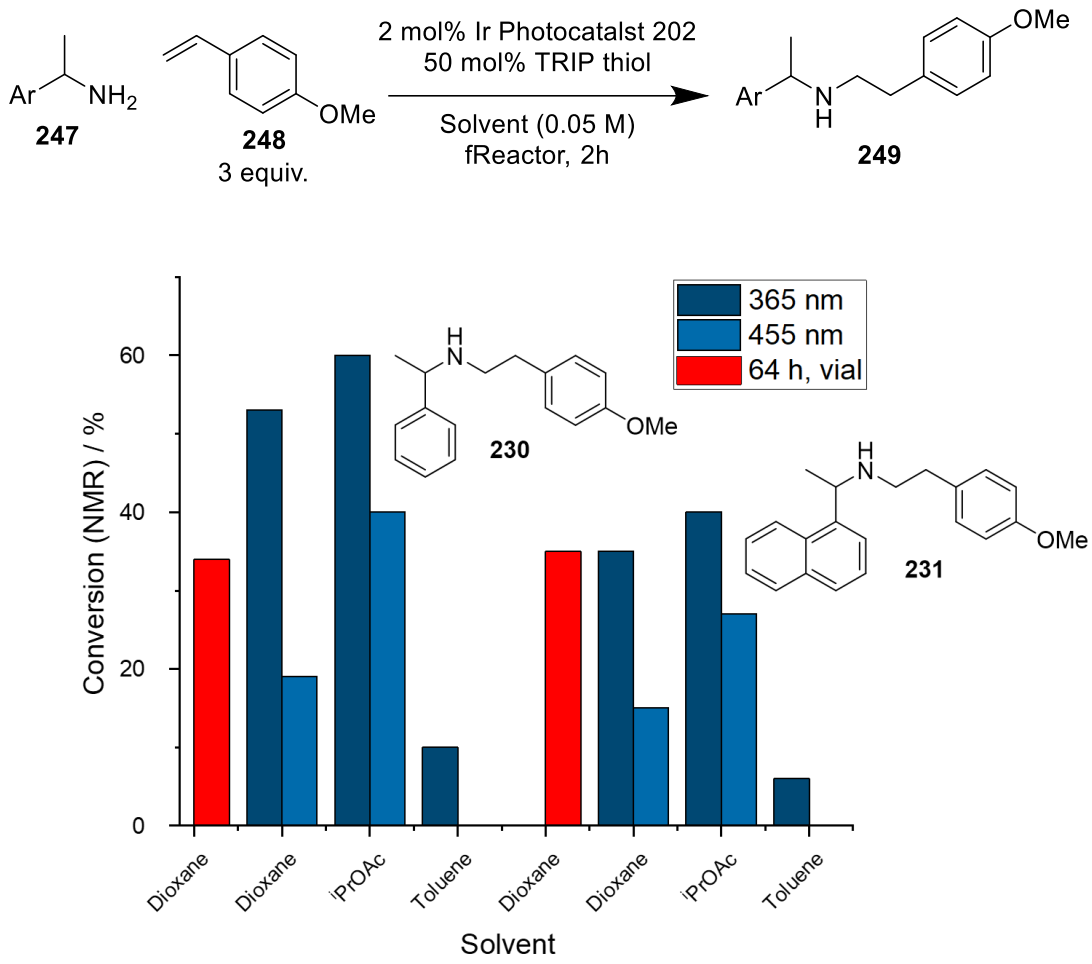

Figure 104: Hydroamination reaction of 4-methoxystyrene with MBA or NEA in the photo fReactor units compared to the same reactions performed in a vial with a 40W Kessil A160WE tuna blue LED. Reactions were performed in dry or degassed solvent (0.05 M), with 3 equivalents of alkene, 2 mol% [Ir(dF(CF₃)ppy)₂(4,4'-CF₃-bpy)PF₆ and 50 mol% TRIP thiol. Conversions were determined by ^{1}H NMR against an internal standard.

The reactions performed with the 365 nm LED resulted in higher yields than those carried out at 455 nm within all three solvents for both primary amines. As the λ_{max} of the photocatalyst is 381 nm, Figure 105, it was expected that the 365 nm light would perform better.

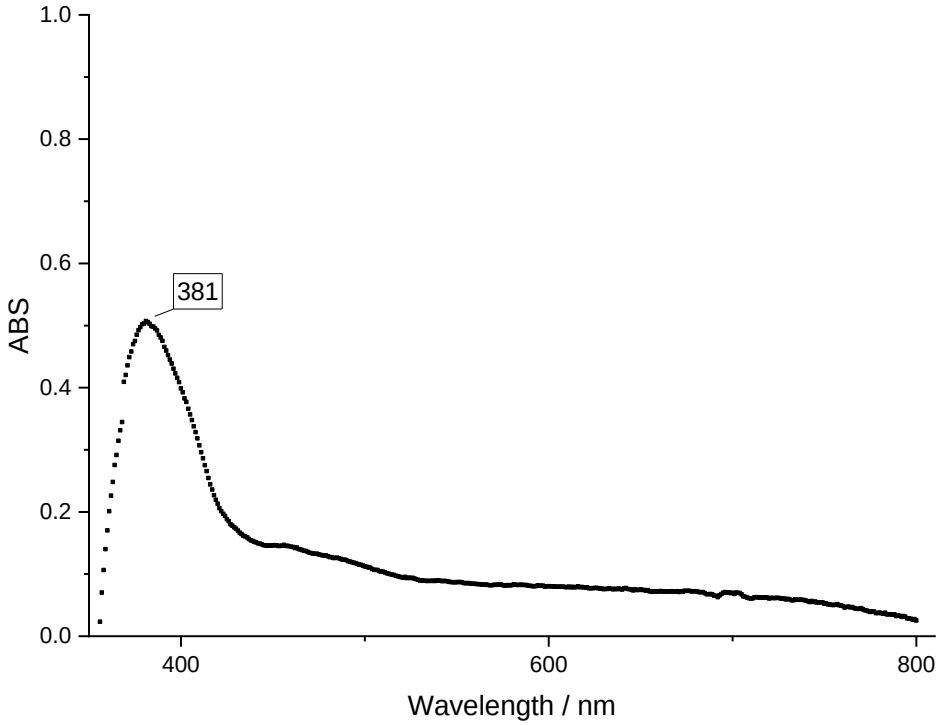

Figure 105: Absorbance spectrum of [Ir(dF(CF$_3$)ppy)$_2$(4,4'-CF$_3$-bpy)PF$_6$.

After 2 h within the fReactor CSTR using the 365 nm light, the yield of each secondary amine was comparable to, or better than, the equivalent reaction in a vial for 64 h in both dioxane and isopropyl acetate. Owing to its compatibility with the upstream lipase-mediated kinetic resolution, all future photo redox hydroamination reactions involving a primary amine and alkene were performed in isopropyl acetate.

3.2.3.2 Optimisation of enecarbamate hydroamination within fReactor CSTRs

The initial conditions for the enecarbamate hydroamination chemistry were taken directly from the literature,[149] in which five equivalents of amine were used. With a chiral amine being generated in the upstream biocatalytic step, using an excess of amine in the hydroamination chemistry effectively wastes precious enantioenriched material that has been formed. To increase the productivity of the telescoped continuous flow system, the equivalency of amine within the reaction needs to be lowered to equimolar amounts or the enecarbamate could even be in excess.

A change of solvent from toluene to isopropyl acetate was also desirable as it would allow the same solvent being used throughout a continuous flow system with an upstream lipase-mediated kinetic resolution.

In addition to the change of solvent and lowering of equivalence, the concentration of the reaction also needs to be doubled, to be representative of the concentration of amine in the product stream of the upstream biocatalytic reaction.

Owing to ease of interpretation of the crude ^{1}H NMR, as well as the commercial availability of *N*-Boc-2,3-dihydropyrrole, it was selected alongside NEA as the substrates in the optimisation studies, Figure 106.

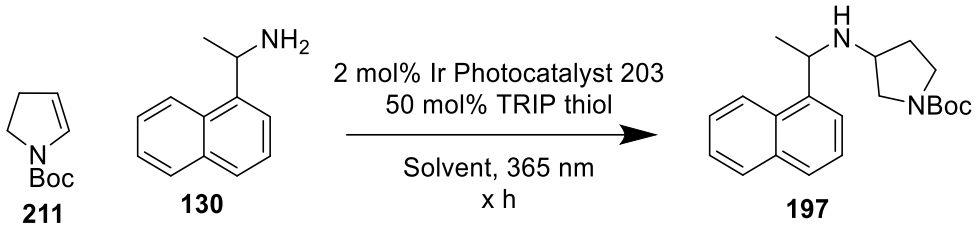

Ratio of enecarbamate : amine	Reaction Time / h	Concentration / mM	Solvent	Reactor	Yield (Isolated) / %
1 : 5	16	50	Toluene	Vial	26 (24)
1 : 2	1	100	^{i}PrOAc	fReactor	18
1.5 : 1	1	100	^{i}PrOAc	fReactor	30
1.5 : 1	2	100	^{i}PrOAc	fReactor	48
1.5 : 1	4	100	^{i}PrOAc	fReactor	63
1.5 : 1	8	100	^{i}PrOAc	fReactor	73

Figure 106: Optimisation of ene-carbamate hydroamination within fReactor CSTRs for the reaction of NEA and N-Boc-2,3-dihydropyrrole. Reactions were performed using 2 mol% $(Ir[dF(CF_3)ppy]_2(dtbpy))PF_6$ and 50 mol% TRIP thiol. Yields were determined from the crude ^1H NMR against an internal standard.

After a reduction in amine equivalents and reaction time as well as an increase in concentration and change of solvent, an 18% yield was observed after just 1 h in the fReactor. Furthermore, when the amine was made the limiting reagent, with 1.5 equivalents of enecarbamate, after just 1 h in the fReactor, the yield was greater than had been previously obtained in a vial.

As the reaction time was doubled, the yield increased linearly up to 8 h of reaction time. Whilst the increase in yield with reaction time was linear, when considering STY within a continuous flow set-up, the most productive reaction time was found to be 1 h. Subsequently, all future hydroamination reactions were therefore performed with a residence time of 1 h.

3.2.4 Compatibility of photoredox hydroamination reactions with the enzymatic product stream

Unlike the reactions earlier within this section, in the continuous flow chemoenzymatic set up, components of the upstream biocatalytic reaction will be present in the downstream chemistry. The compatibility of photoredox hydroamination chemistry in the presence of the extra reaction components, therefore, needed to be examined.

3.2.4.1 Ketone compatibility within photoredox hydroamination chemistry

Results from studies on extractive work-ups demonstrated that unreacted ketone starting material from the transaminase reaction would be found in the organic layer (see 2.1.7) and would subsequently be present in the downstream hydroamination reaction. Subsequently, any potential cross reactivity with unreacted ketone was investigated within the photoredox hydroamination reaction of NEA and 4-methoxystyrene.

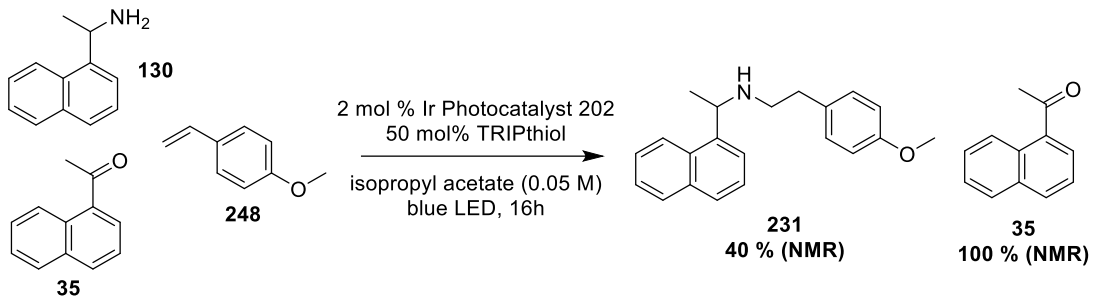

Figure 107: Photoredox hydroamination of NEA with 4-methoxystyrene, doped with 1'-acetonaphthone. The reaction was performed in isopropyl acetate (0.05 M), with 0.5 equivalents of 1'-acetonaphthone, 3 equiv. alkene, 2 mol% iridium photocatalyst A, 50 mol% TRIP thiol and irradiated with blue LEDs for 16 h.

Based on integration of the crude ^{1}H NMR against an internal standard, it was apparent that 1-acetonaphthone had not been consumed within the reaction. Coupled with the yield of the reaction remaining consistent with the yield when the ketone is not present, Figure 97, it can be concluded that presence of the ketone has minimal effect upon the reaction.

3.2.4.2 Amide compatibility within photoredox hydroamination chemistry

As the lipase mediated kinetic resolution produces the *N*-acetyl amide as a by-product and there is no solvent switch between the two stages, the amide would be present in the hydroamination reaction and potential cross-reactivity needed investigating. A reaction of NEA and 4-methoxystyrene was carried out in isopropyl acetate (0.05M) with 1 equivalent of *N*-acetyl-1-(1-naphthyl)ethylamine doped into the reaction mixture, Figure 108.

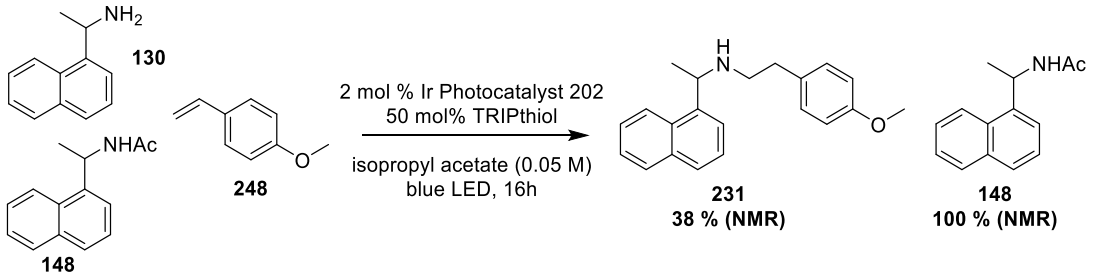

Figure 108: Photoredox hydroamination of NEA with 4-methoxystyrene, doped with N-acetyl-1-(1-naphthyl)ethylamine. The reaction was performed in isopropyl acetate (0.05 M), with 1.0 equivalents

of N-acetyl-1-(1-naphthyl)ethylamine, 3 equiv. alkene, 2 mol% iridium photocatalyst A, 50 mol% TRIP thiol and irradiated with blue LEDs for 16 h. Yields were determined from the crude ^{1}H NMR against an internal standard.

After 16 h of irradiation, no *N*-alkylation of the amide was observed, whilst the yield of the desired product is comparable to when there is no doped amide in the reaction mixture. This therefore demonstrates the compatibility of the lipase product stream within photoredox hydroamination reactions.

3.2.4.3 Retention of stereochemical purity within anti-Markovnikov hydroamination reactions

Iridium-based photocatalysts have previously been employed in photochemical racemisation processes.[101, 303-305] Whilst these reaction conditions differ from those employed to achieve hydroamination, the extent of possible racemisation needed to be assessed.

The hydroamination conditions from the previous section (3.2.3.1) were applied to three combinations of substrates, with enantiopure amine starting materials, Figure 109.

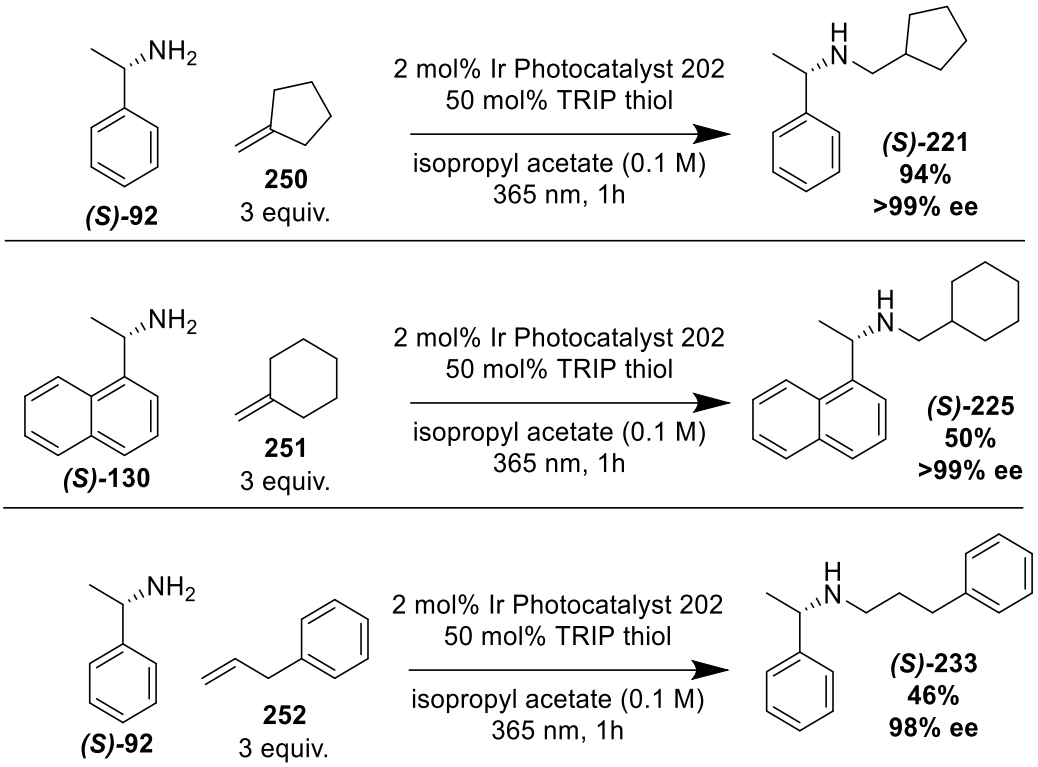

Figure 109: Enantiomeric retention within photoredox hydroamination reactions. Reactions were performed in isopropyl acetate (0.1 M), with 3 equivalents of alkene, 2 mol% [Ir(dF(CF$_3$)ppy)$_2$(4,4'-CF$_3$-bpy)PF$_6$ and 50 mol% TRIP thiol and irradiated at 365 nm for 1h.

Within each of the three substrate combinations, >98%*ee* was observed. This emphasised that a high level of enantiomeric retention would be achieved when photoredox hydroamination is telescoped to an upstream biocatalytic reaction.

3.2.5 Stern-Volmer fluorescence quenching experiments

Due to the consistent observed differences in yields between the two α-aryl amines (MBA, NEA) in the hydroamination reactions with both simple alkenes and enecarbamates, Stern-Volmer quenching experiments were performed on both photocatalysts (202 and 203) and both amines.

Stock solutions of photocatalysts (0.42 mM) and quenchers (360 mM) were prepared in isopropyl acetate. An aliquot of photocatalyst solution was added to a cuvette and irradiated at 380 nm, with luminescence recorded at 582 and 478 nm for photocatalysts 202 and 203 respectively. Aliquots of quencher solution were added

sequentially (2 mM increase in quencher concentration per aliquot) and the samples irradiated, with luminescence recorded twice per sample.

The quenching capabilities of both amines were examined, in addition to cyclohexylamine and 1-(1-naphthyl)ethanol to determine if the naphthyl group itself has any quenching capabilities, which might help to explain the differences in reactivity of MBA and NEA.

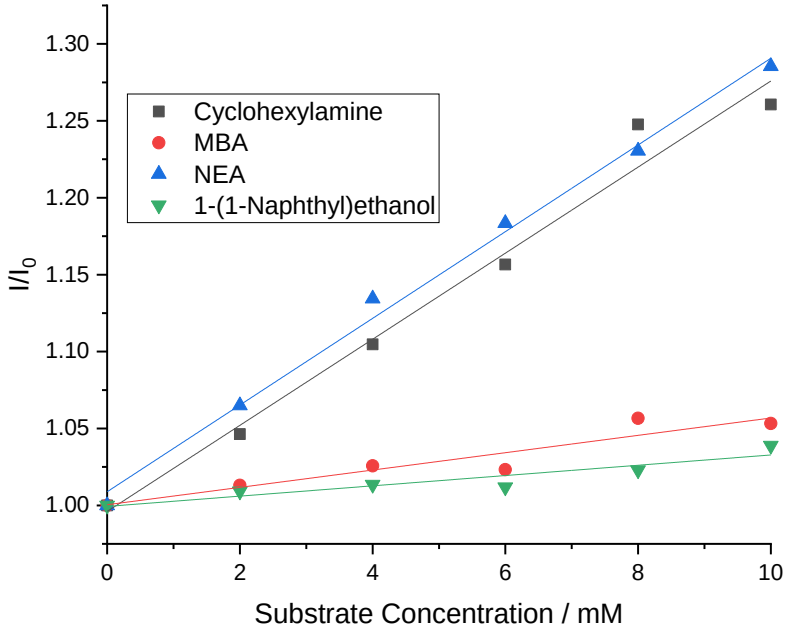

Figure 110: Stern-Volmer fluorescence quenching of catalyst 202 ("F" catalyst). Measurements were performed at 0.42 mM photocatalyst in isopropyl acetate with sequential additions of 20 µL of quencher (360 mM). Photocatalyst was irradiated at 380 nm with the luminescence recorded at 582 nm.

With photocatalyst 202, both cyclohexylamine and NEA exhibit a higher rate of quenching than the other two species. The near flat line of 1-(1-naphthyl)ethanol suggests that there is no quenching of photocatalyst 202 by the naphthyl ring of NEA.

Subsequently the quenching observed with NEA must be due to the formation of an aminium radical cation as required by the reaction mechanism. Despite the

quenching rate of cyclohexylamine and NEA being similar, the conversions of the reactions involving both amines are markedly different. This could be a consequence of a charge transfer from the aminium ion to the long-lived triplet state of the naphthalene group,[306] reducing the productive quenching of NEA.

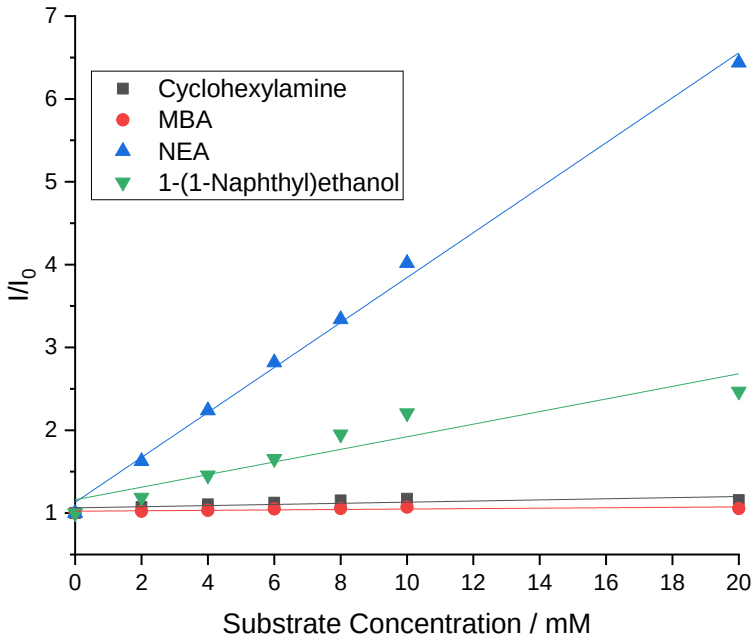

Figure 111: Stern-Volmer fluorescence quenching of catalyst 203 ("CF_3" catalyst). Measurements were performed at 0.42 mM photocatalyst in isopropyl acetate with sequential additions of 20 µL of quencher (360 mM). Photocatalyst was irradiated at 380 nm with the luminescence at 478 nm.

With photocatalyst 203, the quenching profiles for MBA and cyclohexylamine show similarities to the profiles with photocatalyst 202, whereas both compounds containing the naphthyl group both exhibited faster rates of quenching than MBA and cyclohexylamine.

As 1-(1-naphthyl)ethanol demonstrates some quenching behaviour, this suggests that some of the quenching observed with NEA is due to a charge transfer from the excited photocatalyst to the aromatic system.

NEA maintains a higher rate of quench of catalyst B than all the other species. The mechanism of the hydroaminations with enecarbamate substrates is thought to proceed through activation of the enecarbamate, generating an electrophilic radical cation intermediate which can be trapped by an amine nucleophile, Figure 95.[149, 285] As NEA also has a higher rate of quenching than the enecarbamate(s), previously determined by our group,[149] it was proposed that NEA reactions might proceed through a different mechanistic pathway than MBA. To investigate this possibility, parallel hydroamination reactions of NEA and *N*-Boc-2,3-dihydropyrrole were set up with each photocatalyst, Figure 112.

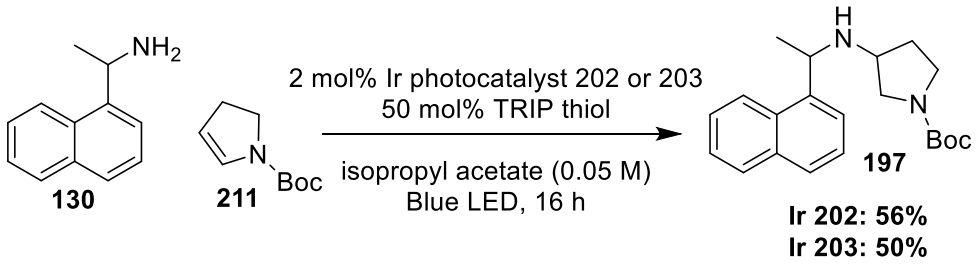

Figure 112: Comparison of the two iridium photocatalyst for the hydroamination reaction of NEA and N-(tert-butoxycarbonyl)-2,3-dihydropyrrole. Reactions were performed using 2 mol% photocatalyst and 50 mol% TRIP thiol. Yields were determined against an internal standard.

Whilst the yield using photocatalyst 202 is greater than for the "conventional" enecarbamate photocatalyst 203, the difference is not definitive enough to suggest an alternative reaction pathway.

It was hypothesized that the reactions involving NEA could be improved with an alternative catalyst with a larger energy difference between its triplet excited state and the triplet excited state of the naphthyl group, to prevent triplet energy transfer from occurring. This could be achieved through a catalyst and/or co-catalyst screen as both the photocatalyst and the HAT co-catalyst influence the productivity of the reaction through successful charge transfers to the substrate(s).

3.3 Chapter summary

Two alternative *N*-alkylation strategies have been employed on the two enzymatically generated α-aryl chiral amines from Chapter 3 with a range of substrates. Reaction conditions for both borrowing hydrogen and photoredox hydroamination chemistries were first applied in batch before being translated and optimised in continuous flow.

Through the translation to continuous flow, the reaction times for each process were drastically reduced (from 20-64h to 1h) whilst also resulting in an increase in yield. Moreover, translation of borrowing hydrogen chemistry to continuous flow enabled a steady state conversion (66.8% ± 0.9%) after just one hour residence time at 140 °C. Furthermore, retention of the stereochemistry was excellent in both the borrowing hydrogen (94-96 %*ee*) and in the hydroamination (98-99 %*ee*) reactions.

Both *N*-alkylation methods were found to be compatible with the by-products of each upstream enzymatic stages which simplifies any extraction stage required between the two reaction zones in the chemoenzymatic cascade.

Within the next chapter the combination of the enzymatic transformations (outlined in 2) will be combined with the two *N*-alkylation methods outlined within this chapter, in a single continuous flow cascade.

4 Access to chiral secondary amines through chemoenzymatic cascades within continuous flow

Traditionally, multi-step reaction sequences are performed in a batch-wise, iterative manner.[108] Not only is this time-consuming, it is also extremely wasteful and often requires the isolation and purification of each intermediate. Consequently, there are considerable environmental, economic and efficiency-based driving forces for implementing cascade reactions in continuous flow. Furthermore, cascading a reaction can be used to drive unfavourable equilibria, whilst also obviating the need for the isolation and purification of intermediates.[108, 116, 117]

A significant challenge associated with chemoenzymatic cascade reactions is the mismatching of the reaction conditions (e.g. different preferred solvents, temperatures, pH and concentrations between enzymatic and chemocatalytic steps),[119] a problem that can be alleviated through telescoping, where each stage of the process takes place in a different reaction zone.[121] In addition, utilisation of immobilised enzymes can vastly enhance the synergy of bio- and chemo-catalysis in a cascade.[118, 122]

Within this chapter, the two biocatalytic steps from 2 will be combined with the two chemocatalytic methods from 3 within a single continuous flow set up.

4.1 Continuous flow chemoenzymatic cascades with an upstream lipase-mediated kinetic resolution

One of the advantages of utilising an upstream lipase-mediated kinetic resolution is the solvent compatibility with the downstream chemistries as demonstrated in 3. This simplifies the continuous flow set up as there is no requirement for a solvent switch or extraction stage between the reaction zones.

Moreover, a lipase-mediated kinetic resolution offers a further advantage which is that the alternative enantiomer is protected against both the downstream chemistries in its acylated form, as demonstrated in 3.1.4 and 3.2.4. This could lead

to excellent enantiomeric excess of the *N*-alkylated secondary amine products after the two synthetic steps.

4.1.1 Lipase-mediated kinetic resolution in cascade with a photoredox hydroamination

As both the lipase-catalysed kinetic resolution and the photoredox hydroamination had been optimised separately (see 2.2.3 and 3.2.3), it was first envisaged that bringing the two systems together with no further optimisation would be possible. A 30 min residence time was maintained for the kinetic resolution and a 60 min residence time in the downstream hydroamination reaction, for a total residence time of 90 min in the chemoenzymatic continuous flow system.

A 200 mM stock of *rac*-amine in isopropyl acetate was first pumped through a PBR containing Novozym 435 with the outlet feeding into a series of 3 CSTR units and irradiated at 365 nm. A solution of photocatalyst (1 mM) and TRIP thiol (50 mM) with either an alkene (300 mM) or enecarbamate (150 mM) in isopropyl acetate was also pumped into the first CSTR of the series. The two streams of stock solutions were pumped into the continuous flow system at the same flow rate (50 µL min^{-1}). The outlet stream was collected in aliquots corresponding to the total reactor volume and the conversion determined at steady state (achieved after 2 h of operation) by ^{1}H NMR against an internal standard.

Figure 113: Photo of the lipase-hydroamination continuous flow cascade with a) the biocatalytic feedstock b) a PBR containing Novozym 435 inside an aluminium heating block c) a syringe pump containing the hydroamination feedstock d) a series of photo fReactor units with the organic outlet of the PBR and the hydroamination feedstock as inlets and e) an external cooling fan.

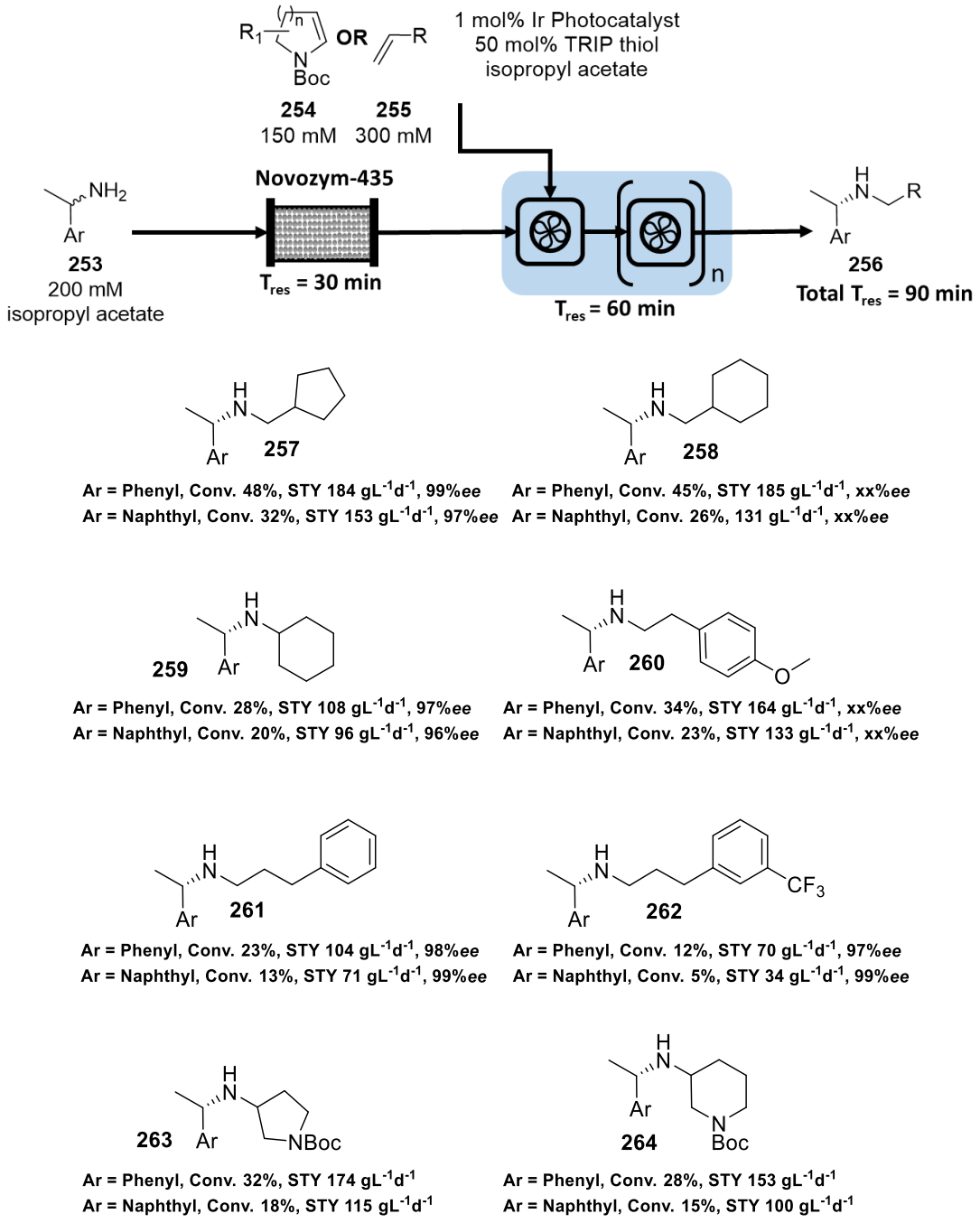

Figure 114: Chemoenzymatic continuously flow synthesis of chiral secondary amines through a lipase-mediated kinetic resolution, hydroamination cascade. Reactions were performed with 200 mM of rac-amine in isopropyl acetate with a separate feed containing photocatalyst (1 mM) and TRIP thiol (50 mM) with either an alkene (300 mM) or enecarbamate (150 mM) in isopropyl acetate for a total residence time of 90 min. Conversions are determined by ^{1}H NMR against an internal standard from the racemic primary amine (maximum theoretical = 50% following kinetic resolution).

It was possible to access 16 products through a lipase-hydroamination continuous flow cascade, with conversions ranging from 5-48%. The highest conversion occurred with a substrate combination of MBA and methylene cyclopentane in a near quantitative yield (48%), considering the 50% maximum theoretical yield imposed by the kinetic resolution.

The poor conversions observed with some of the substrate combinations occur due to the downstream hydroamination reaction, with the mass balance of the product stream highlighting complete kinetic resolution in the upstream reaction (determined by ratio of amide to internal standard in the ^{1}H NMR). The substrate combination leading to cinacalcet **10** resulted in the lowest yield at 5% steady state; however, considering that the hydroamination failed completely under batch conditions using a Kessil lamp (see 3.2.2.1), even this low conversion represents a demonstration of the value of the higher intensity light in our continuous photochemical reactors.

There are two alternative strategies that could be applied to increase the lower conversions observed within the cascade. The first is to extend the residence time for the photoredox hydroamination by adding more photo fReactor units (numbering up). Increasing residence time was previously demonstrated within section 3.2.3.2 and resulted in a linear increase in yield up to 8 h of reaction time but would incur a reduced productivity (STY) of the system. The second strategy involves increasing the loading of the iridium photocatalyst and will be discussed in the next section.

4.1.1.1 Effect of photocatalyst loading in the downstream photoredox hydroamination chemistry

There are two ways in which the catalyst loading can be increased within the continuous flow system. First, the concentration of catalyst within the stock solution of cocatalyst and substrate can be increased. Alternatively, multipoint injection of the same concentration of catalyst can be used to provide a constant infusion of fresh

photocatalyst into each CSTR. Multipoint injection could potentially be the better solution if competing photochemical decomposition of the catalyst is occurring.

Reactions were performed with 200 mM of *rac*-amine in isopropyl acetate with a separate feed containing photocatalyst (1 or 2 mM), TRIP thiol (50 mM) and 4-vinyl anisole (300 mM) in isopropyl acetate for a total residence time of 90 min. For the multipoint injection a third stream containing photocatalyst (1 mM) in isopropyl acetate was injected into the second CSTR in a series of three.

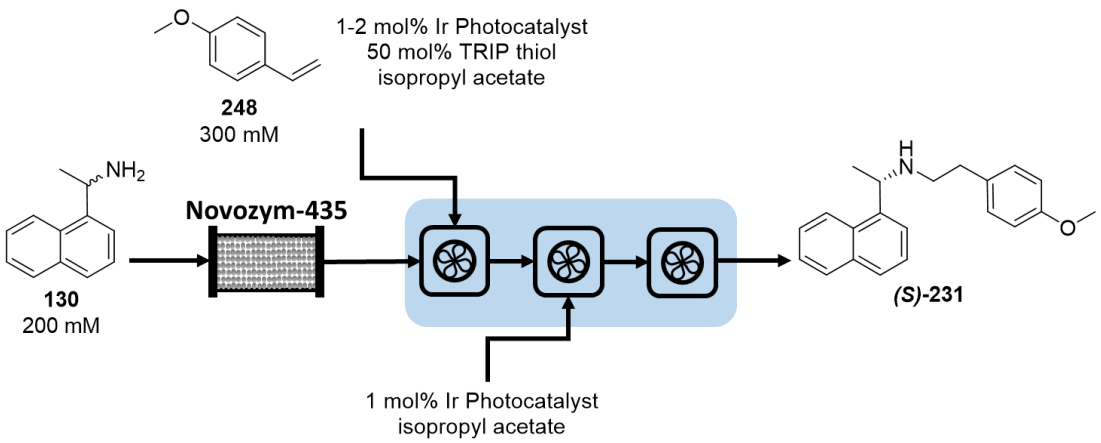

Total Ir loading / mol%	Average Ir loading per reactor / mol%	Conversion (NMR) / %	STY / gd^{-1}	STY / $gL^{-1}d^{-1}$	Mass Balance
1	1	23	1.01	123.7	51% Amide, 26% 1° Amine
2	2	35	1.54	188.2	50% Amide, 15% 1° Amine
2	1.67 *	35	2.04**	250.9**	50% Amide, 15% 1° Amine

*Figure 115: Affect of iridium loading and multipoint injection on the conversion of the lipase-photo chemoenzymatic cascade for the exemplar product (S)-231. *Extra iridium infusion into fReactor 2, **Average flow rate used to calculate. Conversions are determined by ^{1}H NMR against an internal standard.*

Whilst doubling the catalyst concentration resulted in an increase in conversion, the increase was not linear with respect to the catalyst concentration. When multipoint injection is used, the same level of conversion is observed as when the catalyst concentration is doubled, despite a lower effective catalyst loading per reactor. The increase in conversion is closer to being linear with the multipoint injection with respect to the increase in catalyst loading, with conversion expected to be ~38%.

The increase in STY observed for the multipoint injection is a consequence of the faster flow rates within the downstream hydroamination reaction, with the same conversion observed in a shorter residence time (37.6 min) than the doubling of catalyst concentration within a single feed. This suggests that multipoint injection can be implemented to increase the productivity of continuous flow hydroamination reactions.

With the increase in conversion being closer to linear with multipoint injection, the potential cause for the lower conversions with the single infusion of photocatalyst could be due to catalyst degradation. The fresh influx of photocatalyst in the multipoint injection system could be negating this effect.

4.1.2 Lipase-mediated kinetic resolution cascaded with elevated temperature borrowing hydrogen

With the lipase-hydroamination continuous flow cascade yielding 16 products successfully, attention was turned to the alternative downstream *N*-alkylation reaction. The effects of elevated temperature on both conversion and reaction times for borrowing hydrogen reactions on both conversion and reaction times were demonstrated in continuous flow in the previous chapter (3.1.7). Subsequently, the borrowing hydrogen reaction was attached downstream of the lipase-mediated kinetic resolution in a single continuous flow set up.

Reactions were performed with two stock solutions, the first a 200 mM stock of *rac*-amine in isopropyl acetate and the second a solution containing 100 mM of alcohol and 2 mM $[Cp^*IrCl_2]_2$ in a 90:10 mixture of toluene/acetonitrile.

The first solution was pumped through a PBR containing Novozym 435 (T_{res} = 30 min) with the outlet feeding into a series of 3 CSTR units heated to a fluid temperature of 140 °C. A second solution containing alcohol and iridium catalyst was also pumped into the first CSTR of the series. A 100 psi BPR was applied to the system to allow for operation above the atmospheric boiling point of the solvents. The outlet of the system was collected in aliquots corresponding to the total reactor volume and the conversion determined by NMR.

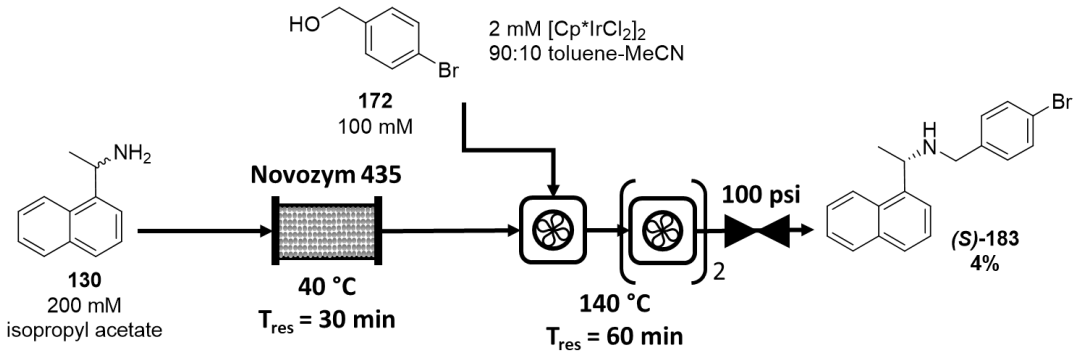

Figure 116: Lipase-mediated kinetic resolution cascade with elevated temperature borrowing hydrogen. Reactions were performed with two stock solutions, the first a 200 mM stock of rac-amine in isopropyl acetate and the second a solution containing 100 mM of alcohol and 2 mM $[Cp^*IrCl_2]_2$ in a 90:10 mixture of toluene/acetonitrile. Resolution was performed at 40 °C with a residence time of 30 min and the borrowing hydrogen performed at a fluid temperature of 140 °C for a residence time of 60 min. A back pressure of 100 psi was applied to the system. Steady state conversion was determined from the crude ^1H NMR against an internal standard.

Despite the good steady state yield observed when the reaction was performed in flow with pre-formed α-methylbenzylamine previously (3.1.7), conversion to the desired product with the upstream lipase reaction was poor. As the only difference between the two reactions is the upstream biocatalytic reaction, it was proposed that a leachate originating from the Novozym support is causing catalyst inhibition in the downstream chemistry, consistent with previous findings.[132]

4.1.2.1 Inhibition of the borrowing hydrogen reaction in the chemoenzymatic continuous flow cascade

To assess whether any potential leachate was inhibiting the downstream borrowing hydrogen reactions, a portion of Novozym 435 was heated at 40 °C in isopropyl acetate for 16 h. After this time, the solvent was sampled and used as the isopropyl acetate component of the solvent system for the reaction in Figure 117.

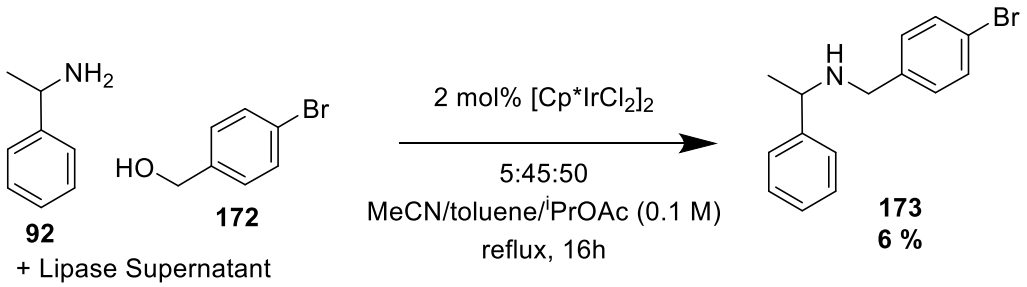

Figure 117: Borrowing hydrogen reaction of MBA and 4-bromobenzylalcohol at 0.1 M using isopropyl acetate containing leachate from Novozym 435 as a component in the solvent system.

The sizeable drop in conversion observed in the reaction performed in the presence of lipase supernatant supports that a leachate coming from the upstream biocatalytic step is likely the cause of the catalyst inhibition.

The lipase supernatant was analysed by Bradford assay which demonstrated that the leachate wasn't protein and, therefore, likely originates in the polymer matrix of the Novozym support. This is in agreement with previous reports, where it has been suggested that a leachate from Novozym has inhibited the SCRAM catalyst.[132]

4.1.2.2 Strategies to overcome catalyst inhibition caused by Novozym leachate

With the cause of the borrowing hydrogen inhibition narrowed down to the lipase support, three alternative strategies to overcome inhibition catalysis by $[Cp^*IrCl_2]_2$ were proposed. Firstly, the steps within the cascade could be reversed with a kinetic resolution of the secondary amine. Alternatively, a capture column could be placed between the reaction zones to absorb any leachate. Each of these strategies will be discussed in the next section.

4.1.2.2.1 Lipase-mediated kinetic resolution of a secondary amine

It was proposed that by swapping the two synthetic steps, it would be possible to access the same chiral secondary amines, as the effects of the leachate would be nullified because there are no steps downstream of the immobilised lipase. To establish the feasibility of a lipase-mediated kinetic resolution of a secondary amine, 4-bromobenzyl(1-phenylethyl)amine was synthesised, Figure 118.

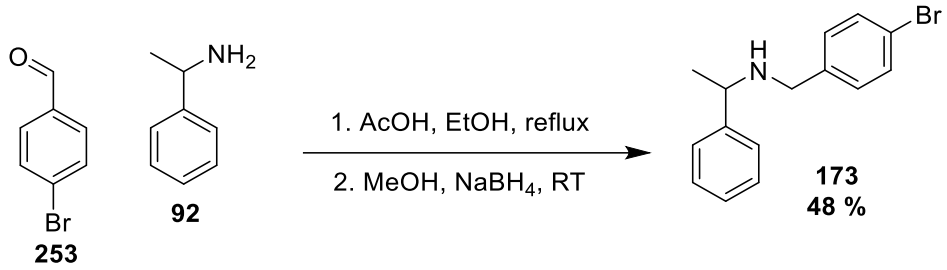

Figure 118: Synthesis of 4-bromobenzyl-(1-phenyl-ethyl)-amine via reductive amination.

The 6 lipases that were initially screened for the kinetic resolution of primary amines in Chapter 3 were screened for the kinetic resolution of 4-bromobenzyl(1-phenylethyl)amine. Whilst there is limited literature precedent for lipase mediated kinetic resolution of secondary amines,[307-309] the simplest solution to catalyst inhibition would be to reverse the steps of the continuous flow system.

Reactions were performed at in isopropyl acetate (0.1 M), with 10 wt% lipase. The lipases screened previously (2.2.2) were used for this reaction. Mixing was provided using a mini roller contained within an incubator held at 40 °C for 16h. Conversion was determined by ^{1}H NMR analysis of the crude material.

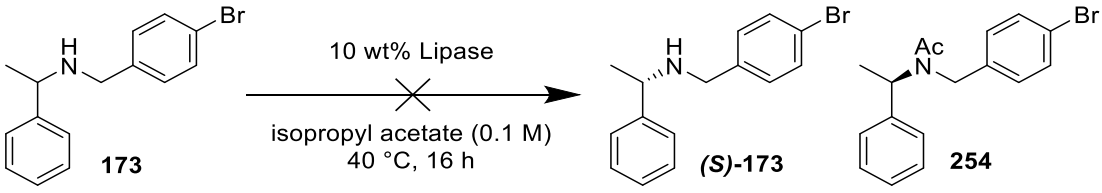

Figure 119: Attempted lipase-mediated kinetic resolution of 4-bromobenzyl-(1-phenyl-ethyl)-amine. Reactions were performed in isopropyl acetate (0.1 M), with 10 wt% lipase at 40 °C for 16h.

None of the 6 lipases tested showed any conversion to the acetylated product, with only unreacted starting material present in the crude NMR. This demonstrated that it would not be possible simply to swap the synthetic steps within the continuous flow cascade to reach the desired product. With future studies, it may be possible to identify (or evolve) a suitable enzyme that could perform a kinetic resolution on secondary amine substrates, however, as we desired to identify a simple solution, an alternative method to prevent catalyst inhibition was required.

4.1.2.2.2 Utilisation of a carbon capture column in between reactor zones

An alternative strategy to prevent catalyst inhibition in the borrowing hydrogen reaction is to use a capture column between the reaction zones, that can absorb the leachate without affecting the amine. By doping batch reactions with activated carbon, the feasibility of a capture column for resolving leachate-caused catalyst inhibition could be assessed.

Reactions were performed with NEA and 4-bromobenzylalcohol at 0.1 M with 1 mol% $[Cp^*IrCl_2]_2$ in a 50:45:5 isopropyl acetate / toluene / acetonitrile solvent mixture, heated at reflux for 16 h. Novozym 435 was heated at 40 °C in isopropyl acetate for 16h, with the supernatant making up the isopropyl acetate component of the solvent mixture. The lipase supernatant was mixed with each additive for 30 min, before addition of catalyst, amine or alcohol.

When the reaction was complete, it was filtered through a short pad of celite washing with isopropyl acetate. The solvent was then removed under reduced pressure and conversion was determined from the crude mixture by ^1H NMR against an internal standard.

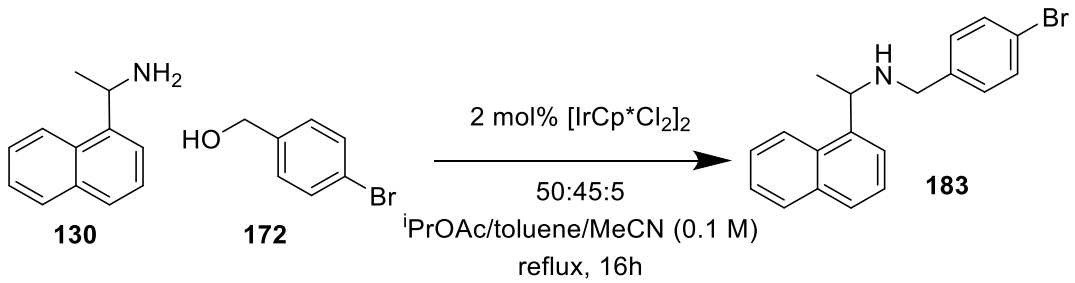

Entry	Additive	Conversion (NMR) / %
1	Supernatant	6
2	Supernatant + graphite	35
3	Supernatant + carbon spheres	*n.d.*
4	Supernatant + activated carbon	*n.d.*
5	No supernatant	86

Figure 120: Affect of different capture column additives on the borrowing hydrogen reaction of NEA and 4-bromobenzyl alcohol. Reactions were performed at 0.1M with 100 mg of additive stirred with the solvent system for 30 min before addition of reagents and catalysts. The reactions were then refluxed for 16h, filtered through celite and analysed by ^{1}H NMR.

The mild increase in conversion in Entry 2 suggests that some of the leachate was absorbed by the graphite, however, conversion was not restored to the level observed in absence of the lipase supernatant (Entry 5).

For Entries 3 and 4, no reaction was observed potentially due to the additive absorbing 4-bromobenzylalcohol, as there was no alcohol present in the crude NMR. As the activated carbon absorbed the alcohol substrate, it would be necessary to remove the carbon additive before addition of the alcohol to the reaction which would not be representative of the system in continuous flow.

It was hypothesised that an in-line separation could also be implemented to remove the inhibitor. For this route to be successful, identification of the inhibitor would be essential to determine its partitioning qualities and adjust the system accordingly. With more time, it could have been possible to formally identify the inhibitor using MALDI-TOF spectrometry.

4.2 Continuous flow chemoenzymatic cascades with an upstream transaminase reaction

Whilst borrowing hydrogen methodologies have been demonstrated in water previously,[133] the use of water as a green solvent wouldn't be possible in continuous flow due to poor substrate and catalyst solubility leading to heterogeneous mixtures. To implement the downstream chemistries with the upstream transaminase reaction, an in-line phase-switch is required, demonstrated in 2.1.7.

Initially, the efficiency of a transaminase-hydroamination cascade, with a surrogate biocatalytic product stream, that had been adjusted to pH 10 was assessed. The buffered solution was pumped through a CSTR with a 1:1 flow rate of isopropyl acetate before the biphasic mixture entered a membrane-based liquid-liquid separator.

The organic outlet of the membrane separator was then connected into a series of photo fReactor units. Within the first CSTR of the series, a solution containing photocatalyst A (1 mM), TRIP thiol (50 mM) and 4-vinyl anisole (300 mM) in isopropyl acetate was also infused. The outlet of the photo fReactor series was collected in aliquots corresponding to the total reactor volume and conversion determined from the crude NMR.

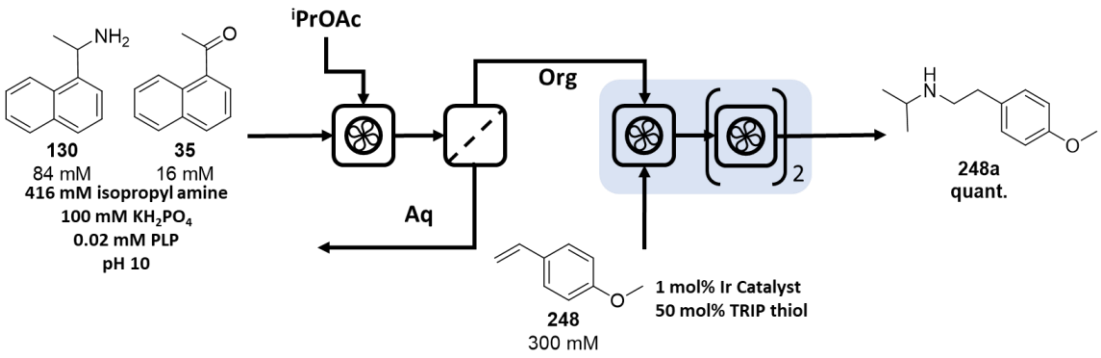

Figure 121: Continuous flow extraction coupled with downstream hydroamination. Reactions were performed with, NEA (84 mM), 1'-acetonaphthone (16 mM), PLP (0.02 mM) and isopropylamine (416 mM) in a buffered solution (100 mM KH_2PO_4, pH 10) and a hydroamination feed containing catalyst A

(1 mM), TRIP thiol (50 mM) and 4-vinyl anisole (300 mM) in isopropyl acetate. Steady state yield was determined by ^{1}H NMR, in reference to an internal standard.

As shown in 2.1.7, at pH 10 isopropylamine is also extracted into the organic phase alongside NEA. When present within the hydroamination reaction zone, isopropylamine out-competes NEA, to give **248a** in quantitative yield (full consumption of **248** observed in ^{1}H NMR).

This highlighted the need to optimize the extraction zone to selectively extract MBA/NEA in preference of isopropylamine, based on pH, before application of a downstream hydroamination reaction. This will be discussed in the next section.

4.2.1 Extraction-hydroamination

Before the upstream PBR was connected to the downstream reaction zones, a continuous flow extraction and separation was performed to assess the efficiency of extraction. Reactions were performed with isopropyl amine (400 mM), NEA (100 mM), 1'-acetonaphthone (50 mM) and PLP (0.02 mM) in a buffered solution (100 mM KH_2PO_4, pH 8).

The buffered solution was pumped through a series of CSTRs. A solution of 0.05 M NaOH was also pumped into the first CSTR at various flow rates, adjusting the pH of the solution. The aqueous mixture then flowed into a second CSTR along with a stream of isopropyl acetate before entering a membrane-based liquid-liquid extraction unit. The organic phase was then analysed by GC and pH of the aqueous phase assessed using an off-line pH probe.

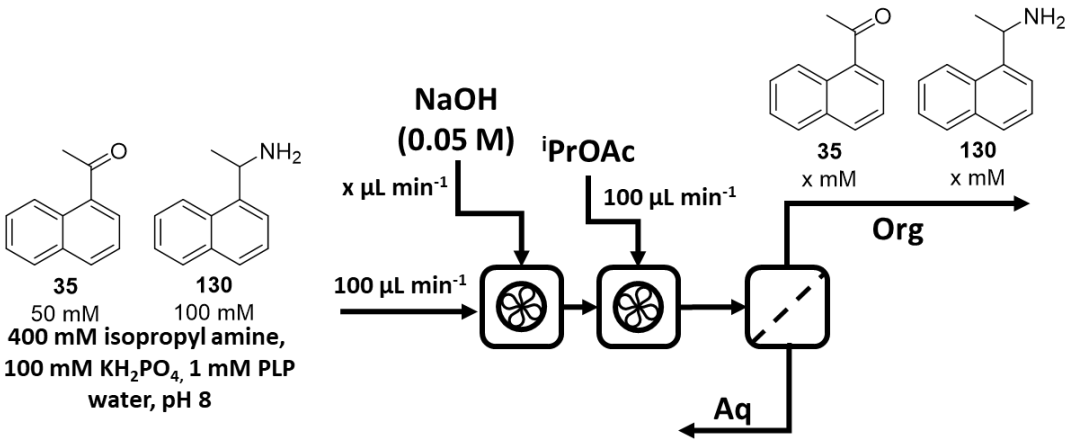

Base Flow Rate / µL min^{-1}	Outlet pH	[NEA] in organic / mM	[ketone] in organic / mM	[^{i}PrNH$_2$] in organic / mM
100	10	75.5 ± 4.1	47.3 ± 1.2	79.5 ± 3.7
50	10	73.7 ± 2.5	47.8 ± 2.3	88.7 ± 4.4
25	9	68.7 ± 3.6	46.9 ± 1.5	0

Figure 122: Continuous flow extraction of NEA from a buffered solution (100 mM KH_2PO_4, pH 8) containing isopropylamine (400 mM), NEA (100 mM), 1'-acetonaphthone (50 mM) and PLP (0.02 mM). pH was adjusted using NaOH (0.05 M) at various flow rates. Concentrations were determined against an internal standard for each compound.

A flow rate of 25 µL min^{-1}, gives an outlet pH of 9 and selective extraction of NEA. At the two faster flow rates (50 and 100 µL min^{-1}), there is a mild increase in the extraction of NEA, however, isopropylamine is also extracted into the organic phase due to the increase in outlet pH. These flow rates and pH optimum to achieve maximum extraction efficiency were also informed by the extraction efficiency models shown in 2.1.7.

Before the PBR containing transaminase was connected upstream of the extraction stage, the conversion of the downstream chemistry when connected to the outlet of the membrane separator was assessed.

Due to the average conversion of the transaminase reaction being 84%, reactions were performed with isopropylamine (416 mM), NEA (84 mM), 1'-acetonaphthone (16 mM) and PLP (0.02 mM) in a buffered solution (100 mM KH_2PO_4, pH 8).

As above, a solution of 0.05 M NaOH was pumped into the first of a series of CSTRs at 25 $\mu Lmin^{-1}$, with the adjusted pH solution then being mixed with a stream of isopropyl acetate before entering a membrane-based liquid-liquid extraction unit.

The organic outlet of the membrane separator was then connected into a series of photo fReactor units. Within the first CSTR of the series, a solution containing photocatalyst A (1 mM), TRIP thiol (50 mM) and 4-vinyl anisole (300 mM) in isopropyl acetate was also infused. The outlet of the photo fReactor series was collected in aliquots corresponding to the total reactor volume and conversion determined from the crude NMR.

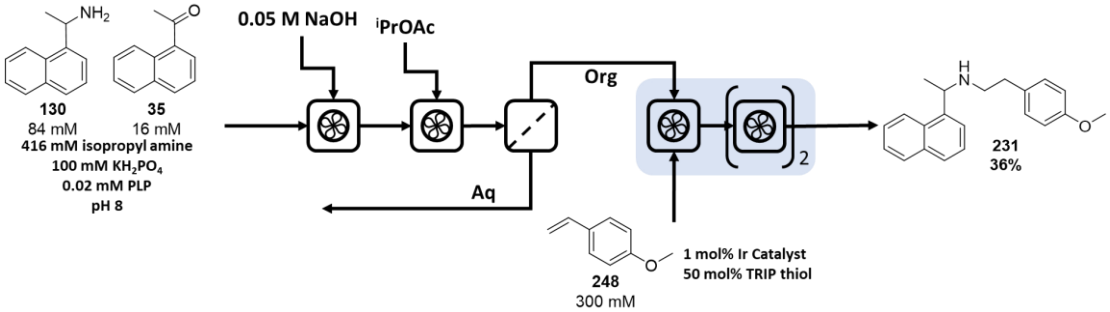

Figure 123: Continuous flow extraction coupled with downstream hydroamination. Reactions were performed with, NEA (84 mM), 1'-acetonaphthone (16 mM), PLP (0.02 mM) and isopropylamine (416 mM) in a buffered solution (100 mM KH_2PO_4, pH 8). NEA was extracted with 0.05 M NaOH and isopropyl acetate, with a hydroamination feed containing catalyst A (1 mM), TRIP thiol (50 mM) and 4-vinyl anisole (300 mM) in isopropyl acetate. Steady state yield was determined by ^1H NMR against an internal standard.

A steady state yield of 36% of the desired product was obtained, which is comparable to the hydroamination yield obtained in the lipase-hydroamination cascade. Moreover, no isopropylamine addition products were observed, confirming the selective extraction of NEA.

4.2.2 Transaminase-hydroamination cascade

After successfully demonstrating the capability of combining an extraction stage with the hydroamination chemistry, a PBR containing BmTA@EziG[1] was attached to the front of the system.

A buffered solution (100 mM KH_2PO_4, pH 8) containing 100 mM ketone, 500 mM isopropylamine and 1 mM PLP was first flowed through a PBR containing BmTA@EziG[1] at a flow rate of 100 µL min^{-1} (equating to a residence time of 30 min). The outlet of the PBR then entered a series of 2 CSTR units, into the first unit NaOH (0.05 M) was also pumped at 25% the flow rate of the transaminase feed (25 µL min^{-1}). Isopropyl acetate was pumped into the second CSTR in series (50 µL min^{-1}), with the biphasic mixture then entering a membrane-based separator.

The organic outlet of the separator was fed into a series of CSTR units and irradiated at 365 nm. A solution of photocatalyst (1 mM) and TRIP thiol (50 mM) with either an alkene (300 mM) or enecarbamate (150 mM) in isopropyl acetate was also fed into the first CSTR of the series. The two streams of stock solutions were pumped into the continuous flow system at the same flow rate (50 µL min^{-1}) to give a residence time of 60 min.

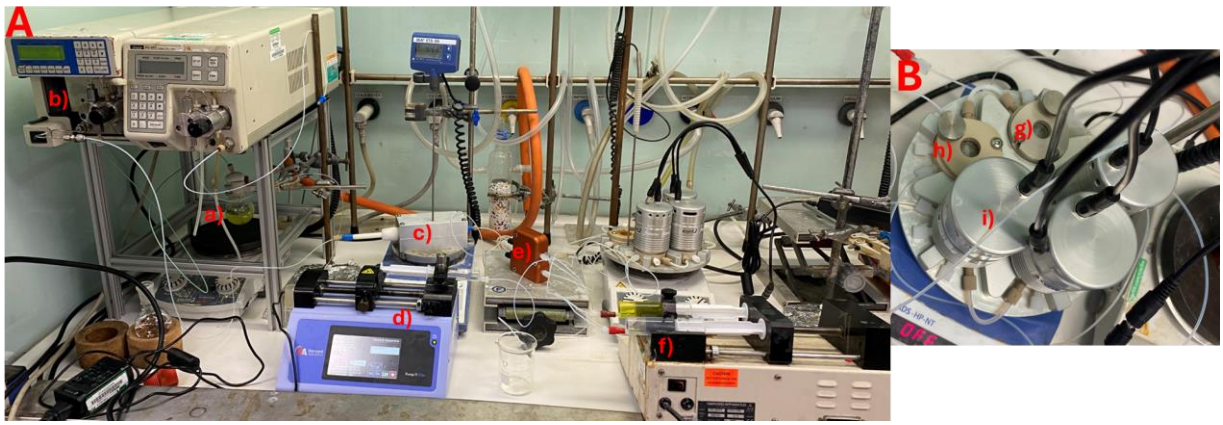

Figure 124: Photos of the transaminase-hydroamination continuous flow cascade. A shows the whole set-up with a) the biocatalytic feedstock b) a JASCO PU-980 HPLC pump c) a PBR containing EmTA@EziG[1] inside an aluminium heating block d) a syringe pump containing 0.05 M NaOH e) a Zaiput

SEP-10 membrane-based separator, fitted with an OB-900 membane and f) a syringe pump fitted with two syringes; one containing isopropyl acetate and the other containing the hydroamination feedstock. B shows a photo of the hotplate containing g) a fReactor unit with the PBR outlet and NaOH as inlets h) a fReactor unit with the basified solution from g) and isopropyl acetate as inlets and h) a series of three photo fReactor units with the organic outlet of the zaiput and the hydroamination feedstock as inlets.

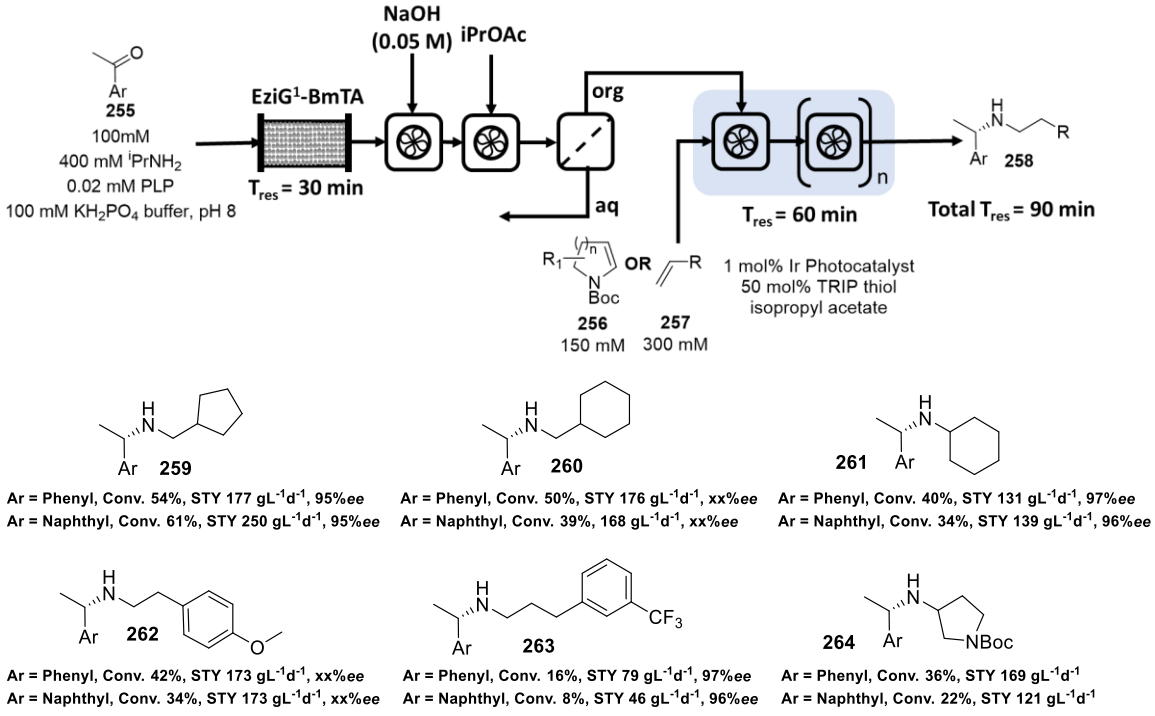

Figure 125: Chemoenzymatic continuous flow synthesis of chiral secondary amines through a transaminase-hydroamination cascade. Reactions were performed with BmTA@EziG[1] and a buffered solution (100 mM KH_2PO_4, pH 8) containing 100 mM ketone, 500 mM isopropylamine and 0.02 mM PLP. Extraction was implemented through basification using NaOH (0.05 M) and isopropyl acetate. A Zaiput membrane separator was used to separate the biphasic mixture and the organic phase fed into a series of CSTR units and irradiated at 365 nm with a separate feed containing photocatalyst (1 mM) and TRIP thiol (50 mM) with either an alkene (300 mM) or enecarbamate (150 mM) in isopropyl acetate for a total residence time of 90 min. Conversions were determined by ^{1}H NMR against an internal standard.

The mass balance of the reactions indicates a steady state conversion of 84% in the biocatalytic reaction for 1'-acetonaphthone and 77% for acetophenone, determined from the crude ^{1}H NMR with the assumption of 100% extraction of residual ketone

into the organic phase, in agreement with the findings of 2.1.7 and 2.1.9. Further, a 18-22% loss of amine was observed within the extraction stage, calculated from HPLC analysis of the aqueous outlet of the separator.

The aqueous outlet of the separator was collected in aliquots corresponding to the reactor volume of the PBR and extracted with isopropyl acetate. After a single wash with isopropyl acetate, ca. 70% of the residual (18-22%) NEA or MBA in the aqueous phase was extracted into isopropyl acetate (resulting in a total extraction efficiency of ca. 90%). This suggests that the loss of amine within the extraction stage could be improved through multi-stage or counter current extraction. Subsequently, this increase in amine concentration within the organic stream could lead to higher conversions in the downstream hydroamination reaction.

Whilst a smaller selection of alkene/enecarbamate substrates were applied to the transaminase-hydroamination cascade compared with the upstream lipase reaction, similar trends between substrates and conversion were observed in each chemoenzymatic flow cascade.

As a consequence of the >50% conversion in the biocatalytic stage, the transaminase-hydroamination cascade results in greater conversions to the same secondary amines compared with lipase-hydroamination cascade, despite the small loss of amine in the extraction.

It was possible to access 12 products through the transaminase-hydroamination continuous flow cascade, with overall conversions ranging from 8-73%. The highest conversion (73%) occurred with a substrate combination of acetophenone and methylene cyclopentane.

As observed with the lipase-hydroamination cascade, the poor conversions observed with some of the substrate combinations are a result of poor performance of the downstream hydroamination reaction, with the substrate combination leading to cinacalcet (**10**) resulting in the lowest yield. These yields could likely be increased

through extending the residence time within the hydroamination stage or through increasing the loading of the photocatalyst (see 4.1.1.1).

4.2.2.1 Ketone substrate scope within transaminase-hydroamination cascade

As the scope of the alkene coupling partner had already been successfully demonstrated within both the lipase and the transaminase cascades, attention was turned to the ketone substrate within the transaminase reaction.

A preliminary batch screen of four ketones (4-bromoacetonaphthone, 1-indanone, 4-chromanone and 4-(3,4-dichlorophenyl)-1-tetralone) was performed. Reactions were performed at 40 °C in an aqueous buffer (100 mM K_2PO_4, 0.02 mM PLP) containing 50 mM ketone and 250 mM $^{i}PrNH_2$ for 24 h.

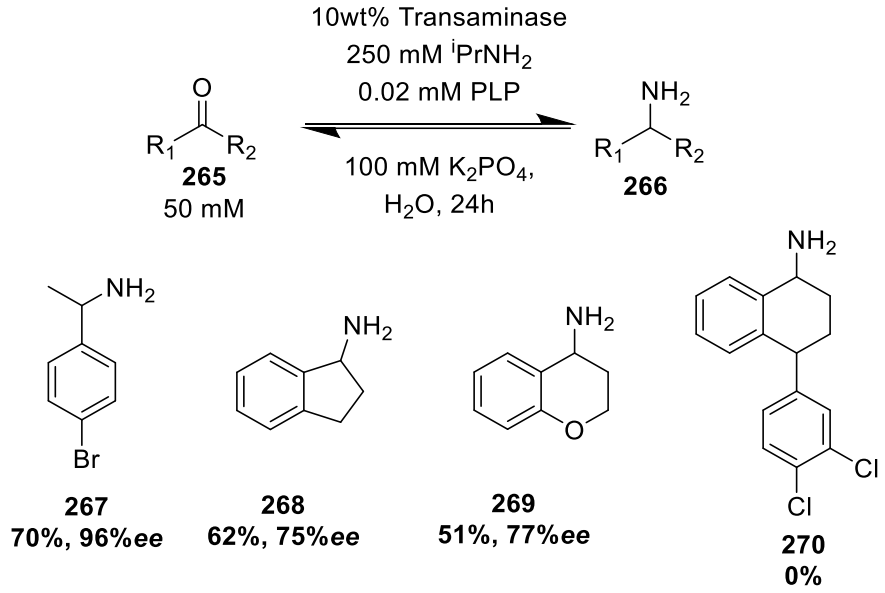

Figure 126: Batch screen of alternative ketones, with view to expand the scope of the transaminase-hydroamination cascade. Reactions were performed at 40 °C in an aqueous buffer (100 mM K_2PO_4, 0.02 mM PLP) containing 50 mM ketone and 250 mM $^{i}PrNH_2$ for 24 h.

Of the four ketones tested, three were successfully transformed into the corresponding amine with moderate to good yields (51-70%) and good to excellent enantiomeric excess (75-96% *ee*). Subsequently, in addition to acetophenone and 1'-acetonaphthone from the previous section (4.2.2), 4-bromoacetonaphthone, 1-

indanone and 4-chromanone were applied to the transaminase-hydroamination cascade with methylenecyclohexane utilised as the alkene substrate.

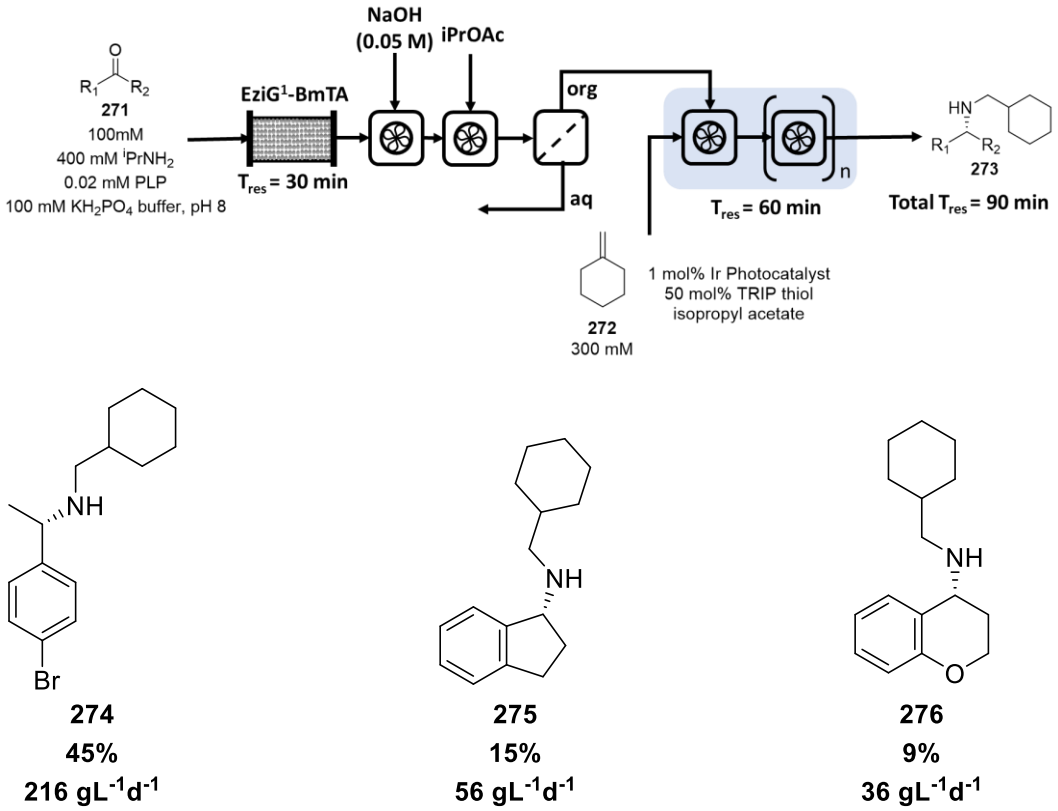

Figure 127: Expansion of the ketone substrate scope within the transaminase-hydroamination continuous flow cascade. Reactions were performed with BmTA@EziG[1] and a buffered solution (100 mM KH_2PO_4, pH 8) containing 100 mM ketone, 500 mM isopropylamine and 0.02 mM PLP. Extraction was implemented through basification using NaOH (0.05 M) and isopropyl acetate. A Zaiput membrane separator was used to separate the biphasic mixture and the organic phase fed into a series of CSTR units and irradiated at 365 nm with a separate feed containing photocatalyst (1 mM) and TRIP thiol (50 mM) with methylenecyclohexane (300 mM) in isopropyl acetate for a total residence time of 90 min. Conversions were determined by ^{1}H NMR against an internal standard.

Each ketone was transformed successfully into the corresponding primary amine (**267-269**) by BmTA with steady state conversions of the transaminase reaction ranging from 51-70% with good to excellent enantioselectivities (75-96 %*ee*).

As observed with MBA and NEA, the 1-(4-bromophenyl)ethylamine, 1-aminoindane and chroman-4-amine transaminase products experienced a loss of 17-21% (9-14

mM) within the extraction stage of the cascade, confirmed by analysis of the aqueous outlet of the membrane separator.

Each of the new amines yielded the desired secondary amine under hydroamination conditions with methylenecyclohexane in poor to excellent steady state yields within the photoredox reaction (22-80%) to give poor to moderate steady state yields across the two steps (9-45%). In combination with the previous section (4.2.2) a total of 15 secondary *N*-alkyl amines were synthesised through a transaminase-hydroamination cascade.

The scope of the transaminase-hydroamination cascade could be further expanded through implementation of different ketones or alkenyl substrates. Aromatic ketones bearing a halogen, like 1-(4-bromophenyl)ethylamine, could be used in various cross-coupling reactions after the two-step cascade allowing for elaboration of the final product. Moreover, through a transaminase screening panel, the steady state conversions of the transaminase reaction could be increased, leading to an increase in the overall productivity of the two-step cascade.

4.3 Chapter summary

Two of the proposed continuous flow chemoenzymatic routes have been successfully demonstrated to yield a range of *N*-alkylated secondary amines in excellent enantiomeric excess.

Through a lipase-hydroamination cascade, 16 products were produced in yields ranging from 5-48% with enantiomeric excess 96-99%. These yields were limited by the performance of the downstream hydroamination reaction with complete kinetic resolution achieved within the upstream lipase step. An increase in some of the lower yields could be achieved through extending the residence time within the hydroamination stage or through multipoint injection of photocatalyst.

Within a transaminase-hydroamination cascade, a smaller panel of alkene substrates were applied to yield 15 products (8-73%). Application of an in-line phase-switch

allowed for the combination of two incompatible reaction zones as well as the selective extraction of amines based on pH.

An attempted combination of a lipase kinetic resolution and borrowing hydrogen methodologies was found to be unsuccessful due to inhibition of the iridium catalyst in the downstream chemistry. It could be possible to realise this chemoenzymatic cascade if the inhibitor is identified and successfully removed from the reaction stream before entering the downstream reaction zone.

As a consequence of time restrictions, a transaminase-borrowing hydrogen cascade was never attempted. It was hypothesized that inhibition problems that restricted the lipase-borrowing hydrogen cascade would not be present with an upstream transaminase reaction as it was proposed the leachate originated from the supported lipase.

5 Thesis Conclusion

Enzymatic access to α-chiral primary amines was successfully achieved through two alternative strategies, a transaminase-mediated reaction from pro-chiral ketones as well as a lipase-mediated kinetic resolution of racemic amines. After initial optimisation in batch, both enzymatic reactions were successfully translated into continuous flow with maximum theoretical conversion observed at steady state for the lipase catalysed kinetic resolution and steady state conversion of up to 84% within the transaminase reaction.

Chapter three describes *N*-alkylation methodologies applied to the primary amines accessed within chapter two. As with the enzymatic reactions, conditions for both borrowing hydrogen and photoredox hydroamination chemistries were first applied in batch before being translated and optimised in continuous flow.

The extended reaction times in batch for the borrowing hydrogen (20h) and the hydroamination (64h) reactions were drastically reduced to 1h when translated to continuous flow, with an increase in yield also observed.

A total of 14 secondary amines were accessed through borrowing hydrogen reactions with the two amines generated in 2, with yields ranging from 31-83%, Figure 128. Translation to continuous flow gave a steady state yield of 67% for an exemplar product (**183**) which is the same as the isolated yield in batch after 20h.

Photoredox hydroamination chemistry provided 22 secondary amines in yields ranging from 4-83%, Figure 128. Through translation to the photo fReactor units, as well as changing the reaction solvent to isopropyl acetate, the reaction time was drastically reduced with yields also increasing compared to reactions performed in vials.

Combination of the results of chapters two and three allowed for the successful development of two continuous flow chemoenzymatic routes, accessing 19 pharmaceutically-relevant α-chiral secondary amines in yields of 5-73% across the two catalytic steps. These two routes combine bio- and chemo-catalytic methodologies with in-line selective extraction of amines.

An unsuccessful combination of a lipase-mediated kinetic resolution with borrowing hydrogen chemistry could potentially have been resolved with use of a carbon capture column between reaction zones.

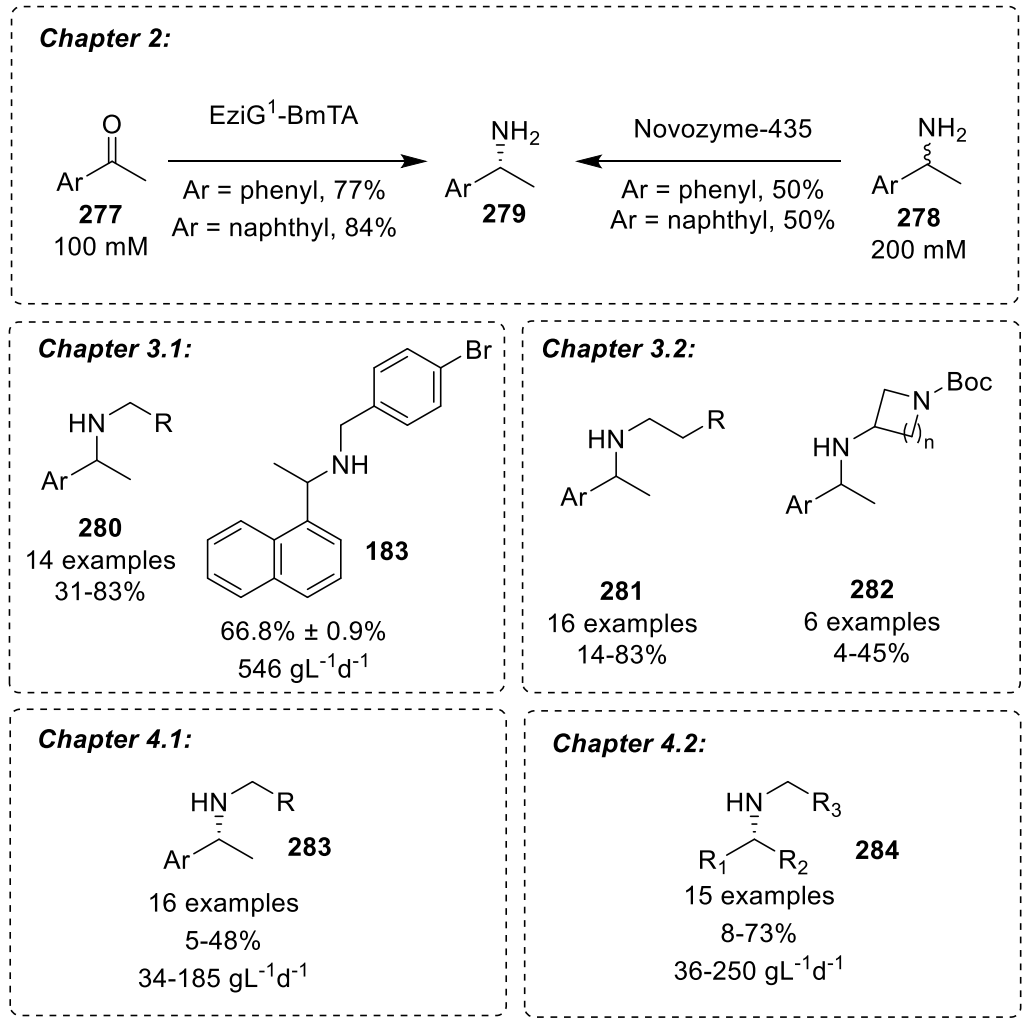

Figure 128: A summary of products accessed in each chapter.

5.1 Future Direction

This work highlights the potential for combining chemoenzymatic synthesis in continuous flow, with the implementation of a continuous, selective extraction enabling a solvent switch between two reaction zones. Within this thesis, however, only two enzymatic and two chemocatalytic systems were employed. Through alteration of enzyme and/or chemocatalytic methods, the scope of products that can be accessed through a two-stage continuous flow chemoenzymatic process would be drastically increased.

Application of amine dehydrogenase[55, 56 47, 57, 62], imine reductase[44-47], reductive aminase[48, 49] or alcohol aminase[310, 311] as alternative biocatalysts would allow access to chiral amines from a more diverse substrate scope. Whilst other synthetically useful enzymes such as alcohol dehydrogenase[63-65, 140] or ketoreductase[312, 313] could afford alternative functional groups (alcohol, carbonyl) that could serve as reactive sites for elaboration by a variety of chemocatalytic methods.

Several cross-coupling reactions, including Buchwald-Hartwig[314-316] and Suzuki-Miyaura[317-319] couplings, have previously been demonstrated in continuous flow. Each of these reactions have also been applied within one-pot batch chemoenzymatic syntheses.[86, 320-322] Harnessing the synthetic capabilities of cross-couplings in continuous flow in conjunction with biocatalytic methods would enable access to a wide variety of industrially-relevant chiral molecules.

Furthermore, within this thesis the biocatalytic reaction preceded the *N*-alykation reaction. Whilst performing these reactions in the opposite order could incur problems, including enzyme inhibition and substrate solubility limitations, it would further increase the scope of continuous flow chemoenzymatic synthesis.

6 Experimental

Commercially available starting materials were obtained from Sigma−Aldrich, Fluorochem and Alfa Aesar. All non-aqueous reactions were performed under nitrogen atmosphere unless otherwise stated. Water-sensitive reactions were performed in anhydrous solvents in oven-dried glassware cooled under nitrogen before use. Anhydrous dichloromethane (DCM), anhydrous tetrahydrofuran (THF), anhydrous toluene, anhydrous diethyl ether, anhydrous ethanol, anhydrous methanol and anhydrous acetonitrile were obtained from a PureSolv MD5 Purification System. Anhydrous dimethylsulfoxide (DMSO) and anhydrous 1,4-dioxane were obtained from SureSeal bottles from Sigma−Aldrich. All other solvents used were of chromatography or analytical grade. Petrol refers to petroleum spirit (b.p. 40-60 °C). An IKA RV 10 rotary evaporator was used to remove the solvents under reduced pressure.

Thin layer chromatography (TLC) was performed using aluminium backed silica (Merck silica gel 60 F254) plates obtained from Merck. Ultraviolet lamp (λ_{max} = 254 nm) and $KMnO_4$ were used for visualization. Flash column chromatography was performed using silica gel 60 (35-70 µm particles) supplied by Merck. A Bruker Daltonics micrOTOF spectrometer with electrospray (ES) ionisation source was used for high-resolution mass spectrometry (HRMS). Perkin-Elmer One FT-IR spectrometer was used to analyse the infrared spectra.

Proton (^{1}H) and carbon (^{13}C) NMR data was collected on a Bruker 300, 400 or 500 MHz spectrometer. Data was collected at 298 K unless otherwise stated. Chemical shifts (δ) are given in parts per million (ppm) and they are referenced to the residual solvent peak. Coupling constants (J) are reported in Hertz (Hz) and splitting patterns are reported in an abbreviated manner: app. (apparent), s (singlet), d (doublet), t (triplet), q (quartet), p (pentet), m (multiplet), br. (broad). Assignments were made using COSY, DEPT, HMQC and NOESY experiments.

6.1 Chiral HPLC general method

To determine enantiomeric excess (*ee*), chiral HPLC was carried out with the following conditions. Analysis was performed using an Agilent 1290 Infinity II HPLC system (Agilent, Santa Clara, CA, United States), with a diode array detector (DAD). Chromatographic separations were performed using the specified column at a column temperature of 25 °C. The mobile phase used is specified for each compound at a flow rate of 1.0 mL/min. The DAD recorded the chromatogram at wavelengths of 230-280 nm.

Enantiomeric excess was calculated from the peak areas of the two enantiomers:

$$Enantiomeric\ excess\ (\%) = \left(\frac{Area\ 1 - Area\ 2}{Area\ 1 + Area\ 2}\right) X\ 100$$

Where Area 1 is larger than Area 2.

6.2 Sequences of ω-transaminases

All DNA or amino acid sequences were taken from literature.[170, 323]

ω-transaminase from Hyphomonas neptunium carrying a His-tag (Hyp-ωTA). Start and stop codons are depicted as lower-case letters and underlined. The His-tag sequence is also underlined.

atgCTGACCTTTCAGAAAGTTCTGACCGGTTTTCAGACCCGTGCAGATGCACGTGCAGAAC
GTACCGATGCATTTGCAGATGGTATTGCATGGATTGAAAATGAATTTGTGCCGATTGGCAA
AGCACGTATTCCGATTCTGGATCAGGGTTTTCTGCATAGCGATCTGACCTATGATGTTCCG
GCAGTTTGGAATGGTCGTATTTTTCGTCTGGATGATCATCTGGATCGTCTGGAAGTTAGCT
GTGCAAAAATGCGTCTGCCGCTGCCGATTGCACGTCCGGAACTGCGTCGTCTGGTTATGG
AACTGGTTAGCCGTAGCGGTCTGCGTGATGCCTATGTTGAAATTATTGTTACCCGTGGCCT
GAAATTTCTGCGTGGTGCACAGGCAGAAGATATTATTCCGAATCTGTATCTGATGGCCGTT
CCGTATGTTTGGATTCTGCCGCTGGAATATCAGAATCATGGTGCACCGGCAGTTGTTACCC
GTACCGTTCGTCGTACACCGCCGGGTGCACTGGATCCGACCATCAAAAATCTGCAGTGGG

GTGATCTGGTTCGTGGTCTGATGGAAGCCGGTGATCGTGATAGCTTTTTTCCGATTCTGCC
GGATGGTGATGGTAATGCAACCGAAGGTGCAGGCTATAACATTGTTCTGGTTCGTAATGG
CGAACTGCATACACCGCGTCGTGGTGTTCTGGAAGGTATTACCCGTCGTACCGTTCTGGAA
ATTGCAGCAGCACGTGGCCTGAAAACACATGTTACCGAAATTCCGATTCAGGCACTGTATG
AATGTGATGAACTGTTTATGTGTAGCACCGCAGGCGGTATTATGCCGCTGGTTCTGCTGGA
TGGTAATATTGTTGGTGATGGCACCGTTGGTCCGGTTACCCGTATGATTTGGGAAGCATAT
TGGGATCTGCATGATGATCCGCAGCTGAGCGAACCGGTTACCTATGCACCGCTCGAGCAC
CACCACCACCACCACtga

MLTFQKVLTGFQTRADARAERTDAFADGIAWIENEFVPIGKARIPILDQGFLHSDLTYDVPAV
WNGRIFRLDDHLDRLEVSCAKMRLPLPIARPELRRLVMELVSRSGLRDAYVEIIVTRGLKFLRGA
QAEDIIPNLYLMAVPYVWILPLEYQNHGAPAVVTRTVRRTPPGALDPTIKNLQWGDLVRGLM
EAGDRDSFFPILPDGDGNATEGAGYNIVLVRNGELHTPRRGVLEGITRRTVLEIAAARGLKTHV
TEIPIQALYECDELFMCSTAGGIMPLVLLDGNIVGDGTVGPVTRMIWEAYWDLHDDPQLSEPV
TYAPLEHHHHHH

ω-transaminase from Bacillus megaterium carrying a His-tag (Bm-ωTA). Start and stop codons are depicted as lower-case letters and underlined. The His-tag sequence is also underlined.

atgAGTTTAACAGTGCAAAAAATAAACTGGGAGCAAGTTAAAGAATGGGATCGTAAATACC
TGATGAGGACGTTTAGTACCCAAAATGAGTATCAACCTGTACCAATTGAATCAACAGAAG
GTGACTATTTGATTATGCCTGATGGCACAAGATTATTAGATTTCTTCAATCAACTTTATTGT
GTCAATTTAGGTCAGAAAAATCAAAAAGTTAATGCTGCAATCAAGGAGGCTTTAGACCGA
TATGGTTTTGTATGGGATACTTATGCAACTGATTATAAAGCCAAAGCAGCAAAGATAATTA
TTGCGGATATTTTAGGTGATGAAGACTGGCCAGGAAAAGTTAGGTTCGTATCAACAGGAA
GTGAAGCAGTGGAAACGGCACTGAATATCGCGAGGTTATATACAAATCGCCCACTAGTGG
TTACACGAGAACACGATTATCATGGTTGGACTGGTGGAGCTGCTACTGTTACTCGATTAAG
GTCATATCGAAGTGGTTTAGTTGGGGAAAATTCAGAATCTTTTTCAGCAGAAATACCCGGG
TCATCATATAATAGTGCTGTTTTGATGGCGCCATCCCCTAACATGTTTCAGGATTCNGACGG
CAACYTGCTAAAAGATGAAAACGGGGAATTGTTGAGTGTAAAGTATACACGTCGTATGAT

CGAAAACTATGGTCCGGAACAAGTGGCAGCAGTGATAACTGAAGTATCGCARGGTGCAG
GCTCTGCTATGCCCCCATATGAATACATTCCACAAATCCGAAAAATGACAAAAGAACTAGG
TGTCCTTTGGATTAATGATGAAGTTCTTACTGGCTTTGGGCGAACAGGGAAGTGGTTTGGA
TATCAGCAYTATGGGGTACAGCCAGATATAATCACTATGGGTAAAGGACTCTCCAGTTCCT
CACTCCCTGCTGGCGCTGTCTTAGTTAGTAAGGAAATTGCAGCGTTTATGGATAAGCACCG
ATGGGAGTCAGTATCCACGTATGCCGGTCATCCAGTTGCGATGGCTGCGGTCTGTGCAAA
TTTAGAAGTGATGATGGAAGAAAACTTTGTTGAGCAAGCGAAGGACAGCGGCGAGTATA
TAAGGAGTAAACTTGAACTTCTGCAAGAAAAGCATAAAAGTATAGGAAATTTCGACGGAT
ATGGCCTTTTATGGATAGTAGATATTGTGAATGCCAAGACTAAGACTCCTTACGTAAAATT
GGACCGGAACTTTACGCACGGGATGAATCCAAATCAAATCCCAACACAAATCATTATGAAA
AAAGCGCTAGAAAAAGGAGTGCTGATTGGTGGAGTAATGCCTAATACAATGAGAATTGGC
GCATCTTTGAATGTTAGTCGCGGAGACATCGATAAAGCAATGGATGCACTGGATTATGCA
CTTGACTATTTAGAAAGTGGAGAATGGCACCACCACCACCACCACtaa

MSLTVQKINWEQVKEWDRKYLMRTFSTQNEYQPVPIESTEGDYLIMPDGTRLLDFFNQLYCV
NLGQKNQKVNAAIKEALDRYGFVWDTYATDYKAKAAKIIIEDILGDEDWPGKVRFVSTGSEAV
ETALNIARLYTNRPLVVTREHDYHGWTGGAATVTRLRSYRSGLVGENSESFSAQIPGSSYNSAV
LMAPSPNMFQDSDGNLLKDENGELLSVKYTRRMIENYGPEQVAAVITEVSQGAGSAMPPYEY
IPQIRKMTKELGVLWINDEVLTGFGRTGKWFGYQHYGVQPDIITMGKGLSSSSLPAGAVLVSK
EIAAFMDKHRWESVSTYAGHPVAMAAVCANLEVMMEENFVEQAKDSGEYIRSKLELLQEKH
KSIGNFDGYGLLWIVDIVNAKTKTPYVKLDRNFTHGMNPNQIPTQIIMKKALEKGVLIGGVMP
NTMRIGASLNVSRGDIDKAMDLDYALDYLESGEWQALEHHHHHH

6.3 Expression and purification of recombinant protein

Expression vector pET-21a was kindly donated by the Turner group from The University of Manchester and was used for gene expression.

The protein expression of ygjG genes in pET21a expression vector was transformed into the strain *E. coli* BL21 (DE3) for yielding E. coli BL21 (pET21a). The freshly-prepared transformed strain (*E. coli* BL21 (pET21a-pATA)) was cultivated in 400 mL of LB medium supplemented with 50 µg/mL ampicillin in 1 L Erlenmeyer flasks at a

rotary shaking rate of 200 rpm at 37 °C. The recombinant protein expression was induced by adding isopropyl β-D-1-thiogalactopyranoside (IPTG) (0.2 mM, final) when A600 reached 0.6 - 0.8. The cell cultures were incubated at 18 °C for 18 h. The cells were harvested by centrifugation (4°C, 3,250 xg, 20 min) and resuspended (1g of wet cell paste/10 mL) in 50 mM TrisHCl, pH 8.0, 300 mM NaCl and 1 mM PLP. The cell pellets were lysed in an iced bath by ultrasonication by Soniprep 150 (10 cycles of 20s on/ 20s off). After centrifugation (4 °C, 16,000 xg, 20 min) the supernatant was used for protein purification by a Ni-NTA agarose column. The enzyme was washed with 50 mM Tris-HCl, 30 mM imidazole and 1 mM PLP at pH 8.0 then eluted with 50mM Tris-HCl, 300 mM imidazole, 100 mM NaCl and 1mM PLP at pH 8.0. The collected fractions were washed twice with 50 mM Tris-HCl buffer containing 1 mM PLP and concentrated in a micropore filter. The enzyme was flash frozen and stored at -80°C. The purity was analysed by SDS/PAGE and the protein was more than 90% pure.[171]

6.4 Immobilisation Procedures

6.4.1 EziG

A vial containing EziG carrier material was cooled down in an ice bath and suspended in immobilization buffer (20 mM KH_2PO_4, 500 mM NaCl, 50 mM imidazole, pH 8). Specific quantities of purified transaminase were suspended in immobilization buffer to give a final concentration of 10 mg mL^{-1}. The suspended transaminase was then added to the carrier suspension, and the mixture shaken with an orbital shaker (120 rpm) for 1 h at room temperature.

Small aliquots from the aqueous phase were sampled before and after the immobilization procedure, their concentrations determined using the Bradford assay (procedure below), and the immobilization yield calculated. The immobilized enzyme was left to sediment, the buffer was removed by pipetting, and the immobilized enzyme was stored at 4 °C until use.

6.4.2 Purolite

6.4.2.1 Epoxy Resins

A vial containing Purolite carrier material was cooled down in an ice bath and washed with immobilization buffer (20 mM KH_2PO_4, pH 8). Specific quantities of purified transaminase was suspended in immobilization buffer to give a final concentration of 10 mg mL^{-1}. The suspended transaminase was then added to the carrier suspension and the mixture was shaken with an orbital shaker (80 rpm) for 18 h at room temperature before being left stationary for a further 20 h.

Small aliquots from the aqueous phase were sampled before and after the immobilization procedure, their concentrations were determined using the Bradford assay (procedure below), and the immobilization yield calculated. The immobilized enzyme was left to sediment, the buffer was removed by pipetting, and the immobilized enzyme was washed with 0.5 M NaCl (x3), filtered and stored at 4 °C until use.

6.4.2.2 Amino Resins

A vial containing Purolite carrier material was cooled down in an ice bath and washed with immobilization buffer (20 mM KH_2PO_4, pH 8). Buffer was removed by pipetting and replaced with glutaraldehyde (2% solution) and the mixture shaken with an orbital shaker (80 rpm) for 1 h at room temperature. The supports were filtered and washed with immobilization buffer. A specific quantity of purified transaminase was suspended in immobilization buffer to give a final concentration of 10 mg mL^{-1}. The suspended transaminase was added to the carrier suspension and the mixture was shaken with an orbital shaker (80 rpm) for 18 h at room temperature.

Small aliquots from the aqueous phase were sampled before and after the immobilization procedure, their concentrations were determined using the Bradford assay (procedure below), and the immobilization yield calculated. The immobilized enzyme was left to sediment, the buffer was removed by pipetting, and the

immobilized enzyme was washed with 0.5 M NaCl (x3), filtered and stored at 4 °C until use.

6.4.2.3 Adsorption Resins

A vial containing Purolite carrier material was cooled down in an ice bath and washed with immobilization buffer (25 mM KH_2PO_4, pH 8). A specific amount of purified transaminase was suspended in immobilization buffer to give a final concentration of 10 mg mL^{-1}. The suspended purified transaminase was added to the carrier suspension and the mixture was shaken with an orbital shaker (80 rpm) for 24 h at room temperature.

Small aliquots from the aqueous phase were sampled before and after the immobilization procedure, their concentrations were determined using the Bradford assay (procedure below), and the immobilization yield calculated. The immobilized enzyme was left to sediment, the buffer was removed by pipetting, and the immobilized enzyme was washed with water (x3), filtered, and stored at 4 °C until use.

6.4.3 Immobeads

A vial containing Immobead carrier material was cooled down in an ice bath and washed with immobilization buffer (20 mM KH_2PO_4, pH 8). Specific amounts of purified transaminase was suspended in immobilization buffer to give a final concentration of 10 mg mL^{-1}. The suspended transaminase was then added to the carrier suspension and the mixture was shaken with an orbital shaker (80 rpm) for 2 h at room temperature before being left for a further 22 h at 4 °C.

Small aliquots from the aqueous phase were sampled before and after the immobilization procedure, their concentrations were determined using the Bradford assay (procedure below), and the immobilization yield calculated. The immobilized enzyme was left to sediment, the buffer was removed by pipetting, and the

immobilized enzyme was washed with water (x5), filtered and stored at 4 °C until use.

6.4.4 Bradford Assay

Coomassie Brilliant blue G250 (50 mg, 1.2 mmol) in methanol (50 mL) was stirred at room temperature until fully dissolved. Then H_3PO_4 (85%, 100 mL) was added and the solution diluted with water (500 mL). The diluted solution was filtered and further diluted with water (350 mL). The stock solution was freshly prepared before use and kept in the dark at 4 °C.

Calibration was performed in the standard range of 125-2000 µg mL^{-1} protein. Samples were prepared by mixing 980 µL stock solution and 20 µL protein sample followed by 5 min incubation at room temperature. Absorption at 595 nm was measured and plotted against the protein concentration. Diluted supernatant from immobilisation assays were then measured to determine concentration.

6.5 General Procedures

6.5.1 General Procedure A (Batch, Transaminase)

Transaminase lysate (20 mg, 10 wt%) was added to a round-bottomed flask containing a buffered solution (KH_2PO_4 (100 mM), pH 8) containing ketone (50 mM) $^{i}PrNH_2$ (250 mM) and pyridoxal 5'-phosphate (PLP) (0.02 mM) and was stirred at 45 °C for 48 h.

The reaction mixture was quenched with aqueous saturated $NaHCO_3$ solution (20 mL), and the product was extracted with EtOAc (2 x 15 mL). The combined organics were dried over $MgSO_4$, filtered, and concentrated in vacuo. The crude product was purified by flash column chromatography.

6.5.2 General Procedure B (Continuous flow, Transaminase)

An Omnifit glass column (10 mm i.d.) was packed with immobilised transaminase (10 wt%, 2.75 mL) and heated to 40 °C. Reagent feeds were introduced into the system

using a JASCO PU-980 HPLC pump or a Harvard Apparatus Model 22 syringe pump. The column was washed with 2x column volume buffered solution (100 mM KH_2PO_4, pH 8). A buffered solution (100 mM KH_2PO_4, pH 8) containing $^{i}PrNH_2$ (500 mM), ketone (100 mM) and PLP (0.2 mM) was then continuously pumped into the reactor (T_{res} = 30 min).

The outlet stream was collected in 2 mL aliquots, extracted with EtOAc and the combined organics were dried over $MgSO_4$, filtered, and concentrated in vacuo. The crude product was purified by flash column chromatography.

6.5.3 General Procedure C (Immobilised Transaminase Activity Retention)

Immobilised transaminase (10 mg) was placed within 1.5 mL Eppendorf tubes and subjected to 0.5 mL of reaction mixture containing 1'-acetonaphthone (50 mM), isopropylamine (250 mM), KH_2PO_4 (100 mM) and PLP (0.02 mM) at pH 8. The Eppendorf tubes were then placed within a thermomixer and shaken (800 rpm) for 16 h at 40 °C. The Eppendorfs were then centrifuged and 100 µL of supernatant sampled, diluted with 900 µL of acetonitrile and analysed by HPLC.

6.5.4 General Procedure D (High Throughput Transaminase Screen)

Reactions were performed in either 384 or 96 well plates with 1 mg lyophilised enzyme in each well. A buffered solution (100 mM KH_2PO_4, pH 9) containing 4-nitrophenethylamine hydrochloride (25 mM), 1'acetonaphthone (10 mM) and PLP (0.2 mM) was added to each well of the plate. The plates were then heated (40 °C) and shaken (500 rpm) for 90 min. After this time, each plate was visually assessed, and the hits identified.

6.5.5 General Procedure E (Batch, Lipase)

Immobilised lipase (10 mg, 15 wt%) was added to a round bottomed flask containing isopropyl acetate (10 mL) and *rac*-amine (300 mM) and was stirred at 40 °C for 16 h. The solvent was removed under reduced pressure and the crude product was purified by flash column chromatography.

6.5.6 General Procedure F (Continuous flow, Lipase)

An Omnifit glass column (10 mm i.d.) was packed with Novozym 435 (2.61 mL) and heated to 40 °C. Reagent feeds were introduced into the system using a JASCO PU-980 HPLC pump or a Harvard Apparatus Model 22 syringe pump. The column was washed with two column volumes of isopropyl acetate. A solution of isopropyl acetate containing *rac*-amine (200 mM) was then continuously pumped into the reactor (T_{res} = 30 min). The outlet stream was collected in 2 mL aliquots, the solvent was removed under reduced pressure and the crude product was purified by flash column chromatography.

6.5.7 General Procedure G (Batch, Borrowing Hydrogen)

To an oven-dried, nitrogen-purged 7 mL screw cap vial containing $[IrCp^*Cl_2]_2$ (8.0 mg, 0.01 mmol) were added the representative alcohol (1 mmol), amine (1 mmol) followed by degassed isopropyl acetate (2 mL). The reaction mixture was then heated at 90 °C for 15 h to 20 h. After the required time, the solvent was removed under vacuum and the resulting residue was purified by column chromatography to give the desired product.

6.5.8 General Procedure H (Continuous flow, Borrowing Hydrogen)

A flask was charged with a solution of degassed 50:45:5 isopropyl acetate/toluene/acetonitrile (0.1 M) containing $[IrCp^*Cl_2]_2$ (5 mol%), amine (1.0 equiv) and alcohol (1.0 equiv). The resulting pale-yellow solution was pumped into fReactor CSTR devices fitted with a back pressure regulator (100 psi) and heated to 140 °C for a residence time of 1h. The product stream was collected in 2 mL aliquots, the solvent removed, and the crude material purified by column chromatography.

6.5.9 General Procedure I (Batch, Hydroamination, in Vials)

An oven-dried 7 mL screw cap vial was equipped with an oven-dried Teflon stir bar and charged with 2,4,6-triisopropylbenzenethiol (TRIP thiol) (29.6 mg, 0.125 mmol, 50 mol%), $[Ir(dF(CF_3)ppy)_2(4,4'\text{-}CF_3\text{-}bpy)PF_6$ (5.7 mg, 0.005 mmol, 2 mol%) and amine

(0.25 mmol, 1.0 equiv). Anhydrous or degassed solvent (5 mL, 0.05 M) was then added via syringe, followed by alkene (0.75 mmol, 3.0 equiv). The resulting pale-yellow solution was irradiated by a single 40W Kessil A160WE tuna blue LED lamp and magnetically stirred for 48-72 h.[289] Throughout irradiation, a small rotary fan was placed adjacent to the vial to cool the reaction. A typical reaction was measured to run at about 25 °C. Once completed, the solvent was removed under reduced pressure and the crude product purified by flash column chromatography.[289]

6.5.10 General Procedure J (Batch, Hydroamination (enecarbamates) in Vials)

An oven-dried 7 mL screw cap culture tube was equipped with an oven-dried Teflon stir bar and charged with 2,4,6-triisopropylbenzenethiol (TRIP thiol) (29.6 mg, 0.125 mmol, 50 mol%), $(Ir[dF(CF_3)ppy]_2(dtbpy))PF_6$ (5.6 mg, 0.005 mmol, 2 mol%), enecarbamate (0.25 mmol, 1.0 equiv.) and amine (1.25 mmol, 5.0 equiv.). The vial was purged with nitrogen for 5 min. Anhydrous toluene (5 mL, 0.05 M) was then added via syringe and the resulting pale-yellow solution was irradiated by a single 40W Kessil A160WE tuna blue LED lamp and magnetically stirred for 16 h.[149] Throughout irradiation, a small rotary fan was placed adjacent to the vial to cool the reaction. A typical reaction was measured to run at about 25 °C. Once completed, the solvent was removed under reduced pressure and the resulting residue was purified by column chromatography to give the desired product.

6.5.1 Photo fReactor set up

Figure 129 shows the equipment layout, with the photo-modules sitting atop the conventional fReactor platform, which in turn sits on a standard laboratory stirrer hotplate. Each photo-module contains a single wavelength LED: for this work, the LEDs used were 365nm with a nominal radiant light output of 4.3 W. The LED is positioned to direct the light through the glass window into the reactor (window diameter 15 mm, with a safety cutout installed so light output is cut if the unit is lifted from the fReactor). Cooling is effected through natural convection around each photo-module unit and can be enhanced with a small external fan.

Extensive details of the single and multiphasic capabilities of the CSTRs are reported elsewhere;[292, 324, 325] briefly, each reaction vessel (PEEK material, volume 1.7ml) contains a single cross stirrer bar and is equipped with 4 standard ports accepting standard low pressure HPLC fittings, allowing for flexibility in connecting reactors to each other (1/8" OD FEP tubing) and to feed sources, sampling ports and instrumentation (e.g. thermocouples). Here, we daisy chain the fReactors together (with a single or dual feed into the first reactor and output from the last) giving an improved residence time distribution when compared to a single larger reactor of equivalent total volume.[324] The fReactor platform sits on a standard stirrer-hotplate, which drives the cross-stirrer within each reactor and allows for heating if required.

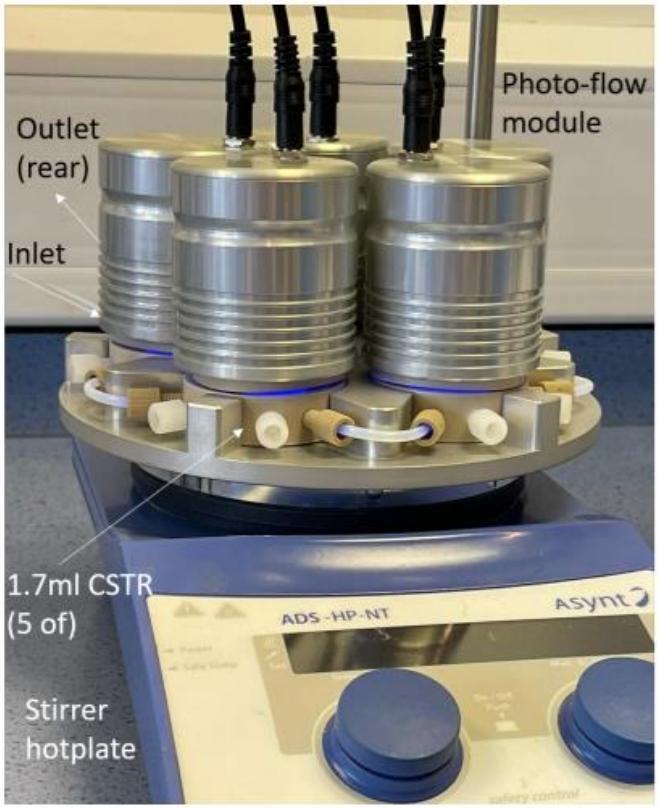

Figure 129: Arrangement of the photo-flow modules on the individual CSTRs. Here, a complete set of five modules in series are shown.

6.5.2 General Procedure K (Batch, Hydroamination, in fReactor)

A fReactor, CSTR, device[292, 324, 325] was charged with a degassed solution of isopropyl acetate (2 mL, 0.05 M) containing 2,4,6-triisopropylbenzenethiol (TRIP thiol) (11.8 mg, 0.05 mmol, 50 mol%), $[Ir(dF(CF_3)ppy)_2(4,4'\text{-}CF_3\text{-}bpy)PF_6$ (2.3 mg, 0.002 mmol, 2 mol%), amine (0.1 mmol, 1.0 equiv) and alkene (0.3 mmol, 3.0 equiv). The resulting pale-yellow solution was irradiated by a single 365 nm LED with a nominal radiant light output of 4.3 W and magnetically stirred for 0.5-2 h. Throughout irradiation, a small rotary fan was placed adjacent to the fReactors to cool the reaction. A typical reaction was measured to run at about 27 °C. Once completed, the reaction mixture was removed from the CSTR, and the device flushed with 5x reaction volume of isopropyl acetate then purified using the specified purification procedure.

6.5.3 General Procedure L (Continuous flow, Hydroamination)

A syringe was charged with a degassed solution of isopropyl acetate containing 2,4,6-triisopropylbenzenethiol (TRIP thiol) (30 mM, 30 mol%), $[Ir(dF(CF_3)ppy)_2(4,4'\text{-}CF_3\text{-}bpy)PF_6$ (1 mM, 1 mol%), amine (100 mM, 1.0 equiv) and alkene (300 mM, 3.0 equiv). The resulting pale-yellow solution was pumped into fReactor CSTR devices[292, 324, 325] and irradiated by 365 nm LEDs with a nominal radiant light output of 4.3 W (T_{res} = 1 h).

Throughout irradiation, a small rotary fan was placed adjacent to the fReactors to cool the reaction. A typical reaction was measured to run at about 27 °C. Conversion was measured by formation of product (secondary amine) against an internal standard and isolated yields were recorded after purification of an aliquot (2 mL) at steady state.

6.5.4 Hydroamination General Workup Procedure

Upon completion of the reaction, the solvent was removed *via* rotary evaporation. The crude residue was then diluted with 40 mL EtOAc and extracted twice with 100 mL 1 N HCl. The combined aqueous layers were washed with Et_2O, then the pH adjusted to pH 10 with 10% (w/w) NaOH solution. The resulting solution was then

extracted with three times with 75 mL DCM. The combined organic extracts were dried over $MgSO_4$ and concentrated under reduced pressure.

6.5.5 General procedure M for the continuous kinetic resolution/photocatalysed hydroamination

An Omnifit glass column (10 mm i.d.) was packed with Novozym 435 (2.61 mL). Solutions of *rac*-amine (200 mM in isopropyl acetate), and the hydroamination feed (relevant iridium photocatalyst 202 or 203 (1 mM), 2,4,6-triisopropylbenzenethiol (50 mM) and alkene (300 mM for alkenes, 150 mM for enecarbamates) in isopropyl acetate) were prepared and degassed. Reagent feeds were introduced into the system using a JASCO PU-980 HPLC pump or a Harvard Apparatus Model 22 syringe pump.

The amine solution was pumped directly into the PBR containing Novozym-435, heated at 40 °C (fluid temperature) at a rate to give a residence time of 30 minutes. The exiting flow stream entered a series of fReactor CSTRs, along with the hydroamination feed through a second inlet at an identical flow rate. The combined streams were irradiated by single wavelength LEDs (365 nm) with a nominal radiant light output of 4.3 W, for a total residence time of 60 min.

Conversion was measured as formation of product (secondary amine) against an internal standard; isolated yields were recorded after purification of an aliquot (2 mL) at steady state.

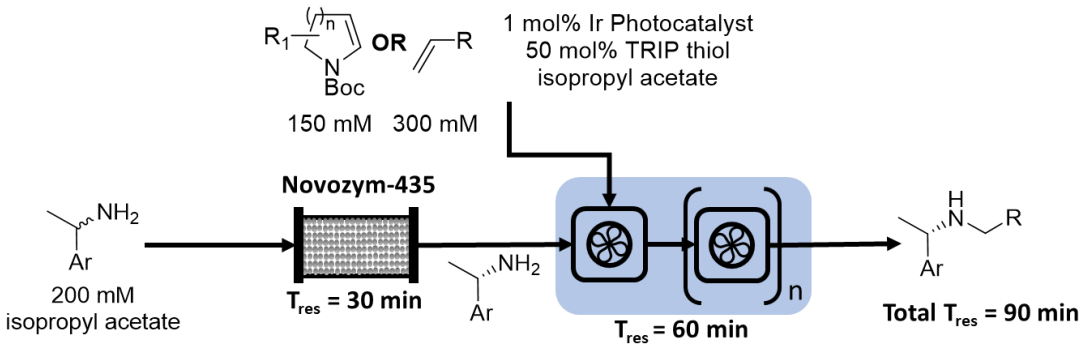

Figure 130: Schematic of enantioselective chemoenzymatic flow synthesis of secondary amines, employing immobilised lipase and hydroamination photochemistry.

6.5.6 General procedure N for the continuous transaminase/photocatalysed hydroamination

An Omnifit glass column (10 mm i.d.) was packed with BmTA@EziG[1] (3.89 mL , 10 wt%). A biocatalysis feed containing 100 mM ketone, 500 mM $^{i}PrNH_2$, 1 mM PLP, 100 mM KH_2PO_4 buffer (pH 8) and the hydroamination feed (relevant iridium photocatalyst 202 or 203 (1 mM), 2,4,6-triisopropylbenzenethiol (50 mM) and alkene (300 mM for alkenes, 150 mM for enecarbamates) in isopropyl acetate) were prepared and degassed. Reagent feeds were introduced into the system using a JASCO PU-980 HPLC pump or a Harvard Apparatus Model 22 syringe pump.

The biocatalysis solution was pumped directly into the PBR containing BmTA@EziG[1], heated at 40 °C (fluid temperature) at a rate to give a residence time of 30 min. The exiting flow stream entered a series of fReactor CSTRs. Within the first CSTR a stream of NaOH (0.05 M) was also fed at ¼ the flow rate of the biocatalysis feed, into the second a stream of isopropyl acetate was pumped (1:1 flow rate with the biocatalysis feed), with the biphasic mixture then entering a Zaiput Sep-10 membrane-based separator, fitted with an OB-900 membane.

The organic outlet of the Zaiput was fed into a series of CSTR units, along with the hydroamination feed through a second inlet at an identical flow rate. The combined streams were irradiated by single wavelength LEDs (365 nm) with a nominal radiant light output of 4.3 W, for a total residence time of 60 min.

Conversion was measured as formation of product (secondary amine) against an internal standard; isolated yields were recorded after purification of an aliquot (2 mL) at steady state.

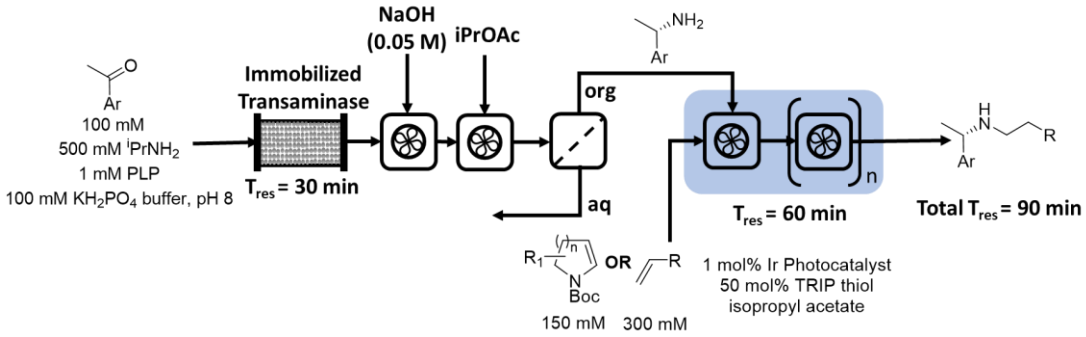

Figure 131: Schematic of enantioselective chemoenzymatic flow synthesis of secondary amines, employing immobilised transaminase and hydroamination photochemistry.

6.5.7 Stern-Volmer Fluorescent Quenching

Stock solutions of photocatalysts (0.42 mM) and quenchers (360 mM) were prepared in isopropyl acetate. An aliquot of photocatalyst solution was added to a cuvette and irradiated at 380 nm, with luminescence recorded at 582 and 478 nm for photocatalysts A and B respectively. Aliquots of quencher solution were added sequentially (2 mM increase in quencher concentration per aliquot) and the samples irradiated, with luminescence recorded twice per sample.

6.6 Characterisation data

6.6.1 Biocatalysis

***rac*-1-(1-Napthyl)ethylamine 130[326]**

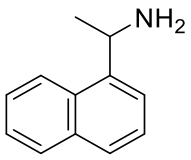

130

1'-Acetonaphthone (2.24 g, 13.2 mmol; 1.00 equiv), hydroxylamine hydrochloride (1.83 g, 26.3 mmol; 2.00 equiv) and sodium acetate (2.16 g, 26.3 mmol; 2.00 equiv) were refluxed in ethanol (30 mL) for 2 h. The solution was then extracted with ethyl acetate (2 x 50 mL), dried over $MgSO_4$, filtered, and concentrated *in vacuo*. Then Pd/C (10 wt%; 200 mg, 1.32 mmol) and ethanol (40 mL) were added to the flask under nitrogen and the atmosphere exchanged to hydrogen. The reaction was stirred for

18 hours at room temperature, then the atmosphere was switched back to nitrogen and the mixture filtered through a short pad of celite. The celite was rinsed with ethanol (3 x 20 mL). The filtrate was concentrated *in vacuo*. The crude product was purified by flash column chromatography, eluting with 67:33 EtOAc−hexane to yield **130** (1.87 g, 83%) as a yellow oil, R_f 0.15 (EtOAc); v_{max}/cm^{-1} 3262, 2557, 1496, 1203, 1112, 685; ^1H NMR ($CDCl_3$, 500 MHz) δ 8.14 (1H, d, *J* = 8.0 Hz, naphthyl 8-H), 7.87 (1H, dd, *J* = 8.0, 1.5 Hz, naphthyl 5-H), 7.75 (1H, d, *J* = 8.1 Hz, naphthyl 4-H), 7.66 (1H, d, *J* = 7.9 Hz, naphthyl 2-H), 7.53 (1H, ddd, *J* = 8.5, 6.8, 1.5 Hz, naphthyl 7-H), 7.51-7.46 (2H, m, naphthyl 3-H and 6-H), 4.97 (1H, q, *J* = 6.6 Hz, ethyl 1-H), 1.64 (2H, br s, N*H*$_2$), 1.56 (3H, d, *J* = 6.6 Hz, ethyl 2-H_3); $^{13}C\{^1H\}$ ($CDCl_3$, 125 MHz) δ 143.5 (napthyl C-1), 134.0 (naphthyl C-4a), 130.9 (naphthyl C-8a), 129.1 (naphthyl C-5), 127.4 (naphthyl C-4), 126.1 (naphthyl C-7), 125.8 (naphthyl C-3 or C-6), 125.6 (naphthyl C-3 or C-6), 123.0 (naphthyl C-8), 121.5 (naphthyl C-2), 46.6 (ethyl C-1), 25.0 (ethyl C-2); HRMS (ESI-TOF) m/z $[M+Na]^+$ Calcd for $C_{12}H_{13}NNa$ 194.0940; Found 194.0931. Spectral data identical to those reported in the literature.[326]

***(R)*-1-(1-Napthyl)ethylamine *(R)*-130**

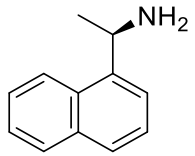

***(R)*-130**

Transaminase from *Hyphomonas neptunium* (HypTA) (2 mg) was added to a 100 mL round bottomed flask containing a buffered solution (KH_2PO_4, pH 8, 35 mL) containing 1'-acetonaphtone (305 mg, 1.87 mmol) $^iPrNH_2$ (553 mg, 9.35 mmol) and pyridoxal 5'-phosphate (PLP) (0.02 mM) and was stirred at 45 ^oC for 48 h.

The reaction mixture was quenched with aqueous saturated $NaHCO_3$ solution (20 mL), and the product was extracted with EtOAc (2 x 15 mL). The EtOAc extract was dried over $MgSO_4$, filtered, and concentrated in vacuo. The crude product was purified by flash column chromatography, eluting with 67:33 EtOAc−hexane to yield ***(R)-130*** (147 mg, 46%, 98% ee) as a yellow oil, R_f 0.15 (EtOAc); $[\alpha]_D^{20}$ +58.7 (*c* 1.00,

MeOH) [lit.:[327] $[\alpha]_D^{20}$ +46.4 (c 1.00, $CHCl_3$)]; spectroscopically identical to the racemate previously prepared. Chiral HPLC was performed with a ChiralPak AS-H column (250 x 4.6 mm), 2% EtOH (0.1% DEA) in hexane (0.1% DEA), 20 min run time (***(S)-130*** 8.61 min, ***(R)-130*** 8.98 min).

***(S)*-1-(1-Napthyl)ethylamine *(S)*-130**

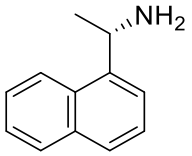

***(S)*-130**

Transaminase from *Bacillus megaterium* (BmTA) (2 mg) was added to a round bottomed flask containing a buffered solution (KH_2PO_4 (100 mM), pH 8, 35 mL) containing 1'-acetonaphtone (305 mg, 1.87 mmol) $^{i}PrNH_2$ (553 mg, 9.35 mmol) and pyridoxal 5'-phosphate (PLP) (0.02 mM) and was stirred at 45 ^{o}C for 48 h.

The reaction mixture was quenched with aqueous saturated $NaHCO_3$ solution (20 mL), and the product was extracted with EtOAc (2 x 15 mL). The EtOAc extract was dried over $MgSO_4$, filtered, and concentrated in vacuo. The crude product was purified by flash column chromatography, eluting with 67:33 EtOAc−hexane to yield ***(S)-130*** in 51% yield (163 mg, 96% ee) as a yellow oil, $[\alpha]_D^{20}$ -58.2 (*c* 1.00, MeOH) [lit.:[328] $[\alpha]_D^{20}$ -34.1 (c 1.00, $CHCl_3$)]; spectroscopically identical to the racemate previously prepared. Chiral HPLC was performed with a ChiralPak AS-H column (250 x 4.6 mm), 2% EtOH (0.1% DEA) in hexane (0.1% DEA), 20 min run time (***(S)-130*** 8.61 min, ***(R)-130*** 8.98 min).

***(S)*-1-(1-Napthyl)ethylamine *(S)*-130**

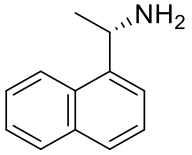

***(S)*-130**

Following general procedure B, using 1'-acetonaphthone. Conversion was determined by HPLC, before the crude material was purified by column chromatography eluting with 67:33 EtOAc−hexane to give an isolated yield of 83% (28.4 mg, 98%*ee*) as a yellow oil, $[\alpha]_D^{20}$ -58.2 (*c* 1.00, MeOH) [lit.:[328] $[\alpha]_D^{20}$ -34.1 (c 1.00, $CHCl_3$)]; spectroscopically identical to the racemate previously prepared. Chiral HPLC was performed with a ChiralPak AS-H column (250 x 4.6 mm), 2% EtOH (0.1% DEA) in hexane (0.1% DEA), 20 min run time (**35** 6.88 min, ***(S)-130*** 8.61 min, ***(R)-130*** 8.98 min).

_N_-Acetyl-1-(1-Naphthyl)ethylamine 148[239]

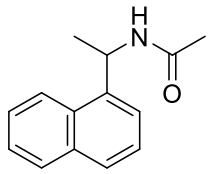

148

1-(1-Napthyl)ethylaminemine (1.03 g, 6 mmol) was dissolved in dichloromethane (7.5 mL) and the mixture cooled to 0 °C. Acetic anhydride (0.6 mL, 6.3 mmol, 1.05 equiv.) was added dropwise under stirring. The mixture was then warmed to room temperature and stirred for 1h. The reaction was then quenched with saturated aqueous sodium bicarbonate (25 mL), the organic phase was then washed with water three times, dried over $MgSO_4$, filtered and concentrated *in vacuo* to yield **148** (1.03 g, 81 %) as an off-white solid; ν_{max}/cm^{-1} 3249, 3085, 1675, 1599, 1543, 775; ^1H NMR ($CDCl_3$, 500 MHz) δ 8.10 (1H, d, *J* = 8.5 Hz, naphthyl 8-H), 7.87 (1H, dd, *J* = 8.0, 1.5 Hz, naphthyl 5-H), 7.80 (1H, d, *J* = 8.1 Hz, naphthyl 4-H), 7.57 – 7.48 (3H, m, naphthyl 2-H, 6-H and 7-H), 7.47 – 7.43 (1H, m, naphthyl 3-H), 5.92 (1H, dq, *J* = 6.8, 6.7 Hz, ethyl 1-H), 5.76 (1H, br d, *J* = 6.7 Hz, N*H*), 1.96 (3H, s, acetyl C*H*$_3$), 1.67 (3H, d, *J* = 6.8 Hz, ethyl 2-H_3); $^{13}C\{^1H\}$ ($CDCl_3$, 125 MHz) δ 169.0 (C=O), 138.3 (naphthyl C-1), 134.1 (naphthyl C-4a), 131.3 (naphthyl C-8a), 128.9 (naphthyl C-5), 128.5 (naphthyl C-4), 126.7 (naphthyl C-7), 126.0 (naphthyl C-6), 125.3 (naphthyl C-3), 123.6 (naphthyl C-8), 122.7 (naphthyl C-2), 44.7 (ethyl C-1), 23.5 (acetyl *C*H_3), 20.8 (ethyl C-2); HRMS

(ESI-TOF) m/z $[M+H]^+$ Calcd for $C_{14}H_{16}NO$ 214.1226; Found 214.1226. Spectral data identical to those reported in the literature.[239]

(*R*)-*N*-Acetyl-1-(1-Naphthyl)ethylamine *(R)*-148

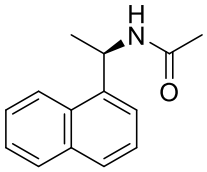

***(R)*-148**

Novozym 435 (10 mg, 15 wt%) was added to a round bottomed flask containing isopropylacetate (10 mL) and 1-(1-Napthyl)ethylamine (171 mg, 1 mmol) and was stirred at 40 °C for 24 h. The solvent was removed under reduced pressure and the crude product purified by column chromatography, eluting with 50:50 EtOAc-hexane to yield ***(R)-148*** (102 mg, 48%, 99% ee) as a white solid, R_f 0.53 (EtOAc); $[\alpha]_D^{20}$ +47.7 (*c* 1.00, MeOH) [lit.:[329] $[\alpha]_D^{27}$ +52.8 (c 0.82, EtOH)]; spectroscopically identical to the racemate previously prepared. Chiral HPLC was performed with a ChiralPak AD-H column (250 x 4.6 mm), 5% EtOH (0.1% DEA) in hexane (0.1% DEA), 20 min run time (***(S)-148*** 14.78 min, ***(R)-148*** 16.52 min).

(*R*)-N-Acetyl-1-(1-Naphthyl)ethylamine *(R)*-148

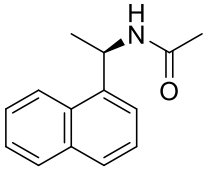

***(R)*-148**

According to general procedure F, using *rac*-1-(1-napthyl)ethylamine. An aliquot was taken for analysis at steady state, conversion was determined from the crude mixture by ^{1}H NMR before the crude material was purified by column chromatography eluting with 50:50 EtOAc-hexane to give an isolated yield of 49% (41.7 mg, 99%*ee*) as a white solid, R_f 0.53 (EtOAc); $[\alpha]_D^{20}$ +47.7 (*c* 1.00, MeOH) [lit.:[329] $[\alpha]_D^{27}$ +52.8 (c 0.82, EtOH)]; spectroscopically identical to the racemate previously prepared. Chiral HPLC was

performed with a ChiralPak AD-H column (250 x 4.6 mm), 5% EtOH (0.1% DEA) in hexane (0.1% DEA), 20 min run time (***(S)-148*** 14.78 min, ***(R)-148*** 16.52 min).

_(S)_-1-(1-Napthyl)ethylamine _(S)_-130

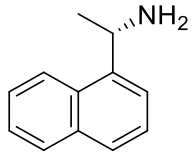

***(S)*-130**

According to general procedure F, using *rac*-1-(1-napthyl)ethylamine. An aliquot was taken for analysis at steady state, conversion was determined from the crude mixture by ^{1}H NMR before the crude material was purified by column chromatography eluting with 50:50 EtOAc-hexane to give an isolated yield of 49% (33.5 mg, 98%*ee*) as a yellow oil, $[\alpha]_D^{20}$ -58.2 (*c* 1.00, MeOH); spectroscopically identical to the racemate previously prepared. Chiral HPLC was performed with a ChiralPak AS-H column (250 x 4.6 mm), 2% EtOH (0.1% DEA) in hexane (0.1% DEA), 20 min run time (**35** 6.88 min, ***(S)-130*** 8.61 min, ***(R)-130*** 8.98 min).

***rac*-1-Phenylethylamine 92[326]**

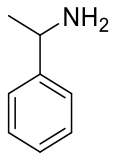

92

Acetophenone (1.6 g, 13.2 mmol; 1.00 equiv), hydroxylamine hydrochloride (1.83 g, 26.3 mmol; 2.00 equiv) and sodium acetate (2.16 g, 26.3 mmol; 2.00 equiv) were refluxed in ethanol (30 mL) for 2 h. The solution was then extracted with ethyl acetate (2 x 50 mL), dried over $MgSO_4$, filtered, and concentrated *in vacuo*. Then Pd/C (10 wt%; 200 mg, 1.32 mmol) and ethanol (40 mL) were added to the flask under nitrogen and the atmosphere exchanged to hydrogen. The reaction was stirred for 18 hours at room temperature, then the atmosphere was switched back to nitrogen and the mixture filtered through a short pad of celite. The celite was rinsed with ethanol (3 x

20 mL). The filtrate was concentrated *in vacuo*. The crude product was purified by flash column chromatography, eluting with 67:33 EtOAc−hexane to yield **92** (1.33 g, 83%) as a pale yellow oil, R_f 0.14 (EtOAc); v_{max}/cm^{-1} 3360, 3059, 2961, 1453, 1280, 1025, 697; ^1H NMR ($CDCl_3$, 500 MHz) δ 7.36-7.29 (4H, m, phenyl 2-H, 3-H, 5-H and 6-H), 7.25-7.20 (1H, m, phenyl 4-H), 4.09 (1H, q, *J* = 6.6 Hz, ethyl 1-H), 1.48 (2H, br s, N*H*$_2$), 1.37 (3H, d, *J* = 6.6 Hz, ethyl 2-H$_3$); $^{13}C\{^1H\}$ ($CDCl_3$, 125 MHz) δ 147.7 (phenyl C-1), 128.3 (phenyl C-3 and C-5), 126.6 (phenyl C-4), 125.6 (phenyl C-2 and C-6), 51.2 (ethyl C-1), 25.6 (ethyl C-2); HRMS (ESI-TOF) m/z $[M+Na]^+$ Calcd for $C_8H_{11}NNa$ 144.0784; Found 144.0787. Spectral data identical to those reported in the literature.[330]

***(S)*-1-Phenylethylamine *(S)*-92**

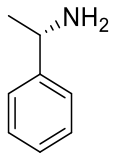

***(S)*-92**

Transaminase from *Bacillus megaterium* (BmTA) (2 mg) was added to a round bottomed flask containing a buffered solution (KH_2PO_4 (100 mM), pH 8, 35 mL) containing acetophenone (210 mg, 1.75 mmol) $^iPrNH_2$ (517 mg, 8.75 mmol) and pyridoxal 5'-phosphate (PLP) (0.02 mM) and was stirred at 45 ^oC for 48 h.

The reaction mixture was quenched with aqueous saturated $NaHCO_3$ solution (20 mL), and the product was extracted with EtOAc (2 x 15 mL). The EtOAc extract was dried over $MgSO_4$, filtered, and concentrated in vacuo. The crude product was purified by flash column chromatography, eluting with 67:33 EtOAc−hexane to yield ***(S)*-92** (95 mg, 45%, 96% ee) as a yellow oil, $[\alpha]_D^{20}$ -17.3 (*c* 1.00, MeOH); spectroscopically identical to the racemate previously prepared. Chiral HPLC was performed with a ChiralPak AS-H column (250 x 4.6 mm), 2% EtOH (0.1% DEA) in hexane (0.1% DEA), 20 min run time (***(S)*-92** 8.17 min, ***(R)*-92** 7.68min).

***(S)*-1-Phenylethylamine *(S)*-92**

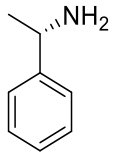

***(S)*-92**

Following general procedure B, using 1'-acetophenone. Conversion was determined by HPLC, before the crude material was purified by column chromatography eluting with 67:33 EtOAc–hexane to give an isolated yield of 76% (18.4 mg, 97%*ee*) as a yellow oil, $[\alpha]_D^{20}$ -17.3 (*c* 1.00, MeOH); spectroscopically identical to the racemate previously prepared. Chiral HPLC was performed with a ChiralPak AS-H column (250 x 4.6 mm), 2% EtOH (0.1% DEA) in hexane (0.1% DEA), 20 min run time (**146** 6.42 min, ***(S)-92*** 8.17 min, ***(R)-92*** 7.68min).

***N*-Acetyl-1-Phenylethylamine 151**[239]

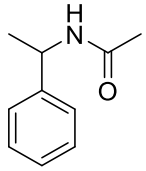

151

1-Phenylethylamine (1.03 g, 6 mmol) was dissolved in dichloromethane (7.5 mL) and the mixture cooled to 0 ºC. Acetic anhydride (0.6 mL, 6.3 mmol, 1.05 equiv.) was added dropwise under stirring. The mixture was then warmed to room temperature and stirred for 1h.

The reaction was then quenched with saturated aqueous sodium bicarbonate (25 mL), the organic phase was then washed with water three times, dried over $MgSO_4$, filtered and concentrated in vacuo to yield **151** (0.68 g, 70 %) as an off-white solid, R_f 0.47 (EtOAc); ν_{max}/cm^{-1} 3261, 2936, 1640, 1561, 1355, 1336, 1097; ^1H NMR ($CDCl_3$, 500 MHz) δ 7.36 – 7.29 (4H, m, phenyl 2-H, 3-H, 5-H and 6-H), 7.28 – 7.24 (1H, m, phenyl 4-H), 5.83 (1H, br s, N*H*), 5.12 (1H, dq, *J* = 6.9, 6.9 Hz, ethyl 1-H), 1.98 (3H, s, acetyl C*H*$_3$), 1.49 (3H, d, *J* = 6.9 Hz, ethyl 2-H$_3$); $^{13}C\{^1H\}$ NMR ($CDCl_3$, 125 MHz) δ 169.2 (C=O), 143.3 (phenyl C-1), 128.8 (phenyl C-3 and C-5), 127.5 (phenyl C-4), 126.3 (phenyl C-2 and C-6), 48.9 (ethyl C-1), 23.6 (acetyl *C*H$_3$), 21.8 (ethyl C-2); HRMS (ESI-

TOF) m/z [M+H]+ Calcd for $C_{10}H_{14}NO$ 164.1070; Found 164.1068. Spectral data identical to those reported in the literature.[239]

***(R)*-N-Acetyl-1-Phenylethylamine *(R)*-151**

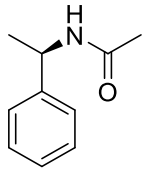

***(R)*-151**

Novozym 435 (10 mg, 15 wt%) was added to a round bottomed flask containing isopropyl acetate (10 mL) and 1-phenyl-ethylamine (120 mg, 1 mmol) and was stirred at 40 °C for 24 h. The solvent was removed under reduced pressure and the crude product purified by column chromatography, eluting with 50:50 EtOAc-hexane to yield ***(R)*-151** (80 mg, 49%, 99%*ee*) as a white solid, $[\alpha]_D^{20}$ +32.4 (*c* 1.00, MeOH); spectroscopically identical to the racemate previously prepared. Chiral HPLC was performed with a ChiralPak AS-H column (250 x 4.6 mm), 2% EtOH (0.1% DEA) in hexane (0.1% DEA), 20 min run time (***(S)*-151** 4.72 min, ***(R)*-151** 5.18 min).

***(R)*-N-Acetyl-1-Phenylethylamine *(R)*-151**

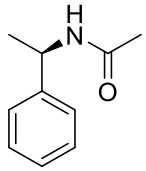

***(R)*-151**

According to general procedure F, using *rac*-methylbenzylamine. An aliquot was taken for analysis at steady state, conversion was determined from the crude mixture by ^{1}H NMR before the crude material was purified by column chromatography eluting with 50:50 EtOAc-hexane to give an isolated yield of 49% (31.9 mg, 99%*ee*) as a white solid, $[\alpha]_D^{20}$ +32.4 (*c* 1.00, MeOH); spectroscopically identical to the racemate previously prepared. Chiral HPLC was performed with a ChiralPak AS-H column (250 x 4.6 mm), 2% EtOH (0.1% DEA) in hexane (0.1% DEA), 20 min run time (***(S)*-151** 4.72 min, ***(R)*-151** 5.18 min).

***(S)*-1-Phenyl-ethylamine *(S)*-92**

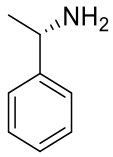

***(S)*-92**

According to general procedure F, using *rac*-methylbenzylamine. An aliquot was taken for analysis at steady state, conversion was determined from the crude mixture by ^{1}H NMR before the crude material was purified by column chromatography eluting with 50:50 EtOAc-hexane to give an isolated yield of 49% (23.7 mg, 98%*ee*) as a yellow oil, $[\alpha]_D^{20}$ -17.3 (*c* 1.00, MeOH); spectroscopically identical to the racemate previously prepared. Chiral HPLC was performed with a ChiralPak AS-H column (250 x 4.6 mm), 2% EtOH (0.1% DEA) in hexane (0.1% DEA), 20 min run time (**146** 6.42 min, ***(S)*-92** 8.17 min, ***(R)*-92** 7.68min).

***(S)*-1-(4-Bromophenyl)ethylamine 267**

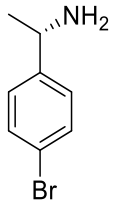

267

Following general procedure B, using 4-bromoacetophenone. Conversion was determined by HPLC, before the crude material was purified by column chromatography eluting with 67:33 EtOAc−hexane to give an isolated yield of 70% (28.0 mg, 96%*ee*) as a yellow oil, $[\alpha]_D^{20}$ -25.6 (*c* 1.00, MeOH); lit.:[331] $[\alpha]_D^{25}$ -30.5 (c 1.00, $CHCl_3$]; ν_{max}/cm^{-1} 3300, 2860, 1547, 1310, 1021, 686; ^{1}H NMR ($CDCl_3$, 500 MHz) δ 7.46-7.41 (2H, m, phenyl 3-H and 5-H), 7.25-7.20 (2H, m, phenyl 2-H and 6-H), 4.09 (1H, q, *J* = 6.6 Hz, ethyl 1-H), 1.35 (3H, d, *J* = 6.6 Hz, ethyl 2-H_3); $^{13}C\{^{1}H\}$ ($CDCl_3$, 125 MHz) δ 146.8 (phenyl C-1), 131.6 (phenyl C-2 and C-6), 127.7 (phenyl C-3 and C-5), 120.6 (phenyl C-4), 50.9 (ethyl C-1), 25.8 (ethyl C-2); HRMS (ESI-TOF) m/z $[M+Na]^+$ Calcd for $C_8H_{11}{}^{79}BrN$ 200.0069; Found 200.0067. Chiral HPLC was performed with a

ChiralPak AS-RH column (250 x 4.6 mm), 40% MeCN (0.1% DEA) in water (0.1% DEA), 10 min run time (***(S)-267*** 4.99 min, ***(R)-267*** 4.23 min).

***(S)*-2,3-Dihydro-*1H*-inden-1-amine 268**

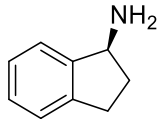

268

Following general procedure B, using 1-indanone. Conversion was determined by HPLC, before the crude material was purified by column chromatography eluting with 67:33 EtOAc–hexane to give an isolated yield of 62% (16.5 mg, 75%*ee*) as a pale yellow oil, R_f 0.13 (50:50 EtOAc-hexane), $[\alpha]_D^{20}$ 20.8 (*c* 1.00, MeOH), lit.:[331] $[\alpha]_D^{25}$ +20.8 (c 1.00, $CHCl_3$]; ν_{max}/cm^{-1} 3361, 2941, 2848, 1586, 1475, 1456, 756, 737; ^1H NMR ($CDCl_3$, 500 MHz) δ 7.35-7.32 (1H, m, 7-H), 7.25-7.18 (3H, m, 4-H, 5-H and 6-H), 4.36 (1H, t, *J* = 7.5 Hz, 1-H), 2.96 (1H, ddd, *J* = 15.8, 8.6, 3.3 Hz, 3-H_a), 2.86-2.77 (1H, m, 3-H_b), 2.55-2.46 (1H, m, 2-H_a), 1.74-1.63 (1H, m, 2-H_b); $^{13}C\{^1H\}$ ($CDCl_3$, 125 MHz) δ 147.6 (C-3a), 143.2 (C-7a), 127.3 (C-5), 126.6 (C-6), 124.8 (C-4), 123.4 (C-7), 57.4 (C-1), 37.5 (C-2), 30.2 (C-3); HRMS (ESI-TOF) m/z $[2M+H]^+$ Calcd for $C_{18}H_{23}N_2$ 267.1858; Found 267.1856. Chiral HPLC was performed with a ChiralPak AS-RH column (250 x 4.6 mm), 20% MeCN (0.1% DEA) in water (0.1% DEA), 20 min run time (***(S)-268*** 9.94 min, ***(R)-268*** 10.49 min).

***(S)*-Chroman-4-amine 269**

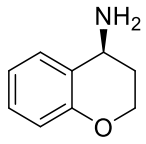

269

Following general procedure B, using 4-chromanone. Conversion was determined by HPLC, before the crude material was purified by column chromatography eluting with 67:33 EtOAc–hexane to give an isolated yield of 51% (15.2 mg, 77% *ee*) as a pale yellow oil, R_f 0.18 (50:50 EtOAc-hexane); $[\alpha]_D^{20}$ -43.2 (*c* 1.00, MeOH), lit.:[332] $[\alpha]_D^{25}$ -

29.8 (c 0.45, $CHCl_3$]; v_{max}/cm^{-1} 3366, 2948, 2873, 1580, 1486, 1451, 1224, 750; ^1H NMR ($CDCl_3$, 500 MHz) δ 7.30 (1H, dd, *J* = 7.6, 1.3 Hz, 5-H), 7.17-7.11 (1H, m, 7-H), 6.91 (1H, ddd, *J* = 7.6, 7.5, 2.9 Hz, 6-H), 6.81 (1H, dd, *J* = 8.2, 1.1 Hz, 8-H), 4.28 (1H, ddd, *J* = 11.8, 9.0, 2.9 Hz, 2-H_a), 4.25-4.20 (1H, m, 2-H_b), 4.05 (1H, t, *J* = 5.3 Hz, 4-H), 2.16 (1H, dddd, *J* = 13.9, 8.8, 5.0, 3.5 Hz, 3-H_a), 1.89-1.80 (1H, m, 3-H_b); $^{13}C\{^1H\}$ ($CDCl_3$, 125 MHz) δ 154.4 (C-8_a), 128.9 (C-5), 128.6 (C-7), 126.8 (C-4_a), 120.6 (C-6), 117.0 (C-8), 62.9 (C-2), 45.2 (C-4), 32.3 (C-3); HRMS (ESI-TOF) m/z $[M+Na]^+$ Calcd for $C_9H_{11}NONa$ 172.0733; Found 172.0736. Chiral HPLC was performed with a ChiralPak AS-RH column (250 x 4.6 mm), 50% MeCN (0.1% DEA) in water (0.1% DEA), 20 min run time ***((S)-269*** 6.29 min, ***(R)-269*** 6.67 min).

2,5-Dimethyl pyrazine 136

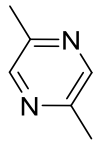

136

Transaminase from *Bacillus megaterium* (BmTA) (2 mg) was added to a round bottomed flask containing a buffered solution (KH_2PO_4 (100 mM), pH 8, 35 mL) containing acetophenone (210 mg, 1.75 mmol) 1,2-diaminopropane (648 mg, 8.75 mmol) and pyridoxal 5'-phosphate (PLP) (0.02 mM) and was stirred at 45 °C for 48 h.

The reaction mixture was quenched with aqueous saturated $NaHCO_3$ solution (20 mL), and the product was extracted with EtOAc (2 x 15 mL). The EtOAc extract was dried over $MgSO_4$, filtered, and concentrated in vacuo. The crude product was purified by flash column chromatography, eluting with 67:33 EtOAc−hexane to yield **136** (43 mg, 23%) as a dark yellow oil, R_f 0.28 (50:50 EtOAc – hexane); v_{max}/cm^{-1} 3386, 3028, 1488, 1379, 1326, 1164, 1035; ^1H NMR ($CDCl_3$, 500 MHz) δ 8.31 (2H, s, 3-H and 6-H), 2.49 (6H, s, C*H*$_3$); $^{13}C\{^1H\}$ NMR ($CDCl_3$, 125 MHz) δ 150.6 (C-2 and C-5), 143.6 (C-3 and C-6), 21.1 (*C*H_3). Spectral data identical to those reported in the literature.[333]

6.6.2 Borrowing Hydrogen

3-(3-(Trifluoromethyl)phenyl)prop-2-yn-1-ol 177[269]

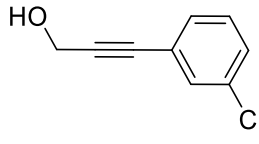

177

3-bromobenzotrifluoride (4.86 g, 21.6 mmol; 1.00 equiv), CuI (123 mg, 0.648 mmol; 3 mol%), $Pd(OAc)_2$ (157 mg, 0.648 mmol; 3 mol%), PPh_3 (340 mg, 1.30 mmol, 6 mol%) and THF (60 mL) were added to an oven-dried two-neck flask under N_2 atmosphere. Then DBU (1,8-diazabicyclo[5.4.0]undec-7-ene; 3.9 mL, 25.9 mmol; 1.20 equiv) was added and the mixture cooled to 0 °C. Propargyl alcohol (1.5 mL, 25.9 mmol; 1.2 equiv) was added dropwise over 15 minutes. The mixture was allowed to warm to room temperature and slowly heated to 55 °C at which temperature it was stirred for 22 hours.

After cooling to room temperature, the reaction mixture was transferred to a separatory funnel using Et_2O (75 mL) and washed with water (25 mL). The aqueous phase was extracted with Et_2O (25 mL). The combined organic phases were washed with HCl (2M, aq., 25 mL), $NaHCO_3$ (sat. aq., 25 mL), brine (25 mL), dried over $MgSO_4$, filtered, and concentrated in vacuo. The crude product was purified by flash column chromatography, eluting with 25:75 EtOAc–hexane to yield **177** (3.66 g, 85%) as a brown oil, R_f 0.32 (25:75 EtOAc-hexane); ν_{max}/cm^{-1} 3322, 2915, 1329, 1094, 1072, 1025, 694; ^1H NMR ($CDCl_3$, 500 MHz) δ 7.70 (1H, s, aryl 2-H), 7.60 (1H, d, *J* = 7.7 Hz, aryl 6-H), 7.57 (1H, d, *J* = 7.9 Hz, aryl 4-H), 7.44 (1H, t, *J* = 7.8 Hz, aryl 5-H), 4.51 (2H, s, propyl 1-H_2), 1.67 (1H, br s, O*H*); $^{13}C\{^1H\}$ NMR ($CDCl_3$, 125 MHz) δ 134.9 (aryl C-6), 131.1 (q, *J* = 32.7 Hz, aryl C-3), 129.0 (aryl C-5), 128.7 (q, *J* = 3.9 Hz, aryl C-2), 125.2 (q, *J* = 3.8 Hz, aryl C-4), 123.8 (q, *J* = 272.4 Hz, *C*F_3), 123.6 (aryl C-1), 88.9 (propyl C-2), 84.4 (propyl C-3), 51.7 (propyl C-1); $^{19}F\{^1H\}$ ($CDCl_3$, 376 MHz) δ -63.0 (*CF*$_3$); HRMS (ESI-TOF) m/z $[M+H]^+$ Calcd for $C_{10}H_8F_3O$ 200.0449; Found 200.0440. Spectral data identical to those reported in the literature.[269]

3-(3-(Trifluoromethyl)phenyl)propan-1-ol 174[269]

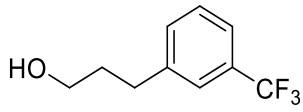

174

An oven-dried flask under nitrogen was equipped with 3-(3-(trifluoromethyl)phenyl)prop-2-yn-1-ol (8.00 g, 40.00 mmol; 1.00 equiv) and ethanol (100 mL). Then Pd/C (10 wt%; 1.45 g, 1.36 mmol; 3.4 mol%) was added and the atmosphere exchanged to hydrogen. The reaction was stirred for 18 hours at room temperature, then the atmosphere was switched back to nitrogen and the mixture filtered through a short pad of celite. The celite was rinsed with ethanol (3 x 20 mL). The filtrate was concentrated in vacuo. Flash chromatography (75:25 hexane-EtOAc) afforded **174** (6.50 g, 80%) as a pale-yellow oil, R_f 0.30 (75:25 hexane-EtOAc); v_{max}-/cm^{-1} 3317, 2939, 2871, 1326, 1117, 1071, 701; ^{1}H NMR ($CDCl_3$, 500 MHz) δ 7.48 – 7.43 (2H, m, aryl 2-H and 6-H), 7.42 – 7.35 (2H, m, aryl 4-H and 5-H), 3.68 (2H, t, *J* = 6.4 Hz, propyl 1-H_2), 2.77 (2H, t, *J = 7.6 Hz*, propyl 3-H_2), 1.94 – 1.87 (2H, m, propyl 2-H_2), 1.46 (brs, 1H); $^{13}C\{^1H\}$ ($CDCl_3$, 125 MHz) δ 142.9 (aryl C1), 132.0 (aryl C-6), 130.8 (q, *J* = 31.9 Hz, aryl C-3), 128.9 (aryl C-5), 125.2 (q, *J* = 3.8 Hz, aryl C-4), 124.4 (q, *J* = 272.2 Hz, *C*F_3), 122.9 (q, *J* = 3.8 Hz, aryl C-2), 62.0 (propyl C-1), 34.0 (propyl C-2), 32.0 (propyl C-3); $^{19}F\{^1H\}$ ($CDCl_3$, 376 MHz) δ -62.6 (C*F*$_3$); HRMS (ESI-TOF) m/z $[M+H]^+$ Calcd for $C_{10}H_{12}F_3O$ 204.0762; Found 204.0760. Spectral data identical to those reported in the literature.[269]

***N*-Boc-3-Hydroxypiperidine 274**

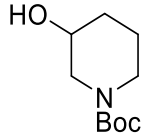

274

3-hydroxypiperidine (1.01 g, 10 mmol) was dissolved in DCM (10 mL) and cooled to 0 °C. Boc_2O (3.28 g, 15 mmol) was then added slowly, and the mixture allowed to warm to RT and stirred for 3 h. The solvent was removed under reduced pressure and the crude residue purified by column chromatography (80:20 DCM-EtOAc), to

yield **274** (1.88 g, 94 %) as a colourless oil, R_f 0.51 (50:50 DCM-EtOAc); v_{max}/cm^{-1} 3463, 2943, 1664, 1431, 1391, 1167, 1071; ^1H NMR (500 MHz, $CDCl_3$) δ 3.75 (1H ddt, *J* = 12.8, 3.7, 1.1 Hz, 2-H_a), 3.70 (1H, ddd, *J* = 11.3, 7.6, 3.7 Hz, 3-H), 3.59-3.48 (1H, brm, 6-H_a), 3.08 (1H, ddd, *J* = 12.6, 9.0, 3.2 Hz, 6-H_b), 3.02 (1H, dd, *J* = 12.8, 7.6 Hz, 2-H_b), 2.25 (1H, brs, O*H*), 1.91-1.84 (1H, m, 4-H_a), 1.73 (1H, ddt, *J* = 13.4, 7.1, 3.5 Hz, 5-H_a), 1.53-1.46 (2H, m, 4-H_b and 5-H_b), 1.44 (9H, s, ^{t}Bu); $^{13}C\{^1H\}$ ($CDCl_3$, 125 MHz) δ 155.4 (C=O), 79.9 (^{t}Bu-*C*), 66.3 (C-3), 50.8 (C-2), 44.1 (C-6), 32.7 (C-4), 28.5 (^{t}Bu *C*H_3), 22.6 (C-5); HRMS (ESI-TOF) m/z $[M+Na]^+$ Calcd for $C_{10}H_{19}NNaO_3$ 244.1257; Found 224.1251.

4-Bromobenzyl-(1-phenylethyl)-amine 173

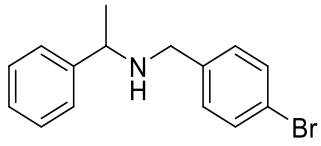

173

According to general procedure G, using 1-phenylethanamine (127 µL, 1 mmol), 4-bromobenzylalcohol (187 µL, 1 mmol), and the title compound was obtained by flash chromatography eluting with 75:25 hexane-EtOAc to yield **173** (231 mg, 80%) as a yellow oil, R_f 0.36 (75:25 hexane-EtOAc); v_{max}/cm^{-1} 2943, 1486, 1433, 1069, 1010, 793; ^1H NMR ($CDCl_3$, 500 MHz) δ 7.45-7.41 (2H, m, aryl 3-H and 5-H), 7.38-7.33 (4H, m, phenyl 2-H, 3-H, 5-H and 6-H), 7.29-7.24 (1H, m, phenyl 4-H), 7.19-7.15 (2H, m, aryl 2-H and 6-H), 3.79 (1H, q, *J* = 6.6 Hz, ethyl 1-H), 3.61 (1H, d, *J* = 13.4 Hz, benzyl C*H*$_a$H$_b$), 3.55 (1H, d, *J* = 13.4 Hz, benzyl CH$_a$*H*$_b$), 1.58 (1H, br s, N*H*), 1.37 (3H, d, *J* = 6.6 Hz, ethyl 2-H_3); $^{13}C\{^1H\}$ ($CDCl_3$, 125 MHz) δ 145.5 (phenyl C-1), 139.8 (aryl C-1), 131.5 (aryl C-3 and C-5), 130.0 (aryl C-2 and C-6), 128.7 (phenyl C-3 or C-5), 128.6 (phenyl C-3 or C-5), 127.2 (phenyl C-4), 126.8 (phenyl C-2 or C-6), 126.7 (phenyl C-2 or C-6), 120.7 (aryl C-4), 57.6 (ethyl C-1), 51.0 (benzyl *C*H_2), 24.6 (ethyl C-2); HRMS (ESI-TOF) m/z $[M+H]^+$ Calcd for $C_{15}H_{17}{}^{79}BrN$ 290.0544; Found 290.0539.

4-Bromobenzyl-(1-phenylethyl)-amine 173

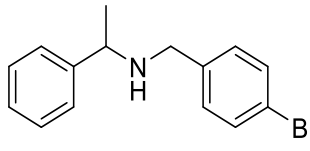

173

4-bromobenzaldehyde (1.85 g, 10 mmol), 1-phenylethanamine (1.22 g, 10 mmol) and a drop of acetic acid were dissolved in ethanol (25 mL) and the mixture refluxed for 24h. The mixture was then cooled to 0 ºC and methanol (5 mL) was added. After 5 mins stirring, $NaBH_4$ (1.0 g, 26 mmol) was added portion-wise. The mixture was warmed to RT and stirred for 20h.

The reaction was then quenched with sat. $NaHCO_3$ (20 mL) and extracted (3x) with DCM. The combined organics were dried over $MgSO_4$, filtered and concentrated in vacuo. The crude product was the purified by flash column chromoatography, eluting with 75:25 hexane-EtOAc to yield **173** (1.39 g, 48%) as a colourless oil, R_f 0.36 (75:25 hexane-EtOAc); spectroscopically identical to the racemate previous prepared.[334]

4-Methylbenzyl-(1-phenylethyl)-amine 181

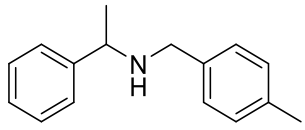

181

According to general procedure G, using 1-phenylethanamine (127 µL, 1 mmol), 4-methylbenzylalcohol (122 mg, 1 mmol), and the title compound was obtained by flash chromatography eluting with 5:95 MeOH-DCM to yield **181** (183 mg, 81%) as a yellow oil; ν_{max}/cm^{-1} 2936, 1450, 1129, 759, 699, 473; ^1H NMR ($CDCl_3$, 500 MHz) δ 7.37-7.34 (4H, m, phenyl 2-H, 3-H, 5-H and 6-H), 7.29-7.26 (1H, m, phenyl 4-H), 7.19-7.16 (2H, m, aryl 2-H and 6-H), 7.13 (2H, d, *J* = 7.8 Hz, aryl 3-H and 5-H), 3.81 (1H, q, *J* = 6.6 Hz, ethyl 1-H), 3.63 (1H, d, *J* = 13.0 Hz, benzyl CH_aH$_b$) 3.56 (1H, d, *J* = 13.0 Hz, benzyl CH$_a$$H_b$), 2.34 (3H, s, 4-aryl C$H_3$), 1.65 (1H, br s, N*H*), 1.36 (3H, d, *J* = 6.6 Hz, ethyl 2-H$_3$); $^{13}C\{^1H\}$ ($CDCl_3$, 125 MHz) δ 145.8 (phenyl C-1), 137.7 (aryl C-1), 136.5 (aryl C-4), 129.4 (aryl C-3 or C-5), 129.1 (aryl C-3 or C-5), 128.6 (phenyl C-3 or C-5), 128.2 (phenyl C-3 or C-5), 127.3 (aryl C-2 and C-6), 127.0 (phenyl C-4), 126.9 (phenyl C-2 and C-6),

57.5 (ethyl C-1), 51.5 (benzyl *C*H_2), 24.6 (ethyl C-2), 21.2 (4-aryl *C*H_3); HRMS (ESI-TOF) m/z $[M+H]^+$ Calcd for $C_{16}H_{20}N$ 226.1596; Found 226.1590.

_N_-(4'-Methoxybenzyl)-1-phenylethanamine 182

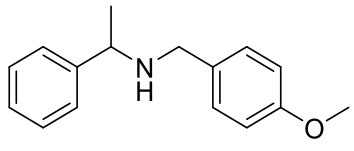

182

According to general procedure G, using 1-phenylethanamine (127 µL, 1 mmol), p-anisyl alcohol (124 µL, 1 mmol), and the title compound was obtained by flash chromatography eluting with 2.5:97.5 MeOH-DCM to yield **182** (139 mg, 58%) as a yellow oil; ν_{max}/cm^{-1} 2959, 1610, 1510, 1451, 1243, 1034, 758, 699; ^1H NMR ($CDCl_3$, 500 MHz) δ 7.36-7.34 (4H, m, phenyl C-2, C-3, C-5 and C-6), 7.28-7.25 (1H, m, phenyl C-4), 7.22-7.18 (2H, m, aryl 2-H and 6-H), 6.87-6.84 (2H, m, aryl 3-H and 5-H), 3.81 (1H, q, *J* = 6.6 Hz, ethyl 1-H), 3.80 (3H, s, methoxy C*H*$_3$), 3.60 (1H, d, *J* = 12.9 Hz, benzyl C*H*$_a$CH$_b$), 3.54 (1H, d, *J* = 12.9 Hz, benzyl CH$_a$C*H*$_b$), 1.56 (1H, br s, N*H*), 1.36 (3H, d, *J* = 6.6 Hz, ethyl 2-H$_3$); $^{13}C\{^1H\}$ ($CDCl_3$, 125 MHz) δ 158.7 (aryl C-4), 145.8 (phenyl C-1), 133.0 (aryl C-1), 129.4 (aryl C-2 and C-6), 128.6 (phenyl C-2 and C-6), 127.0 (phenyl C-4), 126.9 (phenyl C-3 and C-5), 113.9 (aryl C-3 and C-5), 57.5 (ethyl C-1), 55.4 (methoxy *C*H$_3$), 51.1 (benzyl *C*H$_2$), 24.6 (ethyl C-2); HRMS (ESI-TOF) m/z $[M+H]^+$ Calcd for $C_{16}H_{20}NO$ 242.1545; Found 242.1539.

tert-Butyl 3-(1-Phenylethylamino)azetidine-1-carboxylate 193

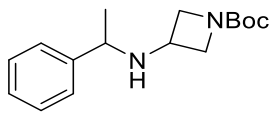

193

According to general procedure G, using 1-phenylethanamine (127 µL, 1.00 mmol) and 1-Boc-3-hydroxyazetidine (173 mg, 1.00 mmol). The solvent was evaporated under reduced pressure to give a crude product which contained an undeterminable mixture of diastereomeric products. The crude product was purified by flash chromatography eluting with 90:10 hexane-acetone to yield **193** (156 mg, 56 %) as a

pale-yellow viscous oil, R_f 0.23 (80:20 hexane-acetone); ν_{max}/cm^{-1} 2972, 1688, 1400, 1365, 1116, 762, 700; ^1H NMR ($CDCl_3$, 500 MHz) δ 7.32-7.28 (2H, m, phenyl 3-H and 5-H), 7.27-2.21 (3H, m, phenyl 2-H, 4-H and 6-H), 4.03-3.97 (1H, m, 2-H_a), 3.89-3.82 (1H, m, 4-H_a), 3.71 (1H, q, *J* = 6.6 Hz, ethyl 1-H), 3.65-3.61 (1H, m, 2-H_b), 3.47-3.39 (2H, m, 3-H and 4-H_b), 1.60 (1H, s, N*H*), 1.39 (9H, s, ^{t}Bu), 1.35 (3H, d, *J* = 6.6 Hz, ethyl 2-H_3); $^{13}C\{^1H\}$ ($CDCl_3$, 125 MHz) δ 156.4 (C=O), 144.8 (phenyl C-1), 128.7 (phenyl C-3 and C-5), 127.5 (C-4), 126.7 (phenyl C-2 and C-6), 79.4 (^{t}Bu *C*), 57.2 (C-2 and C-4), 56.5 (ethyl C-1), 46.2, 28.5 (^{t}Bu *C*H_3), 24.0 (ethyl C-2); HRMS (ESI-TOF) m/z $[M+Na]^+$ Calcd for $C_{16}H_{24}N_2NaO_2$ 299.1730; Found 299.1718.

_N_-(tert-Butoxycarbonyl)-3-(*RS*)-(1'-(*RS*)-Phenylethyl)aminopyrrolidine 194

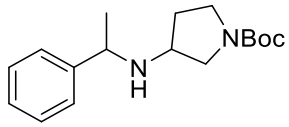

194

According to general procedure G, using 1-phenylethanamine (127 µL, 1.00 mmol), 1-Boc-3-pyrrolidinol (187 µL, 1.00 mmol), and the title compound was obtained by flash chromatography eluting with 50:50 DCM-EtOAc to yield **194** (213 mg, 73%) as a 50:50 mixture of rotameric diastereomers as a yellow oil; ν_{max}/cm^{-1} 3001, 1701, 1390, 1298, 1104, 755, 703; ^1H NMR (d_6-DMSO, 500 MHz, 348K) δ 7.36-7.32 (2H, m, phenyl 2-H and 6-H), 7.32-7.27 (2H, m, phenyl 3-H and 5-H), 7.23-7.18 (1H, m, phenyl 4-h), 3.81-3.71 (1H, m, ethyl 1-H), 3.36-3.31 (1H, m, pyrrolidine 2-H_a^{RotA}, 5-H_a^{RotA}), 3.31-3.26 (0.5H, m, 5-H_a^{RotB}), 3.20-3.14 (0.5H, m, 2-H_b^{RotA}), 3.14-3.09 (1H, m, 5-H_b), 3.05-2.99 (1.5H, m, pyrrolidine 2-H_a^{RotB} and 3-H), 2.83 (0.5H, dd, *J* = 10.7, 5.8 Hz, 2-H_b^{RotB}), 1.93-1.85 (0.5H, m, 4-H_a^{RotB}), 1.81-1.73 (0.5H, m, 4-H_b^{RotA}), 1.71-1.63 (0.5H, m, 4-H_a^{RotA}), 1.58-1.49 (0.5H, m, 4-H_b^{RotB}), 1.39 (4.5H, s, ^{t}Bu), 1.37 (4.5H, s, ^{t}Bu), 1.26 (3H, dd, *J* = 6.6, 4.1 Hz, ethyl 2-H_3); $^{13}C\{^1H\}$ NMR (d_6-DMSO, 125 MHz) δ 153.62, 153.56, 153.5, 153.4 (C=O), 146.2 (phenyl C-1), 128.6, 128.21, 128.15 (phenyl C-3 and C-5), 126.6 (phenyl C-4), 126.5 (phenyl C-2 and C-6), 78.04, 78.01, 77.96, 77.9 (^{t}Bu *C*), 55.9 (ethyl C-1), 55.63 (ethyl C-1), 55.61 (ethyl C-1), 55.0 (pyrrolidine C-3), 54.1 (pyrrolidine C-3), 54.0 (pyrrolidine C-3), 51.9 (pyrrolidine C-2^{RotB}), 51.7 (pyrrolidine C-

2^{RotA}), 51.3 (pyrrolidine C-2^{RotB}), 51.0 (pyrrolidine C-2^{RotA}), 44.2, 44.1, 44.0, 43.9 (pyrrolidine C-5), 31.9 (pyrrolidine C-4^{RotB}), 31.2 (pyrrolidine C-4^{RotA}), 30.8 (pyrrolidine C-4^{RotA}), 30.0 (pyrrolidine C-4^{RotB}), 28.18, 28.16 (^{t}Bu *C*H_3), 24.8, 24.7 (ethyl C-2); HRMS (ESI-TOF) m/z [M+H] Calcd for $C_{17}H_{27}N_2O_2$ 291.2073; Found 291.2067.

***tert*-Butyl 3-(1-Phenylethylamino)piperidine-1-carboxylate 195**

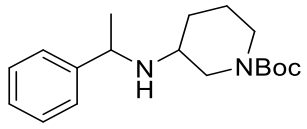

195

According to general procedure G, using 1-phenylethanamine (127 µL, 1.00 mmol), N-boc-3-hydroxypiperidine (201 mg, 1.00 mmol), and the title compound was obtained by flash chromatography eluting with 50:50 hexane-EtOAc to yield **195** as a 50:50 mixture of diastereomers (109.4 mg, 36%) as a viscous yellow oil, R_f 0.17 (50:50 hexane-EtOAc); ν_{max}/cm^{-1} 2989, 1658, 1375, 1301, 1094, 752, 699; ^{1}H NMR ($CDCl_3$, 500 MHz) δ 7.35-7.29 (4H, m, phenyl 2-H, 3-H, 5-H and 6-H), 7.25-7.21 (1H, m, phenyl 4-H), 4.00-3.91 (1H, m, ethyl 1-H), 3.89-3.67 (1.5H, m, piperidine 2-H_{a1}, 2-H_{a2} and 6-H_a), 3.64-3.53 (0.5H, m, piperidine 6-H_a), 3.05-2.96 (0.5H, m, piperidine 6-H_b), 2.95-2.86 (0.5H, br m, piperidine 2-H_b), 2.85-2.76 (0.5H, m, piperidine 6-H_b), 2.67-2.58 (0.5H, m, piperidine 2-H_b), 2.54-2.43 (0.5H, br m, piperidine 3-H), 2.43-2.31 (0.5H, br m, piperidine 3-H), 1.99-1.90 (0.5H, m, piperidine 4-H_a), 1.74-1.68 (0.5H, m, piperidine 4-H_a), 1.67-1.59 (1H, m, piperidine 5-H_{a1} and 5-H_{a2}), 1.45 (4.5H, s, ^{t}Bu), 1.40 (4.5H, s, ^{t}Bu), 1.34 (3H, d, *J* = 6.5 Hz, ethyl 2-H_3), 1.42-1.31 (1.5H, m, piperidine 5-H_{b1}, 5-H_{b2} and 4-H_b), 1.29-1.21 (0.5H, m, piperidine 4-H_b); $^{13}C\{^{1}H\}$ NMR ($CDCl_3$, 125 MHz) δ 155.0 (C=O), 146.0 (phenyl C-1), 128.6 (phenyl C-3 and C-5), 127.1 (phenyl C-4), 126.7, 126.6 (phenyl C-2 and C-6), 79.52 (^{t}Bu *C*), 79.49 (^{t}Bu *C*), 55.1 (ethyl C-1), 50.7 (piperidine C-3), 48.8 (piperidine C-2), 43.9 (piperidine C-6), 32.1, 31.3, 29.9, 29.1 (piperidine C-4), 28.60 (^{t}Bu *C*H_3), 28.56 (^{t}Bu *C*H_3), 25.1 (ethyl C-2), 23.7, 23.4 (piperidine C-5) (21 signals observed of 28 expected); HRMS (ESI-TOF) m/z $[M+H]^+$ Calcd for $C_{18}H_{29}N_2O_2$ 305.2224; Found 305.2224.

4-Bromobenzyl-(1-naphth-1-ylethyl)-amine 183

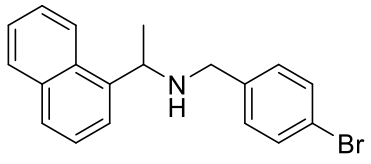

183

According to general procedure G, using 1-(1'-napthyl)ethylamine (161 µL, 1.00 mmol), 4-bromobenzylalcohol (187 µL, 1.00 mmol), and the title compound was obtained by flash chromatography eluting with 75:25 hexane-EtOAc to yield **183** (226.0 mg, 67%) as a yellow oil, R_f 0.28 (75:25 hexane-EtOAc); ν_{max}/cm^{-1} 2977, 2818, 1695, 1593, 1128, 814, 777; ^1H NMR ($CDCl_3$, 500 MHz) δ 8.18-8.12 (1H, m, naphthyl 8-H), 7.91-7.86 (1H, m, naphthyl 5-H), 7.77 (1H, d, *J* = 8.2 Hz, naphthyl 4-H), 7.74 (1H, d, *J* = 7.1 Hz, naphthyl 2-H), 7.54-7.46 (3H, m, naphthyl 3-H, 6-H and 7-H), 7.46-7.41 (2H, m, aryl 3-H and 5-H), 7.21-7.16 (2H, m, aryl 2-H and 6-H), 4.67 (1H, q, *J* = 6.6 Hz, ethyl 1-H), 3.71 (1H, d, *J* = 13.4 Hz, benzyl CH_aH$_b$), 3.65 (1H, d, *J* = 13.4 Hz, benzyl CH$_a$$H_b$), 1.67 (1H, brs, N*H*), 1.52 (3H, d, *J* = 6.6 Hz, ethyl 2-H$_3$); $^{13}C\{^1H\}$ ($CDCl_3$, 125 MHz) δ 140.9 (naphthyl C-1), 139.8 (aryl C-1), 134.2 (naphthyl C-4a), 131.6 (aryl C-3 or C-5 or naphthyl C-8a), 131.5 (aryl C-3 or C-5 or naphthyl C-8a), 130.0 (aryl C-2 and C-6), 129.1 (naphthyl C-5), 127.5 (naphthyl C-4), 125.91 (naphthyl C-3 or C-6 or C-7), 125.88 (naphthyl C-3 or C-6 or C-7), 125.5 (naphthyl C-3 or C-6 or C-7), 123.1 (naphthyl C-8 or C-2), 123.0 (naphthyl C-8 or C-2), 120.8 (aryl C-4), 53.2 (ethyl C-1), 51.3 (benzyl *C*H$_2$), 23.9 (ethyl C-2); HRMS (ESI-TOF) m/z [M+Na] Calcd for $C_{19}H_{18}{}^{79}BrNNa$ 362.0515; Found 362.0503.

4-Bromobenzyl-(1-naphth-1-ylethyl)-amine 183

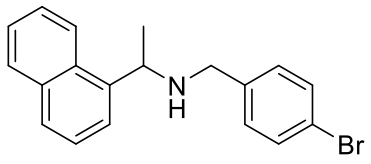

183

According to general procedure G, using 1-(1'-napthyl)ethylamine and 4-bromobenzylalcohol. An aliquot was taken for analysis at steady state, conversion was determined from the crude mixture by ^1H NMR before the crude material was

purified by column chromatography eluting with 75:25 hexane-EtOAc to yield **183** (44.2 mg, 65%) as a yellow oil, R_f 0.28 (75:25 hexane-EtOAc). Spectroscopically identical to the racemate previously prepared.

4-Methylbenzyl-(1-naphthylethyl)-amine 184

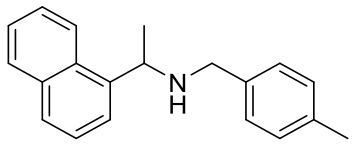

184

According to general procedure G, using 1-(1'-napthyl)ethylamine (161 µL, 1.00 mmol), 4methylbenzylalcohol (122 mg, 1.00 mmol), and the title compound was obtained by flash chromatography eluting with 05:95 MeOH-DCM to yield **184** (199.2 mg, 72 %) as a dark yellow oil, R_f 0.59 (05:95 MeOH-DCM); ν_{max}/cm^{-1} 2971, 1644, 1511, 1447, 1373, 907, 777; ^1H NMR ($CDCl_3$, 500 MHz) δ 8.18-8.14 (1H, m, naphthyl 8-H), 7.91-7.87 (1H, m, naphthyl 5-H), 7.77 (2H, d, *J* = 8.4 Hz, naphthyl 2-H and 4-H), 7.54-7.46 (3H, m, naphthyl 3-H, 5-H and 7-H), 7.20 (2H, d, *J* = 8.0 Hz, aryl 2-H and 6-H), 7.13 (2H, d, *J* = 7.8 Hz, aryl 3-H and 5-H), 4.69 (1H, q, *J* = 6.6 Hz, ethyl 1-H), 3.74 (1H, d, *J* = 13.0 Hz, benzyl C*H*$_a$H$_b$), 3.66 (1H, d, *J* = 13.0 Hz, benzyl CH$_a$C*H*$_b$), 2.35 (3H, s, 4-aryl C*H*$_3$), 1.49 (1H, br s, N*H*), 1.52 (3H, d, *J* = 6.6 Hz, ethyl 2-H$_3$); $^{13}C\{^1H\}$ ($CDCl_3$, 125 MHz) δ 141.2 (naphthyl C-1), 137.7 (aryl C-1), 136.6 (napthyl), 134.1 (naphthyl C-4a), 131.5 (naphthyl C-8a), 129.4 (aryl C-4), 129.2 (aryl C-3 and C-5), 129.1 (aryl C-2 and C-6), 128.3, 127.4, 125.9, 125.4 (naphthyl C-2, C-3, C-4, C-5 and C-7), 123.2 (naphthyl C-2 or C-4 or C-8), 123.1 (naphthyl C-2 or C-4 or C-8), 53.1 (ethyl C-1), 51.7 (benzyl *C*H$_2$), 23.8 (4-aryl *C*H$_3$), 21.3 (ethyl C-2; HRMS (ESI-TOF) m/z $[M+Na]^+$ Calcd for $C_{20}H_{21}NNa$ 298.1566; Found 298.1555.

***N*-(4-Methoxybenzyl)-1-(1-naphthyl)ethylamine 185**

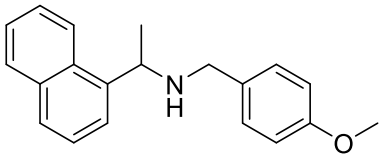

185

According to general procedure G, using 1-(1'-napthyl)ethylamine (161 µL, 1.00 mmol), 4-methoxybenzylalcohol (124 µL, 1.00 mmol), and the title compound was obtained by flash chromatography eluting with 50:49.8:0.2 EtOAc-DCM-methanolic ammonia (7N) to yield **185** (182 mg, 63 %) as a yellow oil; v_{max}/cm^{-1} 2833, 1610, 1509, 1242, 1172, 1032, 776; ^{1}H NMR ($CDCl_3$, 500 MHz) δ 8.21-8.15 (1H, m, naphthyl 8-H), 7.92-7.88 (1H, m, naphthyl 5-H), 7.80-7.78 (1H, m, naphthyl 4-H), 7.78-7.76 (1H, m, naphthyl 2-H), 7.55-7.47 (3H, m, naphthyl 3-H, 6-H and 7-H), 7.26-7.22 (2H, m, aryl 2-H and 6-H), 6.90-6.86 (2H, m, aryl 3-H and 5-H), 4.70 (1H, q, *J* = 6.6 Hz, ethyl 1-H), 3.82 (3H, s, methoxy C*H*$_3$), 3.73 (1H, d, *J* = 12.9 Hz, benzyl C*H*$_a$H$_b$), 3.66 (1H, d, *J* = 12.8 Hz, benzyl CH$_a$*H*$_b$), 1.71 (1H, br s, N*H*), 1.53 (3H, d, *J* = 6.6 Hz, ethyl 2-H$_3$); $^{13}C\{^{1}H\}$ ($CDCl_3$, 125 MHz) δ 158.7 (aryl C-4), 141.2 (naphthyl C-1), 134.1 (naphthyl C-4a), 133.0 (aryl C-1), 131.5 (naphthyl C-8a), 129.5 (aryl C-2 and C-6), 128.8 (naphthyl C-5), 127.3 (naphthyl C-4), 125.88 (naphthyl C-3, C-6 or C-7), 125.82 (naphthyl C-3, C-6 or C-7), 125.4 (naphthyl C-3, C-6 or C-7), 123.2 (naphthyl C-2), 123.0 (naphthyl C-8), 113.9 (aryl C-3 and C-5), 55.4 (ethyl C-1), 53.0 (methoxy *C*H$_3$), 51.4 (benzyl *C*H$_2$), 23.8 (ethyl C-2); HRMS (ESI-TOF) m/z $[M+Na]^+$ Calcd for $C_{20}H_{21}NNaO$ 314.1515; Found 314.1514.

***tert*-Butyl 3-(1-Naphthalen-1-ylethylamino)azetidine-1-carboxylate 196**

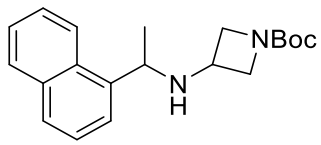

196

According to general procedure G, using 1-(1'-napthyl)ethylamine (161 µL, 1.00 mmol) and 1-Boc-3-hydroxyazetidine (173 mg, 1.00 mmol). The solvent was evaporated under reduced pressure to give a crude product which contained an undeterminable mixture of diastereomeric products. The crude product was purified by flash chromatography eluting with 90:10 DCM-EtOAc to yield **196** (181 mg, 55 %) as a pale-yellow viscous oil, R_f 0.62 (50:50 DCM-EtOAc); v_{max}/cm^{-1} 2972, 1687, 1391, 1365, 1119, 777, 730; ^{1}H NMR ($CDCl_3$, 500 MHz) δ 8.16 (1H, d, *J* = 8.3 Hz, naphthyl 8-H), 7.89-7.85 (1H, m, naphthyl 5-H), 7.76 (1H, d, *J* = 8.2 Hz, naphthyl 4-H), 7.63 (1H,

d, *J* = 6.7 Hz, naphthyl 2-H), 7.54-7.45 (3H, m, naphthyl 3-H, 6-H and 7-H), 4.63 (1H, q, *J* = 6.6 Hz, ethyl 1-H), 4.01 (1H, dd, *J* = 8.7, 6.9 Hz, 2-H_a), 3.97-3.93 (1H, m, 4-H_a), 3.70 (1H, dd, *J* = 8.8, 5.1 Hz, 2-H_b), 3.62-3.56 (1H, m, 4-H_b), 3.54 (1H, ddd, *J* = 10.5, 6.2, 3.5 Hz, 3-H), 1.74 (br s, 1H), 1.51 (3H, d, *J* = 6.6 Hz, ethyl 2-H_3), 1.41 (9H, s, ^{t}Bu); $^{13}C\{^1H\}$ ($CDCl_3$, 125 MHz) δ 156.4 (C=O), 140.4 (naphthyl C-1), 134.1 (naphthyl C-4a), 131.2 (naphthyl C-8a), 129.2 (naphthyl C-5), 127.7 (naphthyl C-4), 126.1 (naphthyl C-3, C-6 or C-7), 125.8 (naphthyl C-3, C-6 or C-7), 125.6 (naphthyl C-3, C-6 or C-7), 123.3 (naphthyl C-2), 122.8 (naphthyl C-8), 79.5 (^{t}Bu *C*), 57.7 (br s, C-2 and C-4), 51.6 (ethyl C-1), 46.3 (C-3), 28.5 (^{t}Bu *C*H_3), 23.6 (ethyl C-2); HRMS (ESI-TOF) m/z $[M+H]^+$ Calcd for $C_{20}H_{27}N_2O_2$ 327.2067; Found 327.2063.

tert-Butyl-3-((1-(Naphthalen-1-yl)ethyl)amino)pyrrolidine-1-carboxylate 197

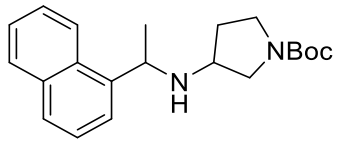

197

According to general procedure G, using 1-(1'-napthyl)ethylamine (161 µL, 1.00 mmol) and 1-Boc-3-pyrrolidinol (187 µL, 1.00 mmol). The solvent was evaporated under reduced pressure to give a crude product which contained a 50:50 mixture of diastereomeric products. The crude product was purified by flash chromatography eluting with 50:50 DCM-EtOAc to yield **197** (281 mg, 83 %) as a 40:60 mixture of diastereomers as a viscous yellow oil, R_f 0.31 (50:50 DCM-EtOAc); ν_{max}/cm^{-1} 2973, 1677, 1402, 1364, 1164, 1117, 777; ^1H NMR ($CDCl_3$, 500 MHz) δ 8.25-8.16 (1H, m, naphthyl 8-H), 7.88 (1H, br d, *J* = 7.5 Hz, naphthyl 5-H), 7.76 (1H, d, *J* = 8.1 Hz, naphthyl 4-H), 7.71-7.62 (1H, m, naphthyl 2-H), 7.56-7.44 (3H, m, naphthyl 3-H, 6-H and 7-H), 4.73 (0.4H, q, *J* = 6.6 Hz, ethyl 1-H), 4.68 (0.6H, q, *J* = 6.4 Hz, ethyl 1-H), 3.60-3.35 (2H, m, pyrrolidine 2-H_a and 5-H_a), 3.32-3.15 (2H, m, pyrrolidine 3-H and 2-H_b), 3.14-2.97 (1H, m, pyrrolidine 5-H_b), 2.04-1.90 (1H, m, pyrrolidine 4-H_a), 1.77-1.60 (1H, m, pyrrolidine 4-H_b), 1.55-1.47 (4H, m, ethyl 2-H_3 and N*H*), 1.47-1.40 (9H, s, ^{t}Bu); $^{13}C\{^1H\}$ ($CDCl_3$, 125 MHz) δ 154.8 (C=O), 141.1 (naphthyl C-1), 141.0 (naphthyl C-1), 134.1 (naphthyl C-4a), 131.3 (naphthyl C-8a), 129.2 (naphthyl C-5), 129.1 (naphthyl C-5),

127.5 (naphthyl C-4), 126.0, 125.83, 125.76, 125.6, 125.5 (naphthyl C-3, C-6 and C-7), 123.1 (naphthyl C-2), 122.9 (naphthyl C-8), 79.3 (^{t}Bu *C*), 79.2 (^{t}Bu *C*), 55.8 (pyrrolidine C-3), 55.7 (pyrrolidine C-3), 55.0 (pyrrolidine C-3), 54.8 (pyrrolidine C-3), 52.3 (ethyl C-1), 51.8 (pyrrolidine C-5), 44.6 (pyrrolidine C-2), 44.2 (pyrrolidine C-2), 32.8, 32.4, 32.1, 31.6, 28.66 (^{t}Bu *C*H$_3$), 28.63 (^{t}Bu *C*H$_3$), 24.5 (ethyl C-2), 24.4 (ethyl C-2), 24.3 (ethyl C-2), 24.0 (ethyl C-2) (36 environments observed); HRMS (ESI-TOF) m/z [M+Na]$^+$ Calcd for $C_{21}H_{28}N_2NaO_2$ 363.2043; Found 363.2038.

***tert*-Butyl 3-(1-Naphthalen-1-ylethylamino)piperidine-1-carboxylate 198**

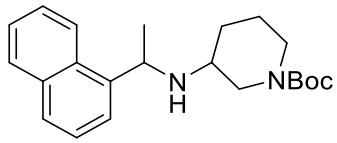

198

According to general procedure G, using 1-(1'-napthyl)ethylamine (161 µL, 1 mmol) and N-boc-3-hydroxypiperidine (201 mg, 1 mmol). The solvent was evaporated under reduced pressure to give a crude product which contained an undermined mixture of diastereomeric products. The crude product was purified by flash chromatography eluting with 96:4 DCM-EtOAc to yield **198** (149 mg, 42 %) as an undetermined mixture of diastereomers as a yellow viscous oil, R_f 0.44 (50:50 DCM-EtOAc); ν_{max}/cm^{-1} 2972, 2930, 1684, 1420, 1364, 1238, 1149, 761, 700; ^{1}H NMR ($CDCl_3$, 500 MHz) δ 8.27-8.14 (1H, m, naphthyl 8-H), 7.87 (1H, d, *J* = 7.9 Hz, naphthyl 5-H), 7.75 (1H, d, *J* = 8.1 Hz, naphthyl 4-H), 7.73-7.65 (1H, br m, naphthyl 2-H), 7.55-7.43 (3H, m, naphthyl 3-H, 6-H and 7-H), 4.92-4.77 (1H, br m, ethyl 1-H), 3.94-3.66 (1.5H, m, piperidine 2-H$_{a1}$, 2-H$_{a2}$, 6-H$_a$), 3.60-3.46 (0.5H, m, piperidine 6-H$_a$), 3.15-3.00 (1H, m, piperidine 2-H$_b$ and 6-H$_b$), 2.87-2.77 (0.5H, m, piperidine 6-H$_b$), 2.77-2.66 (0.5H, m, piperidine 2-H$_b$), 2.65-2.46 (1H, m, piperidine 3-H), 2.01-1.90 (0.5H, m, piperidine 4-H$_a$), 1.89-1.75 (0.5H, m, piperidine 4-H$_a$) 1.71-1.62 (1H, m, piperidine 5-H$_a$), 1.55-1.46 (3H, m, ethyl 2-H$_3$), 1.44-1.31 (9H, m, ^{t}Bu), 1.60-1.30 (2H, m, piperidine 4-H$_b$ and 5-H$_b$); ^{13}C{^{1}H} ($CDCl_3$, 125 MHz) δ 155.0 (C=O), 134.1 (naphthyl C-4a), 131.4 (naphthyl C-8a), 131.2 (naphthyl C-8a), 129.2 (naphthyl C-5), 127.4 (naphthyl C-4), 126.1, 125.8, 125.5 (naphthyl C-3, C-

6 and C-7), 123.1 (naphthyl C-2), 122.9 (naphthyl C-8), 79.6 (^{t}Bu *C*), 51.0 (ethyl C-1 and piperidine C-3), 43.9 (piperidine C-2 and C-6), 28.5 (^{t}Bu *C*H_3), 24.6 (ethyl C-2), 23.8, 23.4 (piperidine C-4 and C-5); HRMS (ESI-TOF) m/z $[M+H]^+$ Calcd for $C_{22}H_{31}N_2O_2$ 355.2380; Found 355.2388.

***N*-(1-Phenylethyl)-3-(3-(trifluoromethyl)phenyl)propan-1-amine 186**

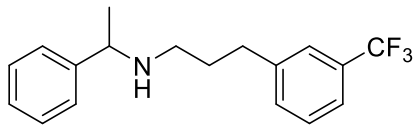

186

According to general procedure G, using methylbenzylamine (127 µL, 1 mmol), 3-(3-(trifluoromethyl)phenyl)propan-1-ol (186 µL, 1 mmol), and the title compound was obtained by flash chromatography eluting with 50:50 DCM-EtOAc to yield **186** (95.6 mg, 31%) as a yellow oil, R_f 0.23 (50:50 DCM-EtOAc); ν_{max}/cm^{-1} 2928, 1450, 1326, 1161, 1118, 1072, 791, 699; ^{1}H NMR ($CDCl_3$, 400 MHz) δ 7.45-7.40 (2H, m, aryl 2-H and 4-H), 7.39-7.35 (1H, m, aryl 5-H), 7.35-7.28 (5H, m, phenyl 2-H, 3-H, 5-H, 6-H and aryl 6-H), 7.27-7.22 (1H, m, phenyl 4-H), 3.75 (1H, q, *J* = 6.6 Hz, ethyl 1-H), 2.71 (1H, ddd, *J* = 14.0, 8.8, 7.1 Hz, propyl 3-H_a), 2.64 (1H, ddd, *J* = 14.0, 8.4, 7.1 Hz, propyl 3-H_b), 2.56 (1H, ddd, *J* = 11.5, 7.5, 6.4 Hz, propyl 1-H_a), 2.47 (1H, app. dt, *J* = 11.5, 7.2 Hz, propyl 1-H_b), 1.87-1.71 (2H, m, propyl 2-H_2), 1.36 (3H, d, *J* = 6.6 Hz, ethyl 2-H_3); $^{13}C\{^1H\}$ ($CDCl_3$, 125 MHz) δ 145.9 (phenyl C-1), 143.3 (aryl C-1), 131.9 (aryl C-6), 130.7 (q, *J* = 31.8 Hz, aryl C-3), 128.8 (phenyl C-3, C-4 or C-5), 128.6 (phenyl C-3, C-4 or C-5), 127.0 (phenyl C-3, C-4 or C-5), 126.7 (aryl C-5), 125.8 (phenyl C-2 and C-6), 125.2 (q, *J* = 3.8 Hz, aryl C-2), 124.4 (q, *J* = 272.3 Hz, *C*F_3), 122.8 (q, *J* = 3.8 Hz, aryl C-4), 58.5 (ethyl C-1), 47.2 (propyl C-1), 33.5 (propyl C-3), 31.9 (propyl C-2), 24.5 (ethyl C-2); $^{19}F\{^1H\}$ NMR ($CDCl_3$, 376 MHz) δ -62.6; HRMS (ESI-TOF) m/z: $[M+H]^+$ Calcd for $C_{18}H_{21}F_3N$ 308.1621; Found 308.1617.

***N*-(1-(Naphthalen-1-yl)ethyl)-3-(3-(trifluoromethyl)phenyl)propan-1-amine 10**

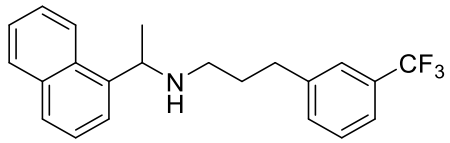

10

According to general procedure G, using 1-(1'-napthyl)ethylamine (161 µL, 1 mmol), 3-(3-(trifluoromethyl)phenyl)propan-1-ol (186 µL, 1 mmol), and the title compound was obtained by flash chromatography eluting with 50:30:20 DCM-EtOAc -hexane to yield **10** (113 mg, 32%) as a yellow oil; ν_{max}/cm^{-1} 3063, 2970, 2929, 2861, 1329, 1161, 1121, 779; ^{1}H NMR ($CDCl_3$, 500 MHz) δ 8.19 (1H, d, *J* = 8.4 Hz, naphthyl 8-H), 7.90 – 7.86 (1H, m, naphthyl 5-H), 7.75 (1H, d, *J* = 8.2 Hz, naphthyl 4-H), 7.64 (1H, d, *J* = 7.0 Hz, naphthyl 2-H), 7.54 – 7.46 (3H, m, naphthyl 3-H, 6-H and 7-H), 7.42 (2H, d, *J* = 8.3 Hz, aryl 2-H and 4-H), 7.36 (1H, app. t, *J* = 5.6 Hz, aryl 5-H), 7.32 (1H, d, *J* = 7.7 Hz, aryl 6-H), 4.62 (1H, q, *J* = 6.6 Hz, ethyl 1-H), 2.78 – 2.55 (4H, m, propyl 1-H_2 and 3-H_2), 1.84 (2H, dddd, *J* = 7.7, 7.5, 7.3, 7.1 Hz, propyl 2-H_2), 1.50 (3H, d, *J* = 6.6 Hz, ethyl 2-H_3); $^{13}C\{^{1}H\}$ NMR ($CDCl_3$, 125 MHz) δ 143.2 (aryl C-1), 141.4 (naphthyl C-1), 134.1 (naphthyl C-4a), 131.91 (aryl C-6 or naphthyl C-2), 131.90 (aryl C-6 or naphthyl C-2), 131.4 (naphthyl C-8a), 131.1 (q, *J* = 31.9 Hz, aryl C-3), 129.1 (naphthyl C-5), 128.8 (aryl C-5), 127.3 (naphthyl C-4), 125.9 (naphthyl C-3 or C-6 or C-7), 125.8 (naphthyl C-3 or C-6 or C-7), 125.5 (naphthyl C-3 or C-6 or C-7), 125.1 (q, *J* = 3.8 Hz, aryl C-2), 124.4 (q, *J* = 272.3 Hz, *C*F_3) 123.1 (naphthyl C-8) 122.9 (q, *J* = 4.3 Hz, aryl C-4), 53.9 (ethyl C-1), 47.4 (propyl C-1), 33.6 (propyl C-3), 32.0 (propyl C-2), 23.8 (ethyl C-2); $^{19}F\{^{1}H\}$ NMR (376 MHz, $CDCl_3$) δ -62.5 (*C*F_3); HRMS (ESI-TOF) m/z: $[M+H]^+$ Calcd for $C_{22}H_{23}F_3N$ 358.1777; Found 358.1783.

6.6.3 Photoredox Hydroamination

2,4,6-Triisopropylbenzenethiol 275[289]

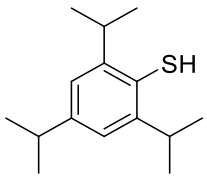

275

A solution of 2,4,6-triisopropylbenzene-1-sulfonyl chloride (6.06 g, 20.0 mmol) in THF (25 mL) was added dropwise to a solution of $LiAlH_4$ (16.7 mL of a 2.4 M solution in THF, 40.0 mmol) at 0 °C. An extra portion of $LiAlH_4$ (16.7 mL of a 2.4 M solution in THF, 40.0 mmol) was then added dropwise. The reaction mixture was then allowed to warm to room temperature and stirred for 16 h. The reaction mixture was cooled to 0 °C and diluted with THF (40 mL). Then, water (3 mL), 10% w/w NaOH solution (5 mL), and water (10 mL) were added dropwise and the mixture allowed to stir at 0 °C for 10 min. $MgSO_4$ was then added and the mixture was allowed to stir at room temperature for 30 min. The white solids were then removed *via* vacuum filtration with THF and Et_2O rinsing. The solvent was then evaporated under reduced pressure to give a yellow semi-solid which was purified by vacuum distillation to yield **275** (1.96 g, 41%) as a pale yellow oil, ν_{max}/cm^{-1} 2958, 2928, 2868, 1429, 1382, 1316, 1102, 1061, 875 and 743; ^1H NMR ($CDCl_3$, 500 MHz) δ 7.00 (2H, s, aryl 3-H and 5-H), 3.50 (2H, hept, *J* = 6.9 Hz, 2,6-isopropyl 2-H_2), 3.07 (1H, s, S*H*), 2.86 (1H, hept, *J* = 6.9 Hz, 4-isopropyl 2-H), 1.26 (12H, d, *J* = 6.9 Hz, 2,6-isopropyl 1-H_3 and 3-H_3), 1.24 (6H, d, *J* = 6.9 Hz, 4-isopropyl 1-H_3 and 3-H_3); $^{13}C\{^1H\}$ ($CDCl_3$, 125 MHz) δ 148.2 (aryl C-2 and C-6), 147.2 (aryl C-4), 124.4 (aryl (C-1), 121.4 (aryl C-3 and C-5), 34.3 (4-isopropyl C-2), 31.9 (2,6-isopropyl C-2), 24.2 (4-isopropyl C-1 and C-3), 23.4 (2,6-isopropyl C-1 and C-3). Spectroscopic data are consistent with those reported in the literature.[289]

3-[(3-Trifluoromethyl)phenyl]-1-propene 216[295]

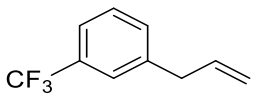

216

In an oven dried flask 3-bromobenzotrifluoride (3.0 g, 13.2 mmol), cesium fluoride (4.0 g, 26.0 mmol), palladium acetate (0.30 g, 1.32 mmol) and triphenylphosphine (1.0 g, 4 mmol) were charged and the flask purged under nitrogen. Dry THF (75 mL) was added *via* a syringe and the mixture was stirred at room temperature for 15 min. Allylboronic acid pinacol ester (4.0 g, 24.0 mmol) in dry THF (30 mL) was then added and the mixture was refluxed for 22 h. After the mixture was allowed to cool to room temperature it was partitioned between H_2O and pentane. The aqueous layer was

washed with pentane (x2) and the combined organic layers were washed with brine, dried over $MgSO_4$, filtered and concentrated under reduced pressure. The crude material was purified via column chromatography eluting with pentane to obtain **216** (1.9 g, 77%) as a colourless oil, R_f 0.76 (pentane); ^{1}H NMR ($CDCl_3$, 500 MHz) δ 7.47 (1H, d, *J* = 7.5 Hz, aryl 4-H), 7.45 (1H, s, aryl 2-H), 7.41 (1H, t, *J* = 7.5 Hz, aryl 5-H), 7.38 (1H, d, *J* = 7.6 Hz, aryl 6-H), 5.96 (1H, ddt, *J* = 16.9, 10.2, 6.7 Hz, 2-H), 5.15-5.08 (2H, m, 3-H_2), 3.45 (2H, d, *J* = 6.7 Hz, 1-H_2); ^{13}C{^{1}H} ($CDCl_3$, 125 MHz) δ 141.1 (aryl C-1), 136.5 (C-2), 132.2 (aryl C-6), 130.9 (q *J* = 32.0 Hz, aryl C-3), 129.0 (aryl C-5), 125.5 (q, *J* = 3.8 Hz, aryl C-2), 123.3 (q, *J* = 272.2 Hz, *C*F_3), 123.1 (q, *J* = 3.9 Hz, aryl C-4), 116.9 (C-1), 40.0 (C-3); ^{19}F{1H} ($CDCl_3$, 376 MHz) δ -62.6 (C*F*$_3$).

1-Boc-3-Tosyloxyazetidine 276[302]

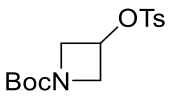

276

1-Boc-3-hydroxyazetidine (3.4 g, 19.6 mmol) was dissolved in pyridine (30 mL) and cooled to 0 °C. *p*-Toluenesulfonylchloride (7.5g, 39.2 mmol) was then added, the flask sealed and stored at -18 ºC for 24h. The solution was then diluted with water and extracted with Et_2O (x3). The combined organics were washed with 1N HCl (x3) then brine and dried over $MgSO_4$. The solvent was removed by rotatory evaporation to yield **x** (6.3 g, 98%) as a yellow oil, ν_{max}/cm^{-1} 2984, 2887, 1693, 1403, 1362, 1178, 1018, 878; ^{1}H NMR ($CDCl_3$, 500 MHz) δ 7.78-7.75 (2H, m, tosyl 2-H and 6-H), 7.37-7.33 (2H, m, tosyl 3-H and 5-H), 4.99 (1H, tt, *J* = 6.8, 4.3 Hz, 3-H), 4.13-4.03 (2H, m, 2-H_a and 4-H_a), 3.96-3.86 (2H, m, 2-H_b and 4-H_b), 2.44 (3H, s, tosyl C*H*$_3$), 1.39 (9H, s, ^{t}Bu); ^{13}C{^{1}H} ($CDCl_3$, 125 MHz) δ 155.9 (C=O), 145.7 (tosyl C-4), 133.0 (tosyl C-1), 130.2 (tosyl C-3 and C-5), 128.0 (tosyl C-2 and C-6), 80.3 (^{t}Bu-*C*), 67.9 (C-3), 56.4 (C-2 and C-4), 28.4 (^{t}Bu-*C*H$_3$), 21.8 (tosyl *C*H$_3$); HRMS (ESI-TOF) m/z: [M+H]+ Calcd for $C_{15}H_{22}NO_5S$ 328.1213; Found 328.1203.

***N*-Boc Azetine 242**[302]

 **242**

1-Boc-3-tosyloxyazetidine (2.0 g, 6.1 mmol), potassium tertbutoxide (1.0 g, 9.2 mmol) were dissolved in tert-butylalcohol (30 mL) and the mixture refluxed for 16h. Water was then added to the mixture which was extracted with hexane (3x). The combined organics were then washed with brine, dried over $MgSO_4$ and reduced in vacuo. The crude material was then purified by column chromatography eluting with 25:75 Et_2O-hexane to yield **242** (330 mg, 35 %) as a colourless oil, R_f 0.66 (50:50 Et_2O-hexane); ν_{max}/cm^{-1} 3100, 2975, 1701, 1391, 1151, 1051, 955, 763, 670; ^1H NMR ($CDCl_3$, 500 MHz) δ 6.57 (1H, s, 1-H), 5.52 (1H, dt, *J* = 1.6, 0.8 Hz, 2-H), 4.38 (2H, t, *J* = 0.8 Hz, 3-H_2), 1.47 (9H, s, ^{t}Bu); $^{13}C\{^1H\}$ ($CDCl_3$, 125 MHz) δ 152.0 (C=O), 138.8 (C-1), 111.9 (C-2), 80.3 (^{t}Bu-*C*), 58.4 (C-3), 28.4 (^{t}Bu-*C*H_3); HRMS (ESI-TOF) m/z: [M+Na]+ Calcd for $C_8H_{13}NaNO_2$ 178.0839; Found 178.0842.

_N_-Boc Piperidine 277[335]

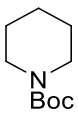 **277**

Piperidine (3.0 mL, 30 mmol) was dissolved in DCM (100 mL) and cooled to 0 °C. Boc_2O (6.4 mL, 28 mmol) was then added dropwise and the mixture allowed to warm to RT and stirred for 16 h. The solvent was then removed under reduced pressure to yield **277** (4.83 g, 93%) as a colourless oil; ν_{max}/cm^{-1} 2934, 2855, 1687, 1417, 1237, 1143, 1025; ^1H NMR ($CDCl_3$, 500 MHz) δ 3.37-3.31 (4H, m, 2-H_2 and 6-H_2), 1.60-1.52 (2H, m, 4-H_2), 1.52-1.46 (4H, m, 3-H_2 and 5-H_2), 1.44 (s, 9H); $^{13}C\{^1H\}$ ($CDCl_3$, 125 MHz) δ 155.1 (C=O), 79.2 (^{t}Bu-*C*), 44.5 (C-2 and C-6), 28.6 (^{t}Bu *C*H_3), 25.9 (C-3 and C-5), 24.6 (4-C); HRMS (ESI-TOF) m/z $[M+Na]^+$ Calcd for $C_{10}H_{19}NaNO_2$ 208.1308; Found 208.1303. Spectroscopic data are consistent with those reported in the literature.[336]

***tert*-Butyl 3,4-dihydropyridine-1(2H)-carboxylate 240[337]**

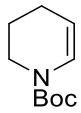

240

An Electrasyn vial (20 mL) with a stir bar was charged with N-Boc piperidine (2.5 g, 13.6 mmol) in anhydrous methanol (17 mL) containing tetraethylammonium tosylate (250 mg, 0.84 mmol) and was electrolysed with graphite electrodes at a constant current of 65 mA at 25 °C. After the passage of 2.5 $Fmol^{-1}$ of electricity, the mixture was concentrated *in vacuo*. The residue was and NH_4Cl (116 mg, 20 mol%) was dissolved in toluene and the mixture stirred at reflux for 4 h. The solvent was removed under reduced pressure and the crude material was then purified by column chromatography eluting with 95:5 hexane-Et_2O to yield **240** as a 40:60 mixture of rotamers (1.53 g, 61%) as a colourless oil, R_f 0.44 (80:20 hexane−Et_2O); ν_{max}/cm^{-1} 2975, 2936, 1686 (C=O), 1363, 1251, 1152, 990, 918, 876 and 729; ^{1}H NMR ($CDCl_3$, 500 MHz) δ 6.84 (0.4H, d, *J* = 7.8 Hz, 2-H), 6.71 (0.6H, d, *J* = 8.3 Hz, 2-H), 4.88 (0.4H, m, 3-H), 4.78 (0.6H, m, 3-H), 3.59–3.47 (2H, m, 6-H_2), 2.05–1.98 (2H, m, 4-H_2), 1.85–1.74 (2H, m, 5-H_2), 1.47 (9H, s, ^{t}Bu); $^{13}C\{^1H\}$ ($CDCl_3$, 125 MHz) δ 152.9 (C=O), 152.5 (C=O), 125.8 (C-2), 125.4 (C-2), 105.8 (C-3), 105.3 (C-3), 80.6 (Boc *C*Me_3), 80.5 (^{t}Bu-*C*), 42.7 (C-6), 41.6 (C-6), 28.5 (^{t}Bu *C*H_3), 21.9, 21.6, 21.5 (C-4 and C-5) (14 out of 16 signals present); HRMS (ESI-TOF) m/z: $[2M+Na]^+$ Calcd for $C_{20}H_{34}N_2NaO_4$ 389.2411; Found 389.2396. Spectroscopic data are consistent with those reported in the literature.[338]

1-Benzylpiperidine-2,6-dione 278[339]

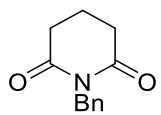

278

Piperidine-2,6-dione (2.26 g, 20 mmol) and potassium carbonate (3.32 g, 24 mmol, 1.2 equiv) were dissolved in anhydrous acetone (40 mL). Benzyl bromide (2.6 mL, 22 mmol, 1.1 equiv) was added and the mixture refluxed for 3 h. The mixture was allowed to cool to room temperature, filtered and the solvent removed under

reduced pressure. The crude material was then purified by column chromatography eluting with 20:80 EtOAc-hexane to yield **278** (2.52 g, 62%) as a colourless oil, Rf 0.14 (20:80 EtOAc-hexane); ν_{max}/cm^{-1} 3305, 3029, 2957, 1690, 1636, 1544, 1453, 1256; ^{1}H NMR ($CDCl_3$, 500 MHz) δ 7.36 (2H, d, *J* = 7.0 Hz, phenyl 2-H and 6-H), 7.28 (2H, t, *J* = 7.3 Hz, phenyl 3-H and 5-H), 7.24 (1H, t, *J* = 7.2 Hz, phenyl 4-H), 4.95 (2H, s, benzyl C*H*$_2$), 2.67 (4H, app. t, *J* = 6.6 Hz, 3-H_2 and 5-H_2), 2.05 (2H, app. p, *J* = 6.6 Hz, 4-H_2); $^{13}C\{^{1}H\}$ ($CDCl_3$, 125 MHz) δ 172.6 (C-2 and C-6), 137.4 (benzyl C-1), 129.0 (benzyl C-2 and C-6), 128.5 (benzyl C-3 and C-5), 127.6 (benzyl C-4), 42.8 (benzyl *C*H_2), 33.1 (C-3 and C-5), 17.2 (C-4); HRMS (ESI-TOF) m/z: $[M+Na]^+$ Calcd for $C_{12}H_{13}NNaO_2$ 226.0838; Found 226.0830. Spectroscopic data are consistent with those reported in the literature.[339]

1-Benzyl-3,4-dihydropyridin-2(1H)-one 279[149]

279

1-Benzylpiperidine-2,6-dione (1.33 g, 6.55 mmol) was dissolved in anhydrous toluene (10 mL) and cooled to – 78 °C. A solution of Superhydride (1M in THF, 7.2 mL, 7.2 mmol) was added dropwise. This mixture was allowed to stir at – 78 °C for 45 minutes followed by the sequential addition of DIPEA (6.5 mL, 37.0 mmol), trifluoroacetic anhydride (1.0 mL, 2.9 mmol) and DMAP (10 mg). The mixture was allowed to warm to room temperature and stirred for 16 h. The reaction was diluted with water and ethyl acetate, the layers separated and the aqueous extracted further with ethyl acetate (3x). The combined organics were dried over $MgSO_4$ and the solvent removed under reduced pressure. The crude material was purified by column chromatography eluting with 15:85 ethyl acetate-hexane to yield **279** (269 mg, 22%) as a yellow oil, Rf 0.27 (20:80 EtOAc-hexane); ν_{max}/cm^{-1} 3294, 3025, 2956, 1703, 1644, 1540, 1466, 1360; ^{1}H NMR ($CDCl_3$, 500 MHz) δ 7.33 (2H, t, *J* = 7.3 Hz, benzyl C-2 and C-6), 7.26-7.22 (3H, m, benzyl C-3, C-4 and C-5), 6.02 (1H, dt, *J* = 7.7, 1.5 Hz, 6-H), 5.17-5.11 (1H, m, 5-H), 4.69 (2H, s, benzyl C*H*$_2$), 2.59 (2H, t, *J* = 8.1 Hz, 3-H_2), 2.38-2.31 (2H, m, 4-H_2);

$^{13}C\{^{1}H\}$ ($CDCl_3$, 125 MHz) δ 169.5 (C-2), 137.4 (benzyl C-1), 129.6 (C-6), 128.8 (benzyl C-2 and C-6), 127.8 (benzyl C-3, C-4 and C-5), 127.6 (C-6), 106.6 (C-5), 49.0 (benzyl *C*H_2), 31.5 (C-3), 20.5 (C-4); HRMS (ESI-TOF) m/z: $[M+H]^+$ Calcd for $C_{12}H_{14}NO$ 188.1070; Found 188.1067. Spectroscopic data are consistent with those reported in the literature.[149]

1-(1-naphthyl)ethanol 280 [340]

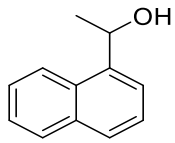

280

1-Acetonaphthone (1.7 g, 10 mmol) was dissolved in ethanol (10 mL) and cooled to 0 °C. Sodium borohydride (756 mg, 20 mmol) was added portion-wise. The mixture was allowed to warm to room temperature and stirred for 3 h. The reaction was then cooled to 0 °C and quenched with 1N HCl. The resultant mixture was extracted (3x) with Et_2O, the combined organics were dried over $MgSO_4$ and the solvent removed under reduced pressure to yield **280** (1.63 g, 95%) as a colourless oil; ν_{max}/cm^{-1} 3247, 2972, 1595, 1108, 1068, 776; ^{1}H NMR ($CDCl_3$, 500 MHz) δ 8.13 (1H, d, *J* = 8.4 Hz, naphthyl 8-H), 7.91-7.85 (1H, m, naphthyl 5-H), 7.79 (1H, d, *J* = 8.2 Hz, naphthyl 4-H), 7.68 (1H, d, *J* = 7.1 Hz, naphthyl 2-H), 7.56-7.46 (3H, m, naphthyl 3-H, 6-H and 7-H), 5.68 (1H, q, *J* = 6.5 Hz, ethyl 1-H), 1.88 (1H, br s, O*H*), 1.68 (3H, d, *J* = 6.5 Hz, ethyl 2-H_3); $^{13}C\{^{1}H\}$ ($CDCl_3$, 125 MHz) δ 141.5 (naphthyl C-1), 133.9 (naphthyl C-4a), 130.4 (naphthyl C-8a), 129.0 (naphthyl C-5), 128.1 (naphthyl C-4), 126.2 (naphthyl C-7), 125.69 (naphthyl C-3 or C-6), 125.67 (naphthyl C-3 or C-6), 123.3 (naphthyl C-8), 122.1 (naphthyl C-2), 67.3 (ethyl C-1), 24.5 (ethyl C-2); HRMS (ESI-TOF) m/z: [M+Na]+ Calcd for $C_{12}H_{12}ONa$ 195.0780; Found 195.0776. Spectroscopic data are consistent with those reported in the literature.[340]

***N*-(Cyclopentylmethyl)cyclohexanamine 220**

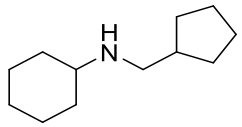

220

The reaction was set up following general procedure I using cyclohexylamine (25 mg, 0.25 mmol) and methylenecyclopentane (62 mg, 0.75 mmol, 3.0 equiv). The reaction was purified by the general workup procedure to give the title compound in an isolated yield of (36.6 mg, 81%); ν_{max}/cm^{-1} 2927, 2853, 1449, 1368, 1129, 890, 844, 730; ^{1}H NMR ($CDCl_3$, 500 MHz) 2.55 (2H, d, *J* =7.2 Hz, methylene 1-H_2), 2.39 (1H, tt, *J* = 10.5, 3.7 Hz, cyclohexyl 1-H), 1.99 (1H, app. septet, *J* = 7.6 Hz, cyclopentyl 1-H), 1.90 – 1.84 (2H, m, cyclohexyl 2-H_a and 6-H_a), 1.81– 1.75 (2H, m, cyclopentyl 2-H_a and 5-H_a), 1.75-1.68 (2H, m, cyclopentyl 3-H_a and 4-H_a), 1.65 – 1.55 (3H, m, cyclohexyl 3-H_a and 4-H_a and N*H*), 1.55-1.48 (2H, m, cyclohexyl 4-H_2) 1.30-1.22 (2H, m, cyclopentyl 3-H_b and 4-H_b) 1.19 (1H, dt, *J* = 12.5, 3.0 Hz, cyclohexyl 3-H_b), 1.17-1.02 (m, 5H, cyclohexyl 2-H_b, 5-H_b and 6-H_b, cyclopentyl 2-H_b and 5-H_b); $^{13}C\{^{1}H\}$ NMR ($CDCl_3$, 125 MHz) 57.3 (cyclohexyl C-1), 53.0 (methyl C-1), 40.3 (cyclopentyl C-1), 33.7 (cyclohexyl C-2 and C-6), 31.1 (cyclopentyl C-2 and C-5), 26.3 (cyclohexyl C-4), 25.5 (cyclohexyl C-3 and C-5), 25.3 (cyclopentyl C-3 and C-4); HRMS (ESI-TOF) m/z: $[M+H]^+$ Calcd for $C_{12}H_{24}N$ 182.1903; Found 182.1908.

***N*-(Cyclopentylmethyl)-1-phenylethanamine 221**

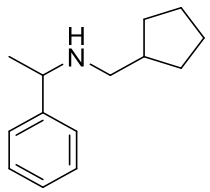

221

The reaction was set up following general procedure I using methylbenzylamine (MBA) (30 mg, 0.25 mmol) and methylenecyclopentane (62 mg, 0.75 mmol, 3.0 equiv). Upon completion of the reaction, the solvent was removed *via* rotary evaporation and the crude material was purified *via* column chromatography eluting with 50:50 hexane-EtOAc to give the title compound (22.8 mg, 45% yield); ν_{max}/cm^{-1}

2935, 2843, 1458, 1378, 1134, 889, 850, 754; ^{1}H NMR ($CDCl_3$, 500 MHz) δ 7.34-7.30 (4H, m, phenyl 2-H, 3-H, 5-H and 6-H), 7.26-7.21 (1H, m, phenyl 4-H), 3.75 (1H, q, *J* = 6.6 Hz, ethyl 1-H), 2.46 (1H, dd, *J* = 11.2, 6.8 Hz, methylene C*H*$_a$CH$_b$), 2.33 (1H, dd, *J* = 11.2, 7.6 Hz, methylene CH$_a$C*H*$_b$), 2.04-1.93 (1H, m, cyclopentyl 1-H), 1.79-1.71 (2H, m, cyclopentyl 2-H$_a$ and 5-H$_a$), 1.60-1.46 (4H, m, cyclopentyl 3-H$_2$ and 4-H$_2$), 1.35 (3H, d, *J* = 6.6 Hz, ethyl 2-H$_3$), 1.15-1.05 (2H, m, cyclopentyl 2-H$_b$ and 5-H$_b$); ^{13}C{^{1}H} NMR ($CDCl_3$, 125 MHz) δ 146.2 (phenyl C-1), 128.5 (phenyl C-3 and C-5), 126.9 (phenyl C-4), 126.7 (phenyl C-2 and C-6), 58.7 (ethyl C-1), 53.8 (methylene C-1), 40.3 (cyclopentyl C-1), 31.01 (cyclopentyl C-2 or C-5), 30.99 (cyclopentyl C-2 or C-5), 25.4 (cyclopentyl C-3 and C-4), 24.7 (ethyl C-2); HRMS (ESI-TOF) m/z [M+H]$^{+}$ Calcd for $C_{14}H_{22}N$ 204.1747; Found 204.1747.

_N_-(Cyclopentylmethyl)-1-naphthalen-1-ylethanamine 222

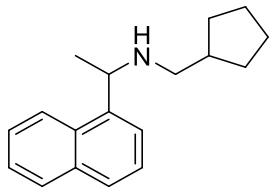

222

The reaction was set up following general procedure I using 1-(1-naphthyl)ethylamine (43 mg, 0.25 mmol) and methylenecyclopentane (62 mg, 0.75 mmol, 3.0 equiv). Upon completion of the reaction, the solvent was removed *via* rotary evaporation and the crude material was purified *via* column chromatography eluting with 50:50 hexane-EtOAc to give the title compound (28.6 mg, 45%); ν_{max}/cm^{-1} 2897, 2845, 1375, 1139, 870, 833, 756; ^{1}H NMR ($CDCl_3$, 500 MHz) δ 8.20 (1H, d, *J* = 8.4 Hz, naphthyl 8-H), 7.89-7.85 (1H, m, naphthyl 5-H), 7.75 (1H, d, *J* = 8.2 Hz, naphthyl 4-H), 7.68 (1H, d, *J* = 7.1 Hz, naphthyl 2-H), 7.53-7.45 (3H, m, naphthyl 3-H, 6-H and 7-H), 4.62 (1H, q, *J* = 6.6 Hz, ethyl 1-H), 2.56 (1H, dd, *J* = 11.2, 6.7 Hz, methyl C*H*$_a$H$_b$), 2.46 (1H, dd, *J* = 11.2, 7.6 Hz, methyl CH$_a$*H*$_b$), 2.09-1.99 (1H, m, cyclopentyl 1-H), 1.82-1.73 (2H, m, cyclopentyl 2-H$_a$ and 5-H$_a$), 1.61-1.51 (4H, m, cyclopentyl 3-H$_2$ and 4-H$_2$), 1.50 (3H, d, *J* = 6.6 Hz, ethyl 2-H$_3$), 1.20-1.08 (2H, m, cyclopentyl 2-H$_b$ and 5-H$_b$); ^{13}C{^{1}H} NMR ($CDCl_3$, 125 MHz) δ 141.6 (naphthyl C-1), 134.1 (naphthyl C-4a),

131.5 (naphthyl C-8a), 129.1 (naphthyl C-5), 127.2 (naphthyl C-4), 125.88 (naphthyl C-3, C-6 or C-7), 125.84 (naphthyl C-3, C-6 or C-7), 125.4 (naphthyl C-3, C-6 or C-7), 123.1 (naphthyl C-8), 122.8 (naphthyl C-2), 54.0 (br s, ethyl C-1 and methyl C-1), 40.4 (cyclopentyl C-1), 31.09 (cyclopentyl C-2 or C-5), 31.06 (cyclopentyl C-2 or C-5), 25.45 (cyclopentyl C-3 and C-4), 25.42 (cyclopentyl C-3 and C-4), 23.8 (ethyl C-2); HRMS (ESI-TOF) m/z $[M+H]^+$ Calcd for $C_{18}H_{24}N$ 254.1903; Found 254.1898.

***N*-(Cyclohexylmethyl)cyclohexanamine 223**

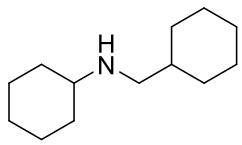

223

The reaction was set up following general procedure I using cyclohexylamine (25 mg, 0.25 mmol) and methylenecyclohexane (72 mg, 0.75 mmol, 3.0 equiv). The reaction was purified by the general workup procedure to give the title compound (40.4 mg, 83%); ν_{max}/cm^{-1} 2920, 2850, 1448, 1347, 1130, 889, 720; ^1H NMR ($CDCl_3$, 500 MHz) δ 2.43 (2H, d, *J* = 6.7 Hz, methyl 1-H_2), 2.35 (1H, tt, *J* = 10.5, 3.7 Hz, 1-H), 1.89-1.83 (2H, m, 2-H_a and 6-H_a), 1.75-1.65 (7H, m, 3-H_a, 5-H_a, cyclohexyl 2-H_a, cyclohexyl 3-H_a, cyclohexyl 5-H_a, cyclohexyl 6-H_a and N*H*), 1.65-1.56 (2H, m, 4-H_a and cyclohexyl 4-H_a), 1.45-1.36 (1H, m, cyclohexyl 1-H), 1.29-1.18 (4H, m, 3-H_b, 5-H_b, cyclohexyl 3-H_b and cyclohexyl 5-H_b), 1.18-1.11 (2H, m, 4-H_b and cyclohexyl 4-H_b), 1.11-0.99 (2H, m, 2-H_b and 6-H_b), 0.93-0.82 (2H, m, cyclohexyl 2-H_b and 6-H_b); $^{13}C\{^1H\}$ NMR ($CDCl_3$, 125 MHz) δ 57.1 (C-1), 53.9 (methyl C-1), 38.3 (cyclohexyl C-1), 33.8 (C-2 and C-6), 31.7 (C-3 and C-5), 26.8 (C-4), 26.4 (cyclohexyl C-4), 26.2 (cyclohexyl C-2 and cyclohexyl C-6 or cyclohexyl C-3 and cyclohexyl C-5), 25.3 (cyclohexyl C-2 and cyclohexyl C-6 or cyclohexyl C-3 and cyclohexyl C-5); HRMS (ESI-TOF) m/z $[M+H]^+$ Calcd $C_{13}H_{26}N$ 196.2065; Found 196.2075.

***N*-(Cyclohexylmethyl)-1-phenylethanamine 224**

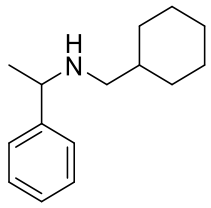

224

The reaction was set up following general procedure I using methylbenzylamine (30 mg, 0.25 mmol) and methylenecyclohexane (72 mg, 0.75 mmol, 3.0 equiv.). Upon completion of the reaction, the solvent was removed *via* rotary evaporation and the crude material was purified *via* column chromatography eluting with 50:50 hexane:EtOAc to give the title compound (19.5 mg, 36%); v_{max}/cm^{-1} 3004, 2901, 1448, 1121, 905, 713; ^{1}H NMR ($CDCl_3$, 500 MHz) δ 7.34-7.29 (4H, m, phenyl 2-H, 3-H, 5-H and 6-H), 7.25-7.21 (1H, m, phenyl 4-H), 3.72 (1H, q, *J* = 6.6 Hz, ethyl 1-H), 2.35 (1H, dd, *J* = 11.5, 6.2 Hz, methylene CH_aH$_b$), 2.24 (1H, dd, *J* = 11.5, 7.1 Hz, methylene CH$_a$$H_b$), 1.78-1.69 (2H, m, cyclohexyl 2-H_2), 1.69-1.61 (2H, m, cyclohexyl 5-H_2), 1.47-1.37 (1H, m, cyclohexyl 1-H), 1.34 (3H, d, *J* = 6.6 Hz, ethyl 2-H_3), 1.28-1.20 (2H, m, cyclohexyl 3-H_2), 1.20-1.08 (2H, m, cyclohexyl 4-H_2), 0.92-0.82 (2H, m, cyclohexyl 6-H_2); $^{13}C\{^{1}H\}$ NMR ($CDCl_3$, 125 MHz) δ 146.2 (phenyl C-1), 128.5 (phenyl C-3 and C-5), 126.9 (phenyl C-4). 126.7 (phenyl C-2 and C-6), 58.6 (ethyl C-1), 54.7 (methyl *C*H_2), 38.3 (cyclohexyl C-1), 31.7 (cyclohexyl C-2 or C-6), 31.6 (cyclohexyl C-2 or C-6), 26.8 (cyclohexyl 3-C), 26.23 (cyclohexyl 4-C), 26.18 (cyclohexyl 5-C), 24.7 (ethyl C-2); HRMS (ESI-TOF) m/z $[M+H]^+$ Calcd for $C_{15}H_{24}N$ 218.1900; Found 218.1901.

_N_-(Cyclohexylmethyl)-1-naphthalen-1-ylethanamine 225

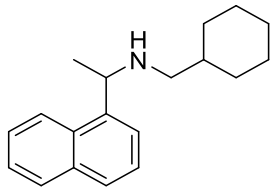

225

The reaction was set up following general procedure I using 1-(1-naphthyl)ethylamine (43 mg, 0.25 mmol) and methylenecyclohexane (72 mg, 0.75 mmol, 3.0 equiv). Upon completion of the reaction, the solvent was removed *via*

rotary evaporation and the crude material was purified *via* column chromatography eluting with 50:50 hexane-EtOAc to give the title compound in an isolated yield of (17.4 mg, 26%). R_f 0.25 (50:50 hexane-EtOAc); ν_{max}/cm^{-1} 2951, 2899, 1501, 1141, 1030, 722; ^1H NMR ($CDCl_3$, 500 MHz) δ 8.19 (1H, d, *J* = 8.4 Hz, naphthyl 8-H), 7.90-7.85 (1H, m, naphthyl 5-H), 7.74 (1H, d, *J* = 8.2 Hz, naphthyl 4-H), 7.68 (1H, d, *J* = 7.1 Hz, naphthyl 2-H), 7.54-7.44 (3H, m, naphthyl 3-H, 6-H and 7-H), 4.63 (1H, q, *J* = 6.6 Hz, ethyl 1-H), 2.56 (1H, dd, *J* = 11.2, 6.7 Hz, methylene 1-H_a) , 2.46 (1H, dd, *J* = 11.2, 7.6 Hz, methylene 1-H_b), 2.04 (1H, app. septet, *J* = 7.7 Hz, cyclohexyl 1-H), 1.82-1.72 (2H, m, 4-H_2), 1.59-1.52 (4H, m, cyclohexyl 2-H_2 and 6-H_2), 1.50 (3H, d, *J* = 6.6 Hz, ethyl 2-H_3), 1.29-1.23 (2H, m, 3-H_a and 5-H_a), 1.20-1.08 (2H, m, 3-H_b and 5-H_b); $^{13}C\{^1H\}$ ($CDCl_3$, 125 MHz) δ 141.5 (naphthyl C-1), 134.1 (naphthyl C-4a), 131.5 (naphthyl C-8a), 129.1 (naphthyl C-5), 127.2 (naphthyl C-4), 125.88 (naphthyl C-3, C-6 or C-7), 125.86 (naphthyl C-3, C-6 or C-7), 125.4 (naphthyl C-3, C-6 or C-7), 123.1 (naphthyl C-8), 122.8 (naphthyl C-2), 54.0 (ethyl C-1), 40.4 (cyclohexyl C-1), 31.09 (cyclohexyl C-3, C-4 or C-5), 31.06 (cyclohexyl C-3, C-4 or C-5), 29.9 (cyclohexyl C-3, C-4 or C-5), 26.5 (cyclohexyl C-2 or C-6), 26.4 (cyclohexyl C-2 or C-6), 23.8 (ethyl C-2); HRMS (ESI-TOF) m/z $[M+H]^+$ Calcd for $C_{19}H_{26}N$ 268.2060; Found 268.2067.

***N,N*-Dicyclohexylamine 226**

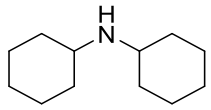

226

The reaction was set up following general general procedure I using cyclohexylamine (25 mg, 0.25 mmol) and cyclohexene (62 mg, 0.75 mmol, 3.0 equiv). The reaction was purified by the general workup procedure to give the title compound (28.5 mg, 63%); ν_{max}/cm^{-1} 3310, 2852, 1464, 1448, 1368, 1126, 888, 705; ^1H NMR ($CDCl_3$, 500 MHz) δ 2.62-2.53 (2H, tt, *J* = 10.6, 3.6 Hz, 1-H), 1.91-1.78 (4H, m, 2-H_a and 6-H_a), 1.76-1.64 (4H, m, 2-H_b and 6-H_b), 1.64-1.57 (2H, m, 4-H_a), 1.31-1.16 (5H, m, 3-H_a, 5-H_a and N*H*), 1.15-1.06 (2H, m, 3-H_b), 1.06-0.93 (4H, m, 4-H_2 and 5-H_b); $^{13}C\{^1H\}$ ($CDCl_3$, 125 MHz) δ

53.2 (C-1), 34.5 (C-2 and C-6), 26.3 (C-3 and C-5), 25.4 (C-4); HRMS (ESI-TOF) m/z $[M+H]^+$ Calcd for $C_{12}H_{24}N$ 182.1903; Found 182.1902.

***N*-(1-Phenylethyl)cyclohexanamine 227**

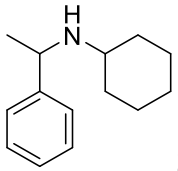

227

The reaction was set up following general procedure I using methylbenzylamine (30 mg, 0.25 mmol) and cyclohexene (62 mg, 0.75 mmol, 3.0 equiv). Upon completion of the reaction, the solvent was removed *via* rotary evaporation and the crude material was purified *via* column chromatography eluting with 50:50 hexane-EtOAc to give the title compound as a yellow oil (13.2 mg, 26%), R_f 0.15 (EtOAc); ν_{max}/cm^{-1} 2921, 2850, 1491, 1448, 1366, 1127, 760, 699; ^1H NMR ($CDCl_3$, 500 MHz) δ 7.34-7.28 (4H, m, phenyl 2-H, 3-H, 5-H and 6-H), 7.25-7.21 (1H, m, phenyl 4-H), 3.96 (1H, q, *J* = 6.6 Hz, ethyl 1-H), 2.27 (1H, tt, *J* = 10.1, 3.7 Hz, cyclohexyl 1-H), 1.98 (1H, app. d, *J* = 12.4 Hz, cyclohexyl 2-H_a), 1.74-1.61 (3H, m, cyclohexyl 3-H_a, 5-H_a and 6-H_a), 1.59-1.50 (1H, m, cyclohexyl 4-H_a), 1.33 (3H, d, *J* = 6.6 Hz, ethyl 2-H_3), 1.20-0.96 (5H, m, cyclohexyl 2-H_b, 3-H_b, 4-H_b, 5-H_b and 6-H_b); $^{13}C\{^1H\}$ ($CDCl_3$, 125 MHz) δ 146.4, (phenyl C-1), 128.5 (phenyl C-3 and C-5), 126.8 (phenyl C-4), 126.6 (phenyl C-2 and C-6), 54.6 (ethyl C-1), 53.8 (cyclohexyl C-1), 34.7 (cyclohexyl C-6), 33.3 (cyclohexyl C-2), 26.3 (cyclohexyl C-4), 25.4, 25.2 (cyclohexyl C-3 and C-5), 25.1 (ethyl C-2); HRMS (ESI-TOF) m/z $[M+H]^+$ Calcd for $C_{14}H_{22}N$ 204.1747; Found 204.1439.

***N*-[1-(Naphthalen-2-yl)ethyl]cyclohexanamine 228**

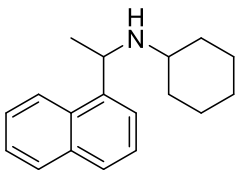

228

The reaction was set up following general procedure I using 1-(1-naphthyl)ethylamine (43 mg, 0.25 mmol) and cyclohexene (62 mg, 0.75 mmol, 3.0 equiv). Upon completion of the reaction, the solvent was removed *via* rotary evaporation and the crude material was purified *via* column chromatography eluting with 50:50 hexane-EtOAc to give the title compound as a yellow oil (13.9 mg, 22%), R_f 0.54 (EtOAc); v_{max}/cm^{-1} 3051, 2920, 1506, 1457, 1446, 1365, 1128, 887, 744; ^1H NMR ($CDCl_3$, 500 MHz) δ 8.19 (1H, d, *J* = 8.4 Hz, naphthyl 8-H), 7.90-7.85 (1H, m, naphthyl 5-H), 7.74 (1H, d, *J* = 8.2 Hz, naphthyl 4-H), 7.65 (1H, d, *J* = 7.0 Hz, naphthyl 2-H), 7.54-7.45 (3H, m, naphthyl 3-H, 6-H and 7-H), 4.85 (1H, q, *J* = 6.5 Hz, ethyl 1-H), 2.45-2.37 (1H, br m, cyclohexyl 1-H), 2.03-1.95 (1H, br m, cyclohexyl 2-H_a), 1.86-1.81 (1H, br m, cyclohexyl 6-H_a), 1.71-1.61 (2H, br m, cyclohexyl 3-H_a and 5-H_a), 1.58-1.52 (1H, br m, cyclohexyl 4-H_a), 1.47 (3H, d, *J* = 6.0 Hz, ethyl 2-H_3), 1.21-1.02 (5H, m, cyclohexyl 2-H_b, 3-H_b, 4-H_b, 5-H_b and 6-H_b); $^{13}C\{^1H\}$ ($CDCl_3$, 125 MHz) δ 142.1 (naphthyl C-1), 134.1 (naphthyl C-4a), 131.4 (naphthyl C-8a), 129.1 (naphthyl C-5), 127.1 (naphthyl C-4), 125.9, 125.4 (naphthyl C-3 C-6 and C-7), 123.0 (naphthyl C-8), 122.8 (naphthyl C-2), 54.0 (ethyl C-1), 49.7 (cyclohexyl C-1), 34.7 (cyclohexyl C-6), 33.8 (cyclohexyl C-2), 26.3 (cyclohexyl C-4), 25.5, 25.2 (cyclohexyl C-3 and C-5), 24.6 (ethyl C-2); HRMS (ESI-TOF) m/z $[M+H]^+$ Calcd for $C_{18}H_{24}N$ 254.1903; Found 254.1906.

***N*-Cyclohexyl-4-methoxybenzeneethanamine 229**

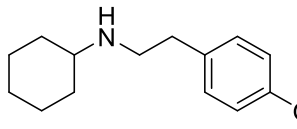

229

The reaction was set up following general procedure I using cyclohexylamine (25 mg, 0.25 mmol) and 4-vinylanisole (101 mg, 0.75 mmol, 3.0 equiv). The reaction was purified by the general workup procedure to give the title compound as a yellow oil (44.1 mg, 76%); v_{max}/cm^{-1} 2991, 2843, 1548, 1445, 1130, 901, 705; ^1H NMR ($CDCl_3$, 500 MHz) δ 7.15-7.08 (2H, m, aryl 2-H and 6-H), 6.86-6.81 (2H, m, aryl 3-H and 5-H), 3.79 (3H, s, methoxy CH_3), 2.89-2.84 (2H, m, ethyl 1-H_2), 2.77-2.72 (2H, m, ethyl 2-H_2), 2.42 (1H, tt, *J* = 10.6, 3.7 Hz, cyclohexyl 1-H), 1.90 – 1.82 (2H, m, cyclohexyl 2-H_a

and 6-H_a), 1.74– 1.67 (3H, m, cyclohexyl 4-H_2 and 3-H_a), 1.25 (1H, br s, N*H*) 1.18-0.99 (5H, m, cyclohexyl 2-H_b, 3-H_b, 5-H_2 and 6-H_b); $^{13}C\{^1H\}$ ($CDCl_3$, 125 MHz) δ 158.1 (aryl C-4), 132.3 (aryl C-1), 129.8 (aryl C-2 and C-6), 114.0 (aryl C-3 and C-5), 56.9 (cyclohexyl C-1), 55.4 (methoxy *C*H_3), 48.6 (ethyl C-1), 35.8 (ethyl C-2), 33.7 (cyclohexyl C-2 and C-6), 29.8 (cyclohexyl C-3 and C-5), 25.2 (cyclohexyl C-4); HRMS (ESI-TOF) m/z $[M+H]^+$ Calcd for $C_{15}H_{24}NO$ 234.1852; Found 234.1858.

***N*-[2-(4-Methoxyphenyl)ethyl]-1-phenylethanamine 230**

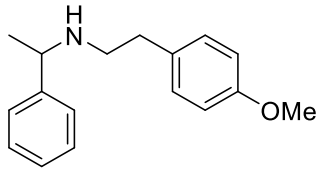

230

The reaction was set up following general procedure I using methylbenzylamine (MBA) (30 mg, 0.25 mmol) and 4-vinylanisole (101 mg, 0.75 mmol, 3.0 equiv). Upon completion of the reaction, the solvent was removed *via* rotary evaporation and the crude material was purified *via* column chromatography eluting with 96:4 DCM-MeOH to give the title compound as a dark brown oil (21.7 mg, 34%), R_f 0.28 (96:4 DCM-MeOH); v_{max}/cm^{-1} 3001, 2934, 1555, 1459, 1136, 888, 699; ^1H NMR ($CDCl_3$, 500 MHz) δ 7.34-7.29 (2H, m, phenyl 3-H and 5-H), 7.28-7.20 (3H, m, phenyl 2-H, 4-H and 6-H), 7.07 (2H, d, *J* = 8.5 Hz, aryl 2-H and 6-H) 6.81 (2H, d, *J* = 8.6 Hz, aryl 3-H and 5-H), 3.81-3.75 (4H, m, 1-H and methoxy C*H*$_3$), 2.78-2.64 (4H, m, ethyl 1-H_2 and 2-H_2), 1.67 (1H, br s, N*H*), 1.34 (3H, d, *J* = 6.6 Hz, 2-H_3); $^{13}C\{^1H\}$ ($CDCl_3$, 125 MHz) δ 158.1 (aryl C-4), 145.5 (phenyl C-1), 132.1 (aryl C-1), 129.7 (aryl C-2 and C-6), 128.6 (phenyl C-3 and C-5), 127.1 (phenyl C-4), 126.7 (phenyl C-2 and C-6), 114.0 (aryl C-3 and C-5), 58.4 (C-1), 55.4 (methoxy *C*H_3), 49.2 (ethyl C-1), 35.5 (ethyl C-2), 24.3 (C-2); HRMS (ESI-TOF) m/z $[M+H]^+$ Calcd for $C_{17}H_{22}NO$ 256.1696; Found 256.1707.

***N*-[2-(4-Methoxyphenyl)ethyl]-1-naphthalen-1-ylethanamine 231**

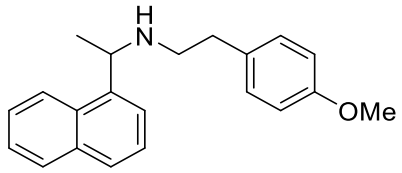

231

The reaction was set up following general procedure I using 1-(1-naphthyl)ethylamine (43 mg, 0.25 mmol) and 4-vinylanisole (101 mg, 0.75 mmol, 3.0 equiv). Upon completion of the reaction, the solvent was removed *via* rotary evaporation and the crude material was purified *via* column chromatography eluting with 50:50 hexane-EtOAc to give the title compound as a yellow oil (27.0 mg, 35%); v_{max}/cm^{-1} 2994, 2915, 1531, 1465, 1130, 843, 708; ^{1}H NMR ($CDCl_3$, 500 MHz) δ 8.12-8.07 (1H, m, naphthyl 8-H), 7.88-7.84 (1H, m, naphthyl 5-H), 7.75 (1H, d, *J* = 8.2 Hz, naphthyl 4-H), 7.58 (1H, d, *J* = 7.0 Hz, naphthyl 2-H), 7.51-7.43 (3H, m, naphthyl 3-H, 6-H and 7-H), 7.07 (2H, d, *J* = 8.6 Hz, aryl 2-H and 6-H), 6.80 (2H, d, *J* = 8.6 Hz, aryl 3-H and 5-H), 4.69 (1H, q, *J* = 6.4 Hz, 1-H), 3.78 (3H, s, methoxy C*H*$_3$), 2.90-2.74 (4H, m, ethyl 1-H_2 and 2-H_2), 1.52 (3H, m, *J* = 6.5 Hz, 2-H_3); $^{13}C\{^{1}H\}$ ($CDCl_3$, 125 MHz) δ 158.2 (aryl C-1), 141.3 (naphthyl C-1), 134.1 (naphthyl C-4a), 132.2 (aryl C-4), 131.4 (naphthyl C-8a), 129.8 (aryl C-2 and C-6), 129.1 (naphthyl C-5), 127.5 (naphthyl C-4), 126.1, 125.9, 125.5 (naphthyl C-3 C-6 and C-7), 122.9, 122.8 (naphthyl C-2 and C-8), 114.0 (aryl C-3 and C-5), 55.4 (methoxy *C*H_3), 53.7 (C-1), 49.2 (ethyl C-1), 35.3 (ethyl C-2), 23.4 (C-2); HRMS (ESI-TOF) m/z $[M+H]^+$ Calcd for $C_{21}H_{24}NO$ 306.1852; Found 306.1850.

_N_-(3-Phenylpropyl)cyclohexanamine 232

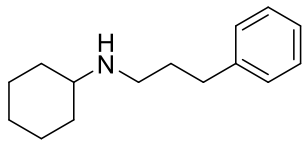

232

The reaction was set up following general procedure I using cyclohexylamine (25 mg, 0.25 mmol) and allylbenzene (89 mg, 0.75 mmol, 3.0 equiv). The reaction was purified by the general workup procedure to give the title compound (25.5 mg, 47%);

v_{max}/cm^{-1} 3298, 1609, 1488, 1447, 1279, 699; ^{1}H NMR ($CDCl_3$, 500 MHz) δ 7.32-7.27 (2H, m, phenyl 3-H and 5-H), 7.20-7.17 (3H, m, phenyl 2-H, 4-H and 6-H), 2.69-2.62 (4H, m, propyl 1-H_2 and 3-H_2), 2.40 (1H, tt, *J* = 10.6, 3.7 Hz, 1-H), 1.89-1.68 (7H, m, propyl 2-H_2, 2-H_a, 3-H_a, 4-H_2 and 6-H_a), 1.64-1.57 (2H, m, 3-H_b, 5-H_a), 1.17-1.12 (1H, m, 5-H_b), 1.10-1.00 (2H, m, 2-H_b and 6-H_b); $^{13}C\{^{1}H\}$ ($CDCl_3$, 125 MHz) δ 142.3 (phenyl C-1), 128.52 (phenyl C-3 and C-5), 128.46 (phenyl C-2 and C-6) 125.9 (phenyl C-4), 57.0 (C-1), 46.7 (propyl C-1), 33.9 (propyl C-3), 33.7 (propyl C-2), 32.1, 29.8 (C-2 and C-6), 26.3 (C-3 and C-5), 25.3 (C-4); HRMS (ESI-TOF) m/z $[M+H]^+$ Calcd for $C_{15}H_{24}N$ 218.1903; Found 218.1910.

3-Phenyl-*N*-(1-phenylethyl)-1-propanamine 233

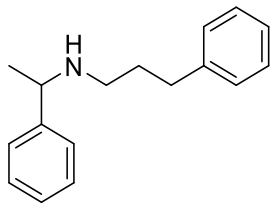

233

The reaction was set up following general procedure I using methylbenzylamine (MBA) (30 mg, 0.25 mmol) and allylbenzene (89 mg, 0.75 mmol, 3.0 equiv). Upon completion of the reaction, the solvent was removed *via* rotary evaporation and the crude material was purified *via* column chromatography eluting with 50:50 EtOAc-hexane to give the title compound as a colourless oil (14.9 mg, 25%), R_f 0.29 (EtOAc); v_{max}/cm^{-1} 3311, 1603, 1495, 1453, 1368, 734, 700; ^{1}H NMR ($CDCl_3$, 500 MHz) δ 7.34-7.27 (4H, m, phenylethyl 2-H, 3-H, 5-H and 6-H), 7.25-7.21 (3H, m, phenylethyl 4-H, phenyl 3-H and 5-H), 7.18-7.11 (3H, m, phenyl 2-H, 4-H and 6-H), 3.74 (1H, q, *J* = 6.6 Hz, ethyl 1-H), 2.67-2.51 (3H, m, propyl 1-H_a and 3-H_2), 2.50-2.43 (1H, m, propyl 1-H_b), 1.85-1.71 (2H, m, propyl 2-H_2), 1.34 (3H, d, *J* = 6.6 Hz, ethyl 1-H_3); $^{13}C\{^{1}H\}$ ($CDCl_3$, 125 MHz) δ 145.9 (phenylethyl C-1), 142.3 (phenyl C-1), 128.55, 128.49, 128.4 (phenylethyl C-3, C-5, phenyl C-2, C-3, C-5 and C-6), 127.0 (phenyl C-4), 126.7 (phenylethyl C-2 and C-6), 125.9 (phenylethyl C-4), 58.5 (ethyl C-1), 47.5 (propyl C-1),

33.8 (propyl C-3), 32.0 (propyl C-2), 24.5 (ethyl C-2); HRMS (ESI-TOF) m/z $[M+H]^+$ Calcd for $C_{17}H_{22}N$ 240.1747; Found 240.1746.

***N*-(3-Phenylpropyl)-1-(1-naphthyl)ethylamine 234**

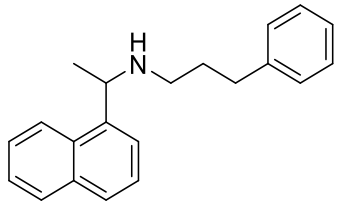

234

(Note: hydroamination in batch failed; alternative preparation to make racemic standard).

To an oven dried, nitrogen purged 7mL screw cap vial containing $[IrCp^*Cl_2]_2$ (8.0 mg, 0.01 mmol) were added 1-(1-naphthyl)ethylamine (171 mg, 1.0 mmol) and 3-phenyl-1-propanol (136 mg, 1.0 mmol) followed by toluene (2 mL). The reaction mixture was then heated at reflux for 20 h. The solvent was removed under vacuum and the resulting residue was purified by column chromatography eluting with 50:50 EtOAc-hexane to give the title compound as a yellow oil (121 mg, 42%), R_f 0.32 (EtOAc); ν_{max}/cm^{-1} 3350, 1596, 1509, 1496, 1369, 779, 699; ^1H NMR ($CDCl_3$, 500 MHz) δ 8.18 (1H, d, *J* = 8.2 Hz, naphthyl 8-H), 7.90 – 7.85 (1H, m, naphthyl 5-H), 7.75 (1H, d, *J* = 8.1 Hz, naphthyl 4-H), 7.67 (1H, d, *J* = 6.2 Hz, naphthyl 2-H), 7.54 – 7.45 (3H, m, naphthyl 3-H, 6-H and 7-H), 7.24 (2H, d, *J* = 7.5 Hz, aryl 3-H and 5-H), 7.18-7.11 (3H, m, aryl 2-H, 4-H and 6-H), 4.64 (1H, q, *J* = 5.9 Hz, ethyl 1-H), 2.70 – 2.56 (4H, m, propyl 1-H_2 and 3-H_2), 1.91-1.80 (2H, m, propyl 2-H_2), 1.51 (3H, d, *J* = 6.6 Hz, ethyl 2-H_3); $^{13}C\{^1H\}$ NMR ($CDCl_3$, 125 MHz) δ 142.3 (aryl C-1), 134.1 (naphthyl C-4a), 131.4 (naphthyl C-8a), 129.1 (naphthyl C-5), 128.5 (aryl C-3 and C-5), 128.4 (aryl C-2 and C-6), 127.4 (naphthyl C-4), 125.94, 125.88 (naphthyl C-3, C-6 and C-7), 125.5 (aryl C-4), 123.0 (naphthyl C-8), 122.9 (naphthyl C-2), 53.8 (ethyl C-1), 47.6 (propyl C-1), 33.8 (propyl C-3), 32.1 (propyl C-2), 23.7 (ethyl C-2) (17 signals observed of 19 expected); HRMS (ESI-TOF) m/z: $[M+H]^+$ Calcd for $C_{21}H_{24}N$ 290.1903; Found 290.1905.

***N*-(3-(3-(Trifluoromethyl)phenyl)propyl)cyclohexanamine 235**

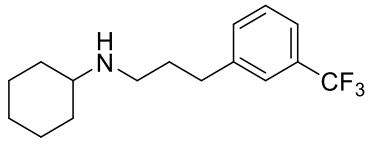

235

The reaction was set up following general procedure I using cyclohexylamine (25 mg, 0.25 mmol) and 3-[(3-trifluoromethyl)phenyl]-1-propene (140 mg, 0.75 mmol, 3.0 equiv). The reaction was purified by the general workup procedure to give the title compound (9.0 mg, 13%); v_{max}/cm^{-1} 3230, 3002, 1289, 1101, 723; ^{1}H NMR ($CDCl_3$, 400 MHz) δ 7.46-7.41 (2H, m, aryl 2-H and 4-H), 7.40-7.34 (2H, m, aryl 5-H and 6-H), 2.71 (2H, br t, *J* = 7.7 Hz, propyl 1-H_2), 2.65 (2H, br t, *J* = 7.2 Hz, propyl 3-H_2), 2.39 (1H, tt, *J* = 10.5, 3.7 Hz, 1-H), 1.90-1.77 (4H, m, propyl 2-H_2, 2-H_a and 6-H_a), 1.76-1.66 (2H, m, 4-H_2), 1.65-1.56 (1H, m, 3-H_a), 1.31-1.11 (3H, m, 3-H_b and 5-H_2), 1.10-0.98 (2H, m, 2-H_b and 6-H_b); $^{13}C\{^{1}H\}$ NMR ($CDCl_3$, 125 MHz) δ 143.2 (aryl C-1), 131.9 (aryl C-6), 130.7 (q, *J* = 31.7 Hz, aryl C-3), 128.8 (aryl C-5), 125.2 (q, *J* = 3.6 Hz, aryl C-2), 124.1 (q, *J* = 272.3, *C*F_3), 122.8 (q, *J* = 3.8 Hz, aryl C-4), 57.0 (C-1), 46.5 (propyl C-3), 33.9 (C-2), 33.7 (C-6), 32.2 (propyl C-1), 26.3 (C-4), 25.2 (C-3 and C-5); $^{19}F\{^{1}H\}$ NMR ($CDCl_3$, 376 MHz) δ -62.6; HRMS (ESI-TOF) m/z: $[M+H]^+$ Calcd for $C_{16}H_{23}F_3N$ 286.1777; Found 286.1779.

***N*-(1-Phenylethyl)-3-(3-(trifluoromethyl)phenyl)propan-1-amine 186**

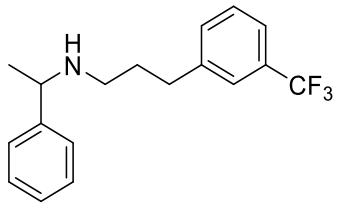

186

The reaction was set up following general procedure I using methylbenzylamine (30 mg, 0.25 mmol) and 3-[(3-trifluoromethyl)phenyl]-1-propene (140 mg, 0.75 mmol, 3.0 equiv). Upon completion of the reaction, the solvent was removed *via* rotary evaporation and the crude material was purified *via* column chromatography eluting with 5:95 EtOAc-hexane to give the title compound as a yellow oil (10.6 mg, 14%), R_f 0.23 (50:50 DCM-EtOAc); v_{max}/cm^{-1} 3041, 2985, 2932, 1333, 1163, 771; ^{1}H NMR

($CDCl_3$, 500 MHz) δ 7.45-7.40 (2H, m, aryl 2-H and 4-H), 7.39-7.35 (1H, m, aryl 5-H), 7.35-7.28 (5H, m, phenyl 2-H, 3-H, 5-H, 6-H and aryl 6-H), 7.27-7.22 (1H, m, phenyl 4-H), 3.75 (1H, q, *J* = 6.6 Hz, ethyl 1-H), 2.71 (1H, ddd, *J* = 14.0, 8.8, 7.1 Hz, propyl 3-H_a), 2.64 (1H, ddd, *J* = 14.0, 8.4, 7.1 Hz, propyl 3-H_b), 2.56 (1H, ddd, *J* = 11.5, 7.5, 6.4 Hz, propyl 1-H_a), 2.47 (1H, app. dt, *J* = 11.5, 7.2 Hz, propyl 1-H_b), 1.87-1.71 (2H, m, propyl 2-H_2), 1.36 (3H, d, *J* = 6.6 Hz, ethyl 2-H_3); $^{13}C\{^1H\}$ NMR ($CDCl_3$, 125 MHz) δ 145.9 (phenyl C-1), 143.3 (aryl C-1), 131.9 (aryl C-6), 130.7 (q, *J* = 31.8 Hz, aryl C-3), 128.8 (phenyl C-3, C-4 or C-5), 128.6 (phenyl C-3, C-4 or C-5), 127.0 (phenyl C-3, C-4 or C-5), 126.7 (aryl C-5), 125.8 (phenyl C-2 and C-6), 125.2 (q, *J* = 3.8 Hz, aryl C-2), 124.4 (q, *J* = 272.3 Hz, *C*F_3), 122.8 (q, *J* = 3.8 Hz, aryl C-4), 58.5 (ethyl C-1), 47.2 (propyl C-1), 33.5 (propyl C-3), 31.9 (propyl C-2), 24.5 (ethyl C-2); $^{19}F\{^1H\}$ NMR ($CDCl_3$, 376 MHz) δ -62.6; HRMS (ESI-TOF) m/z: $[M+H]^+$ Calcd for $C_{18}H_{21}F_3N$ 308.1621; Found 308.1617.

_N_-(1-(Naphthalen-1-yl)ethyl)-3-(3-(trifluoromethyl)phenyl)propan-1-amine 10 (Cinacalcet) [341]

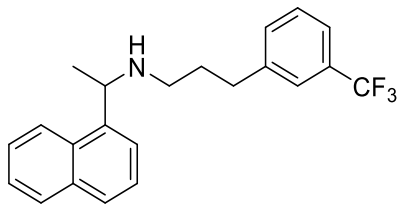

10

(Note: hydroamination in batch failed; alternative preparation to make racemic standard).

1-(1-Naphthyl)ethylamine (1.54 g, 9.0 mmol) and 3-[3-(trifluoromethyl)phenyl]propanal (2.02 g, 10.0 mmol, 1.1 equiv.) were dissolved in methanol (20 mL) and stirred at room temperature for 15 min. Sodium triacetoxyborohydride (2.12 g, 10.0 mmol, 1.1 equiv.) was added portion-wise and the mixture stirred at room temperature for 4 h. After the reaction was completed, the solid was removed by filtration and the solvent removed under reduced pressure. The residue was suspended in toluene and then washed with HCl (2M), NaOH (1M) and water. The organic phase was died over MgSO4 and concentrated under reduced

pressure. The resultant crude mixture was purified by column chromatography eluting with 25:75 EtOAc-heptane to yield the title compound (2.86 g, 89%) as a yellow oil; v_{max}/cm^{-1} 3063, 2970, 2929, 2861, 1329, 1161, 1121, 779; ^{1}H NMR ($CDCl_3$, 500 MHz) δ 8.19 (1H, d, *J* = 8.4 Hz, naphthyl 8-H), 7.90 – 7.86 (1H, m, naphthyl 5-H), 7.75 (1H, d, *J* = 8.2 Hz, naphthyl 4-H), 7.64 (1H, d, *J* = 7.0 Hz, naphthyl 2-H), 7.54 – 7.46 (3H, m, naphthyl 3-H, 6-H and 7-H), 7.42 (2H, d, *J* = 8.3 Hz, aryl 2-H and 4-H), 7.36 (1H, app. t, *J* = 5.6 Hz, aryl 5-H), 7.32 (1H, d, *J* = 7.7 Hz, aryl 6-H), 4.62 (1H, q, *J* = 6.6 Hz, ethyl 1-H), 2.78 – 2.55 (4H, m, propyl 1-H_2 and 3-H_2), 1.84 (2H, dddd, *J* = 7.7, 7.5, 7.3, 7.1 Hz, propyl 2-H_2), 1.50 (3H, d, *J* = 6.6 Hz, ethyl 2-H_3); $^{13}C\{^{1}H\}$ NMR ($CDCl_3$, 125 MHz) δ 143.2 (aryl C-1), 141.4 (naphthyl C-1), 134.1 (naphthyl C-4a), 131.91 (aryl C-6 or naphthyl C-2), 131.90 (aryl C-6 or naphthyl C-2),, 131.4 (naphthyl C-8a), 131.1 (q, *J* = 31.9 Hz, aryl C-3), 129.1 (naphthyl C-5), 128.8 (aryl C-5), 127.3 (naphthyl C-4), 125.9 (naphthyl C-3 or C-6 or C-7), 125.8 (naphthyl C-3 or C-6 or C-7), 125.5 (naphthyl C-3 or C-6 or C-7), 125.1 (q, *J* = 3.8 Hz, aryl C-2), 124.4 (q, *J* = 272.3 Hz, *C*F_3) 123.1 (naphthyl C-8) 122.9 (q, *J* = 4.3 Hz, aryl C-4), 53.9 (ethyl C-1), 47.4 (propyl C-1), 33.6 (propyl C-3), 32.0 (propyl C-2), 23.8 (ethyl C-2); $^{19}F\{^{1}H\}$ NMR (376 MHz, $CDCl_3$) δ -62.5 (C*F*$_3$); HRMS (ESI-TOF) m/z: $[M+H]^+$ Calcd for $C_{22}H_{23}F_3N$ 358.1777; Found 358.1783.

tert-Butyl 3-(1-phenylethylamino)azetidine-1-carboxylate 193

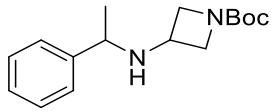

193

According to general procedure J, using methylbenzylamine (MBA) (151 mg, 1.25 mmol) and N-Boc azetine (39 mg, 0.25 mmol). The solvent was evaporated under reduced pressure and the crude product was purified by flash chromatography eluting with 90:10 hexane-acetone to yield **193** (3.4 mg, 5 %) as a pale-yellow viscous oil, R_f 0.23 (80:20 hexane-acetone); v_{max}/cm^{-1} 2972, 1688, 1400, 1365, 1116, 762, 700; ^{1}H NMR ($CDCl_3$, 500 MHz) δ 7.32-7.28 (2H, m, phenyl 3-H and 5-H), 7.27-2.21 (3H, m, phenyl 2-H, 4-H and 6-H), 4.03-3.97 (1H, m, 2-H_a), 3.89-3.82 (1H, m, 4-H_a), 3.71 (1H, q, *J* = 6.6 Hz, ethyl 1-H), 3.65-3.61 (1H, m, 2-H_b), 3.47-3.39 (2H, m, 3-H and 4-H_b), 1.60 (1H, s, N*H*), 1.39 (9H, s, ^{t}Bu), 1.35 (3H, d, *J* = 6.6 Hz, ethyl 2-H_3); $^{13}C\{^{1}H\}$

($CDCl_3$, 125 MHz) δ 156.4 (C=O), 144.8 (phenyl C-1), 128.7 (phenyl C-3 and C-5), 127.5 (C-4), 126.7 (phenyl C-2 and C-6), 79.4 (^{t}Bu *C*), 57.2 (C-2 and C-4), 56.5 (ethyl C-1), 46.2, 28.5 (^{t}Bu *C*H_3), 24.0 (ethyl C-2); HRMS (ESI-TOF) m/z [M+Na]+ Calcd for $C_{16}H_{24}N_2NaO_2$ 299.1730; Found 299.1718.

_N_-(_tert_-Butoxycarbonyl)-3-(1-phenylethyl)aminopyrrolidine 194

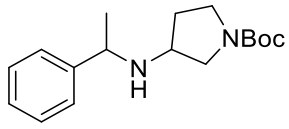

194

According to general procedure J, using methylbenzylamine (151 mg, 1.25 mmol) and *N*-(*tert*-butoxycarbonyl)-2,3-dihydropyrrole (43 mg, 0.25 mmol). The solvent was evaporated under reduced pressure to give a crude product which contained a 50:50 mixture of diastereomeric products. The crude product was purified by flash chromatography eluting with 50:50 hexane-EtOAc to give a 50:50 mixture of diastereomers with each diastereomer appearing as a 50:50 mixture of rotamers (32.5 mg, 45 %) as a viscous yellow oil, R_f 0.18 (50:50 hexane-EtOAc); ν_{max}/cm^{-1} 3001, 1701, 1390, 1298, 1104, 755, 703; ^{1}H NMR (d_6-DMSO, 500 MHz, 348K) δ 7.36-7.32 (2H, m, phenyl 2-H and 6-H), 7.32-7.27 (2H, m, phenyl 3-H and 5-H), 7.23-7.18 (1H, m, phenyl 4-H), 3.81-3.71 (1H, m, ethyl 1-H), 3.36-3.31 (1H, m, pyrrolidine 2-H_a^{RotA}, 5-H_a^{RotA}), 3.31-3.26 (0.5H, m, 5-H_a^{RotB}), 3.20-3.14 (0.5H, m, 2-H_b^{RotA}), 3.14-3.09 (1H, m, 5-H_b), 3.05-2.99 (1.5H, m, pyrrolidine 2-H_a^{RotB} and 3-H), 2.83 (0.5H, dd, *J* = 10.7, 5.8 Hz, 2-H_b^{RotB}), 1.93-1.85 (0.5H, m, 4-H_a^{RotB}), 1.81-1.73 (0.5H, m, 4-H_b^{RotA}), 1.71-1.63 (0.5H, m, 4-H_a^{RotA}), 1.58-1.49 (0.5H, m, 4-H_b^{RotB}), 1.39 (4.5H, s, ^{t}Bu), 1.37 (4.5H, s, ^{t}Bu), 1.26 (3H, dd, *J* = 6.6, 4.1 Hz, ethyl 2-H_3); $^{13}C\{^1H\}$ NMR (d_6-DMSO, 125 MHz) δ 153.62, 153.56, 153.5, 153.4 (C=O), 146.2 (phenyl C-1), 128.6, 128.21, 128.15 (phenyl C-3 and C-5), 126.6 (phenyl C-4), 126.5 (phenyl C-2 and C-6), 78.04, 78.01, 77.96, 77.9 (^{t}Bu *C*), 55.9 (ethyl C-1), 55.63 (ethyl C-1), 55.61 (ethyl C-1), 55.0 (pyrrolidine C-3), 54.1 (pyrrolidine C-3), 54.0 (pyrrolidine C-3), 51.9 (pyrrolidine C-2^{RotB}), 51.7 (pyrrolidine C-2^{RotA}), 51.3 (pyrrolidine C-2^{RotB}), 51.0 (pyrrolidine C-2^{RotA}), 44.2, 44.1, 44.0, 43.9 (pyrrolidine C-5), 31.9 (pyrrolidine C-4^{RotB}), 31.2 (pyrrolidine C-4^{RotA}), 30.8 (pyrrolidine

C-4^{RotA}), 30.0 (pyrrolidine C-4^{RotB}), 28.18, 28.16 (^{t}Bu *C*H$_3$), 24.8, 24.7 (ethyl C-2) (36 signals of 52 expected observed); HRMS (ESI-TOF) m/z [M+H]$^+$ Calcd for $C_{17}H_{27}N_2O_2$ 291.2073; Found 291.2067.

***tert*-Butyl 3-(1-phenylethylamino)piperidine-1-carboxylate 195**

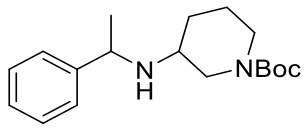

195

According to general procedure J, using methylbenzylamine (151 mg, 1.25 mmol) and tert-butyl-1,2,3,4-tetrahydropyridine-1-carboxylate (46 mg, 0.25 mmol). The solvent was evaporated under reduced pressure to give a crude product which contained a 50:50 mixture of diastereomeric products. The crude product was purified by flash chromatography eluting with 50:50 hexane-EtOAc to a give 50:50 mixture of diastereomers (16.0 mg, 21%) as a viscous yellow oil, R_f 0.17 (50:50 hexane-EtOAc); ν_{max}/cm^{-1} 2989, 1658, 1375, 1301, 1094, 752, 699; ^{1}H NMR ($CDCl_3$, 500 MHz) δ 7.35-7.29 (4H, m, phenyl 2-H, 3-H, 5-H and 6-H), 7.25-7.21 (1H, m, phenyl 4-H), 4.00-3.91 (1H, m, ethyl 1-H), 3.89-3.67 (1.5H, m, piperidine 2-H$_{a1}$, 2-H$_{a2}$ and 6-H$_a$), 3.64-3.53 (0.5H, m, piperidine 6-H$_a$), 3.05-2.96 (0.5H, m, piperidine 6-H$_b$), 2.95-2.86 (0.5H, br m, piperidine 2-H$_b$), 2.85-2.76 (0.5H, m, piperidine 6-H$_b$), 2.67-2.58 (0.5H, m, piperidine 2-H$_b$), 2.54-2.43 (0.5H, br m, piperidine 3-H), 2.43-2.31 (0.5H, br m, piperidine 3-H), 1.99-1.90 (0.5H, m, piperidine 4-H$_a$), 1.74-1.68 (0.5H, m, piperidine 4-H$_a$), 1.67-1.59 (1H, m, piperidine 5-H$_{a1}$ and 5-H$_{a2}$), 1.45 (4.5H, s, ^{t}Bu), 1.40 (4.5H, s, ^{t}Bu), 1.34 (3H, d, *J* = 6.5 Hz, ethyl 2-H$_3$), 1.42-1.31 (1.5H, m, piperidine 5-H$_{b1}$, 5-H$_{b2}$ and 4-H$_b$), 1.29-1.21 (0.5H, m, piperidine 4-H$_b$); ^{13}C{^{1}H} NMR ($CDCl_3$, 125 MHz) δ 155.0 (C=O), 146.0 (phenyl C-1), 128.6 (phenyl C-3 and C-5), 127.1 (phenyl C-4), 126.7, 126.6 (phenyl C-2 and C-6), 79.52 (^{t}Bu *C*), 79.49 (^{t}Bu *C*), 55.1 (ethyl C-1), 50.7 (piperidine C-3), 48.8 (piperidine C-2), 43.9 (piperidine C-6), 32.1, 31.3, 29.9, 29.1 (piperidine C-4), 28.60 (^{t}Bu *C*H$_3$), 28.56 (^{t}Bu *C*H$_3$), 25.1 (ethyl C-2), 23.7, 23.4 (piperidine C-5) (21 signals observed of 28 expected); HRMS (ESI-TOF) m/z [M+H]$^+$ Calcd for $C_{18}H_{29}N_2O_2$ 305.2224; Found 305.2224.

tert-Butyl 3-(1-naphthalen-1-ylethylamino)azetidine-1-carboxylate 196

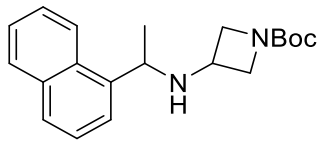

196

According to general procedure J, using 1-(1'-napthyl)ethylamine (200 µL, 1.25 mmol) and N-Boc azetine (39 mg, 0.25 mmol). The solvent was evaporated under reduced pressure and the crude product was purified by flash chromatography eluting with 90:10 DCM-EtOAc to yield **196** (53.1 mg, 65 %) as a pale-yellow viscous oil, R_f 0.62 (50:50 DCM-EtOAc); ν_{max}/cm^{-1} 2972, 1687, 1391, 1365, 1119, 777, 730; ^1H NMR ($CDCl_3$, 500 MHz) δ 8.16 (1H, d, *J* = 8.3 Hz, naphthyl 8-H), 7.89-7.85 (1H, m, naphthyl 5-H), 7.76 (1H, d, *J* = 8.2 Hz, naphthyl 4-H), 7.63 (1H, d, *J* = 6.7 Hz, naphthyl 2-H), 7.54-7.45 (3H, m, naphthyl 3-H, 6-H and 7-H), 4.63 (1H, q, *J* = 6.6 Hz, ethyl 1-H), 4.01 (1H, dd, *J* = 8.7, 6.9 Hz, 2-H_a), 3.97-3.93 (1H, m, 4-H_a), 3.70 (1H, dd, *J* = 8.8, 5.1 Hz, 2-H_b), 3.62-3.56 (1H, m, 4-H_b), 3.54 (1H, ddd, *J* = 10.5, 6.2, 3.5 Hz, 3-H), 1.74 (1H, br s, *N*H), 1.51 (3H, d, *J* = 6.6 Hz, ethyl 2-H_3), 1.41 (9H, s, ^{t}Bu); $^{13}C\{^1H\}$ ($CDCl_3$, 125 MHz) δ 156.4 (C=O), 140.4 (naphthyl C-1), 134.1 (naphthyl C-4a), 131.2 (naphthyl C-8a), 129.2 (naphthyl C-5), 127.7 (naphthyl C-4), 126.1 (naphthyl C-3, C-6 or C-7), 125.8 (naphthyl C-3, C-6 or C-7), 125.6 (naphthyl C-3, C-6 or C-7), 123.3 (naphthyl C-2), 122.8 (naphthyl C-8), 79.5 (^{t}Bu *C*), 57.7 (br s, C-2 and C-4), 51.6 (ethyl C-1), 46.3 (C-3), 28.5 (^{t}Bu *C*H_3), 23.6 (ethyl C-2); HRMS (ESI-TOF) m/z [M+H]+ Calcd for $C_{20}H_{27}N_2O_2$ 327.2067; Found 327.2063.

***tert*-Butyl-3-((1-(naphthalen-1-yl)ethyl)amino)pyrrolidine-1-carboxylate 197**

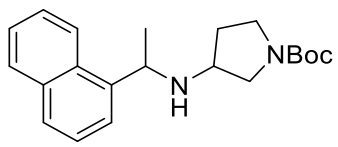

197

According to general procedure J, using 1-(1'-napthyl)ethylamine (200 µL, 1.25 mmol) and *N*-(*tert*-butoxycarbonyl)-2,3-dihydropyrrole (43 mg, 0.25 mmol). The

solvent was evaporated under reduced pressure to give a crude product which contained a 50:50 mixture of diastereomeric products. The crude product was purified by flash chromatography eluting with 50:50 DCM-EtOAc to give a 60:40 mixture of diastereomers (20.7 mg, 24 %) as a viscous yellow oil, R_f 0.31 (50:50 DCM-EtOAc); ν_{max}/cm^{-1} 2973, 1677, 1402, 1364, 1164, 1117, 777; ^1H NMR ($CDCl_3$, 500 MHz) δ 8.25-8.16 (1H, m, naphthyl 8-H), 7.88 (1H, br d, *J* = 7.5 Hz, naphthyl 5-H), 7.76 (1H, d, *J* = 8.1 Hz, naphthyl 4-H), 7.71-7.62 (1H, m, naphthyl 2-H), 7.56-7.44 (3H, m, naphthyl 3-H, 6-H and 7-H), 4.73 (0.4H, q, *J* = 6.6 Hz, ethyl 1-H), 4.68 (0.6H, q, *J* = 6.4 Hz, ethyl 1-H), 3.60-3.35 (2H, m, pyrrolidine 2-H_a and 5-H_a), 3.32-3.15 (2H, m, pyrrolidine 3-H and 2-H_b), 3.14-2.97 (1H, m, pyrrolidine 5-H_b), 2.04-1.90 (1H, m, pyrrolidine 4-H_a), 1.77-1.60 (1H, m, pyrrolidine 4-H_b), 1.55-1.47 (4H, m, ethyl 2-H_3 and N*H*), 1.47-1.40 (9H, s, ^{t}Bu); $^{13}C\{^1H\}$ ($CDCl_3$, 125 MHz) δ 154.8 (C=O), 141.1 (naphthyl C-1), 141.0 (naphthyl C-1), 134.1 (naphthyl C-4a), 131.3 (naphthyl C-8a), 129.2 (naphthyl C-5), 129.1 (naphthyl C-5), 127.5 (naphthyl C-4), 126.0, 125.83, 125.76, 125.6, 125.5 (naphthyl C-3, C-6 and C-7), 123.1 (naphthyl C-2), 122.9 (naphthyl C-8), 79.3 (^{t}Bu *C*), 79.2 (^{t}Bu *C*), 55.8 (pyrrolidine C-3), 55.7 (pyrrolidine C-3), 55.0 (pyrrolidine C-3), 54.8 (pyrrolidine C-3), 52.3 (ethyl C-1), 51.8 (pyrrolidine C-5), 44.6 (pyrrolidine C-2), 44.2 (pyrrolidine C-2), 32.8, 32.4, 32.1, 31.6, 28.66 (^{t}Bu *C*H_3), 28.63 (^{t}Bu *C*H_3), 24.5 (ethyl C-2), 24.4 (ethyl C-2), 24.3 (ethyl C-2), 24.0 (ethyl C-2) (35 signals of 38 expected observed); HRMS (ESI-TOF) m/z $[M+Na]^+$ Calcd for $C_{21}H_{28}N_2NaO_2$ 363.2043; Found 363.2038.

tert-Butyl 3-(1-naphthalen-1-ylethylamino)piperidine-1-carboxylate 198

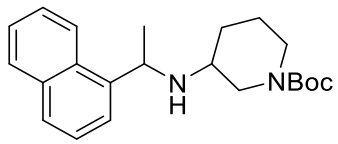

198

According to general procedure J, using 1-(1'-napthyl)ethylamine (200 µL, 1.25 mmol) and *tert*-butyl 1,2,3,4-tetrahydropyridine-1-carboxylate (46 mg, 0.25 mmol). The solvent was evaporated under reduced pressure to give a crude product which

contained a 50:50 mixture of diastereomeric products. The crude product was purified by flash chromatography eluting with 50:50 hexane-EtOAc to give an 50:50 mixture of diastereomers (8.5 mg, 10%) as a yellow viscous oil, R_f 0.31 (50:50 hexane-EtOAc); v_{max}/cm^{-1} 2972, 2930, 1684, 1420, 1364, 1238, 1149, 761, 700; ^1H NMR ($CDCl_3$, 500 MHz) δ 8.27-8.14 (1H, m, naphthyl 8-H), 7.87 (1H, d, *J* = 7.9 Hz, naphthyl 5-H), 7.75 (1H, d, *J* = 8.1 Hz, naphthyl 4-H), 7.73-7.65 (1H, br m, naphthyl 2-H), 7.55-7.43 (3H, m, naphthyl 3-H, 6-H and 7-H), 4.92-4.77 (1H, br m, ethyl 1-H), 3.94-3.66 (1.5H, m, piperidine 2-H_{a1}, 2-H_{a2}, 6-H_a), 3.60-3.46 (0.5H, m, piperidine 6-H_a), 3.15-3.00 (1H, m, piperidine 2-H_b and 6-H_b), 2.87-2.77 (0.5H, m, piperidine 6-H_b), 2.77-2.66 (0.5H, m, piperidine 2-H_b), 2.65-2.46 (1H, m, piperidine 3-H), 2.01-1.90 (0.5H, m, piperidine 4-H_a), 1.89-1.75 (0.5H, m, piperidine 4-H_a) 1.71-1.62 (1H, m, piperidine 5-H_a), 1.55-1.46 (3H, m, ethyl 2-H_3), 1.44-1.31 (9H, m, ^{t}Bu), 1.60-1.30 (2H, m, piperidine 4-H_b and 5-H_b); $^{13}C\{^1H\}$ ($CDCl_3$, 125 MHz) δ 155.0 (C=O), 134.1 (naphthyl C-4a), 131.4 (naphthyl C-8a), 131.2 (naphthyl C-8a), 129.2 (naphthyl C-5), 127.4 (naphthyl C-4), 126.1, 125.8, 125.5 (naphthyl C-3, C-6 and C-7), 123.1 (naphthyl C-2), 122.9 (naphthyl C-8), 79.5, 79.4 (^{t}Bu *C*), 51.0 (ethyl C-1 and piperidine C-3), 43.9 (piperidine C-2 and C-6), 28.5 (^{t}Bu *C*H_3), 24.6 (ethyl C-2), 23.8, 23.4 (piperidine C-4 and C-5) (19 signals of 40 expected observed); HRMS (ESI-TOF) m/z $[M+H]^+$ Calcd for $C_{22}H_{31}N_2O_2$ 355.2380; Found 355.2388.

1-(4-Bromophenyl)-*N*-(cyclohexylmethyl)ethanamine 268

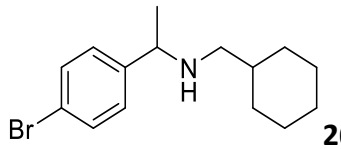

268

According to general procedure I, using 4-bromophenylethylamine (50.0 mg, 0.25 mmol) and methylenecyclohexane (72.0 mg, 0.75 mmol, 3.0 equiv). Upon completion of the reaction, the solvent was removed *via* rotary evaporation and the crude material was purified *via* column chromatography eluting with 50:50 EtOAc-hexane to give the title compound as a yellow oil (59.2 mg, 80%), R_f 0.41 (EtOAc); v_{max}/cm^{-1}

3021, 2918, 2848, 1447, 742; ^{1}H NMR ($CDCl_3$, 500 MHz) δ 7.46-7.41 (2H, m, phenyl 2-H and 6-H), 7.22-7.17 (2H, m, phenyl 3-H and 5-H), 3.70 (1H, q, *J* = 6.6 Hz, ethyl 1-H), 2.33 (1H, dd, *J* = 11.5, 6.2 Hz, methyl 1-H_a), 2.19 (1H, dd, *J* = 11.5, 7.1 Hz, methyl 1-H_b), 1.78-1.59 (4H, m, cyclohexyl 2-H_a, 3-H_a, 5-H_a and 6-H_a), 1.43-1.36 (1H, m, cyclohexyl 1-H), 1.31 (3H, d, *J* = 6.6 Hz, ethyl 2-H_3), 1.28-1.06 (4H, m, cyclohexyl 3-H_b, 4-H_2, 5-H_b), 0.96-0.77 (2H, m, cyclohexyl 2-H_b and 6-H_b); ^{13}C{^{1}H} NMR ($CDCl_3$, 125 MHz) δ 131.6 (phenyl C-3 and C-5), 128.6 (phenyl C-2 and C-6), 58.1 (ethyl C-1), 54.7 (methyl C-1), 38.2 (cyclohexyl C-1), 31.7, 31.6 (cyclohexyl C-2 and C-6), 29.9 (cyclohexyl C-4), 26.21, 26.16 (cyclohexyl C-3 and C-5), 24.6 (ethyl C-2); HRMS (ESI-TOF) m/z: $[M+H]^+$ Calcd for $C_{15}H_{23}BrN$ 296.1008; Found 296.1006.

***N*-(Cyclohexylmethyl)-2,3-dihydro-1H-inden-1-amine 269**

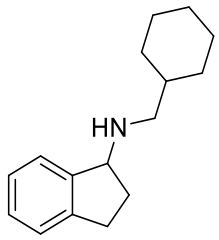

269

According to general procedure I, using 2,3-dihydro-1H-inden-1-amine (33.3 mg, 0.25 mmol) and methylenecyclohexane (72.0 mg, 0.75 mmol, 3.0 equiv). Upon completion of the reaction, the solvent was removed *via* rotary evaporation and the crude material was purified *via* column chromatography eluting with 50:50 EtOAc-hexane to yield **269** (10.9 mg, 19%) as a yellow oil, R_f 0.31 (EtOAc); v_{max}/cm^{-1} 2919, 2484, 1583, 1487, 1448, 1222, 751; ^{1}H NMR ($CDCl_3$, 500 MHz) δ 7.36-7.31 (1H, m, 4-H), 7.24-7.15 (3H, m,5-H, 6-H and 7-H), 4.22 (1H, t, *J* = 6.7 Hz, 1-H), 2.99 (1H, ddd, *J* = 15.8, 8.6, 4.6 Hz, 3-H_a), 2.80 (1H, dt, *J* = 15.8, 7.8 Hz, 3-H_b), 2.56 (1H, dd, *J* = 11.4, 6.5 Hz, methyl 1-H_a), 2.53 (1H, dd, *J* = 11.4, 6.7 Hz, methyl 1-H_b), 2.44-2.33 (1H, m, 2-H_a), 1.87-1.63 (5H, m, 2-H_b and cyclohexyl 2-H_a, 3-H_a, 5-H_a and 6-H_a), 1.59-1.40 (1H, m, cyclohexyl 1-H), 1.32-1.09 (4H, m, cyclohexyl 3-H_b, 4-H_2 and 5-H_b), 0.99-0.86 (2H, m, cyclohexyl 2-H_b and 6-H_b); ^{13}C{^{1}H} NMR ($CDCl_3$, 125 MHz) δ 145.7 (C-7_a), 143.8 (C-3_a), 127.4, 126.3 (C-5 and C-6), 124.9 (C-7), 124.2 (C-4), 63.6 (C-1), 54.3 (methyl C-1), 38.6

(cyclohexyl C-1), 33.7 (C-2), 31.8, 31.7 (cyclohexyl C-2 and C-6)), 30.5 (C-3), 26.9 (cyclohexyl C-4), 26.26, 26.24 (cyclohexyl C-3 and C-5); HRMS (ESI-TOF) m/z: $[M+H]^+$ Calcd for $C_{16}H_{24}N$ 230.1903; Found 230.1899.

_N_-(Cyclohexylmethyl)-3,4-dihydro-2H-chromen-4-amine 270

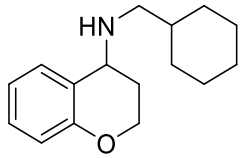

270

According to general procedure I, using chroman-4-ylamine (37.3 mg, 0.25 mmol) and methylenecyclohexane (72.0 mg, 0.75 mmol, 3.0 equiv). Upon completion of the reaction, the solvent was removed *via* rotary evaporation and the crude material was purified *via* column chromatography eluting with 25:75 EtOAc-hexane to give the title compound as a yellow oil (8.6 mg, 14%), R_f 0.68 (50:50 EtOAc-hexane); ν_{max}/cm^{-1} 3360, 2948, 2871, 1609, 1575, 1490, 1549, 1230, 749; ^1H NMR ($CDCl_3$, 500 MHz) δ 7.24 (1H, dd, *J* = 7.6, 1.5 Hz, 5-H), 7.16-7.11 (1H, m, 7-H), 6.87 (1H, ddd, *J* = 7.5, 7.4, 1.2 Hz, 6-H), 6.81 (1H, dd, *J* = 8.2, 1.0 Hz, 8-H), 4.33 (1H, ddd, *J* = 10.5, 10.4, 2.9 Hz, 2-H_a), 4.22-4.16 (1H, m, 2-H_b), 3.73 (1H, t, *J* = 4.2 Hz, 4-H), 2.55 (2H, d, *J* = 6.6 Hz, methyl 1-H_2), 2.04-1.90 (2H, m, 3-H_2), 1.86-1.79 (1H, m, cyclohexyl 2-H_a), 1.79-1.64 (3H, m, cyclohexyl 3-H_a, 5-H_a and 6-H_a), 1.49-1.39 (1H, m, cyclohexyl 1-H), 1.30-1.11 (4H, m, cyclohexyl 3-H_b, 4-H_2, 5-H_b), 1.01-0.87 (2H, m, cyclohexyl 2-H_b and 6-H_b); $^{13}C\{^1H\}$ NMR ($CDCl_3$, 125 MHz) δ 154.9 (C-8_a), 129.7 (C-5), 128.6 (C-7), 125.2 (C-4_a), 120.2 (C-6), 117.0 (C-8), 62.7 (C-2), 54.1 (methyl C-1), 51.5 (C-4), 38.5 (cyclohexyl C-1), 31.73, 31.69 (cyclohexyl C-2 and C-6), 27.7 (C-3), 26.9 (cyclohexyl C-4), 26.3, 26.2 (cyclohexyl C-3 and C-5); HRMS (ESI-TOF) m/z: $[M+H]^+$ Calcd for $C_{16}H_{24}NO$ 246.1852; Found 246.1849.

tert-Butyl 3-((2,4,6-triisopropylphenyl)thio)azetidine-1-carboxylate 244

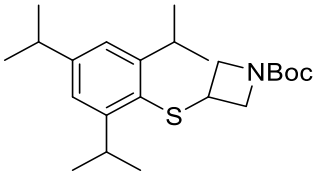

244

According to general procedure J, using methylbenzylamine (MBA) (151 mg, 1.25 mmol) and N-Boc azetine (39 mg, 0.25 mmol). Upon completion of the reaction, the solvent was removed via rotary evaporation and the crude material was purified via column chromatography eluting with 10:90 acetone-hexane to yield **244** (47.5 mg, 97%) as a yellow oil, R_f 0.61 (20:80 acetone-hexane); v_{max}/cm^{-1} 2960, 2871, 1703, 1388, 1364, 1127, 731; ^1H NMR ($CDCl_3$, 500 MHz) δ 7.01 (2H, s, aryl 3-H and 5-H), 4.17 (2H, app. t, *J* = 8.8 Hz, 2-H_a 4-H_a), 3.88 (2H, dd, *J* = 9.2, 5.8 Hz, 2-H_b 4-H_b), 3.84 (2H, hept, *J* = 6.9 Hz, 2,6-isopropyl 2-H_2), 3.57 (1H, tt, *J* = 8.1, 6.9 Hz, 3-H), 2.87 (1H, hept, *J* = 6.9 Hz, 4-isopropyl 2-H), 1.43 (9H, s, ^{t}Bu), 1.25 (6H, d, *J* = 6.9 Hz, 4-isopropyl 1-H_3 and 3-H_3) 1.22 (12H, d, *J* = 6.9 Hz, 2,6-isopropyl 1-H_3 and 3-H_3); $^{13}C\{^1H\}$ ($CDCl_3$, 125 MHz) δ 156.3 (C=O), 153.1 (aryl C-2 and C-6), 150.2 (aryl C-4), 127.1 (aryl C-1), 122.1 (aryl C-3 and C-5), 79.8 (^{t}Bu-*C*), 56.9 (br s, C-2 and C-4), 37.6 (C-3), 34.4 (4-isopropyl C-2), 31.8 (2,6-isopropyl C-2), 28.5 (^{t}Bu-*C*H_3), 24.5 (2,6-isopropyl C-1 and C-3), 24.0 (4-isopropyl C-1 and C-3); HRMS (ESI-TOF) m/z: $[M+H]^+$ Calcd for $C_{23}H_{38}NO_2S$ 392.2618; Found 392.2616.

1,2,3,4-Tetrahydronaphthalen-2-ol 281[342]

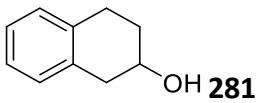

281

Sodium borohydride ($NaBH_4$) (257 mg, 6.8 mmol) was added portion wise to a solution of 1,2,3,4-tetrahydronaphthalen-2-one (500 mg, 3.4 mmol) in MeOH (5 mL) at 0 ºC. The solution was warmed to RT and stirred for 1h, after which the reaction was quenched with ice cold water (5 mL) and concentrated under reduced pressure. The crude mixture was then diluted with water and extracted with EtOAc (x2). The

combined organic layers were dried over $MgSO_4$ and concentrated to yield **281** (448 mg, 89%) as a dark yellow oil, ν_{max}/cm^{-1} 3321, 2924, 1581, 1495, 1038, 741; ^1H NMR ($CDCl_3$, 500 MHz) δ 7.15-7.12 (1H, m, 6-H), 7.12-7.07 (3H, m, 5-H, 7-H and 8-H), 4.17 (1H, dddd, *J* = 9.7, 8.0, 5.8, 4.6 Hz, 2-H), 3.10 (1H, dd, *J* = 16.3, 4.6 Hz, 3-H_a), 2.97 (1H, dt, *J* = 17.0, 5.7 Hz, 1-H_a), 2.85 (1H, m, 1-H_b), 2.78 (1H, dd, *J* = 16.4, 7.9 Hz, 3-H_b), 2.07 (1H, m, 4-H_a), 1.83 (1H, m, 4-H_b), 1.75 (1H, s, O*H*); $^{13}C\{^1H\}$ ($CDCl_3$, 125 MHz) δ 135.8 (C-8a), 134.4 (C-4a), 129.6 (C-5 or C-8), 128.7, 126.1 (C-6 or C-7), 126.0 (C-6 or C-7), 67.4 (C-2), 38.5 (C-3), 31.6 (C-4), 27.1 (C-1); HRMS (ESI-TOF) m/z: [M+Na]+ Calcd for $C_{10}H_{12}NaO$ 171.0780; Found 171.0776.

6.6.4 Continuous kinetic resolution/hydroaminations

***(S)-N*-(Cyclopentylmethyl)-1-phenylethanamine *(S)*-221**

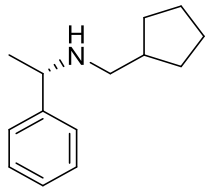

(S)-221

The reaction was set up following general procedure M, using methylbenzylamine and methylenecyclopentane. An aliquot was taken for analysis at steady state, conversion was determined from the crude mixture by ^1H NMR before the crude material was purified by column chromatography eluting with 50:50 EtOAc-hexane to give an isolated yield of 47% (38.0 mg) as a yellow oil; $[\alpha]_D^{20}$ -34.8 (*c* 1.00, MeOH, >99% *ee*) [lit.:[343] $[\alpha]_D^{24}$ -36.0 (c 1.00, CH_2Cl_2)]; spectroscopically identical to the racemate previously prepared. Chiral HPLC was performed with a ChiralPak AD-RH column (250 x 4.6 mm), 50% MeCN (0.1% DEA) in water (0.1% DEA), 15 min run time (***(S)*-221** 8.84 min, ***(R)*-221** 10.72min).

***(S)-N*-(Cyclopentylmethyl)-1-naphthalen-1-ylethanamine *(S)*-222**

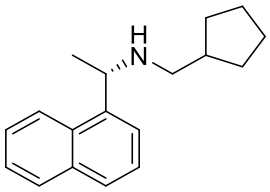

(S)-222

The reaction was set up following general procedure M, using 1-(1-naphthyl)ethylamine and methylenecyclopentane. An aliquot was taken for analysis at steady state, conversion was determined from the crude mixture by ^{1}H NMR before the crude material was purified by column chromatography eluting with 50:50 EtOAc-hexane to give an isolated yield of 32% (31.7 mg) as a yellow oil; $[\alpha]_D^{20}$ -23.8 (*c* 1.00, MeOH, 97% *ee*); spectroscopically identical to the racemate previously prepared. Chiral HPLC was performed with a ChiralPak AS-RH column (250 x 4.6 mm), 40% MeCN (0.1% DEA) in water (0.1% DEA), 20 min run time (***(S)*-222** 11.41 min, ***(R)*-222** 13.28 min).

***(S)*-*N*-(Cyclohexylmethyl)-1-phenylethanamine *(S)*-224**

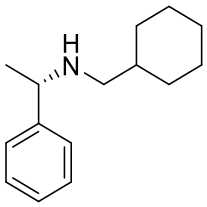

(S)-224

The reaction was set up following general procedure M, using methylbenzylamine and methylenecyclohexane. An aliquot was taken for analysis at steady state, conversion was determined from the crude mixture by ^{1}H NMR before the crude material was purified by column chromatography eluting with 50:50 EtOAc-hexane to give an isolated yield of 43% (37.1 mg) as a yellow oil; $[\alpha]_D^{20}$ -27.9 (*c* 1.00, MeOH, xx% *ee*) [lit.:[343] $[\alpha]_D^{24}$ -30.6 (c 1.00, CH_2Cl_2)]; spectroscopically identical to the racemate previously prepared. Chiral HPLC was performed with a ChiralPak AS-RH column (250 x 4.6 mm), 40% MeCN (0.1% DEA) in water (0.1% DEA), 20 min run time (***(S)*-224** 5.74 min, ***(R)*-224** 5.15 min).

***(S)*-*N*-(Cyclohexylmethyl)-1-naphthalen-1-ylethanamine *(S)*-225**

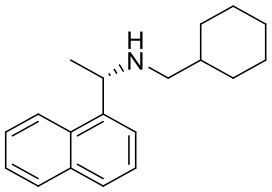

***(S)*-225**

The reaction was set up following general procedure M, using 1-(1-naphthyl)ethylamine and methylenecyclohexane. An aliquot was taken for analysis at steady state, conversion was determined from the crude mixture by ^{1}H NMR before the crude material was purified by column chromatography eluting with 50:50 EtOAc-hexane to give an isolated yield of 25% (26.5 mg) as a yellow oil; $[\alpha]_D^{20}$ -32.3 (*c* 1.00, MeOH, xx% *ee*); spectroscopically identical to the racemate previously prepared. Chiral HPLC was performed with a ChiralCel OD-RH column (250 x 4.6 mm), 40% MeCN (0.1% DEA) in water (0.1% DEA), 20 min run time (***(S)*-225** 13.06 min, ***(R)*-225** 14.40 min).

***(S)*-*N*-(1-Phenylethyl)cyclohexanamine *(S)*-227**

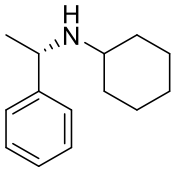

***(S)*-227**

The reaction was set up following general procedure M, using methylbenzylamine and cyclohexene. An aliquot was taken for analysis at steady state, conversion was determined from the crude mixture by ^{1}H NMR before the crude material was purified by column chromatography eluting with 50:50 EtOAc-hexane to give an isolated yield of 47% (38.0 mg) as a yellow oil; $[\alpha]_D^{20}$ -66.3 (*c* 1.00, MeOH, 97% *ee*) [lit.:[344] $[\alpha]_D^{25}$ -68.8 (c 1.00, CH_2Cl_2)]; spectroscopically identical to the racemate previously prepared. Chiral HPLC was performed with a ChiralPak AS-RH column (250 x 4.6 mm), 40% MeCN (0.1% DEA) in water (0.1% DEA), 20 min run time (***(S)*-227** 9.28 min, ***(R)*-227** 10.48min).

***(S)*-*N*-[1-(Naphthalen-2-yl)ethyl]cyclohexanamine *(S)*-228**

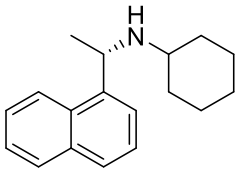

***(S)*-228**

The reaction was set up following general procedure M, using 1-(1-naphthyl)ethylamine and cyclohexene. An aliquot was taken for analysis at steady state, conversion was determined from the crude mixture by ^{1}H NMR before the crude material was purified by column chromatography eluting with 50:50 EtOAc-hexane to give an isolated yield of 18% (18.2 mg) as a yellow oil; $[\alpha]_D^{20}$ -35.1 (*c* 1.00, MeOH, 96% *ee*); spectroscopically identical to the racemate previously prepared. Chiral HPLC was performed with a ChiralCel OD-RH column (250 x 4.6 mm), 40% MeCN (0.1% DEA) in water (0.1% DEA), 20 min run time (***(S)*-228** 8.61 min, ***(R)*-228** 9.17 min).

***(S)*-*N*-[2-(4-Methoxyphenyl)ethyl]-1-phenylethanamine *(S)*-230**

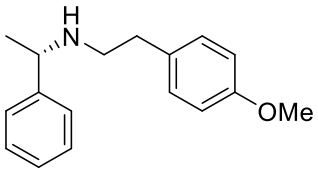

***(S)*-230**

The reaction was set up following general procedure M, using methylbenzylamine and 4-vinyl anisole. An aliquot was taken for analysis at steady state, conversion was determined from the crude mixture by ^{1}H NMR before the crude material was purified by column chromatography eluting with 50:50 EtOAc-hexane to give an isolated yield of 31% (31.4 mg) as a yellow oil; $[\alpha]_D^{20}$ -38.0 (*c* 1.00, MeOH, xx% *ee*) [lit.:[343] $[\alpha]_D^{24}$ -16.4 (c 0.0073, CH_2Cl_2)]; spectroscopically identical to the racemate previously prepared. Chiral HPLC was performed with a ChiralPak AS-RH column (250 x 4.6 mm), 40% MeCN (0.1% DEA) in water (0.1% DEA), 20 min run time (***(S)*-230** 17.42 min, ***(R)*-230** 13.41 min).

***(S)*-*N*-[2-(4-Methoxyphenyl)ethyl]-1-naphthalen-1-ylethanamine *(S)*-231**

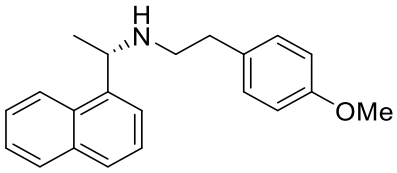

***(S)*-231**

The reaction was set up following general procedure M, using 1-(1-naphthyl)ethylamine and 4-vinyl anisole. An aliquot was taken for analysis at steady state, conversion was determined from the crude mixture by ^{1}H NMR before the crude material was purified by column chromatography eluting with 50:50 EtOAc-hexane to give an isolated yield of 23% (27.7 mg) as a yellow oil; $[\alpha]_D^{20}$ -24.9 (*c* 1.00, MeOH, xx% *ee*); spectroscopically identical to the racemate previously prepared. Chiral HPLC was performed with a ChiralPak AD-RH column (250 x 4.6 mm), 40% MeCN (0.1% DEA) in water (0.1% DEA), 20 min run time (***(S)*-231** 6.43 min, ***(R)*-231** 7.64 min).

***(S)*-*N*-(3-Phenylpropyl)-1-phenylethylamine *(S)*-233**

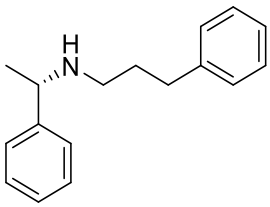

***(S)*-233**

The reaction was set up following general procedure M, using methylbenzylamine and allylbenzene. An aliquot was taken for analysis at steady state, conversion was determined from the crude mixture by ^{1}H NMR before the crude material was purified by column chromatography eluting with 50:50 EtOAc-hexane to give an isolated yield of 23% (21.7 mg) as a yellow oil; $[\alpha]_D^{20}$ -36.8 (*c* 1.00, MeOH, 98% *ee*) lit. $[\alpha]_D$ -40.0 (c 1.10, $CHCl_3$)[36]; spectroscopically identical to the racemate previously prepared. Chiral HPLC was performed with a ChiralPak AS-RH column (250 x 4.6 mm), 45% MeCN (0.1% DEA) in water (0.1% DEA), 20 min run time (***(S)*-233** 7.29 min, ***(R)*-233** 7.91 min).

***(S)*-*N*-(3-Phenylpropyl)-1-(1-naphthyl)ethylamine *(S)*-234**

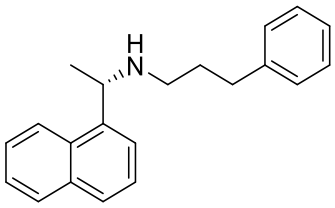

***(S)*-234**

The reaction was set up following general procedure M, using 1-(1-naphthyl)ethylamine and allylbenzene. An aliquot was taken for analysis at steady state, conversion was determined from the crude mixture by ^{1}H NMR before the crude material was purified by column chromatography eluting with 50:50 EtOAc-hexane to give an isolated yield of 12% (14.2 mg) as a yellow oil; $[\alpha]_D^{20}$ -28.2 (*c* 1.00, MeOH, >99% *ee*); spectroscopically identical to the racemate previously prepared. Chiral HPLC was performed with a ChiralCel OD-RH column (250 x 4.6 mm), 40% MeCN (0.1% DEA) in water (0.1% DEA), 20 min run time (***(S)*-234** 10.81 min, ***(R)*-234** 9.12 min).

***(S)*-*N*-(1-Phenylethyl)-3-(3-(trifluoromethyl)phenyl)propan-1-amine *(S)*-186**

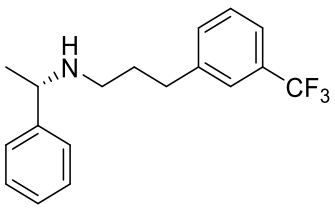

***(S)*-186**

The reaction was set up following general procedure M, using methylbenzylamine and 3-[(3-trifluoromethyl)phenyl]-1-propene. An aliquot was taken for analysis at steady state, conversion was determined from the crude mixture by ^{1}H NMR before the crude material was purified by column chromatography eluting with 20:80 EtOAc-hexane to give an isolated yield of 11% (13.5 mg) as a yellow oil; $[\alpha]_D^{20}$ -21.2 (*c* 1.00, MeOH, 97% *ee*); spectroscopically identical to the racemate previously prepared. Chiral HPLC was performed with a ChiralCel OD-RH column (250 x 4.6 mm), 30% MeCN (0.1% DEA) in water (0.1% DEA), 20 min run time (***(S)*-186** 10.16 min, ***(R)*-186** 11.12 min).

***(S)*-*N*-(1-(naphthalen-1-yl)ethyl)-3-(3-(trifluoromethyl)phenyl)propan-1-amine *(S)*-10 (cinacalcet)**

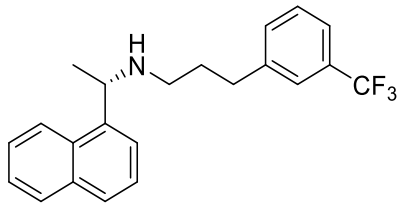

***(S)*-10**

The reaction was set up following general procedure M, using 1-(1-naphthyl)ethylamine and 3-[(3-Trifluoromethyl)phenyl]-1-propene. An aliquot was taken for analysis at steady state, conversion was determined from the crude mixture by ^{1}H NMR before the crude material was purified by column chromatography eluting with 20:80 EtOAc-hexane to give an isolated yield of 5% (7.1 mg) as a yellow oil; $[\alpha]_D^{20}$ -18.6 (*c* 1.00, MeOH, >99% *ee*) lit. $[\alpha]_D$ -23.0 (c 1.30, CH_2Cl_2)[345]; spectroscopically identical to the racemate previously prepared. Chiral HPLC was performed with a ChiralCel OD-RH column (250 x 4.6 mm), 40% MeCN (0.1% DEA) in water (0.1% DEA), 20 min run time (***(S)*-10** 12.32 min, ***(R)*-10** 11.19 min).

***N*-(*tert*-Butoxycarbonyl)-3-(1-phenylethyl)aminopyrrolidine 194**

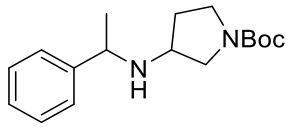

194

The reaction was set up following general procedure M, using methylbenzylamine and *N*-(*tert*-butoxycarbonyl)-2,3-dihydropyrrole. An aliquot was taken for analysis at steady state, conversion was determined from the crude mixture by ^{1}H NMR before the crude material was purified by column chromatography eluting with 50:50 EtOAc-hexane to give a 50:50 mixture of diastereomers with each diastereomer appearing as a 50:50 mixture of rotamers in an isolated yield of 32% (37.1 mg) as a viscous yellow oil, R_f 0.18 (50:50 hexane-EtOAc); spectroscopically identical to the racemate previously prepared.

***tert*-Butyl-3-((1-(naphthalen-1-yl)ethyl)amino)pyrrolidine-1-carboxylate 197**

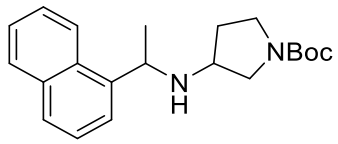

197

The reaction was set up following general procedure M, using 1-(1-naphthyl)ethylamine and *N*-(*tert*-butoxycarbonyl)-2,3-dihydropyrrole. An aliquot was taken for analysis at steady state, conversion was determined from the crude mixture by ^{1}H NMR before the crude material was purified by column chromatography eluting with 50:50 DCM-EtOAc to give a 50:50 mixture of diastereomers in an isolated yield of 18% (24.5 mg) as a viscous yellow oil, R_f 0.31 (50:50 DCM-EtOAc); spectroscopically identical to the racemate previously prepared.

***tert*-Butyl 3-(1-phenylethylamino)piperidine-1-carboxylate 195**

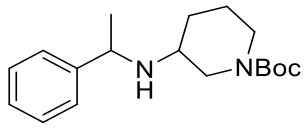

195

The reaction was set up following general procedure M, using methylbenzylamine and tert-butyl-1,2,3,4-tetrahydropyridine-1-carboxylate. An aliquot was taken for analysis at steady state, conversion was determined from the crude mixture by ^{1}H NMR before the crude material was purified by column chromatography eluting with50:50 hexane-EtOAc to give a 50:50 mixture of diastereomers in an isolated yield of 28% (34.0 mg) as a viscous yellow oil, R_f 0.17 (50:50 hexane-EtOAc); spectroscopically identical to the racemate previously prepared.

***tert*-Butyl 3-(1-naphthalen-1-ylethylamino)piperidine-1-carboxylate 198**

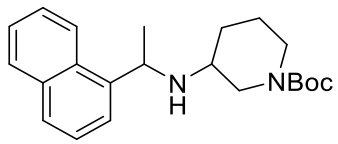

198

The reaction was set up following general procedure M, using 1-(1-naphthyl)ethylamine and tert-butyl-1,2,3,4-tetrahydropyridine-1-carboxylate. An aliquot was taken for analysis at steady state, conversion was determined from the crude mixture by ^{1}H NMR before the crude material was purified by column chromatography eluting with 50:50 hexane-EtOAc to give a 50:50 mixture of diastereomers in an isolated yield of 15% (21.2 mg) as a viscous yellow oil, R_f 0.31 (50:50 hexane-EtOAc); spectroscopically identical to the racemate previously prepared.

6.6.5 Continuous transaminase/hydroaminations

***(S)*-*N*-(Cyclopentylmethyl)-1-phenylethanamine *(S)*-221**

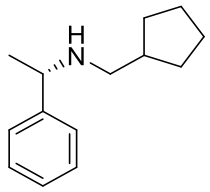

***(S)*-221**

The reaction was set up following general procedure N, using acetophenone and methylenecyclopentane. An aliquot was taken for analysis at steady state, conversion was determined from the crude mixture by ^{1}H NMR before the crude material was purified by column chromatography eluting with 50:50 EtOAc-hexane to give an isolated yield of 73% (29.6 mg) as a yellow oil; $[\alpha]_D^{20}$ -34.8 (*c* 1.00, MeOH, 95% *ee*) [lit.:[343] $[\alpha]_D^{24}$ -36.0 (c 1.00, CH_2Cl_2)]; spectroscopically identical to the racemate previously prepared. Chiral HPLC was performed with a ChiralPak AD-RH column (250 x 4.6 mm), 50% MeCN (0.1% DEA) in water (0.1% DEA), 15 min run time (***(S)*-221** 8.84 min, ***(R)*-221** 10.72min).

***(S)*-*N*-(Cyclopentylmethyl)-1-naphthalen-1-ylethanamine *(S)*-222**

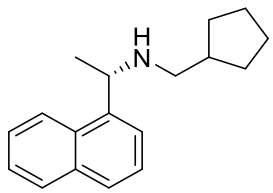

***(S)*-222**

The reaction was set up following general procedure N, using 1'-acetonaphthone and methylenecyclopentane. An aliquot was taken for analysis at steady state, conversion was determined from the crude mixture by ^{1}H NMR before the crude material was purified by column chromatography eluting with 50:50 EtOAc-hexane to give an isolated yield of 61% (30.9 mg) as a yellow oil; $[\alpha]_D^{20}$ -23.8 (*c* 1.00, MeOH, 95% *ee*); spectroscopically identical to the racemate previously prepared. Chiral HPLC was performed with a ChiralPak AS-RH column (250 x 4.6 mm), 40% MeCN (0.1% DEA) in water (0.1% DEA), 20 min run time (***(S)*-222** 11.41 min, ***(R)*-222** 13.28 min).

***(S)*-*N*-(Cyclohexylmethyl)-1-phenylethanamine *(S)*-224**

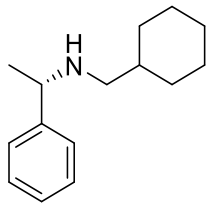

***(S)*-224**

The reaction was set up following general procedure N, using acetophenone and methylenecyclohexane. An aliquot was taken for analysis at steady state, conversion was determined from the crude mixture by ^{1}H NMR before the crude material was purified by column chromatography eluting with 50:50 EtOAc-hexane to give an isolated yield of 61% (26.5 mg) as a yellow oil; $[\alpha]_D^{20}$ -27.9 (*c* 1.00, MeOH, xx% *ee*) [lit.:[343] $[\alpha]_D^{24}$ -30.6 (c 1.00, CH_2Cl_2)]; spectroscopically identical to the racemate previously prepared. Chiral HPLC was performed with a ChiralPak AS-RH column (250 x 4.6 mm), 40% MeCN (0.1% DEA) in water (0.1% DEA), 20 min run time (***(S)*-224** 5.74 min, ***(R)*-224** 5.15 min).

***(S)*-*N*-(Cyclohexylmethyl)-1-naphthalen-1-ylethanamine *(S)*-225**

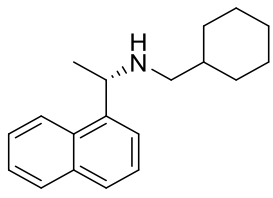

***(S)*-225**

The reaction was set up following general procedure N, using 1'-acetonaphthone and methylenecyclohexane. An aliquot was taken for analysis at steady state, conversion was determined from the crude mixture by ^{1}H NMR before the crude material was purified by column chromatography eluting with 50:50 EtOAc-hexane to give an isolated yield of 39% (20.8 mg) as a yellow oil; $[\alpha]_D^{20}$ -32.3 (*c* 1.00, MeOH, xx% *ee*); spectroscopically identical to the racemate previously prepared. Chiral HPLC was performed with a ChiralCel OD-RH column (250 x 4.6 mm), 40% MeCN (0.1% DEA) in water (0.1% DEA), 20 min run time (***(S)*-225** 13.06 min, ***(R)*-225** 14.40 min).

***(S)*-*N*-(1-Phenylethyl)cyclohexanamine *(S)*-227**

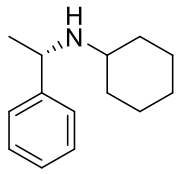

***(S)*-227**

The reaction was set up following general procedure N, using acetophenone and cyclohexene. An aliquot was taken for analysis at steady state, conversion was determined from the crude mixture by ^{1}H NMR before the crude material was purified by column chromatography eluting with 50:50 EtOAc-hexane to give an isolated yield of 40% (16.2 mg) as a yellow oil; $[\alpha]_D^{20}$ -66.3 (*c* 1.00, MeOH, 97% *ee*) [lit.:[344] $[\alpha]_D^{25}$ -68.8 (c 1.00, CH_2Cl_2)]; spectroscopically identical to the racemate previously prepared. Chiral HPLC was performed with a ChiralPak AS-RH column (250 x 4.6 mm), 40% MeCN (0.1% DEA) in water (0.1% DEA), 20 min run time (***(S)*-227** 9.28 min, ***(R)*-227** 10.48min).

***(S)*-*N*-[1-(Naphthalen-2-yl)ethyl]cyclohexanamine *(S)*-228**

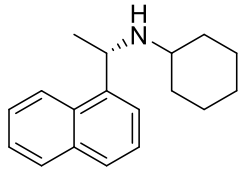

***(S)*-228**

The reaction was set up following general procedure N, using 1'-acetonaphthone and cyclohexene. An aliquot was taken for analysis at steady state, conversion was determined from the crude mixture by ^{1}H NMR before the crude material was purified by column chromatography eluting with 50:50 EtOAc-hexane to give an isolated yield of 34% (17.2 mg) as a yellow oil; $[\alpha]_D^{20}$ -35.1 (*c* 1.00, MeOH, 96% *ee*); spectroscopically identical to the racemate previously prepared. Chiral HPLC was performed with a ChiralCel OD-RH column (250 x 4.6 mm), 40% MeCN (0.1% DEA) in water (0.1% DEA), 20 min run time (***(S)*-228** 8.61 min, ***(R)*-228** 9.17 min).

***(S)*-*N*-[2-(4-Methoxyphenyl)ethyl]-1-phenylethanamine *(S)*-230**

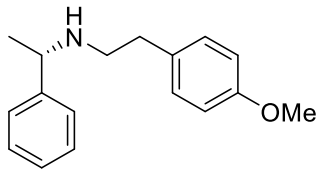

***(S)*-230**

The reaction was set up following general procedure N, using acetophenone and 4-vinyl anisole. An aliquot was taken for analysis at steady state, conversion was determined from the crude mixture by ^{1}H NMR before the crude material was purified by column chromatography eluting with 50:50 EtOAc-hexane to give an isolated yield of 42% (21.4 mg) as a yellow oil; $[\alpha]_D^{20}$ -38.0 (*c* 1.00, MeOH, xx% *ee*) [lit.:[343] $[\alpha]_D^{24}$ -16.4 (c 0.0073, CH_2Cl_2)]; spectroscopically identical to the racemate previously prepared. Chiral HPLC was performed with a ChiralPak AS-RH column (250 x 4.6 mm), 40% MeCN (0.1% DEA) in water (0.1% DEA), 20 min run time (***(S)*-230** 17.42 min, ***(R)*-230** 13.41 min).

***(S)*-*N*-[2-(4-Methoxyphenyl)ethyl]-1-naphthalen-1-ylethanamine *(S)*-231**

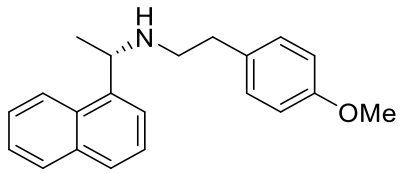

***(S)*-231**

The reaction was set up following general procedure N, using 1'-acetonaphthone and 4-vinyl anisole. An aliquot was taken for analysis at steady state, conversion was determined from the crude mixture by ^{1}H NMR before the crude material was purified by column chromatography eluting with 50:50 EtOAc-hexane to give an isolated yield of 34% (20.7 mg) as a yellow oil; $[\alpha]_D^{20}$ -xx.x (*c* 1.00, MeOH, xx% *ee*); spectroscopically identical to the racemate previously prepared. Chiral HPLC was performed with a ChiralPak AD-RH column (250 x 4.6 mm), 40% MeCN (0.1% DEA) in water (0.1% DEA), 20 min run time (***(S)*-231** 6.43 min, ***(R)*-231** 7.64 min).

***(S)*-*N*-(1-Phenylethyl)-3-(3-(trifluoromethyl)phenyl)propan-1-amine *(S)*-186**

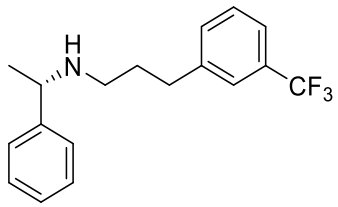

***(S)*-186**

The reaction was set up following general procedure N, using acetophenone and 3-[(3-trifluoromethyl)phenyl]-1-propene. An aliquot was taken for analysis at steady state, conversion was determined from the crude mixture by ^{1}H NMR before the crude material was purified by column chromatography eluting with 20:80 EtOAc-hexane to give an isolated yield of 16% (9.8 mg) as a yellow oil; $[\alpha]_D^{20}$ -21.2 (*c* 1.00, MeOH, 97% *ee*); spectroscopically identical to the racemate previously prepared. Chiral HPLC was performed with a ChiralCel OD-RH column (250 x 4.6 mm), 30% MeCN (0.1% DEA) in water (0.1% DEA), 20 min run time (***(S)*-186** 10.16 min, ***(R)*-186** 11.12 min).

***(S)*-*N*-(1-(Naphthalen-1-yl)ethyl)-3-(3-(trifluoromethyl)phenyl)propan-1-amine *(S)*-10 (cinacalcet)**

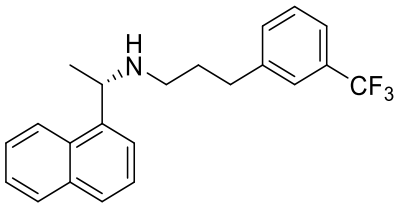

***(S)*-10**

The reaction was set up following general procedure N, using 1'-acetonaphthone and 3-[(3-Trifluoromethyl)phenyl]-1-propene. An aliquot was taken for analysis at steady state, conversion was determined from the crude mixture by ^{1}H NMR before the crude material was purified by column chromatography eluting with 20:80 EtOAc-hexane to give an isolated yield of 8% (5.7 mg) as a yellow oil; $[\alpha]_D^{20}$ -18.6 (*c* 1.00, MeOH, 96% *ee*) lit. $[\alpha]_D$ -23.0 (c 1.30, CH_2Cl_2)[345]; spectroscopically identical to the racemate previously prepared. Chiral HPLC was performed with a ChiralCel OD-RH column (250 x 4.6 mm), 40% MeCN (0.1% DEA) in water (0.1% DEA), 20 min run time (***(S)*-10** 12.32 min, ***(R)*-10** 11.19 min).

***N*-(*tert*-Butoxycarbonyl)-3-(1-Phenylethyl)aminopyrrolidine 194**

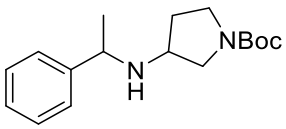

194

The reaction was set up following general procedure N, using acetophenone and *N*-(*tert*-butoxycarbonyl)-2,3-dihydropyrrole. An aliquot was taken for analysis at steady state, conversion was determined from the crude mixture by ^{1}H NMR before the crude material was purified by column chromatography eluting with 50:50 EtOAc-hexane to give a 50:50 mixture of diastereomers with each diastereomer appearing as a 50:50 mixture of rotamers in an isolated yield of 36% (20.9 mg) as a viscous yellow oil, R_f 0.18 (50:50 hexane-EtOAc); spectroscopically identical to the racemate previously prepared.

***tert*-Butyl-3-((1-(Naphthalen-1-yl)ethyl)amino)pyrrolidine-1-carboxylate 197**

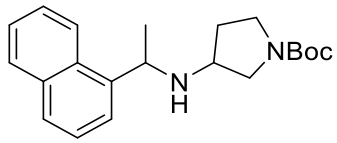

197

The reaction was set up following general procedure N, using 1'-acetonaphthone and *N*-(*tert*-butoxycarbonyl)-2,3-dihydropyrrole. An aliquot was taken for analysis at steady state, conversion was determined from the crude mixture by ^{1}H NMR before the crude material was purified by column chromatography eluting with 50:50 DCM-EtOAc to give a 50:50 mixture of diastereomers in an isolated yield of 22% (15.0 mg) as a viscous yellow oil, R_f 0.31 (50:50 DCM-EtOAc); spectroscopically identical to the racemate previously prepared.

1-(4-Bromophenyl)-*N*-(cyclohexylmethyl)ethanamine 274

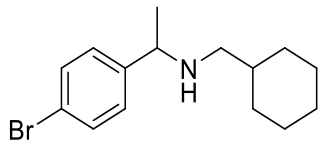

274

The reaction was set up following general procedure N, using 4-bromoacetophenone and methylenecyclohexane. An aliquot was taken for analysis at steady state, conversion was determined from the crude mixture by ^{1}H NMR before the crude material was purified by column chromatography eluting with 50:50 EtOAc-hexane to give an isolated yield of 42% (24.9 mg) as a yellow oil, R_f 0.41 (EtOAc); spectroscopically identical to the racemate previously prepared.

***N*-(Cyclohexylmethyl)-2,3-dihydro-1H-inden-1-amine 275**

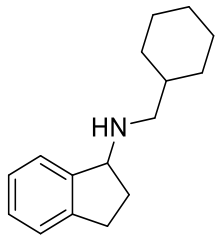

275

The reaction was set up following general procedure N, using 1-indanone and methylenecyclohexane. An aliquot was taken for analysis at steady state, conversion was determined from the crude mixture by ^{1}H NMR before the crude material was purified by column chromatography eluting with 50:50 EtOAc-hexane to give an isolated yield of 15% (6.9 mg) as a yellow oil, R_f 0.31 (EtOAc); spectroscopically identical to the racemate previously prepared.

***N*-(Cyclohexylmethyl)-3,4-dihydro-2H-chromen-4-amine 276**

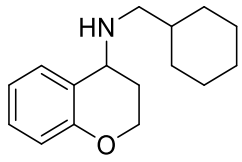

276

The reaction was set up following general procedure N, using 4-chromanone and methylenecyclohexane. An aliquot was taken for analysis at steady state, conversion was determined from the crude mixture by ^{1}H NMR before the crude material was purified by column chromatography eluting with 25:75 EtOAc-hexane to give an isolated yield of 9% (4.4 mg) as a yellow oil, R_f 0.68 (50:50 EtOAc-hexane); spectroscopically identical to the racemate previously prepared.

References

1. J. H. Schrittwieser, S. Velikogne, M. Hall and W. Kroutil, *Chem. Rev.*, 2018, **118**, 270-348.
2. A. D. Clayton, R. Labes and A. J. Blacker, *Current Opinion in Green and Sustainable Chemistry*, 2020, **26**.
3. T. C. Nugent and M. El-Shazly, *Advanced Synthesis & Catalysis*, 2010, **352**, 753-819.
4. A. Cabre, X. Verdaguer and A. Riera, *Chem. Rev.*, 2022, **122**, 269-339.
5. M. Höhne and U. T. Bornscheuer, *ChemCatChem*, 2009, **1**, 42-51.
6. R. Kadyrov, T. H. Riermeier, U. Dingerdissen, V. Tararov and A. Borner, *The Journal of Organic Chemistry*, 2003, **68**, 4067-4070.
7. Z. Wu, W. Wang, H. Guo, G. Gao, H. Huang and M. Chang, *Nature Communications*, 2022, **13**, 3344.
8. G. K. M. Verzijl, C. Schuster, T. Dax, A. H. M. de Vries and L. Lefort, *Organic Process Research & Development*, 2018, **22**, 1817-1822.
9. H. Huang, Y. Zhao, Y. Yang, L. Zhou and M. Chang, *Organic Letters*, 2017, **19**, 1942-1945.
10. H. Huang, X. Liu, L. Zhou, M. Chang and X. Zhang, *Angewandte Chemie International Edition*, 2016, **55**, 5309-5312.
11. E. Salomo, A. Gallen, G. Sciortino, G. Ujaque, A. Grabulosa, A. Lledos, A. Riera and X. Verdaguer, *Journal of the American Chemical Society*, 2018, **140**, 16967-16970.
12. Z. Han, Z. Wang, X. Zhang and K. Ding, *Angewandte Chemie International Edition*, 2009, **48**, 5345-5349.
13. A. Ros, A. Magriz, H. Dietrich, M. Ford, R. Fernández and J. M. Lassaletta, *Advanced Synthesis & Catalysis*, 2005, **347**, 1917-1920.
14. P. Schnider, G. Koch, R. Prétôt, G. Wang, F. M. Bohnen, C. Krüger and A. Pfaltz, *Chemistry: A European Journal*, 1997, **3**, 887-892.
15. M. P. Thompson, S. R. Derrington, R. S. Heath, J. L. Porter, J. Mangas-Sanchez, P. N. Devine, M. D. Truppo and N. J. Turner, *Tetrahedron*, 2019, **75**, 327-334.
16. J. M. Woodley, *Current Opinion in Green and Sustainable Chemistry*, 2020, **21**, 22-26.
17. J. Puetz and F. M. Wurm, *Processes*, 2019, **7**.
18. R. A. Sheldon and J. M. Woodley, *Chem. Rev.*, 2018, **118**, 801-838.
19. M. P. Thompson, I. Peñafiel, S. C. Cosgrove and N. J. Turner, *Organic Process Research & Development*, 2018, **23**, 9-18.
20. E. L. Bell, W. Finnigan, S. P. France, A. P. Green, M. A. Hayes, L. J. Hepworth, S. L. Lovelock, H. Niikura, S. Osuna, E. Romero, K. S. Ryan, N. J. Turner and S. L. Flitsch, *Nature Reviews Methods Primers*, 2021, **1**.
21. S. Basler, S. Studer, Y. Zou, T. Mori, Y. Ota, A. Camus, H. A. Bunzel, R. C. Helgeson, K. N. Houk, G. Jimenez-Oses and D. Hilvert, *Nature Chemistry*, 2021, **13**, 231-235.
22. Z. Liu and F. H. Arnold, *Current Opinion in Biotechnology*, 2021, **69**, 43-51.

23. H.-U. Blaser, H.-P. Buser, H.-P. Jalett, B. Pugin and F. Spindler, *Synlett*, 1999, **1999**, 867-868.
24. Y. Tian, L. a. Hu, Y.-Z. Wang, X. Zhang and Q. Yin, *Organic Chemistry Frontiers*, 2021, **8**, 2328-2342.
25. C. Li, B. Villa-Marcos and J. Xiao, *Journal of the American Chemical Society*, 2009, **131**, 6967-6969.
26. J. Smith, A. Kacmaz, C. Wang, B. Villa-Marcos and J. Xiao, *Organic and Biomolecular Chemistry*, 2021, **19**, 279-284.
27. S. Zhou, S. Fleischer, H. Jiao, K. Junge and M. Beller, *Advanced Synthesis & Catalysis*, 2014, **356**, 3451-3455.
28. M. Chang, S. Liu, K. Huang and X. Zhang, *Organic Letters*, 2013, **15**, 4354-4357.
29. Z.-P. Chen, S.-B. Hu, J. Zhou and Y.-G. Zhou, *ACS Catalysis*, 2015, **5**, 6086-6089.
30. P. Yang, L. H. Lim, P. Chuanprasit, H. Hirao and J. S. Zhou, *Angewandte Chemie International Edition*, 2016, **55**, 12083-12087.
31. R. I. Storer, D. E. Carrera, Y. Ni and D. W. MacMillan, *Journal of the American Chemical Society*, 2006, **128**, 84-86.
32. V. N. Wakchaure, J. Zhou, S. Hoffmann and B. List, *Angewandte Chemie International Edition*, 2010, **49**, 4612-4614.
33. C. Zhu and T. Akiyama, *Organic Letters*, 2009, **11**, 4180-4183.
34. K. Saito and T. Akiyama, *Chem. Commun.*, 2012, **48**, 4573-4575.
35. A. Henseler, M. Kato, K. Mori and T. Akiyama, *Angewandte Chemie International Edition*, 2011, **50**, 8180-8183.
36. F. M. Gautier, S. Jones, X. Li and S. J. Martin, *Organic and Biomolecular Chemistry*, 2011, **9**, 7860-7868.
37. V. Skrypai, S. E. Varjosaari, F. Azam, T. M. Gilbert and M. J. Adler, *The Journal of Organic Chemistry*, 2019, **84**, 5021-5026.
38. A. V. Malkov, S. Stoncius and P. Kocovsky, *Angewandte Chemie International Edition*, 2007, **46**, 3722-3724.
39. Z. Pan, L. Shen, D. Song, Z. Xie, F. Ling and W. Zhong, *The Journal of Organic Chemistry*, 2018, **83**, 11502-11509.
40. Q. Zhou, W. Meng, J. Yang and H. Du, *Angewandte Chemie International Edition*, 2018, **57**, 12111-12115.
41. Z. Zhang, P. Jain and J. C. Antilla, *Angewandte Chemie International Edition*, 2011, **50**, 10961-10964.
42. Z. Wu, H. He, M. Chen, L. Zhu, W. Zheng, Y. Cao and J. C. Antilla, *Organic Letters*, 2022, **24**, 9436-9441.
43. T. Li, Q. Zhou, F. Meng, W. Cui, Q. Li, J. Zhu and Y. Cao, *European Journal of Organic Chemistry*, 2023, DOI: 10.1002/ejoc.202300507.
44. S. P. France, R. M. Howard, J. Steflik, N. J. Weise, J. Mangas-Sanchez, S. L. Montgomery, R. Crook, R. Kumar and N. J. Turner, *ChemCatChem*, 2018, **10**, 510-514.
45. G.-D. Roiban, M. Kern, Z. Liu, J. Hyslop, P. L. Tey, M. S. Levine, L. S. Jordan, K. K. Brown, T. Hadi, L. A. F. Ihnken and M. J. B. Brown, *ChemCatChem*, 2017, **9**, 4475-4479.

46. P. N. Scheller, M. Lenz, S. C. Hammer, B. Hauer and B. M. Nestl, *ChemCatChem*, 2015, **7**, 3239-3242.
47. A. K. Gilio, T. W. Thorpe, N. Turner and G. Grogan, *Chemical Science*, 2022, **13**, 4697-4713.
48. K. Zhang, Y. He, J. Zhu, Q. Zhang, L. Tang, L. Cui and Y. Feng, *Front. Bioeng. Biotechnol.*, 2021, **9**, 798147.
49. G. A. Aleku, S. P. France, H. Man, J. Mangas-Sanchez, S. L. Montgomery, M. Sharma, F. Leipold, S. Hussain, G. Grogan and N. J. Turner, *Nature Chemistry*, 2017, **9**, 961-969.
50. R. E. Ruscoe, J. I. Ramsden and N. J. Turner, *Current Opinion in Chemical Engineering*, 2020, **30**, 60-68.
51. J. Mangas-Sanchez, S. P. France, S. L. Montgomery, G. A. Aleku, H. Man, M. Sharma, J. I. Ramsden, G. Grogan and N. J. Turner, *Current Opinion in Chemical Biology*, 2017, **37**, 19-25.
52. P. Matzel, L. Krautschick and M. Hohne, *Chembiochem*, 2017, **18**, 2022-2027.
53. R. D. Lewis, S. P. France and C. A. Martinez, *ACS Catalysis*, 2023, **13**, 5571-5577.
54. C. Iglesias, A. Tijman, G. López, M. I. Lapaz, M. J. Pianzzola, P. Panizza and S. Rodríguez Giordano, *Frontiers in Catalysis*, 2021, **1**.
55. L. Liu, D.-H. Wang, F.-F. Chen, Z.-J. Zhang, Q. Chen, J.-H. Xu, Z.-L. Wang and G.-W. Zheng, *Catal. Sci. Technol.*, 2020, **10**, 2353-2358.
56. O. Mayol, K. Bastard, L. Beloti, A. Frese, J. P. Turkenburg, J.-L. Petit, A. Mariage, A. Debard, V. Pellouin, A. Perret, V. de Berardinis, A. Zaparucha, G. Grogan and C. Vergne-Vaxelaire, *Nature Catalysis*, 2019, **2**, 324-333.
57. V. Tseliou, M. F. Masman, W. Bohmer, T. Knaus and F. G. Mutti, *ChemBioChem*, 2019, **20**, 800-812.
58. C. K. Winkler, J. H. Schrittwieser and W. Kroutil, *ACS Central Science*, 2021, **7**, 55-71.
59. W. Liu and P. Wang, *Biotechnology Advances*, 2007, **25**, 369-384.
60. Y. J. Yoo, Y. Feng, Y.-H. Kim and C. F. J. Yagonia, *Fundamentals of Enzyme Engineering*, Springer, 1 edn., 2017.
61. S. T. Morthensen, S. B. Sigurdardóttir, A. S. Meyer, H. Jørgensen and M. Pinelo, *Journal of Membrane Science*, 2017, **523**, 327-335.
62. T. Knaus, W. Bohmer and F. G. Mutti, *Green Chemistry*, 2017, **19**, 453-463.
63. F. G. Mutti, T. Knaus, N. S. Scrutton, M. Breuer and N. J. Turner, *Science*, 2015, **349**, 1525-1529.
64. F.-F. Chen, Y.-Y. Liu, G.-W. Zheng and J.-H. Xu, *ChemCatChem*, 2015, **7**, 3838-3841.
65. S. L. Montgomery, J. Mangas-Sanchez, M. P. Thompson, G. A. Aleku, B. Dominguez and N. J. Turner, *Angewandte Chemie International Edition*, 2017, **56**, 10491-10494.
66. L. Bering, J. Thompson and J. Micklefield, *Trends in Chemistry*, 2022, **4**, 392-408.
67. F. Rudroff, M. D. Mihovilovic, H. Gröger, R. Snajdrova, H. Iding and U. T. Bornscheuer, *Nature Catalysis*, 2018, **1**, 12-22.

68. S. Simic, E. Zukic, L. Schmermund, K. Faber, C. K. Winkler and W. Kroutil, *Chem. Rev.*, 2022, **122**, 1052-1126.
69. P. K. Robinson, *Essays in Biochemistry*, 2015, **59**, 1-41.
70. S. L. Hooe, G. A. Ellis and I. L. Medintz, *RSC Chemical Biology*, 2022, **3**, 1301-1313.
71. T. Sugai, S. Higashibayashi and K. Hanaya, *Tetrahedron*, 2018, **74**, 3469-3487.
72. S. A. Loskot, D. K. Romney, F. H. Arnold and B. M. Stoltz, *Journal of the American Chemical Society*, 2017, **139**, 10196-10199.
73. B. M. Trost, C. E. Stivala, D. R. Fandrick, K. L. Hull, A. Huang, C. Poock and R. Kalkofen, *Journal of the American Chemical Society*, 2016, **138**, 11690-11701.
74. U. T. Bornscheuer, G. W. Huisman, R. J. Kazlauskas, S. Lutz, J. C. Moore and K. Robins, *Nature*, 2012, **485**, 185-194.
75. G. Hughes and J. C. Lewis, *Chem. Rev.*, 2018, **118**, 1-3.
76. R. C. Simon, F. G. Mutti and W. Kroutil, *Drug Discovery Today: Technologies*, 2013, **10**, e37-44.
77. C. K. Savile, J. M. Janey, E. C. Mundorff, J. C. Moore, S. Tam, W. R. Jarvis, J. C. Colbeck, A. Krebber, F. J. Fleitz, J. Brands, P. N. Devine, G. W. Huisman and G. J. Hughes, *Science*, 2010, **329**, 305-309.
78. G. Ma, Z. Xu, P. Zhang, J. Liu, X. Hao, J. Ouyang, P. Liang, S. You and X. Jia, *Organic Process Research & Development*, 2014, **18**, 1169-1174.
79. L. Marx, N. Rios-Lombardia, J. F. Farnberger, W. Kroutil, A. I. Benitez-Mateos, F. Lopez-Gallego, F. Moris, J. Gonzalez-Sabin and P. Berglund, *Advanced Synthesis & Catalysis*, 2018, **360**, 2157-2165.
80. G. Rajendra, K. Ganesh, G. Rajulu G, G. Sambasivam, R. Selvaraj, C. Kumar G, S. C. Ravikumar, P. C. Acharya and N. Shivashankarappa, *ChemistrySelect*, 2023, **8**.
81. J. Paris, N. Ríos-Lombardía, F. Morís, H. Gröger and J. González-Sabín, *ChemCatChem*, 2018, **10**, 4417-4423.
82. R. Kourist and J. González-Sabín, *ChemCatChem*, 2020, **12**, 1903-1912.
83. R. Villa, R. Porcar, S. Nieto, A. Donaire, E. Garcia-Verdugo, S. V. Luis and P. Lozano, *Green Chemistry*, 2021, **23**, 4191-4200.
84. R. Porcar, V. Sans, N. Ríos-Lombardía, V. Gotor-Fernández, V. Gotor, M. I. Burguete, E. García-Verdugo and S. V. Luis, *ACS Catalysis*, 2012, **2**, 1976-1983.
85. S. Sun, G. Yang, Y. Bi and F. Xiao, *Biotechnology Letters*, 2009, **31**, 1885-1889.
86. S. C. Cosgrove, M. P. Thompson, S. T. Ahmed, F. Parmeggiani and N. J. Turner, *Angewandte Chemie International Edition*, 2020, **59**, 18156-18160.
87. C. J. Hastings, N. P. Adams, J. Bushi and S. J. Kolb, *Green Chemistry*, 2020, **22**, 6187-6193.
88. H. Groger, F. Gallou and B. H. Lipshutz, *Chem. Rev.*, 2023, **123**, 5262-5296.
89. J. McNulty, S. Cheekoori, T. P. Bender and J. A. Coggan, *European Journal of Organic Chemistry*, 2007, **2007**, 1423-1428.
90. B. Kudłak, K. Owczarek and J. Namieśnik, *Environmental Science and Pollution Research*, 2015, **22**, 11975-11992.
91. A. Satlewal, R. Agrawal, S. Bhagia, J. Sangoro and A. J. Ragauskas, *Biotechnol Adv*, 2018, **36**, 2032-2050.

92. S. Sowmiah, V. Srinivasadesikan, M. C. Tseng and Y. H. Chu, *Molecules*, 2009, **14**, 3780-3813.
93. Y. Chen and T. Mu, *Green Chemical Engineering*, 2021, **2**, 174-186.
94. S. Randström, M. Montanino, G. B. Appetecchi, C. Lagergren, A. Moreno and S. Passerini, *Electrochimica Acta*, 2008, **53**, 6397-6401.
95. D. Kumar, K. Seth, D. N. Kommi, S. Bhagat and A. K. Chakraborti, *RSC Advances*, 2013, **3**.
96. P. Luan, Y. Liu, Y. Li, R. Chen, C. Huang, J. Gao, F. Hollmann and Y. Jiang, *Green Chemistry*, 2021, **23**, 1960-1964.
97. D. J. Mansell, H. S. Toogood, J. Waller, J. M. Hughes, C. W. Levy, J. M. Gardiner and N. S. Scrutton, *ACS Catalysis*, 2013, **3**, 370-379.
98. F. Taday, R. Cairns, A. O'Connell and E. O'Reilly, *Chem. Commun.*, 2022, **58**, 1697-1700.
99. R. A. Sheldon, *ACS Sustainable Chemistry & Engineering*, 2017, **6**, 32-48.
100. G. E. M. Crisenza and P. Melchiorre, *Nature Communications*, 2020, **11**, 803.
101. Q. Yang, F. Zhao, N. Zhang, M. Liu, H. Hu, J. Zhang and S. Zhou, *Chem. Commun.*, 2018, **54**, 14065-14068.
102. X. Ding, C. L. Dong, Z. Guan and Y. H. He, *Angewandte Chemie International Edition*, 2019, **58**, 118-124.
103. L.-L. Wu, Y. Xiang, D.-C. Yang, Z. Guan and Y.-H. He, *Catal. Sci. Technol.*, 2016, **6**, 3963-3970.
104. Z. J. Yang, Q. T. Gong, Y. Yu, W. F. Lu, Z. N. Wu, N. Wang and X. Q. Yu, *Bioorganic Chemistry*, 2021, **107**, 104607.
105. Z. B. Xie, N. Wang, W. X. Wu, Z. G. Le and X. Q. Yu, *J. Biotechnol.*, 2014, **170**, 1-5.
106. Y.-L. Chen, W. Li, Y. Liu, Z. Guan and Y.-H. He, *Journal of Molecular Catalysis B: Enzymatic*, 2013, **87**, 83-87.
107. R. C. Betori, C. M. May and K. A. Scheidt, *Angewandte Chemie International Edition*, 2019, **58**, 16490-16494.
108. D. Webb and T. F. Jamison, *Chemical Science*, 2010, **1**, 675-680.
109. P. T. Anastas and M. M. Kirchhoff, *Accounts of Chemical Research*, 2002, **35**, 686-694.
110. T. Hudlicky, *Chem. Rev.*, 1996, **96**, 3-30.
111. B. M. Trost, *Science*, 1991, **254**, 1471-1477.
112. M. S. Tichenor and D. L. Boger, *Natural Product Reports*, 2008, **25**, 220-226.
113. B. P. Mason, K. E. Price, J. L. Steinbacher, A. R. Bogdan and D. T. McQuade, *Chem. Rev.*, 2007, **107**, 2300-2318.
114. R. L. Hartman and K. F. Jensen, *Lab Chip*, 2009, **9**, 2495-2507.
115. Y. Hayashi, *The Journal of Organic Chemistry*, 2021, **86**, 1-23.
116. R. A. Sheldon and P. C. Pereira, *Chemical Society Reviews*, 2017, **46**, 2678-2691.
117. E. T. Hwang and S. Lee, *ACS Catalysis*, 2019, **9**, 4402-4425.
118. R. A. Sheldon, *Advanced Synthesis & Catalysis*, 2007, **349**, 1289-1307.
119. P. Gruber, M. P. C. Marques, B. O'Sullivan, F. Baganz, R. Wohlgemuth and N. Szita, *Biotechnology Journal*, 2017, **12**.

120. S. Gandomkar, A. Zadlo-Dobrowolska and W. Kroutil, *ChemCatChem*, 2019, **11**, 225-243.
121. Y. Hayashi, *Chemical Science*, 2016, **7**, 866-880.
122. M. Romero-Fernandez and F. Paradisi, *Current Opinion in Chemical Biology*, 2020, **55**, 1-8.
123. R. L. Hartman, J. R. Naber, S. L. Buchwald and K. F. Jensen, *Angewandte Chemie International Edition*, 2010, **49**, 899-903.
124. P. Falus, L. Cerioli, G. Bajnóczi, Z. Boros, D. Weiser, J. Nagy, D. Tessaro, S. Servi and L. Poppe, *Advanced Synthesis & Catalysis*, 2016, **358**, 1608-1617.
125. M. Corovic, M. Mihailovic, K. Banjanac, M. Carevic, A. Milivojevic, N. Milosavic and D. Bezbradica, *Bioprocess. Biosyst. Eng.*, 2017, **40**, 23-34.
126. E. Farkas, M. Olah, A. Foldi, J. Koti, J. Eles, J. Nagy, C. A. Gal, C. Paizs, G. Hornyanszky and L. Poppe, *Organic Letters*, 2018, **20**, 8052-8056.
127. A. S. de Miranda, M. V. de M. Silva, F. C. Dias, S. P. de Souza, R. A. C. Leão and R. O. M. A. de Souza, *Reaction Chemistry & Engineering*, 2017, **2**, 375-381.
128. S. Wuyts, J. Wahlen, P. A. Jacobs and D. E. De Vos, *Green Chemistry*, 2007, **9**.
129. B. Grabner, A. K. Schweiger, K. Gavric, R. Kourist and H. Gruber-Woelfler, *Reaction Chemistry & Engineering*, 2020, **5**, 263-269.
130. D. R. Padrosa and M. L. Contente, *Tetrahedron Letters*, 2021, **86**.
131. M. L. Contente, S. Farris, L. Tamborini, F. Molinari and F. Paradisi, *Green Chemistry*, 2019, **21**, 3263-3266.
132. L. A. Thompson, Chemo- and Bio-Catalysis for the Synthesis of Chiral Amines in Continuous Flow Reactors, University of Leeds, 2017.
133. O. Saidi, A. J. Blacker, M. M. Farah, S. P. Marsden and J. M. Williams, *Chem. Commun.*, 2010, **46**, 1541-1543.
134. V. De Vitis, F. Dall'Oglio, A. Pinto, C. De Micheli, F. Molinari, P. Conti, D. Romano and L. Tamborini, *ChemistryOpen*, 2017, **6**, 668-673.
135. M. M. Delville, K. Koch, J. C. van Hest and F. P. Rutjes, *Organic and Biomolecular Chemistry*, 2015, **13**, 1634-1638.
136. K. Koch, R. J. van den Berg, P. J. Nieuwland, R. Wijtmans, H. E. Schoemaker, J. C. van Hest and F. P. Rutjes, *Biotechnology and Bioengineering*, 2008, **99**, 1028-1033.
137. K. Koch, R. Vandenberg, P. Nieuwland, R. Wijtmans, M. Wubbolts, H. Schoemaker, F. Rutjes and J. Vanhest, *Chemical Engineering Journal*, 2008, **135**, S89-S92.
138. FLLEX, https://www.syrris.com/, (accessed January, 2022).
139. G. Rulli, N. Duangdee, W. Hummel, A. Berkessel and H. Gröger, *European Journal of Organic Chemistry*, 2017, **2017**, 812-817.
140. L. Schober, F. Tonin, U. Hanefeld and H. Gröger, *European Journal of Organic Chemistry*, 2022, **2022**.
141. M. D. Hopkin, I. R. Baxendale and S. V. Ley, *Chem. Commun.*, 2010, **46**, 2450-2452.
142. R. L. Hartman, H. R. Sahoo, B. C. Yen and K. F. Jensen, *Lab Chip*, 2009, **9**, 1843-1849.
143. J. G. Kralj, H. R. Sahoo and K. F. Jensen, *Lab Chip*, 2007, **7**, 256-263.

144. H. R. Sahoo, J. G. Kralj and K. F. Jensen, *Angewandte Chemie International Edition*, 2007, **46**, 5704-5708.
145. M. Argyle and C. Bartholomew, *Catalysts*, 2015, **5**, 145-269.
146. M. Irfan, T. N. Glasnov and C. O. Kappe, *ChemSusChem*, 2011, **4**, 300-316.
147. D. Cantillo and C. O. Kappe, *ChemCatChem*, 2014, **6**, 3286-3305.
148. O. Saidi, A. J. Blacker, M. M. Farah, S. P. Marsden and J. M. Williams, *Angewandte Chemie International Edition*, 2009, **48**, 7375-7378.
149. D. Francis, A. Nelson and S. P. Marsden, *Chemistry*, 2020, **26**, 14861-14865.
150. R. Lanaro, New catalysts for amine alkylation reactions promoted by hydrogen borrowing, University of Leeds, 2015.
151. M. R. Shannon, New organometallic catalysts for process-friendly redox neutral alkylations, University of Leeds, 2019.
152. L. Tamborini, P. Fernandes, F. Paradisi and F. Molinari, *Trends Biotechnol*, 2018, **36**, 73-88.
153. J. Britton, S. Majumdar and G. A. Weiss, *Chemical Society Reviews*, 2018, **47**, 5891-5918.
154. R. A. Sheldon and S. van Pelt, *Chemical Society Reviews*, 2013, **42**, 6223-6235.
155. U. Hanefeld, L. Gardossi and E. Magner, *Chemical Society Reviews*, 2009, **38**, 453-468.
156. S. Cantone, V. Ferrario, L. Corici, C. Ebert, D. Fattor, P. Spizzo and L. Gardossi, *Chemical Society Reviews*, 2013, **42**, 6262-6276.
157. N. Milozic, G. Stojkovic, A. Vogel, D. Bouwes and P. Znidarsic-Plazl, *New Biotechnology*, 2018, **47**, 18-24.
158. A. P. Green, N. J. Turner and E. O'Reilly, *Angewandte Chemie International Edition*, 2014, **53**, 10714-10717.
159. L. Nagy-Gyor, E. Abahazi, V. Bodai, P. Satorhelyi, B. Erdelyi, D. Balogh-Weiser, C. Paizs, G. Hornyanszky and L. Poppe, *ChemBioChem*, 2018, **19**, 1845-1848.
160. S. A. Kelly, S. Pohle, S. Wharry, S. Mix, C. C. R. Allen, T. S. Moody and B. F. Gilmore, *Chem. Rev.*, 2018, **118**, 349-367.
161. A. Gomm and E. O'Reilly, *Current Opinion in Chemical Biology*, 2018, **43**, 106-112.
162. K. Yonaha, M. Nishie and S. Aibara, *The Journal of Biological Chemistry*, 1992, **267**, 12506-12510.
163. K. Yonaha, S. Toyama and K. Kagamiyama, *The Journal of Biological Chemistry*, 1983, **258**, 2260-2668.
164. K. Szmejda, T. Florczak, I. Jodłowska and M. Turkiewicz, *Biotechnology and Food Science*, 2017, **81**.
165. N. J. Turner and M. D. Truppo, in *Sustainable Catalysis Challenges and Practices for the Pharmaceutical and Fine Chemical Industries*, 2013, ch. 3, pp. 63-74.
166. J.-S. Shin and B.-G. Kim, *The Journal of Organic Chemistry*, 2002, **67**, 2848-2853.
167. P. Tufvesson, J. Lima-Ramos, J. S. Jensen, N. Al-Haque, W. Neto and J. M. Woodley, *Biotechnology and Bioengineering*, 2011, **108**, 1479-1493.
168. A. M. Ferreira, H. Passos, A. Okafuji, A. P. M. Tavares, H. Ohno, M. G. Freire and J. A. P. Coutinho, *Green Chemistry*, 2018, **20**, 1218-1223.

169. P. Sagmeister, R. Lebl, I. Castillo, J. Rehrl, J. Kruisz, M. Sipek, M. Horn, S. Sacher, D. Cantillo, J. D. Williams and C. O. Kappe, *Angewandte Chemie International Edition*, 2021, **60**, 8139-8148.
170. R. L. Hanson, B. L. Davis, Y. Chen, S. L. Goldberg, W. L. Parker, T. P. Tully, M. A. Montana and R. N. Patel, *Advanced Synthesis & Catalysis*, 2008, **350**, 1367-1375.
171. I. Slabu, J. L. Galman, N. J. Weise, R. C. Lloyd and N. J. Turner, *ChemCatChem*, 2016, **8**, 1038-1042.
172. I. Slabu, J. L. Galman, R. C. Lloyd and N. J. Turner, *ACS Catalysis*, 2017, **7**, 8263-8284.
173. X. Gao, X. Zhang, N. Zhu, Y. Mou, H. Zhang, X. Liu and P. Wei, *Appl Microbiol Biotechnol*, 2020, **104**, 3959-3969.
174. F. Guo and P. Berglund, *Green Chemistry*, 2017, **19**, 333-360.
175. F. G. Mutti, C. S. Fuchs, D. Pressnitz, J. H. Sattler and W. Kroutil, *Advanced Synthesis & Catalysis*, 2011, **353**, 3227-3233.
176. A. P. Mattey, G. J. Ford, J. Citoler, C. Baldwin, J. R. Marshall, R. B. Palmer, M. Thompson, N. J. Turner, S. C. Cosgrove and S. L. Flitsch, *Angewandte Chemie International Edition*, 2021, **60**, 18660-18665.
177. Z. Molnár, E. Farkas, Á. Lakó, B. Erdélyi, W. Kroutil, B. G. Vértessy, C. Paizs and L. Poppe, *Catalysts*, 2019, **9**.
178. P. Kelefiotis-Stratidakis, T. Tyrikos-Ergas and I. V. Pavlidis, *Organic and Biomolecular Chemistry*, 2019, **17**, 1634-1642.
179. J.-S. Shin and B.-G. Kim, *Biotechnology and Bioengineering*, 1999, **65**, 206-211.
180. D. Koszelewski, I. Lavandera, D. Clay, D. Rozzell and W. Kroutil, *Advanced Synthesis & Catalysis*, 2008, **350**, 2761-2766.
181. D. Koszelewski, I. Lavandera, D. Clay, G. M. Guebitz, D. Rozzell and W. Kroutil, *Angewandte Chemie International Edition*, 2008, **47**, 9337-9340.
182. M. Hohne, S. Kuhl, K. Robins and U. T. Bornscheuer, *ChemBioChem*, 2008, **9**, 363-365.
183. K. E. Cassimjee, C. Branneby, V. Abedi, A. Wells and P. Berglund, *Chem. Commun.*, 2010, **46**, 5569-5571.
184. E.-S. Park, J.-Y. Dong and J.-S. Shin, *ChemCatChem*, 2013, **5**, 3538-3542.
185. S. E. Payer, J. H. Schrittwieser and W. Kroutil, *European Journal of Organic Chemistry*, 2017, **2017**, 2553-2559.
186. A. Gomm, S. Grigoriou, C. Peel, J. Ryan, N. Mujtaba, T. Clarke, E. Kulcinskaja and E. O'Reilly, *European Journal of Organic Chemistry*, 2018, **2018**, 5282-5284.
187. A. Gomm, W. Lewis, A. P. Green and E. O'Reilly, *Chemistry*, 2016, **22**, 12692-12695.
188. E. E. Ferrandi and D. Monti, *World Journal of Microbiology and Biotechnology*, 2017, **34**, 13.
189. U. Novak, D. Lavric and P. Žnidaršič-Plazl, *Journal of Flow Chemistry*, 2016, **6**, 33-38.
190. A. Liese and L. Hilterhaus, *Chemical Society Reviews*, 2013, **42**, 6236-6249.

191. M. Planchestainer, M. L. Contente, J. Cassidy, F. Molinari, L. Tamborini and F. Paradisi, *Green Chemistry*, 2017, **19**, 372-375.
192. F. Secundo, *Chemical Society Reviews*, 2013, **42**, 6250-6261.
193. E. Magner, *Chemical Society Reviews*, 2013, **42**, 6213-6222.
194. M. S. Doscher and F. M. Richards, *The Journal of Biological Chemistry*, 1963, **238**, 2399-2406.
195. R. Schoevaart, M. W. Wolbers, M. Golubovic, M. Ottens, A. P. Kieboom, F. van Rantwijk, L. A. van der Wielen and R. A. Sheldon, *Biotechnology and Bioengineering*, 2004, **87**, 754-762.
196. H.-Z. Ma, X.-W. Yu, C. Song, Q.-l. Xue and B. Jiang, *Journal of Molecular Catalysis B: Enzymatic*, 2016, **127**, 76-81.
197. M. Schlieker and K.-D. Vorlop, in *Immobilization of Enzymes and Cells*, ed. J. M. Walker, Humana Press, 2 edn., 2006, pp. 333-343.
198. G. Czichocki, H. Dautzenberg, E. Capan and K.-D. Vorlop, *Biotechnology Letters*, 2001, **23**, 1303-1307.
199. J. M. Nelson and E. G. Griffin, *Journal of the American Chemical Society*, 2002, **38**, 1109-1115.
200. J. Krenkova and F. Foret, *Electrophoresis*, 2004, **25**, 3550-3563.
201. D. N. Tran and K. J. Balkus, *ACS Catalysis*, 2011, **1**, 956-968.
202. M. Mihailović, M. Stojanović, K. Banjanac, M. Carević, N. Prlainović, N. Milosavić and D. Bezbradica, *Process Biochemistry*, 2014, **49**, 637-646.
203. E. Abaházi, P. Sátorhelyi, B. Erdélyi, B. G. Vértessy, H. Land, C. Paizs, P. Berglund and L. Poppe, *Biochemical Engineering Journal*, 2018, **132**, 270-278.
204. W. Neto, M. Schürmann, L. Panella, A. Vogel and J. M. Woodley, *Journal of Molecular Catalysis B: Enzymatic*, 2015, **117**, 54-61.
205. Purolite Immobilisation, https://www.purolite.com/dam/jcr:3c5b978b-3829-4f92-8654-390863042f09/Lifetech%20ECR%20immobilization%20procedures.pdf, (accessed March 2020).
206. E. Hochuli, W. Bannwarth, H. Döbeli, R. Gentz and D. Stüber, *Nat. Biotechnol.*, 1988, **6**, 1321-1325.
207. M. M. Bradford, *Analytical Biochemistry*, 1976, **72**, 248-254.
208. A. R. Turner, A. T. Turner, G. P. Howell, M. A. Y. Gall, K. R. Mulholland, N. K. Adlington, Z. Tian, B. Liu, Q. Gong and W. Yu, *Journal*, 2022.
209. A. Markham, *Drugs*, 2021, **81**, 1665-1670.
210. S. P. France, E. A. Lindsey, E. L. McInturff, S. Berritt, D. W. Carney, J. C. DeForest, S. J. Fink, A. C. Flick, T. S. Gibson, K. Gray, A. M. Johnson, C. A. Leverett, Y. Liu, S. Mahapatra and R. B. Watson, *J Med Chem*, 2024, DOI: 10.1021/acs.jmedchem.3c02374.
211. D. N. Jumbam, R. A. Skilton, A. J. Parrott, R. A. Bourne and M. Poliakoff, *Journal of Flow Chemistry*, 2012, **2**, 24-27.
212. R. A. Sheldon, *Green Chemistry*, 2007, **9**.
213. F. Uthoff, J. Lowe, C. Harms, K. Donsbach and H. Groger, *The Journal of Organic Chemistry*, 2019, **84**, 4856-4866.

214. A. S. de Miranda, L. S. Miranda and R. O. de Souza, *Organic and Biomolecular Chemistry*, 2013, **11**, 3332-3336.
215. E. M. Anderson, K. M. Larsson and O. Kirk, *Biocatalysis and Biotransformation*, 2009, **16**, 181-204.
216. T. Kobayashi and S. Adachi, *Biotechnology Letters*, 2004, **26**, 1461-1468.
217. A. Ghanem and H. Y. Aboul-Enein, *Tetrahedron: Asymmetry*, 2004, **15**, 3331-3351.
218. A. Kumar, K. Dhar, S. S. Kanwar and P. K. Arora, *Biological Procedures Online*, 2016, **18**, 2.
219. R. C. Simon, N. Richter, E. Busto and W. Kroutil, *ACS Catalysis*, 2013, **4**, 129-143.
220. C. R. Johnson and S. J. Bis, *Tetrahedron Letters*, 1992, **33**, 7287-7290.
221. F. P. Byrne, S. Jin, G. Paggiola, T. H. M. Petchey, J. H. Clark, T. J. Farmer, A. J. Hunt, C. Robert McElroy and J. Sherwood, *Sustainable Chemical Processes*, 2016, **4**.
222. S. D. Shinde and G. D. Yadav, *Process Biochemistry*, 2015, **50**, 230-236.
223. J. A. C. da Silva, V. F. Soares, R. Fernandez- Lafuente, A. C. Habert and D. M. G. Freire, *Journal of Molecular Catalysis B: Enzymatic*, 2015, **122**, 323-329.
224. S. Arana-Peña, Y. Lokha and R. Fernández-Lafuente, *Catalysts*, 2018, **8**.
225. S. Arana-Pena, Y. Lokha and R. Fernandez-Lafuente, *Biotechnology Progress*, 2019, **35**, e2735.
226. O. Kirk and M. W. Christensen, *Organic Process Research & Development*, 2002, **6**, 446-451.
227. V. Gotor-Fernández, E. Busto and V. Gotor, *Advanced Synthesis & Catalysis*, 2006, **348**, 797-812.
228. B. Chen, M. E. Miller and R. A. Gross, *Langmuir*, 2007, **23**, 6467-6474.
229. Y. Mei, L. Miller, W. Gao and R. A. Gross, *Biomacromolecules*, 2003, **4**, 70-74.
230. B. Chen, J. Hu, E. M. Miller, W. Xie, M. Cai and R. A. Gross, *Biomacromolecules*, 2008, **9**, 463-471.
231. L. Rubio-Perez, F. J. Perez-Flores, P. Sharma, L. Velasco and A. Cabrera, *Organic Letters*, 2009, **11**, 265-268.
232. C. Ortiz, M. L. Ferreira, O. Barbosa, J. C. S. dos Santos, R. C. Rodrigues, Á. Berenguer-Murcia, L. E. Briand and R. Fernandez-Lafuente, *Catal. Sci. Technol.*, 2019, **9**, 2380-2420.
233. N. Rueda, J. C. S. dos Santos, R. Torres, C. Ortiz, O. Barbosa and R. Fernandez-Lafuente, *RSC Advances*, 2015, **5**, 11212-11222.
234. H. Zhao and Z. Song, *Biochemical Engineering Journal*, 2010, **49**, 113-118.
235. C. José and L. E. Briand, *Reaction Kinetics, Mechanisms and Catalysis*, 2010, **99**, 17-22.
236. M. V. Toledo, C. José, S. E. Collins, M. L. Ferreira and L. E. Briand, *Journal of Molecular Catalysis B: Enzymatic*, 2015, **118**, 52-61.
237. M. V. Toledo, C. José, S. E. Collins, R. D. Bonetto, M. L. Ferreira and L. E. Briand, *Journal of Molecular Catalysis B: Enzymatic*, 2012, **83**, 108-119.

238. C. José, R. D. Bonetto, L. A. Gambaro, M. d. P. G. Torres, M. L. Foresti, M. L. Ferreira and L. E. Briand, *Journal of Molecular Catalysis B: Enzymatic*, 2011, **71**, 95-107.
239. F. Xu, Q. Wu, X. Chen, X. Lin and Q. Wu, *European Journal of Organic Chemistry*, 2015, **2015**, 5393-5401.
240. J. Leonard, A. J. Blacker, S. P. Marsden, M. F. Jones, K. R. Mulholland and R. Newton, *Organic Process Research & Development*, 2015, **19**, 1400-1410.
241. D. J. C. Constable, P. J. Dunn, J. D. Hayler, G. R. Humphrey, J. J. L. Leazer, R. J. Linderman, K. Lorenz, J. Manley, B. A. Pearlman, A. Wells, A. Zaks and T. Y. Zhang, *Green Chemistry*, 2007, **9**, 411-420.
242. J. S. Carey, D. Laffan, C. Thomson and M. T. Williams, *Organic and Biomolecular Chemistry*, 2006, **4**, 2337-2347.
243. J. R. Cabrero-Antonino, R. Adam and M. Beller, *Angewandte Chemie International Edition*, 2019, **58**, 12820-12838.
244. B. Appiagyei, S. Bhatia, G. L. Keeney, T. Dolmetsch and J. E. Jackson, *Green Chemistry*, 2020, **22**, 860-869.
245. , !!! INVALID CITATION !!! 5-7.
246. K. Bui The, C. Concilio and G. Porzi, *The Journal of Organic Chemistry*, 2002, **46**, 1759-1760.
247. Y. Watanabe, Y. Tsuji and Y. Ohsugi, *Tetrahedron Letters*, 1981, **22**, 2667-2670.
248. R. Grigg, T. R. B. Mitchell, S. Sutthivaiyakit and N. Tongpenyai, *Journal of the Chemical Society, Chemical Communications*, 1981, DOI: 10.1039/c39810000611.
249. B. G. Reed-Berendt, D. E. Latham, M. B. Dambatta and L. C. Morrill, *ACS Central Science*, 2021, **7**, 570-585.
250. N. Luo, Y. Zhong, H. Wen and R. Luo, *ACS Omega*, 2020, **5**, 27723-27732.
251. S. Genc, B. Arslan, S. Gulcemal, S. Gunnaz, B. Cetinkaya and D. Gulcemal, *The Journal of Organic Chemistry*, 2019, **84**, 6286-6297.
252. B. G. Reed-Berendt, K. Polidano and L. C. Morrill, *Organic and Biomolecular Chemistry*, 2019, **17**, 1595-1607.
253. C. Heider, A. Winter, V. Voß, D. Vogt and T. Seidensticker, *ChemCatChem*, 2023, **15**.
254. R. Labes, C. Mateos, C. Battilocchio, Y. Chen, P. Dingwall, G. R. Cumming, J. A. Rincón, M. J. Nieves-Remacha and S. V. Ley, *Green Chemistry*, 2019, **21**, 59-63.
255. K.-i. Fujita, Y. Enoki and R. Yamaguchi, *Tetrahedron*, 2008, **64**, 1943-1954.
256. P. Fristrup, M. Tursky and R. Madsen, *Organic and Biomolecular Chemistry*, 2012, **10**, 2569-2577.
257. S. J. Lucas, B. D. Crossley, A. J. Pettman, A. D. Vassileiou, T. E. Screen, A. J. Blacker and P. C. McGowan, *Chem. Commun.*, 2013, **49**, 5562-5564.
258. S. Hashiguchi, A. Fujii, J. Takehara, T. Ikariya and R. Noyori, *Journal of the American Chemical Society*, 2002, **117**, 7562-7563.
259. US10717754B2, 2020.
260. G. E. Dobereiner and R. H. Crabtree, *Chem. Rev.*, 2010, **110**, 681-703.
261. A. J. Blacker, M. J. Stirling and M. I. Page, *Organic Process Research & Development*, 2007, **11**, 642-648.

262. M. H. T. Kwan, J. Breen, M. Bowden, L. Conway, B. Crossley, M. F. Jones, R. Munday, N. P. B. Pokar, T. Screen and A. J. Blacker, *The Journal of Organic Chemistry*, 2021, **86**, 2458-2473.
263. G. J. Sherborne, M. R. Chapman, A. J. Blacker, R. A. Bourne, T. W. Chamberlain, B. D. Crossley, S. J. Lucas, P. C. McGowan, M. A. Newton, T. E. Screen, P. Thompson, C. E. Willans and B. N. Nguyen, *Journal of the American Chemical Society*, 2015, **137**, 4151-4157.
264. D. Balcells, A. Nova, E. Clot, D. Gnanamgari, R. H. Crabtree and O. Eisenstein, *Organometallics*, 2008, **27**, 2529-2535.
265. L. U. Nordstrom and R. Madsen, *Chem. Commun.*, 2007, DOI: 10.1039/b712685a, 5034-5036.
266. R. Kawahara, K. Fujita and R. Yamaguchi, *Journal of the American Chemical Society*, 2010, **132**, 15108-15111.
267. R. Kawahara, K.-i. Fujita and R. Yamaguchi, *Advanced Synthesis & Catalysis*, 2011, **353**, 1161-1168.
268. P. Qu, C. Sun, J. Ma and F. Li, *Advanced Synthesis & Catalysis*, 2014, **356**, 447-459.
269. S. Kramer, *Organic Letters*, 2019, **21**, 65-69.
270. *United States Pat.,* US6211244B1, 2001.
271. *United States Pat.,* US6750255B2, 2004.
272. *United States Pat.,* US20100279936A1, 2010.
273. A. C. Flick, C. A. Leverett, H. X. Ding, E. McInturff, S. J. Fink, C. J. Helal, J. C. DeForest, P. D. Morse, S. Mahapatra and C. J. O'Donnell, *Journal of Medicinal Chemistry*, 2020, **63**, 10652-10704.
274. H. Miyazaki, Y. Ikeda, O. Sakurai, T. Miyake, R. Tsubota, J. Okabe, M. Kuroda, Y. Hisada, T. Yanagida, H. Yoneda, Y. Tsukumo, S. Tokunaga, T. Kawata, R. Ohashi, H. Fukuda, K. Kojima, A. Kannami, T. Kifuji, N. Sato, A. Idei, T. Iguchi, T. Sakairi and Y. Moritani, *Bioorganic & Medicinal Chemistry Letters*, 2018, **28**, 2055-2060.
275. K. Leach, K. J. Gregory, I. Kufareva, E. Khajehali, A. E. Cook, R. Abagyan, A. D. Conigrave, P. M. Sexton and A. Christopoulos, *Cell Research*, 2016, **26**, 574-592.
276. S. C. Palmer, I. Nistor, J. C. Craig, F. Pellegrini, P. Messa, M. Tonelli, A. Covic and G. F. Strippoli, *PLOS Medicine*, 2013, **10**, e1001436.
277. C. Wang, A. Pettman, J. Basca and J. Xiao, *Angewandte Chemie International Edition*, 2010, **49**, 7548-7552.
278. W. P. Liu, M. L. Yuan, X. H. Yang, K. Li, J. H. Xie and Q. L. Zhou, *Chem. Commun.*, 2015, **51**, 6123-6125.
279. C. K. Prier, D. A. Rankic and D. W. MacMillan, *Chem. Rev.*, 2013, **113**, 5322-5363.
280. M. H. Shaw, J. Twilton and D. W. MacMillan, *The Journal of Organic Chemistry*, 2016, **81**, 6898-6926.
281. J. Michaux, V. Terrasson, S. Marque, J. Wehbe, D. Prim and J.-M. Campagne, *European Journal of Organic Chemistry*, 2007, **2007**, 2601-2603.

282. M. Kawatsura and J. F. Hartwig, *Journal of the American Chemical Society*, 2000, **122**, 9546-9547.
283. S. Tobisch, *Chemistry*, 2016, **22**, 8290-8300.
284. M. Utsunomiya and J. F. Hartwig, *Journal of the American Chemical Society*, 2003, **125**, 14286-14287.
285. A. J. Musacchio, B. C. Lainhart, X. Zhang, S. G. Naguib, T. C. Sherwood and R. R. Knowles, *Science*, 2017, **355**, 727-730.
286. M. Utsunomiya and J. F. Hartwig, *Journal of the American Chemical Society*, 2004, **126**, 2702-2703.
287. Q. Zhu, D. E. Graff and R. R. Knowles, *Journal of the American Chemical Society*, 2018, **140**, 741-747.
288. T. M. Nguyen and D. A. Nicewicz, *Journal of the American Chemical Society*, 2013, **135**, 9588-9591.
289. D. C. Miller, J. M. Ganley, A. J. Musacchio, T. C. Sherwood, W. R. Ewing and R. R. Knowles, *Journal of the American Chemical Society*, 2019, **141**, 16590-16594.
290. S. D. A. Zondag, D. Mazzarella and T. Noel, *Annual Review of Chemical and Biomolecular Engineering*, 2023, **14**, 283-300.
291. K. Donnelly and M. Baumann, *Journal of Flow Chemistry*, 2021, **11**, 223-241.
292. D. Francis, A. J. Blacker, N. Kapur and S. P. Marsden, *Organic Process Research & Development*, 2021, **26**, 215-221.
293. F. Politano and G. Oksdath-Mansilla, *Organic Process Research & Development*, 2018, **22**, 1045-1062.
294. Y. Qin, Q. Zhu, R. Sun, J. M. Ganley, R. R. Knowles and D. G. Nocera, *Journal of the American Chemical Society*, 2021, **143**, 10232-10242.
295. S. Fang, X. Wang, F. Yin, P. Cai, H. Yang and L. Kong, *Organic Letters*, 2019, **21**, 1841-1844.
296. T. Shono, Y. Matsumura and K. Tsubata, *Journal of the American Chemical Society*, 2002, **103**, 1172-1176.
297. T. Shono, H. Hamaguchi and Y. Matsumura, *Journal of the American Chemical Society*, 2002, **97**, 4264-4268.
298. A. M. Jones and C. E. Banks, *Beilstein Journal of Organic Chemistry*, 2014, **10**, 3056-3072.
299. A. F. Trindade, E. L. Faulkner, A. G. Leach, A. Nelson and S. P. Marsden, *Chem. Commun.*, 2020, **56**, 8802-8805.
300. S. S. Libendi, Y. Demizu, Y. Matsumura and O. Onomura, *Tetrahedron*, 2008, **64**, 3935-3942.
301. D. F. Oliveira, P. C. Miranda and C. R. Correia, *The Journal of Organic Chemistry*, 1999, **64**, 6646-6652.
302. R. I. McDonald, G. W. Wong, R. P. Neupane, S. S. Stahl and C. R. Landis, *Journal of the American Chemical Society*, 2010, **132**, 14027-14029.
303. X. Guo, Y. Okamoto, M. R. Schreier, T. R. Ward and O. S. Wenger, *Chemical Science*, 2018, **9**, 5052-5056.
304. Z. Shen, M. A. Vargas-Rivera, E. L. Rigby, S. Chen and J. A. Ellman, *ACS Catalysis*, 2022, **12**, 12860-12868.

305. Z. Shen, M. M. Walker, S. Chen, G. A. Parada, D. M. Chu, S. Dongbang, J. M. Mayer, K. N. Houk and J. A. Ellman, *Journal of the American Chemical Society*, 2021, **143**, 126-131.
306. S. L. Murov, I. Carmichael and G. L. Hug, *Handbook of photochemistry*, Crc Press, 1993.
307. T. A. Paál, E. Forró, A. Liljeblad, L. T. Kanerva and F. Fülöp, *Tetrahedron: Asymmetry*, 2007, **18**, 1428-1433.
308. Z. S. Seddigi, M. S. Malik, S. A. Ahmed, A. O. Babalghith and A. Kamal, *Coordination Chemistry Reviews*, 2017, **348**, 54-70.
309. S. Alatorre-Santamaria, M. Rodriguez-Mata, V. Gotor-Fernandez, M. C. de Mattos, F. J. Sayago, A. I. Jimenez, C. Cativiela and V. Gotor, *Tetrahedron Asymmetry*, 2009, **19**, 1714-1719.
310. V. Tseliou, D. Schilder, M. F. Masman, T. Knaus and F. G. Mutti, *Chemistry*, 2021, **27**, 3315-3325.
311. H. Ming, B. Yuan, G. Qu and Z. Sun, *Catal. Sci. Technol.*, 2022, **12**, 5952-5960.
312. Z. Li, H. Yang, J. Liu, Z. Huang and F. Chen, *Chem Rec*, 2021, **21**, 1611-1630.
313. T. M. Penning, *Chem Biol Interact*, 2015, **234**, 236-246.
314. S. K. Kashani, J. E. Jessiman and S. G. Newman, *Organic Process Research & Development*, 2020, **24**, 1948-1954.
315. P. Yaseneva, P. Hodgson, J. Zakrzewski, S. Falß, R. E. Meadows and A. A. Lapkin, *Reaction Chemistry & Engineering*, 2016, **1**, 229-238.
316. J. R. Naber and S. L. Buchwald, *Angew Chem Int Ed Engl*, 2010, **49**, 9469-9474.
317. J.-C. Wang, C.-X. Liu, X. Kan, X.-W. Wu, J.-L. Kan and Y.-B. Dong, *Green Chemistry*, 2020, **22**, 1150-1155.
318. J. Jiao, W. Nie, T. Yu, F. Yang, Q. Zhang, F. Aihemaiti, T. Yang, X. Liu, J. Wang and P. Li, *Chemistry*, 2021, **27**, 4817-4838.
319. H. Soutome, K. Maekawa, Y. Ashikari and A. Nagaki, *Organic Process Research & Development*, 2024, DOI: 10.1021/acs.oprd.4c00021.
320. L. Bering, E. J. Craven, S. A. Sowerby Thomas, S. A. Shepherd and J. Micklefield, *Nat Commun*, 2022, **13**, 380.
321. Z. Xu, J. Feng, P. Yao, Q. Wu and D. Zhu, *Green Chemistry*, 2023, **25**, 4667-4673.
322. J. E. Dander, M. Giroud, S. Racine, E. R. Darzi, O. Alvizo, D. Entwistle and N. K. Garg, *Communications Chemistry*, 2019, **2**.
323. A. Iwasaki, K. Matsumoto, J. Hasegawa and Y. Yasohara, *Applied Microbiology and Biotechnology*, 2012, **93**, 1563-1573.
324. M. R. Chapman, M. H. T. Kwan, G. King, K. E. Jolley, M. Hussain, S. Hussain, I. E. Salama, C. González Niño, L. A. Thompson, M. E. Bayana, A. D. Clayton, B. N. Nguyen, N. J. Turner, N. Kapur and A. J. Blacker, *Organic Process Research & Development*, 2017, **21**, 1294-1301.
325. F. Guan, N. Kapur, L. Sim, C. J. Taylor, J. Wen, X. Zhang and A. J. Blacker, *Reaction Chemistry & Engineering*, 2020, **5**, 1903-1908.
326. P. Falus, Z. Boros, G. Hornyánszky, J. Nagy, F. Darvas, L. Ürge and L. Poppe, *Tetrahedron Letters*, 2011, **52**, 1310-1312.
327. X. Tan, S. Gao, W. Zeng, S. Xin, Q. Yin and X. Zhang, *Journal of the American Chemical Society*, 2018, **140**, 2024-2027.

328. M. Nechab, N. Azzi, N. Vanthuyne, M. Bertrand, S. Gastaldi and G. Gil, *The Journal of Organic Chemistry*, 2007, **72**, 6918-6923.
329. J. L. Núñez-Rico, P. Etayo, H. Fernández-Pérez and A. Vidal-Ferran, *Advanced Synthesis & Catalysis*, 2012, **354**, 3025-3035.
330. S. Liu, Y. Yang, X. Zhen, J. Li, H. He, J. Feng and A. Whiting, *Organic and Biomolecular Chemistry*, 2012, **10**, 663-670.
331. M. Päiviö, P. Perkiö and L. T. Kanerva, *Tetrahedron: Asymmetry*, 2012, **23**, 230-236.
332. D. Pressnitz, C. S. Fuchs, J. H. Sattler, T. Knaus, P. Macheroux, F. G. Mutti and W. Kroutil, *ACS Catalysis*, 2013, **3**, 555-559.
333. S. A. Sadler, H. Tajuddin, I. A. Mkhalid, A. S. Batsanov, D. Albesa-Jove, M. S. Cheung, A. C. Maxwell, L. Shukla, B. Roberts, D. C. Blakemore, Z. Lin, T. B. Marder and P. G. Steel, *Organic and Biomolecular Chemistry*, 2014, **12**, 7318-7327.
334. G. Lu, F. Zheng, L. Wang, Y. Guo, X. Li, X. Cao, C. Wang, H. Chi, Y. Dong and Z. Zhang, *Tetrahedron: Asymmetry*, 2016, **27**, 732-739.
335. B. Abadie, D. Jardel, G. Pozzi, P. Toullec and J. M. Vincent, *Chemistry*, 2019, **25**, 16120-16127.
336. N. J. Taylor, E. Emer, S. Preshlock, M. Schedler, M. Tredwell, S. Verhoog, J. Mercier, C. Genicot and V. Gouverneur, *Journal of the American Chemical Society*, 2017, **139**, 8267-8276.
337. J. Yu, V. Truc, P. Riebel, E. Hierl and B. Mudryk, *Tetrahedron Letters*, 2005, **46**, 4011-4013.
338. O. D. Tereshchenko, M. Y. Perebiynis, I. V. Knysh, O. V. Vasylets, A. A. Sorochenko, E. Y. Slobodyanyuk, E. B. Rusanov, O. V. Borysov, S. V. Kolotilov, S. V. Ryabukhin and D. M. Volochnyuk, *Advanced Synthesis & Catalysis*, 2020, **362**, 3229-3242.
339. T. Song, S. Arseniyadis and J. Cossy, *Chemistry*, 2018, **24**, 8076-8080.
340. A. Hu, H. L. Ngo and W. Lin, *Organic Letters*, 2004, **6**, 2937-2940.
341. Y. Chen, X. Yi, Y. Cheng, A. Huang, Z. Yang, X. Zhao, F. Ling and W. Zhong, *The Journal of Organic Chemistry*, 2022, **87**, 7864-7874.
342. B. Pujala, A. K. Agarwal, S. Middya, M. Banerjee, A. Surya, A. K. Nayak, A. Gupta, S. Khare, R. Guguloth, N. A. Randive, B. U. Shinde, A. Thakur, D. I. Patel, M. Raja, M. J. Green, J. Alfaro, P. Avila, F. Perez de Arce, R. G. Almirez, S. Kanno, S. Bernales, D. T. Hung, S. Chakravarty, E. McCullagh, K. P. Quinn, R. Rai and S. M. Pham, *ACS Medicinal Chemistry Letters*, 2016, **7**, 1161-1166.
343. P. Kang, K. M. Lee, W. K. Lee, K. H. Lee, B. Lee, J. Cho and N. H. Hur, *RSC Advances*, 2014, **4**, 46203-46207.
344. G. Dayaker, W. Erb, M. Hedidi, F. Chevallier, M. Blot, P. C. Gros, G. Hilmersson, T. Roisnel, V. Dorcet, G. Bentabed-Ababsa and F. Mongin, *New Journal of Chemistry*, 2021, **45**, 22579-22590.
345. Y. F. Zhang, X. Y. Dong, J. T. Cheng, N. Y. Yang, L. L. Wang, F. L. Wang, C. Luan, J. Liu, Z. L. Li, Q. S. Gu and X. Y. Liu, *Journal of the American Chemical Society*, 2021, **143**, 15413-15419.

266

7 Appendix

7.1 HPLC Chromatograms

***rac*-1-(1-Napthyl)ethylamine 130**

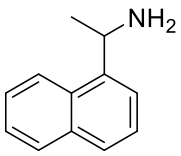

130

Chiral HPLC was performed with a ChiralPak AS-H column (250 x 4.6 mm), 2% EtOH 0.1% DEA) in hexane (0.1% DEA), 20 min run time (***(S)-130*** 7.23 min, ***(R)-130*** 7.72 min).

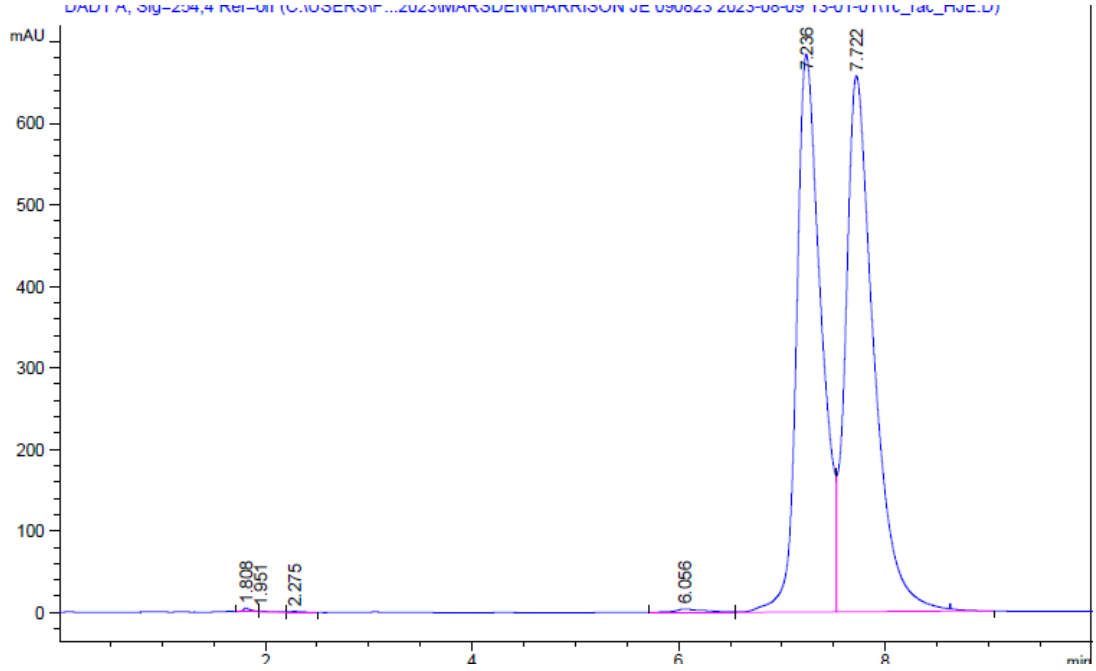

***(S)*-1-(1-Napthyl)ethylamine *(S)*-130**

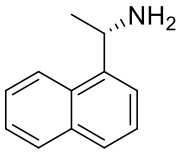

***(S)*-130**

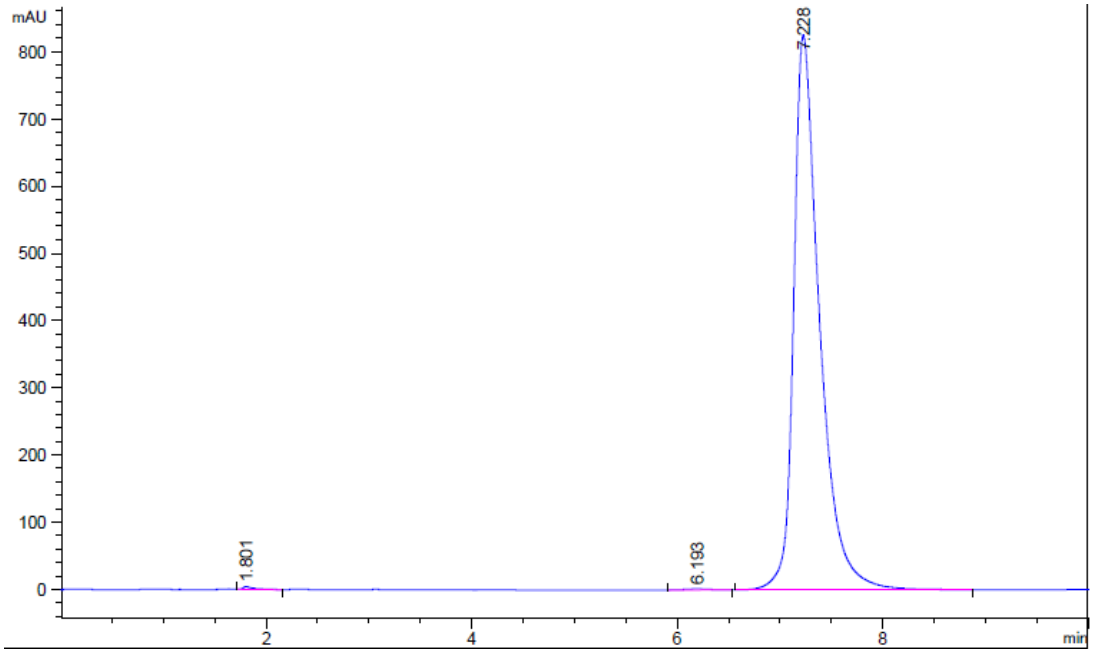

***N*-Acetyl-1-(1-Naphthyl)ethylamine 148**

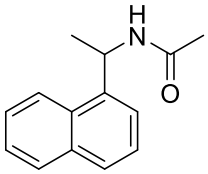

148

Chiral HPLC was performed with a ChiralPak AD-H column (250 x 4.6 mm), 5% EtOH (0.1% DEA) in hexane (0.1% DEA), 20 min run time (***(S)-148*** 4.29 min, ***(R)-148*** 5.22 min).

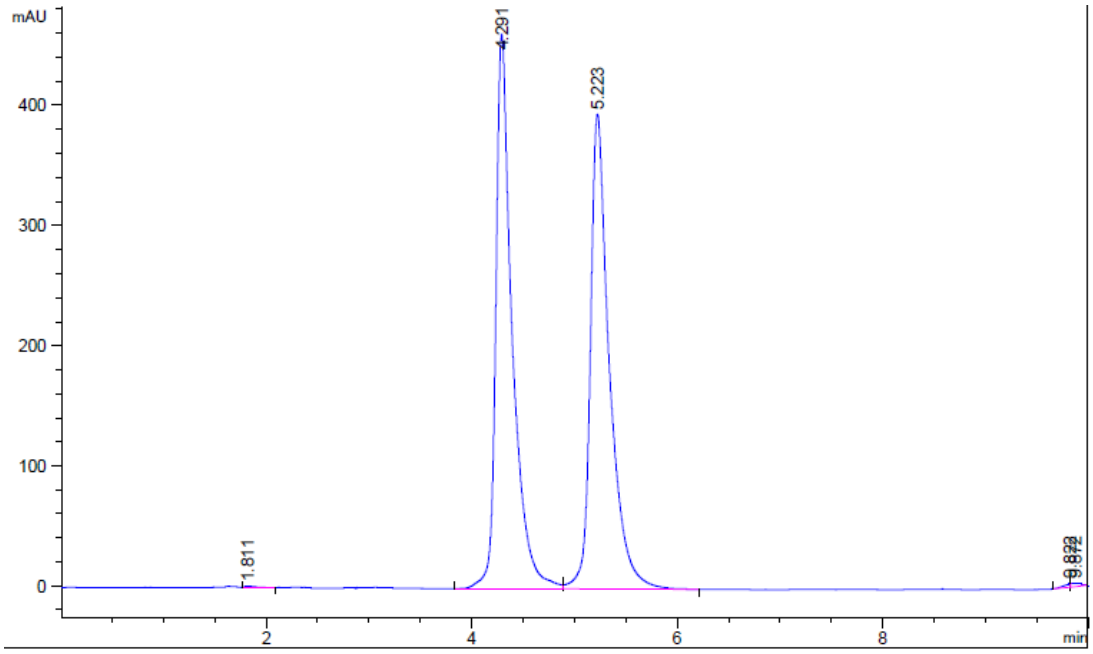

1-Phenylethylamine 92

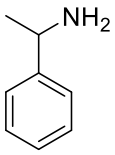

92

Chiral HPLC was performed with a ChiralPak AS-H column (250 x 4.6 mm), 2% EtOH (0.1% DEA) in hexane (0.1% DEA), 20 min run time (***(S)-92*** 8.17 min, ***(R)-92*** 7.68min).

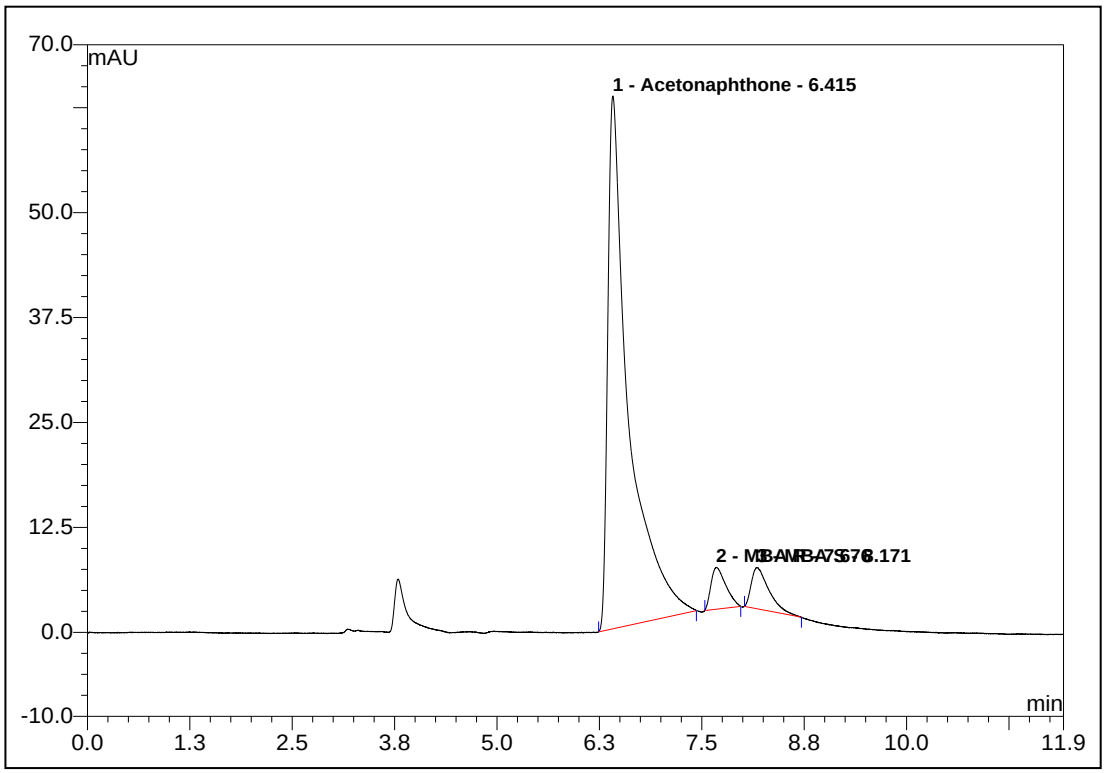

***N*-Acetyl-1-Phenylethylamine 151**

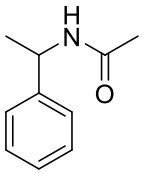

151

Chiral HPLC was performed with a ChiralPak AS-H column (250 x 4.6 mm), 2% EtOH (0.1% DEA) in hexane (0.1% DEA), 20 min run time (***(S)-151*** 4.72 min, ***(R)-151*** 5.18 min).

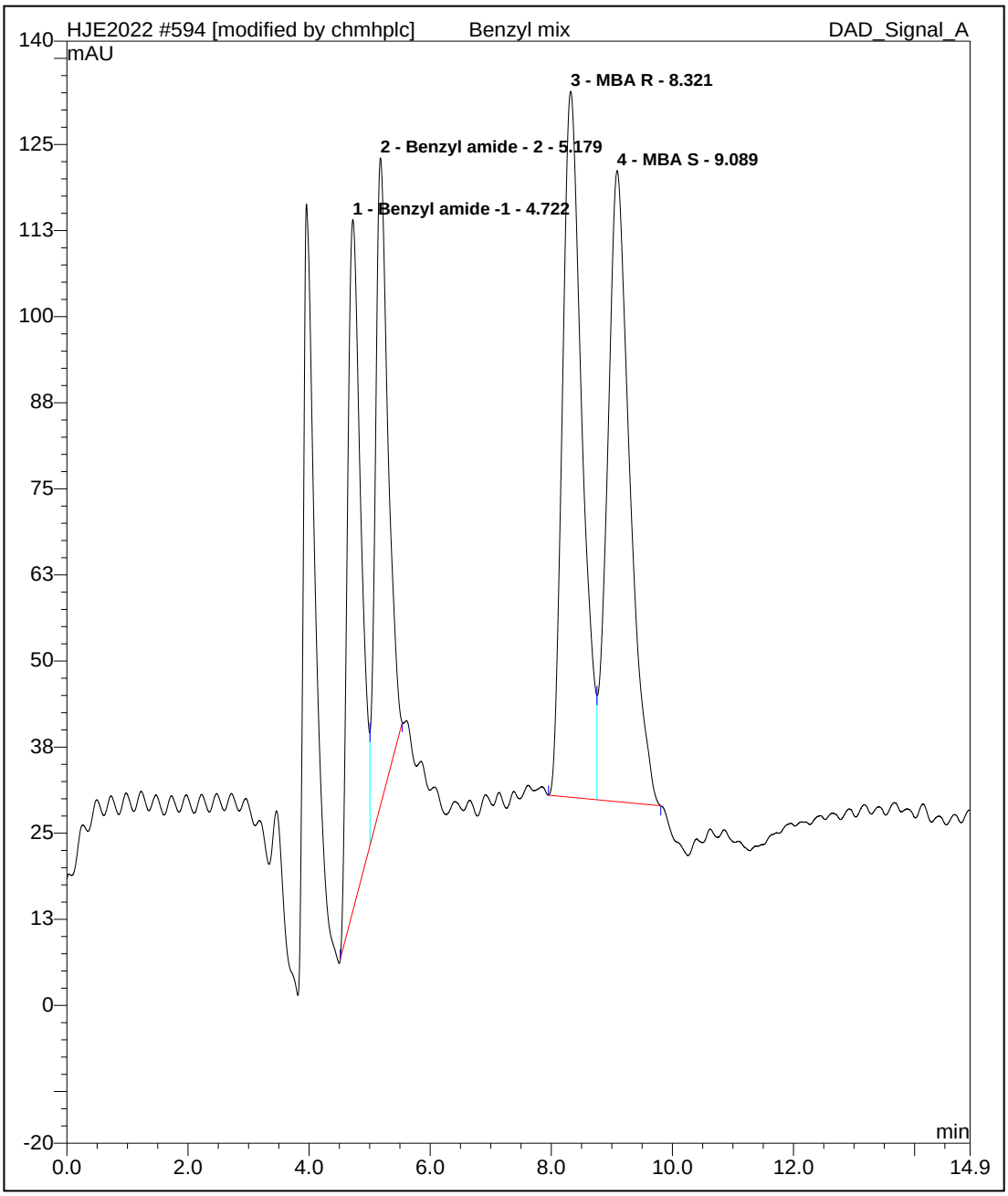

_N_-(Cyclopentylmethyl)-1-phenylethanamine 221

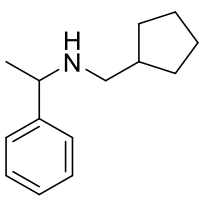

221

Chiral HPLC was performed with a ChiralPak AD-RH column (250 x 4.6 mm), 50% MeCN (0.1% DEA) in water (0.1% DEA), 15 min run time (***(S)*-221** 8.84 min, ***(R)*-221** 10.72min).

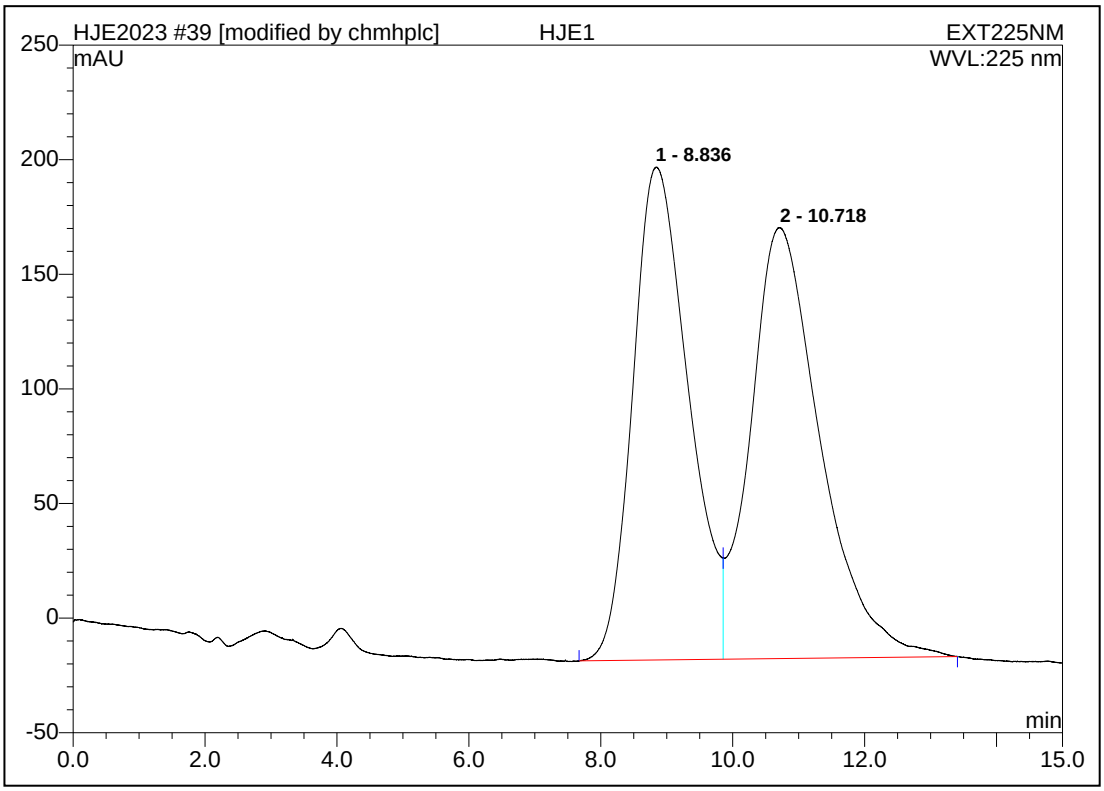

***(S)*-*N*-(Cyclopentylmethyl)-1-phenylethanamine *(S)*-221**

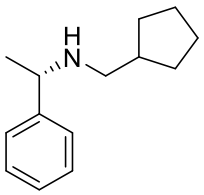

***(S)*-221**

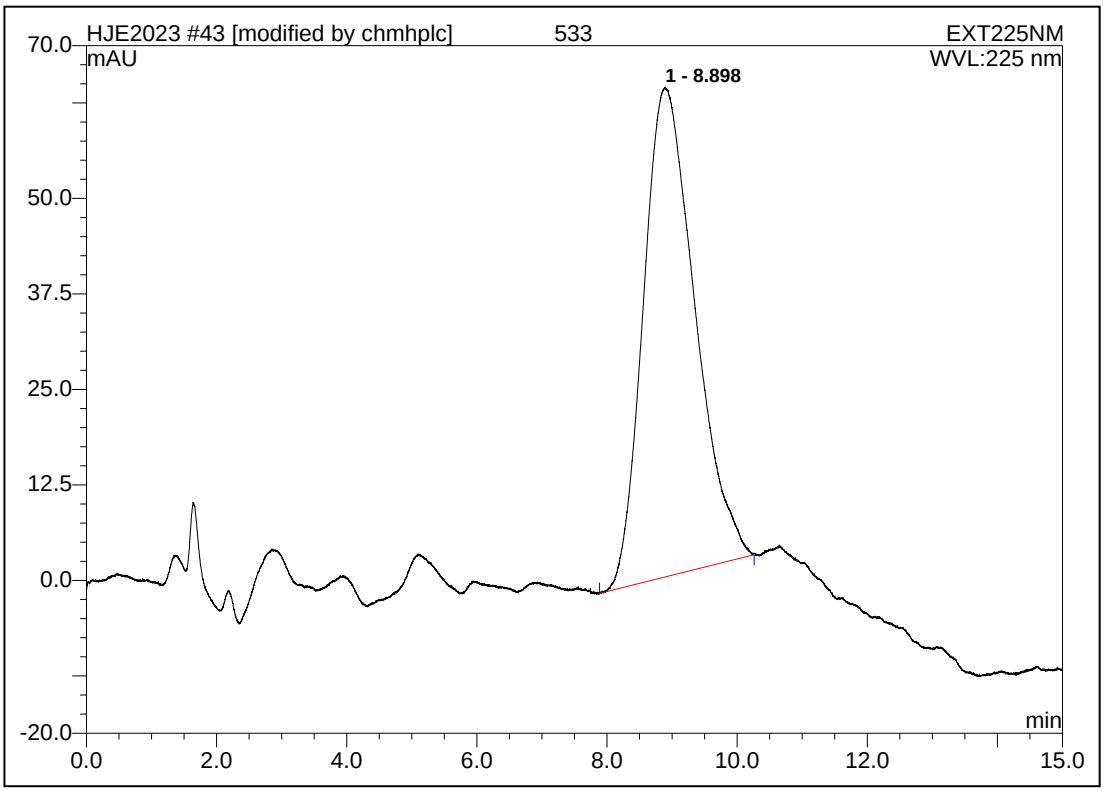

***N*-(Cyclohexylmethyl)-1-naphthalen-1-ylethanamine 225**

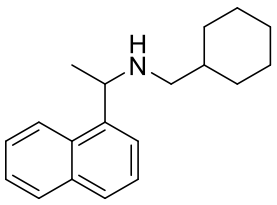

225

Chiral HPLC was performed with a ChiralCel OD-RH column (250 x 4.6 mm), 40% MeCN (0.1% DEA) in water (0.1% DEA), 20 min run time (***(S)*-225** 13.06 min, ***(R)*-225** 14.40 min).

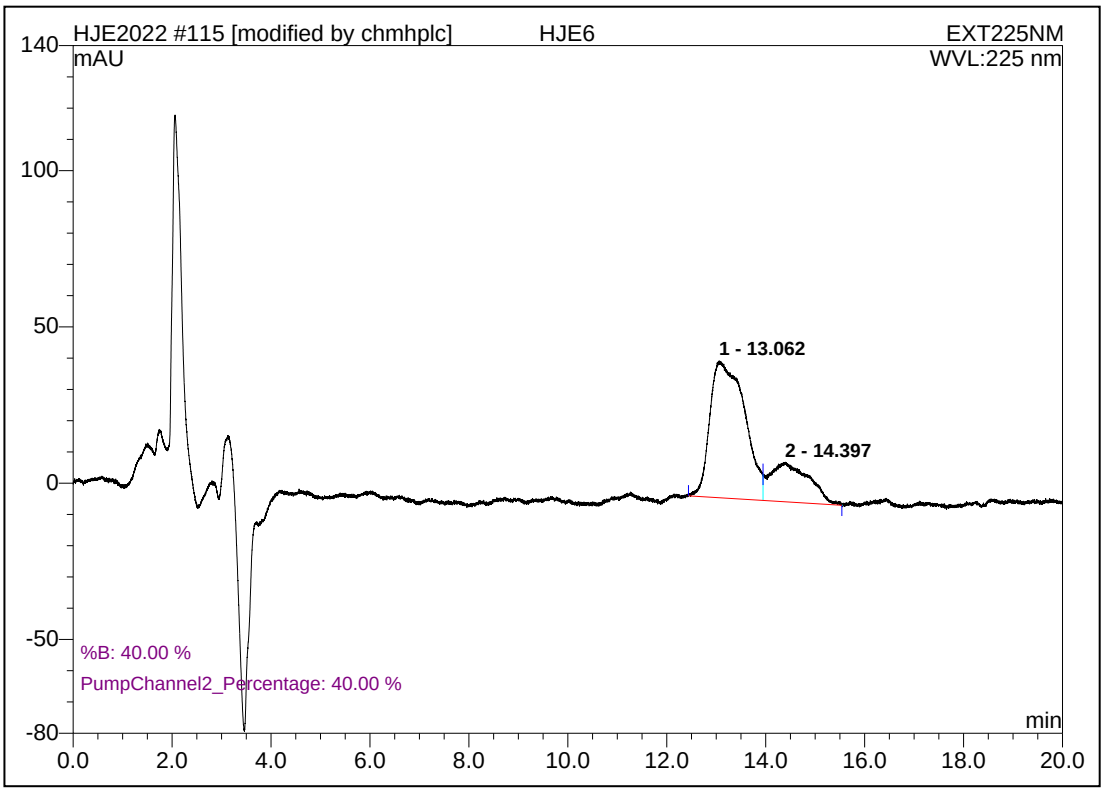

***(S)*-*N*-(Cyclohexylmethyl)-1-naphthalen-1-ylethanamine 225**

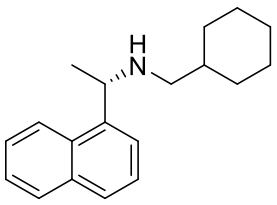

***(S)*-225**

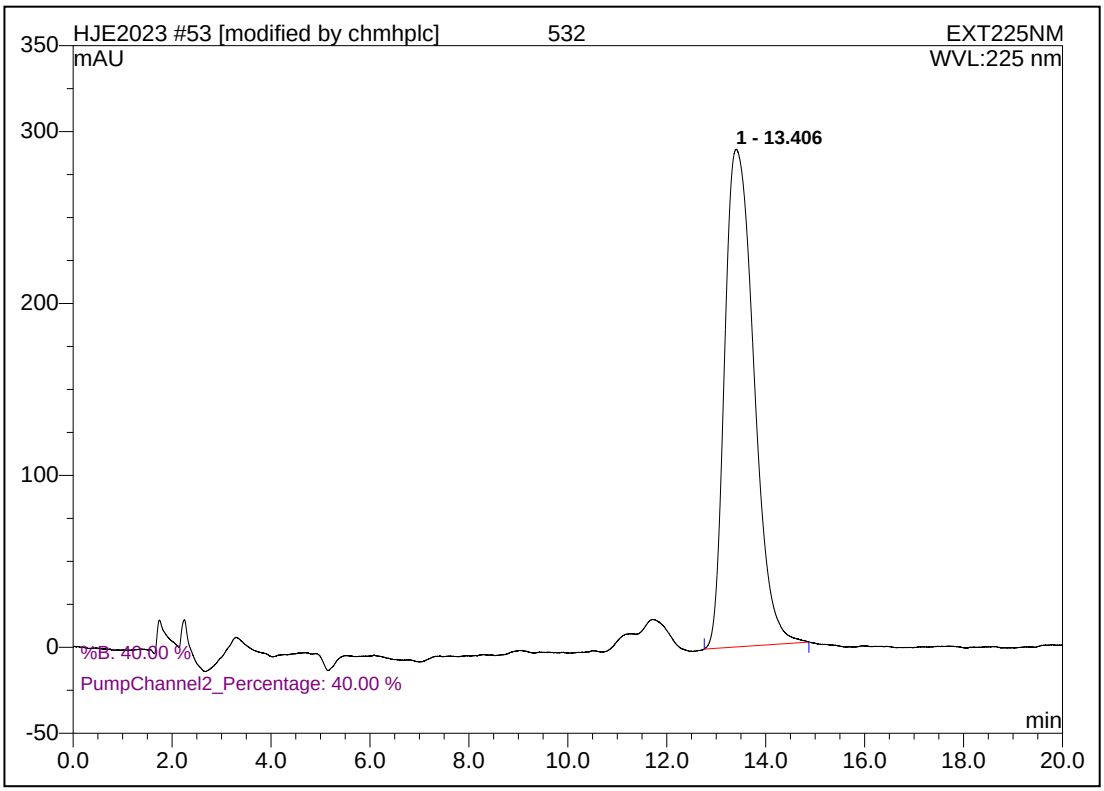

***(S)*-*N*-(1-Phenylethyl)cyclohexanamine *(S)*-227**

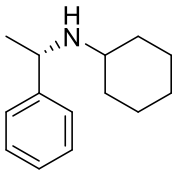

***(S)*-227**

Chiral HPLC was performed with a ChiralPak AS-RH column (250 x 4.6 mm), 40% MeCN (0.1% DEA) in water (0.1% DEA), 20 min run time (***(S)*-227** 10.61 min, ***(R)*-227** 12.67 min).

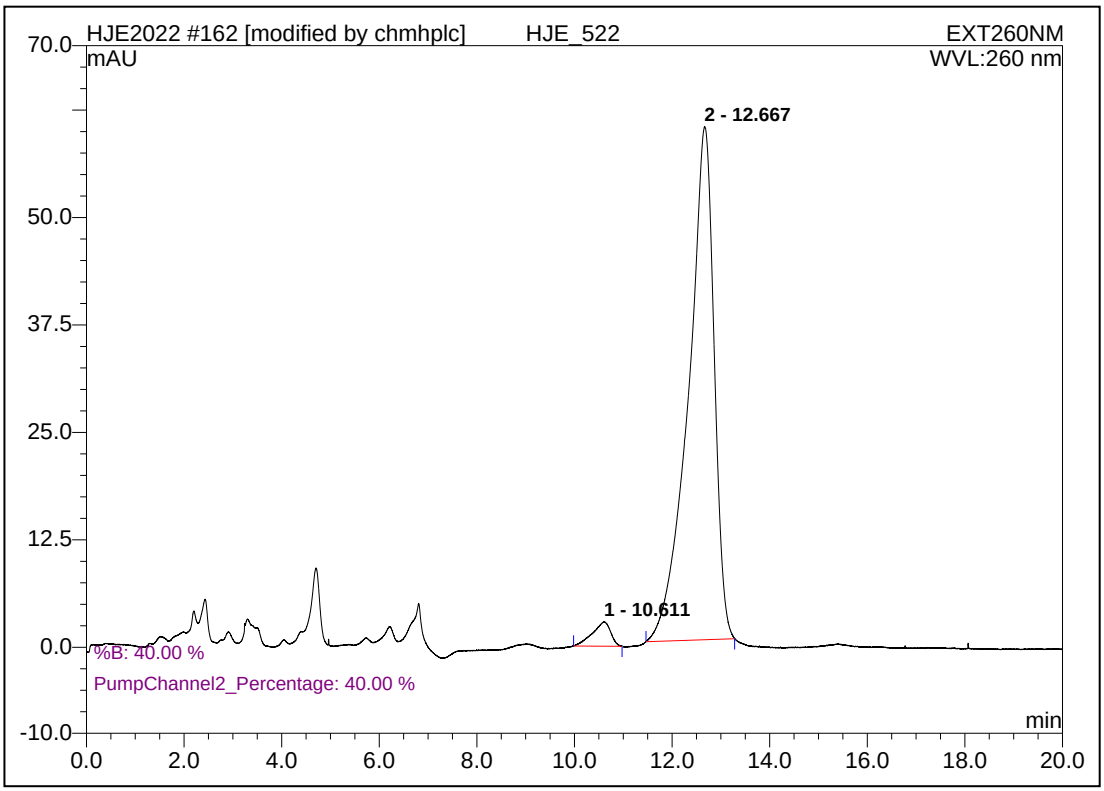

***(S)*-*N*-[2-(4-Methoxyphenyl)ethyl]-1-phenylethanamine *(S)*-230**

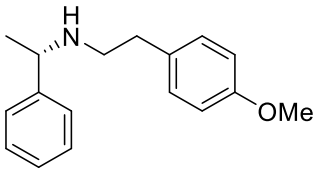

***(S)*-230**

Chiral HPLC was performed with a ChiralPak AS-RH column (250 x 4.6 mm), 40% MeCN (0.1% DEA) in water (0.1% DEA), 20 min run time (***(S)*-230** 17.42 min, ***(R)*-230** 13.41 min).

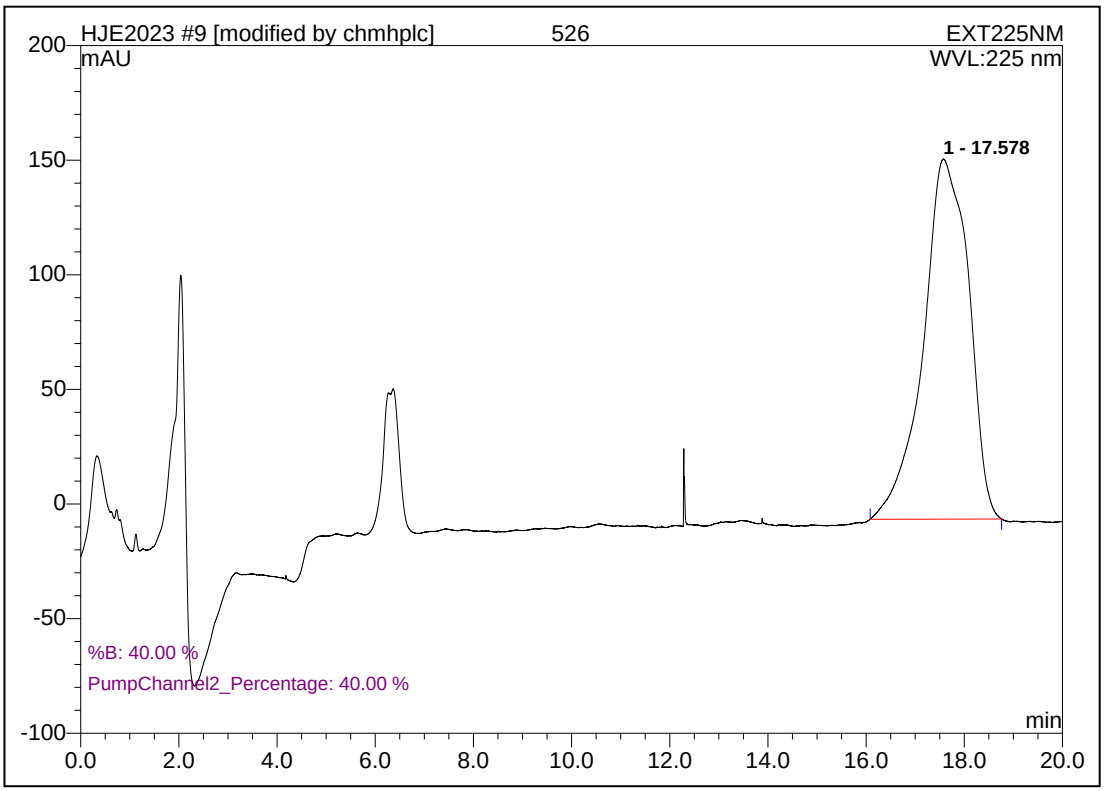

***(S)*-*N*-(3-Phenylpropyl)-1-phenylethylamine 233**

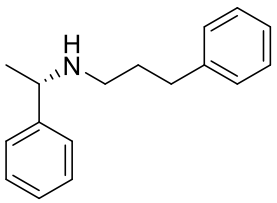

***(S)*-233**

Chiral HPLC was performed with a ChiralPak AS-RH column (250 x 4.6 mm), 45% MeCN (0.1% DEA) in water (0.1% DEA), 20 min run time (***(S)*-233** 11.84 min, ***(R)*-233** 9.90 min).

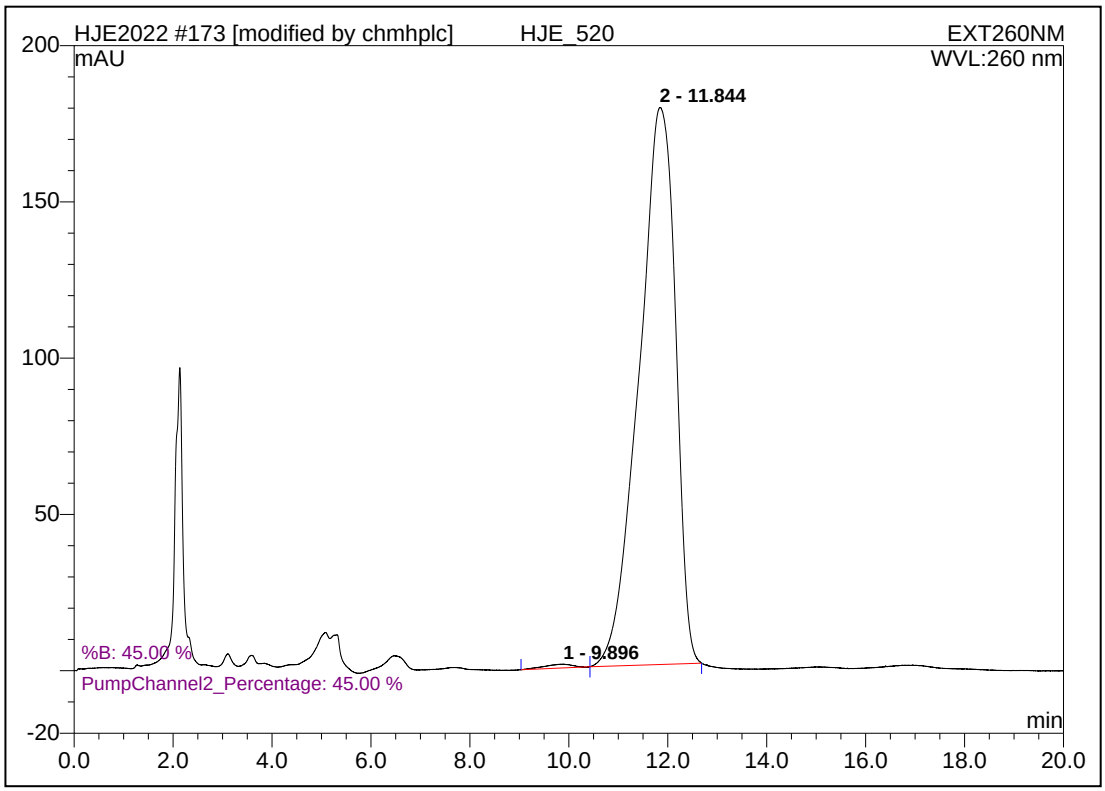

***N*-(3-Phenylpropyl)-1-(1-naphthyl)ethylamine 234**

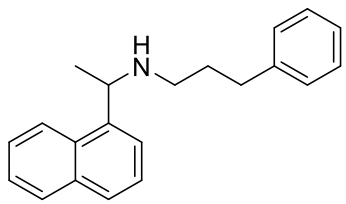

234

Chiral HPLC was performed with a ChiralCel OD-RH column (250 x 4.6 mm), 40% MeCN (0.1% DEA) in water (0.1% DEA), 15 min run time (***(S)*-234** 8.43 min, ***(R)*-234** 9.20 min).

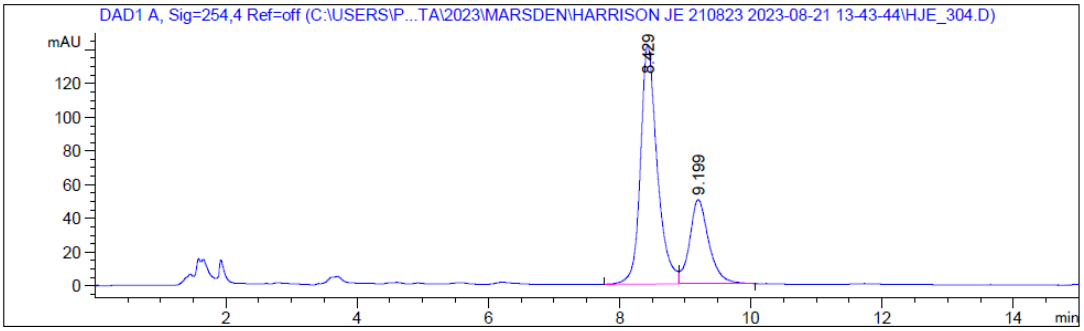

***N*-(1-(naphthalen-1-yl)ethyl)-3-(3-(trifluoromethyl)phenyl)propan-1-amine 10 (cinacalcet)**

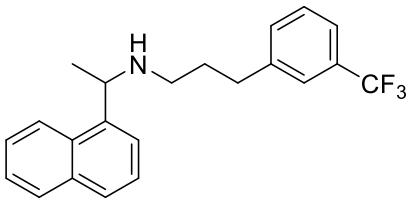

10

Chiral HPLC was performed with a ChiralCel OD-RH column (250 x 4.6 mm), 40% MeCN (0.1% DEA) in water (0.1% DEA), 20 min run time (***(S)*-10** 12.32 min, ***(R)*-10** 11.19 min).

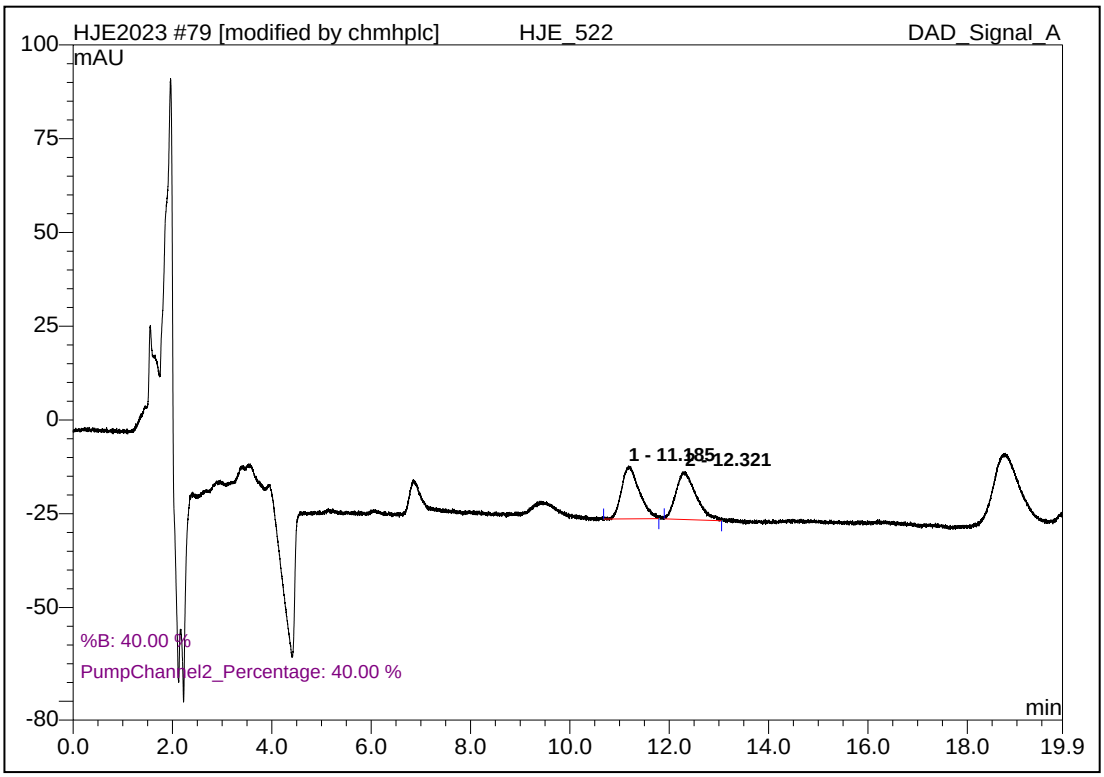

***(S)-N*-(1-(naphthalen-1-yl)ethyl)-3-(3-(trifluoromethyl)phenyl)propan-1-amine *(S)*-10 (cinacalcet)**

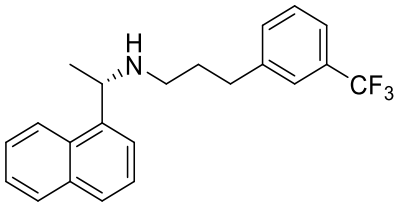

***(S)*-10**

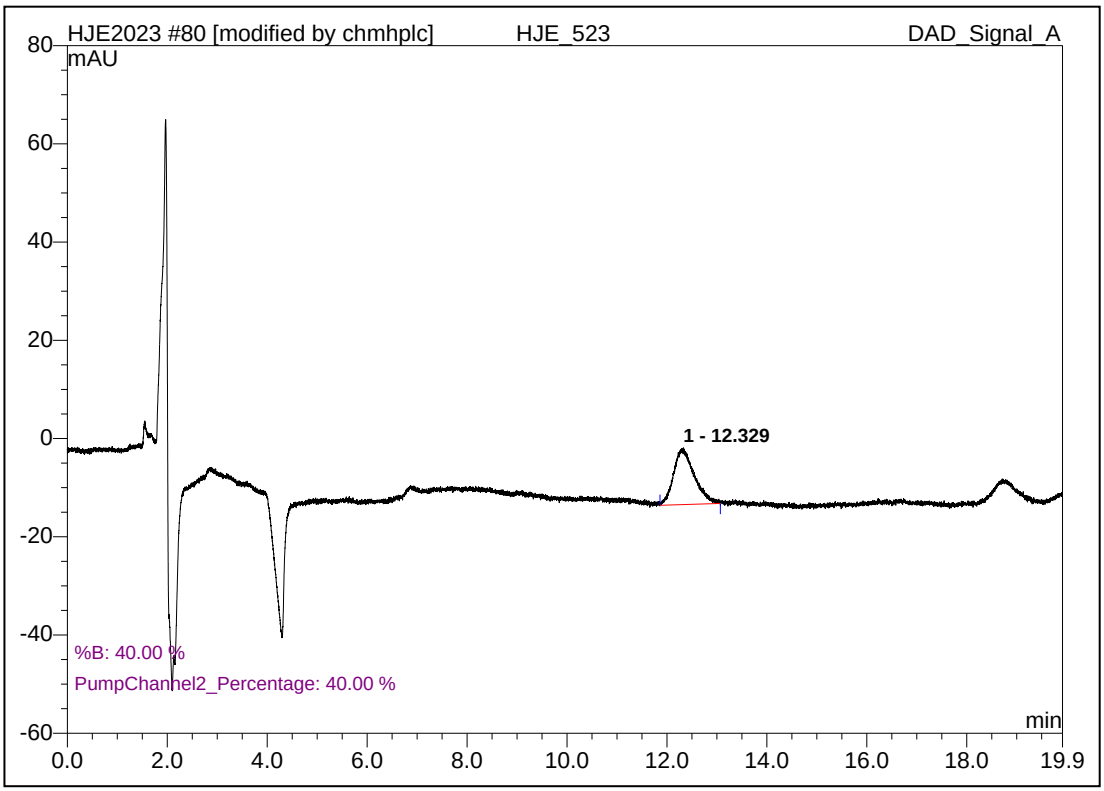

***(S)*-1-(4-Bromophenyl)ethylamine 267**

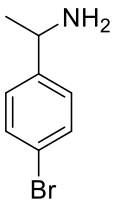

267

Chiral HPLC was performed with a ChiralPak AS-RH column (250 x 4.6 mm), 40% MeCN (0.1% DEA) in water (0.1% DEA), 10 min run time (***(S)-267*** 4.60 min, ***(R)-267*** 4.16 min).

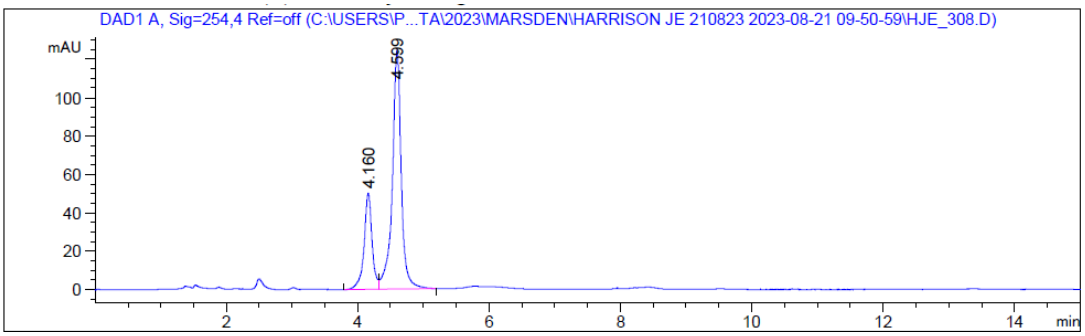

2,3-Dihydro-*1H*-inden-1-amine 268

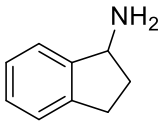

268

Chiral HPLC was performed with a ChiralPak AS-RH column (250 x 4.6 mm), 20% MeCN (0.1% DEA) in water (0.1% DEA), 20 min run time (***(S)-268*** 9.94 min, ***(R)-268*** 10.49 min).

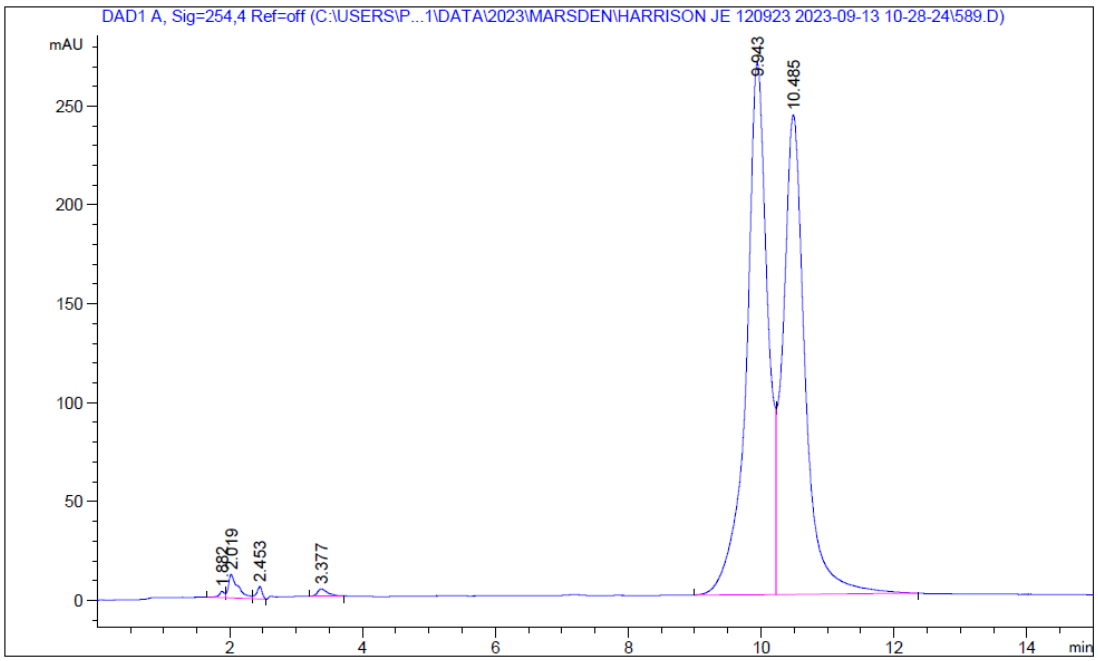

Chroman-4-amine 269

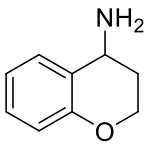

269

Chiral HPLC was performed with a ChiralPak AS-RH column (250 x 4.6 mm), 50% MeCN (0.1% DEA) in water (0.1% DEA), 20 min run time (***(S)-269*** 6.29 min, ***(R)-269*** 6.67 min).

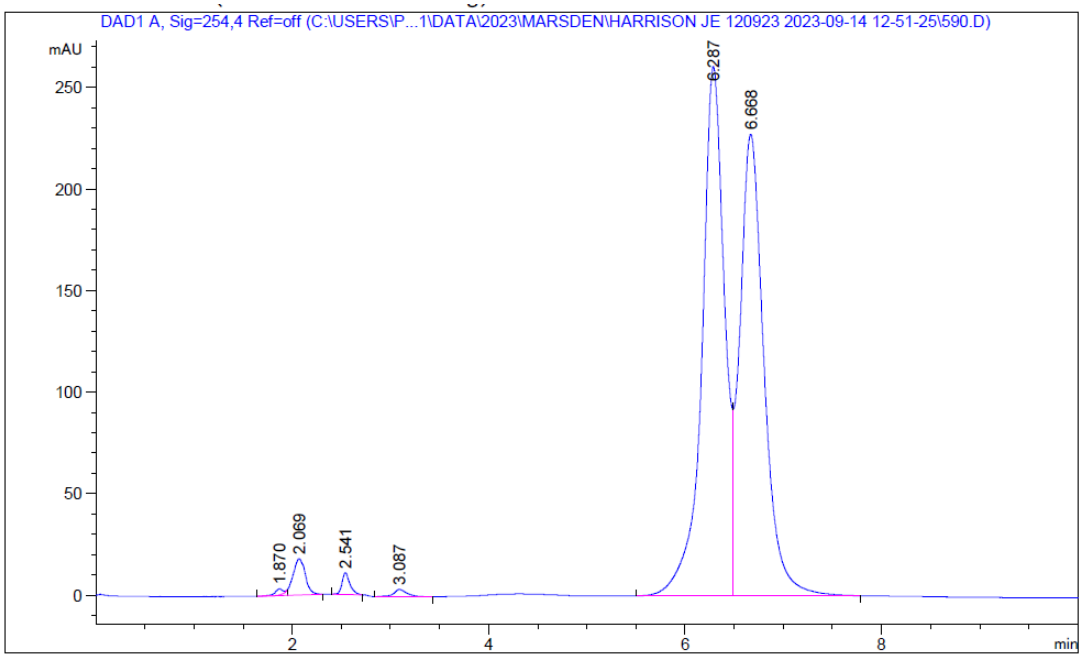
DAD1 A, Sig=254,4 Ref=off (C:\USERS\P...1\DATA\2023\MARSDEN\HARRISON JE 120923 2023-09-14 12-51-25\590.D)
mAU
250
200
150
100
50
0
1.870
2.069
2.541
3.087
6.287
6.668
2
4
6
8
min